Human longevity : crosstalk between the brain and periphery
Akintola, A.A.

Author: Akintola, Abimbola
Title: Human longevity : crosstalk between the brain and periphery
Issue Date: 2016-11-16

HUMAN LONGEVITY:
CROSSTALK BETWEEN THE BRAIN AND PERIPHERY

ABIMBOLA AKINTOLA

HUMAN LONGEVITY:

CROSSTALK BETWEEN THE BRAIN AND PERIPHERY

Abimbola A. Akintola

Colofon

Author:	Abimbola (Abi) Akintola
Design / lay-out:	Abi Akintola, Mirakels Ontwerp
Printing:	Gildeprint - The Netherlands
ISBN:	978-94-6233-433-5

The work described in this thesis was supported by the European commission project Switchbox (FP7, Health-F2-2010-259772).

HUMAN LONGEVITY:

CROSSTALK BETWEEN THE BRAIN AND PERIPHERY

Proefschrift

ter verkrijging van
de graad van Doctor aan de Universiteit Leiden
op gezag van Rector Magnificus prof. mr. C.J.J.M. Stolker
volgens besluit van het College voor Promoties
te verdedigen op woensdag 16 november 2016
klokke 11:15 uur

door

Abimbola Abike Akintola

Geboren te Lagos, Nigeria

Promotor

Prof. Dr. R. G. J. Westendorp

Co-promotores

Dr. Ir. Diana van Heemst

Dr. Jeroen van der Grond

Leden promotiecommissie

Prof. Dr. Hanno Pijl

Prof. Dr. Joke Meijer

Prof. Dr. Manfred Hallschmid (University of Tübingen, Germany)

Prof. Dr. Nuno Sousa (University of Minho, Braga, Portugal)

Even in old age they will still be thriving, they will remain vigorous and fresh

The former things have passed away

(Psalm 92:14, Revelation 21:4)

CONTENTS

LIST OF ABBREVIATIONS

ANN	Average of NN intervals
ARD	Absolute relative difference
ARD	Absolute relative difference
AUC	Area Under the Curve
BPM	Beats per minute
CMB	Cerebral micro-bleeds
CGM	Continuous glucose monitor
CONGA	Continuous overlapping net glycemic action
CONGA1	Continuous overlapping net glycemic action over one hour
CONGA4	Continuous overlapping net glycemic action over four hours
CV	Coefficient of variation
ECG	Electrocardiogram
EQ02	Equivital EQ02 lifemonitor
FAST	FMRIB's automated segmentation tool
FLAIR	Fluid attenuated inversion recovery
FMRIB	Functional MRI of the brain
FSL	FMRIB Software Library
GM	Gray Matter
Holter	Holter ambulatory ECG monitor
HOMA-IR	Homeostatic Model Assessment of Insulin Resistance
HOMA-IS	Homeostatic Model Assessment of Insulin Sensitivity
HR	Heart rate
HRV	Heart rate variability
IQR	Interquartile range
LLS	Leiden longevity study
MAGE	Mean amplitude of glycemic excursions
MARD	Mean absolute relative difference
MNI152	Montreal Neurological Institute 152
MRI	Magnetic Resonance Imaging
ms	Milliseconds
MTI	Magnetization Transfer Imaging

MTR	Magnetization Transfer Ratio
NN	Normal- to- normal sinus rhythm interval
NN50	Number of adjacent NN intervals with a difference less than 50ms
OGTT	Oral Glucose Tolerance Test
pNN50	Ratio of a NN50 to total number of NN intervals
RD	Relative difference
RR	interval between the R wave peaks of the recorded QRS complex
RMSSD	Square root of the mean squared differences of successive intervals
SD	Standard deviation
SDws1	Standard deviation within time series of one hour
SDws4	Standard deviation within time series of four hours
SDANN	Standard deviation of 5 minute averages of NN intervals
SDNN	Standard deviation of NN intervals
SDNNi	Mean of the standard deviation of 5 minute NN intervals
SDSD	Standard deviation of successive differences of NN intervals
SE	Standard error
SIENAX	Structural Image Evaluation, using Normalization, of Atrophy
SMBG	Self-monitoring of blood glucose
TFCE	Threshold- Free Cluster Enhancement
Type 2 DM	Type 2 Diabetes Mellitus
VOI	Voxels of Interest
WM	White Matter
WMH	White Matter Hyper-intensities

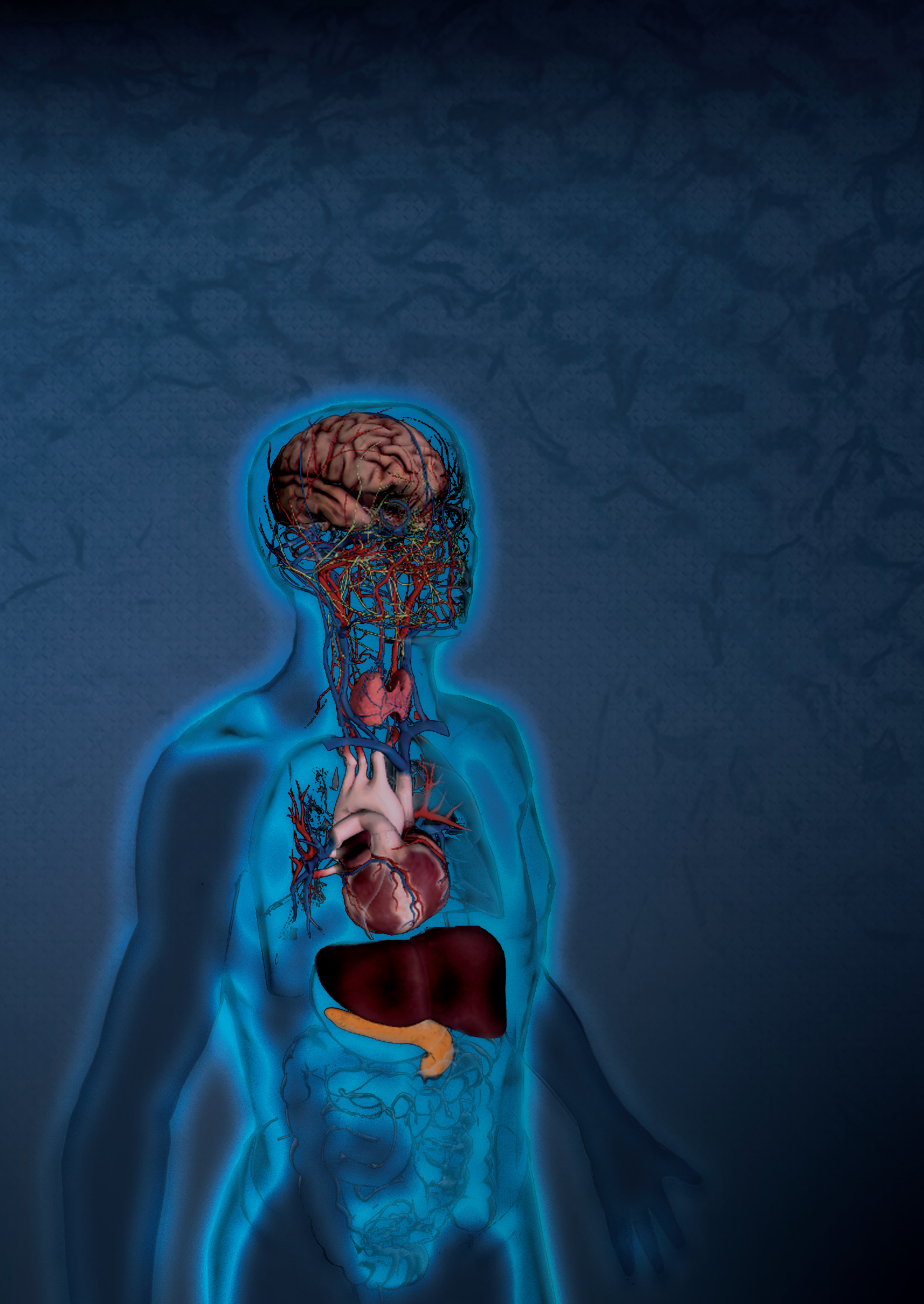

CHAPTER 1

GENERAL INTRODUCTION

GENERAL INTRODUCTION

1

Chapter 1

Even though mortality in old age has significantly decreased over the last fifty years in the developed world [1], there still remains a large inter- individual variability in ageing trajectories, morbidity and mortality [2]. The ageing process is associated with numerous physiological alterations across multiple organ systems, including the brain. Thus, the need to better understand the physiological mechanisms and processes that underlie the ageing process is vital.

Longevity potential is determined by genetic and environmental factors [2, 3]. Various attempts have been made to delineate the regulatory pathways that underlie human longevity. Studies in model organisms suggest that longevity is promoted by conserved genetic mechanisms that orchestrate the organism's responses to its changing environment, such as insulin/insulin-like growth factor-1 (IGF-1) signaling [4, 5]. Also in humans, the ability to maintain the stability of the body's internal environment while dynamically adapting to changes in external conditions, known as homeostasis, has been identified as being a key to healthy longevity [6]. This maintenance is brought about by an intact communication between the brain and the peripheral bodily functions. Loss of homeostatic control is hypothesized to contribute to both bodily and cognitive decline.

Crosstalk between brain and periphery

Homeostasis is essential for health throughout lifetime, since age- related changes to physiology accumulate from early life [7, 8]. Homeostatic control is a complex mechanism requiring reciprocal projections from the brain to the periphery, and have at least three interdependent components: receptor/sensor, control center and effector [9]. Homeostasis requires the integration of numerous peripheral cues (sensor) by the hypothalamus and nearby brain structures (control center), to mount a coordinated response to adapt and maintain the internal environment within narrow limits. Tight regulation of these systems is key to healthy ageing.

Among the key modifiers of the ageing process identified are insulin/ IGF-1 signaling (IIS), the hypothalamic/ pituitary/thyroid (HPT) axis, the hypothalamic/ pituitary/ adrenal (HPA) axis and the autonomic nervous system. While a healthy interaction between these systems is crucial for maintenance of homeostasis of vital parameters (figure 1), a lack of communication or their dysregulation is implicated in accelerated and unhealthy ageing.

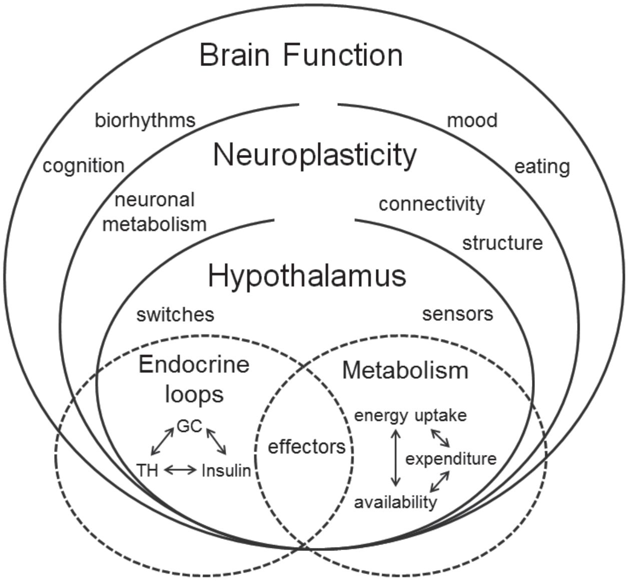

FIGURE 1.1 | Schematic figure depicting the brain-periphery dialogue. Taken with permission from the Switchbox project proposal.

In this thesis, emphasis will be placed on three key modifiers of the ageing process, namely the communication between the brain and glucose and insulin metabolism, HPT axis and the autonomic nervous system, using data from the Leiden Longevity Study and the Switchbox study.

Data Sources- the Leiden Longevity Study

The Leiden Longevity study (LLS) was designed to identify determinants of human longevity by studying offspring of long- lived siblings and their partners. Between 2002 and 2006, some 421 Dutch Caucasian families were recruited of which at least two long-lived siblings were alive and aged 89 years or older for men and 91 years or older for women, without selection on health or demographic characteristics. Furthermore, the offspring of these long- lived nonagenarians and their partners, were also enrolled (figure 2). These offspring carry 50% of the genetic advantage of their long- lived parent and were shown to have a 35% lower mortality rate compared to their birth cohort [10]. Their partners with whom most have had a relationship and shared environment for decades, were included as population-based, environment- matched controls.

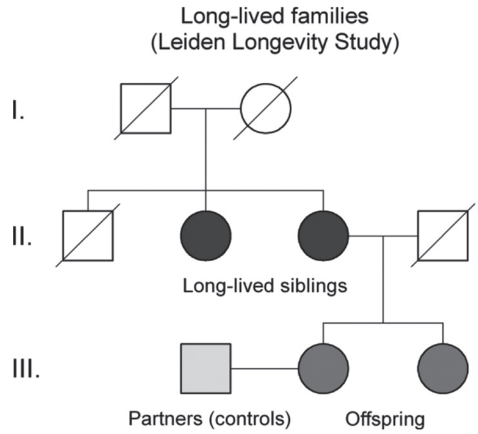

FIGURE 1.2 | Study design of the Leiden Longevity Study.

Brain MRI data from offspring and partners in the LLS were used to study the relation between parameters of glucose metabolism and brain function.

Data Sources- the Switchbox Study

The Switchbox study is a satellite study from the LLS. The study is entitled 'Maintaining health in old age through homeostasis', and has the acronym 'Switchbox'. It is an European project comprising partners from Paris, Munich, Budapest, Braga and Leiden, with the collective aim of improving healthy longevity by studying the brain- periphery dialogue with a view to re-setting the critical hypothalamic set-points. In Leiden, Switchbox was conducted in two phases- Phases I & II, over a period of 4.5 years (figure 3). The first phase (phase I) was an observational study of offspring of long- lived siblings and their partners, while phase II was a randomised controlled clinical trial involving healthy volunteers from the general population.

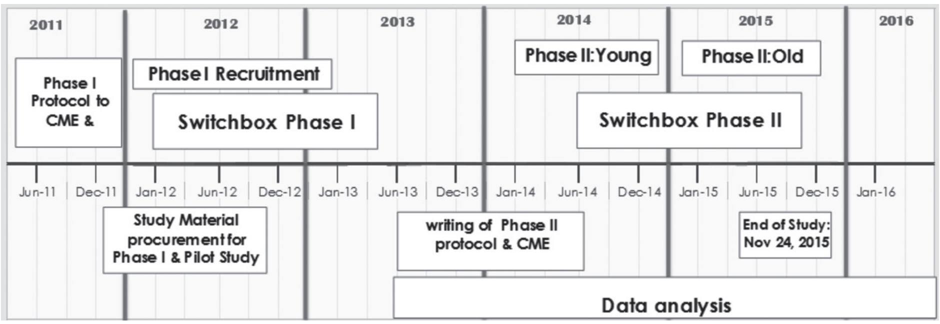

FIGURE 1.3 | Switchbox timeline covering the period of 4.5 years during which the Switchbox study was conducted.

Switchbox Phase I

The hypothesis of the Switchbox phase I study is that control of homeostasis would be better preserved in the offspring of long-lived sibling, who grow older in better health compared to their partners who show 'regular' ageing. This was hypothesized to be reflected in differences in brain function, neuro-endocrine output and peripheral metabolism. Thus, we examined the links between the three main signaling axes- Hypothalamo-adrenal axis (HPA), Hypothalamo- thyroid axis (HPT) & Insulin- IGF-1 signaling axis (IIS) and critical measures that deteriorate during the ageing process, such as metabolism, brain structure and function, and heart rate and heart rate variability.

Between March 2012 and July 2013, 135 offspring and partners from the LLS were included for Switchbox phase I. Inclusion criteria were being middle-aged (55-77 years) and having a stable body mass index (BMI) between 19 kg/m2 < BMI < 33 kg/m2. All women in the study were postmenopausal. Participants were excluded if their fasting plasma glucose was above 7 mmol/L, if they had any significant chronic, renal, hepatic or endocrine disease, or if they used any medication known to influence lipolysis, thyroid function, glucose metabolism, GH/IGF-1 secretion or any other hormonal axis. Other exclusion criteria were difficulties to insert and maintain an intravenous catheter, anaemia (Hemoglobin < 7.1 mmol/L), blood donation within the last two months, smoking and alcohol addiction, severe claustrophobia and extreme diet therapies. Data for comparison of measures of brain function (structural and functional brain MRI, cognitive tests), neuro-endocrine output (24-hour hormone rhythms), and peripheral metabolism (continuous glucose monitoring, indirect calorimetry, diaries), cardiac parameters (continuous ambulatory ECG monitoring) to estimate sympathetic/ parasympathetic tone and motion (continuous tri-axial accelerometry) were collected over five days (figure 4) from offspring and their partners, to identify parameters most relevant for a slower pace of ageing.

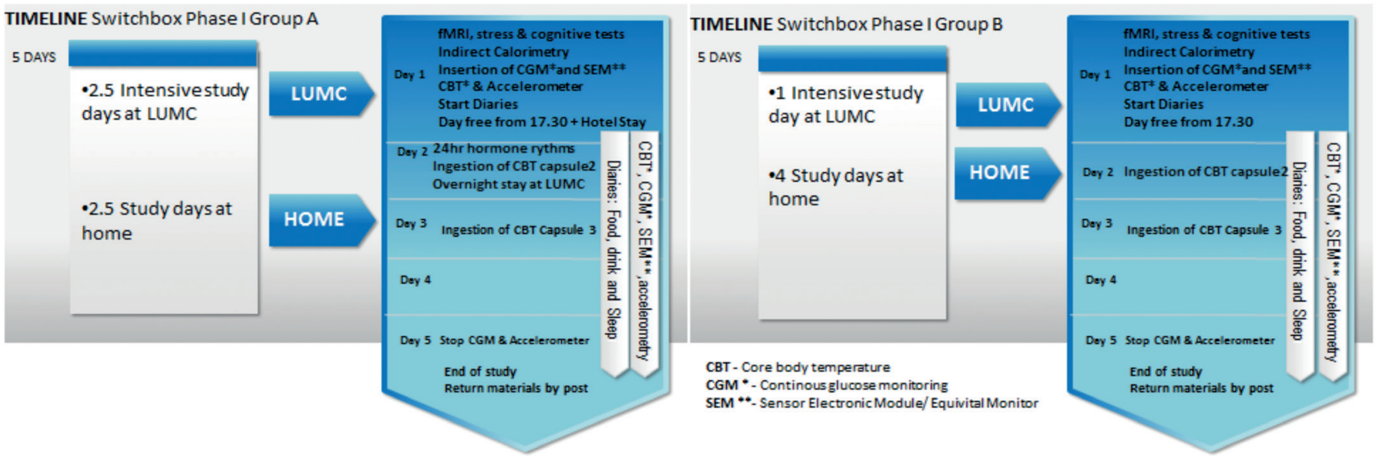

FIGURE 1.4 | Study protocol followed by both groups of Switchbox phase I participants.

Switchbox Phase II

Insulin is an important modulator of brain functions, including central regulation of energy homeostasis, cognitive functions, neuronal activity and other behavioral, cellular, biochemical, and molecular functions [11, 12]. Due to the presence of direct pathways from the nasal cavity to the CNS, insulin can be delivered, non- invasively and rapidly to the CNS through the intranasal route without being absorbed into the blood stream or having direct systemic effects [13].

Phase II involved testing whether and to what extent parameters identified in Phase I could be modulated by intranasal insulin application. To this end intranasal insulin and placebo were administered to 19 adults (8 young and 11 elderly) volunteers from the general population in a blinded, cross- over designed randomized clinical trial in which each participant served as his own control. Participants were randomized into two groups for the order of intranasal application of insulin and placebo (insulin first or placebo first groups), In addition, the younger participants additionally received either 75 gr glucose solution or water during the MRI protocol. Thus, the younger participants were randomized to four study days (insulin and glucose, insulin and water, placebo and glucose, placebo and water) (figure 5) whereas the older had two visits (insulin and water and placebo and water).

In this thesis, we report on the neuro-endocrine, metabolic and autonomic characteristics that appear to be pertinent for slower pace of ageing.

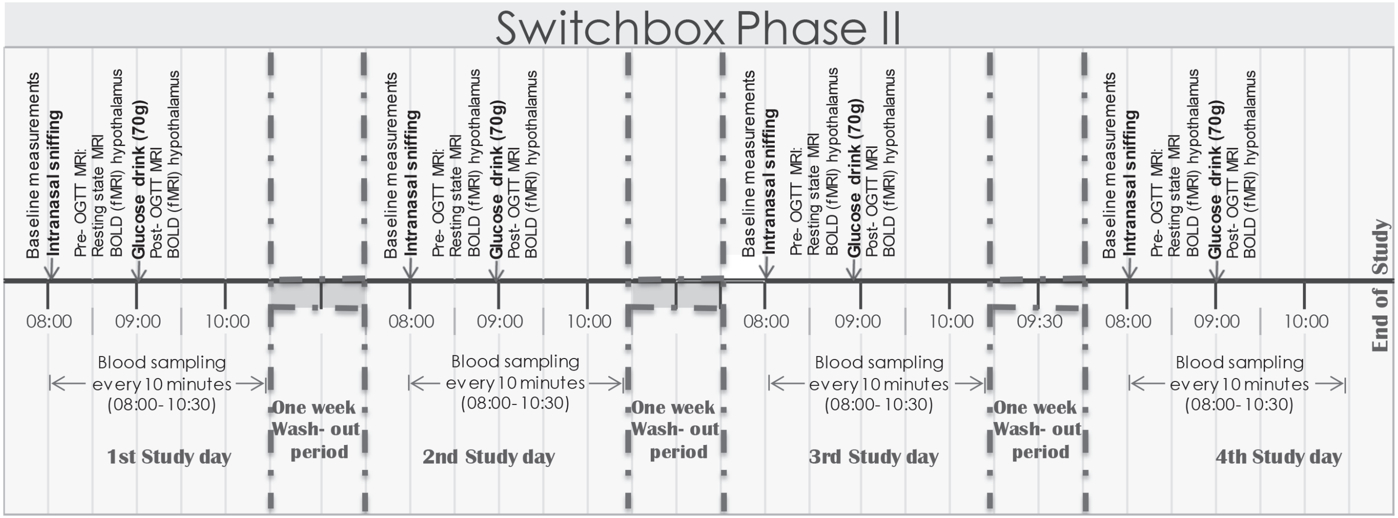

FIGURE 1.5 | Study protocol followed by Switchbox phase II participants.

REFERENCES:

1. Oeppen J, Vaupel JW. Demography. Broken limits to life expectancy. Science. 2002;237:1029
2. Westendorp RG. What is healthy ageing in the 21st century? Am J Clin Nutr. 2006;83:404S-9S
3. Zwaan BJ. The evolutionary genetics of ageing and longevity. Heredity (Edinb). 1999;82 (Pt6):589-97
4. Holzenberger M,Dupont J,Ducos B, Leneuve P, Geloen A, Even PC, et al. IGF-1 receptor regulates lifespan and resistance to oxidative stress in mice. Nature. (2003) 421(6919):182–7. doi:10.1038/nature01298
5. Bartke A, Chandrashekar V, Dominici F, Turyn D, Kinney B, Steger R, et al. Insulin-like growth factor 1 (IGF-1) and E: controversies and new insights. Biogerontology. (2003) 4(1):1–8. doi:10.1023/A:1022448532248
6. Marieb, Elaine N., Hoehn, Katja N. (2009). Essentials of Human Anatomy & Physiology (9th ed.). San Francisco, CA: Pearson/Benjamin Cummings. ISBN 0321513428.
7. Gavrilov LA, Gavrilova NS. Early-life programming of aging and longevity: the idea of high initial damage load (the HIDL hypothesis). Annals of the New York Academy of Sciences. 2004;1019:496-501.
8. Gillman MW. Developmental origins of health and disease. The New England journal of medicine. 2005;353(17):1848-50.
9. Source: Boundless. "Homeostatic Control." Boundless Anatomy and Physiology. Boundless, 21 Jul. 2015. Retrieved 09 Oct. 2015 from https://www.boundless.com/physiology/textbooks/boundless-anatomy-and-physiology-textbook/introduction-to-human-anatomy-and-physiology-1/homeostasis-32/homeostatic-control-284-3141/
10. Schoenmaker M, de Craen AJ, de Meijer PH, Beekman M, Blauw GJ, Slagboom PE, Westendorp RG (2006) Evidence of genetic enrichment for exceptional survival using a family approach: the Leiden Longevity Study. Eur J Hum Genet. 14:79–84. doi:10.1038/sj.ejhg.5201508
11. Duarte AI, Moreira PI, Oliveira CR. Insulin in central nervous system: more than just a peripheral hormone. JAging Res. 2012;2012:384017.
12. Schwartz MW, Seeley RJ, Tschop MH, Woods SC, Morton GJ, Myers MG, et al. Cooperation between brain and islet in glucose homeostasis and diabetes. Nature. 2013;503(7474):59-66.
13. Hallschmid M, Benedict C, Schultes B, Perras B, Fehm HL, Kern W, et al. Towards the therapeutic use of intranasal neuropeptide administration in metabolic and cognitive disorders. Regulatory peptides. 2008;149(1-3):79-83.

OUTLINE OF THIS THESIS

The main objective of this thesis is to provide new insights into the crosstalk between the brain and the periphery, with a focus on glucose and insulin metabolism, the thyroid axis and the autonomic nervous system. Each section begins with the validation of a measurement device for use for a key parameter in this crosstalk.

Part I of this thesis discusses the role of the brain in glucose and insulin metabolism, in both offspring of families enriched for familial longevity and their partners. Since glucose metabolism was previously shown to associate with longevity potential, we explored ways to measure glucose levels non-invasively. Thus, we started in **chapter 2** with the validation of a continuous glucose monitor for non-invasive glucose measurement in older persons. Based on the hypothesis that maintenance of glucose metabolism is important not just for metabolic health but also for the brain, we assessed the relation between glucose and insulin metabolism on brain macro- and microstructure in **chapter 3**. Then, we further tested the effect of age and being a descendant of families enriched for familial longevity on the relation between parameters of glucose metabolism and the brain integrity in **chapter 4**. To gain mechanistic insights into the role of the brain in glucose metabolism, we examined the effect of intranasal administration of insulin on the brain, as it was found previously to improve cognition in humans. In **chapter 5**, we examined the effect of intranasally administered insulin on cerebral blood flow and perfusion in young and older adults. Part I concludes with **chapter 6**, where we reviewed the crosstalk between glucose and insulin metabolism, ageing and the brain.

In **Part II** of this thesis, we investigated another system that is implicated in human longevity; i.e. the thyroid axis. Thus, we set out to characterize the thyroid axis. First, we devised a versatile method for frequent blood collection in older participants. This is presented as **chapter 7**. Then, in **chapter 8**, from frequently sampled blood, we investigated the thyroid stimulating hormone (TSH) secretion pattern on the one hand, and whole body energy metabolism on the other hand in relation to longevity. In **chapter 9**, via a systematic review and meta-analysis of existing literature, we further looked at the effect of subclinically raised TSH levels on cognition.

Summarily, our study of the thyroid axis showed that human longevity is characterized by higher TSH levels, but without differences in basal metabolism. Since the thyroid gland is innervated by the autonomic nervous system, and its activity might be affected by the sympathetic/ para-sympathetic tone, we tested the influence of the autonomic nervous system, using heart rate and heart rate variability as a proxy, on human longevity. This forms the basis for the **third part (Part III)** of this thesis. In this part, in **chapter 10**, we first validated a device- the Equivital (EQ02) lifemonitor- for non-invasive measurement of ambulatory ECG, heart rate and heart rate variability in older adults. Then, in **chapter 11**, we examined the role of heart rate rhythms and heart rate variability in familial longevity.

Finally, in **chapter 12**, the key findings of this thesis are summarized. These are then discussed in context of current knowledge of human longevity.

PART I:

CROSSTALK WITH INSULIN AND GLUCOSE

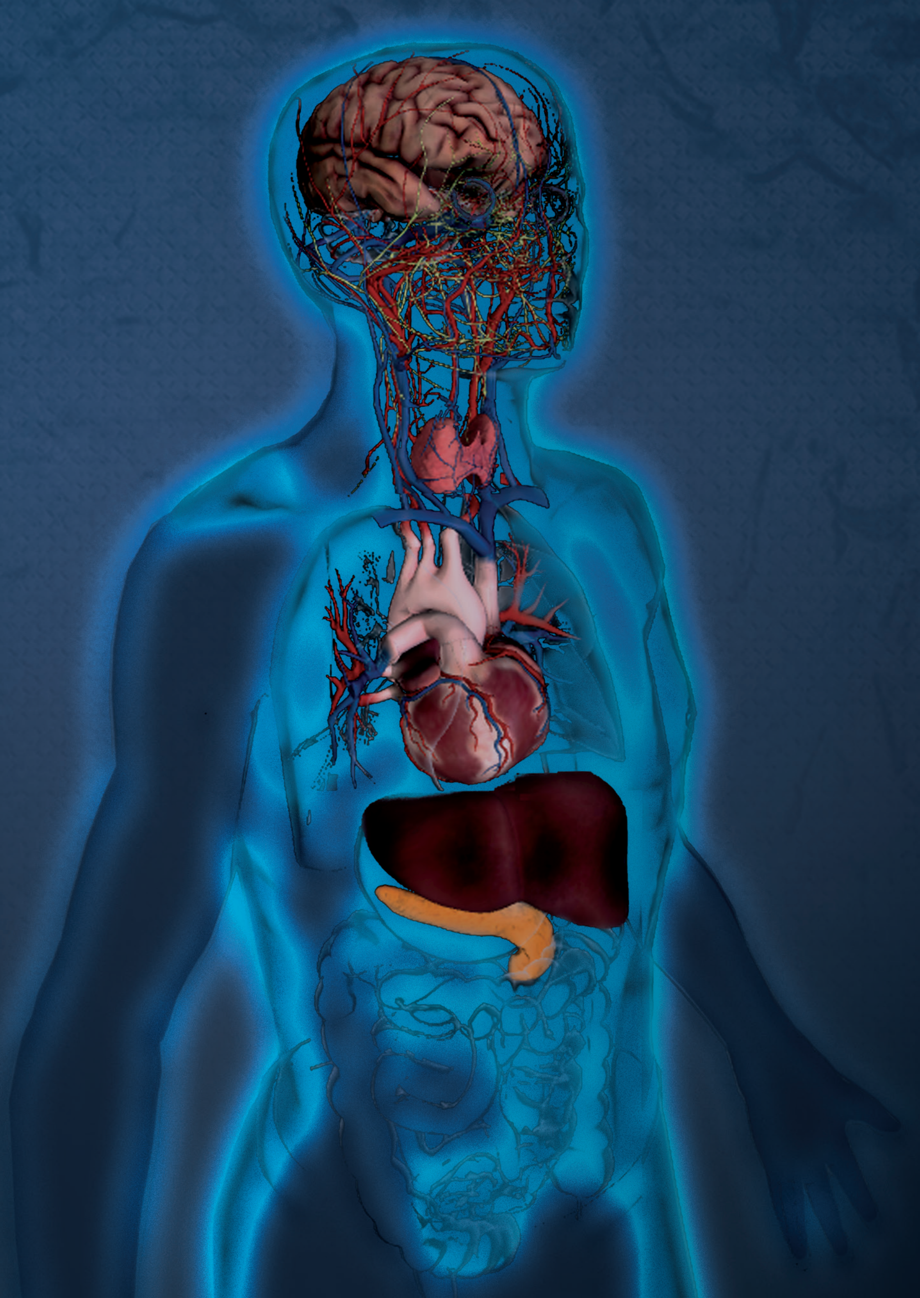

CHAPTER 2

ACCURACY OF CONTINUOUS GLUCOSE MONITORING MEASUREMENTS IN NORMO-GLYCEMIC INDIVIDUALS

Abimbola A. Akintola
Raymond Noordam
Steffy W. Jansen
Anton J.M. de Craen
Bart E. Ballieux
Christa M. Cobbaert
Simon P. Mooijaart
Hanno Pijl
Rudi G.J. Westendorp
Diana van Heemst

PLoS One. 2015 Oct 7;10(10):e0139973.

ABSTRACT

The validity of continuous glucose monitoring (CGM) is well established in diabetic patients. CGM is also increasingly used for research purposes in normo-glycemic individuals, but the CGM validity in such individuals is unknown. We studied the accuracy of CGM measurements in normo-glycemic individuals by comparing CGM-derived versus venous blood-derived glucose levels and measures of glycemia and glycemic variability.

In 34 healthy participants (mean age 65.7 years), glucose was simultaneously measured every 10 minutes, via both an Enlite® CGM sensor, and in venous blood sampled over a 24-hour period. Validity of CGM-derived individual glucose measurements, calculated measures of glycemia over daytime (09:00h-23:00h) and nighttime (23:00h-09:00h), and calculated measures of glycemic variability (e.g. 24h standard deviation [SD]) were assessed by Pearson correlation coefficients, mean absolute relative difference (MARD) and paired t-tests.

The median correlation coefficient between CGM and venous glucose measurements per participant was 0.68 (interquartile range: 0.40–0.78), and the MARD was 17.6% (SD = 17%). Compared with venous sampling, the calculated measure of glycemia during daytime was 0.22 mmol/L higher when derived from CGM, but no difference was observed during nighttime. Most measures of glycemic variability were lower with CGM than with venous blood sampling (e.g., 24h SD: 1.07 with CGM and 1.26 with venous blood; p-value = 0.004).

In normo-glycemic individuals, CGM-derived glucose measurements had good agreement with venous glucose levels. However, the measure of glycemia was higher during the day and most measures of glycemic variability were lower when derived from CGM.

INTRODUCTION

Continuous glucose monitoring (CGM) is a minimally invasive method that has been approved for ambulant glucose monitoring in patients with diabetes mellitus [(1)]. For the purpose of patient care, the validity of different CGM devices has been studied against glucose measures obtained with another CGM device [(2)], glucometers [(3, 4)], capillary blood [(5, 6)] and venous blood taken at random time points [(7)]. Recently, studies have also been conducted in which CGM glucose measurements were compared with frequently sampled venous blood glucose measurements [(8-11)]. In general, these studies have shown that glucose measurements derived with a CGM device were comparable to venous blood glucose measurements [(8-11)]. For example, the CGM Enlite® provides accurate glucose readings (correct detection of existing or predicted hypo- and hyperglycemia) for up to six consecutive days in diabetic patients when calibrated against capillary glucose three to four times a day [(8)].

In addition to patient care, CGM has also been increasingly used in epidemiological studies in healthy volunteers [(12-14)]. For research, the main advantage of CGM is that the device is portable, easy to use, cost effective, and can be used during normal daily activities. After processing, the device provides information on 24-hour glucose rhythms for up to six consecutive days. From this data, measures of glycemia and glycemic variability can be calculated. However, to date, the validity of the estimates for glycemia and glycemic variability as well as the glucose levels themselves have not been studied in normo-glycemic individuals.

In the present study, we conducted a validation study of glucose measurements obtained with CGM using the Enlite® sensor in normo-glycemic individuals. For this, we studied accuracy of CGM measurements by comparing CGM-derived glucose levels and measures of glycemia and glycemic variability with those obtained from simultaneously sampled venous blood.

MATERIALS AND METHODS

Ethics statement

The Medical Ethical Committee of Leiden University Medical Center approved this study, and all investigations have been conducted according to the principles expressed in the Declaration of Helsinki. Written informed consent was obtained from all study participants.

Study participants

The present study was embedded in the Switchbox Study [15], which was a sub-study of the Leiden Longevity Study (LLS). The LLS was originally designed to investigate genetic and phenotypic biomarkers associated with human longevity. In total, the LLS comprised 2,415 participants (1,671 offspring from nonagenarian siblings and 744 partners thereof). A more detailed description of the study design and recruitment strategy has been described elsewhere [16].

Of these, a subsample of 38 non-diabetic participants underwent 24-hour venous blood sampling. To be included, the participants had to have a fasting glucose level <7 mmol/L, hemoglobin >7.1 mmol/L, a body mass index (BMI) between 19 kg/m2 and 33 kg/m2 and be free of any significant chronic disease. Exclusion criteria that were considered for participation in the 24-hour venous blood sampling included, among others, use of any medication known to influence lipolysis, thyroid function, glucose metabolism, growth hormone secretion or any other hormonal axis, difficulties in inserting and maintaining an intravenous catheter, blood donation within the last two months, smoking and alcohol addiction, and extreme diet therapies, as has been described in more detail elsewhere [17]. Of the 38 participants, 34 had simultaneously measured glucose levels from CGM and venous blood (no CGM data could be uploaded for four participants).

Study and sampling procedure

After an overnight fast of 10-14 hours, a catheter, for the purpose of venous blood sampling, was inserted in the non-dominant hand before the start of the study. Blood sampling started at 09.00h and continued for 24 hours. During this period, 2 ml of blood were collected every 10 minutes in a serum separator (SST)-tube.

During the study period, participants received three standardized meals at three fixed time points (namely, between 09.00h-10.00h, 12.00h-13.00h and 18.00h-19.00h). All meals consisted of 600 kcal Nutridrink (Nutricia Advanced Medical Nutrition, Zoetermeer, the Netherlands). All participants were sampled in the same room with standardized ambient conditions. Participants were not allowed to sleep during the day; lights were turned off between 23.00h to 08.00h to allow the participants to sleep.

Continuous glucose monitoring

Each participant was assigned to a iPro® 2 MiniMed® continuous glucose monitoring System (Medtronic MiniMed Inc., Northridge, CA, USA). The system comprised of (i) a sterile, single use electrode sensor system (ENLiTE®; Medtronic MiniMed Inc., released 2010), inserted into the interstitial fluid, that continuously generates an electrical current proportional to the glucose concentration, (ii) a Sen-serter for sensor insertion, (iii) a iPro2 recorder that digitally stores the average sensor current every 5 minutes, and (iv) a dock wired to a personal computer (PC) with CareLink® iPro, through which data from iPro2 is uploaded through dock to PC with Internet connection to CareLink iPro. The glucose sensor was inserted into the subcutaneous abdominal fat tissue the day before the study, to allow for sensor equilibration and for resolution of any insertion-induced micro-hematoma. This procedure has been validated previously and provides accurate CGM glucose recordings over a longer period [8].

The CGM glucose recordings were retrospectively calibrated using capillary glucose (fingersticks) values from a self- monitored blood glucose (SMBG) meter (Contour ® by Bayer), as specified by the manufacturer [18]. The SMBG values were measured four times during the study, namely before breakfast, before lunch, before dinner, and before sleeping.

At the end of the study, data from the sensor as well as SMBG values were uploaded via internet connection to CareLink iPro (https://carelink.minimed.eu/ipro/hcp/) to calibrate the CGM measurements against the capillary glucose measurements. CGM provides calibrated continuous glucose readings every 5 minutes, which were downloaded and used for analyses.

Processing of venous blood samples

After blood withdrawal, the serum tubes were kept at room temperature to clot and immediately centrifuged when the samples were clotted. Serum was aliquoted into 500µl tubes and promptly stored at -80°C. Glucose levels were measured using fully automated equipment with the Hitachi Modular P800 from Roche Diagnostics (Almere, the Netherlands). Coefficient of variation for measurements ranged between 0.9-3.0%.

Anthropometrics

At the study center, height, weight, body fat percentage, and waist and hip circumference were measured. Weight (in kilograms) was divided by the squared height (in meters) to calculate the body mass index (BMI). The percentage of body fat was measured using a bioelectrical impedance analysis (BIA) meter at a fixed frequency of 50kHz (Bodystat® 1500 Ltd, Isle of Man, British Isles).

Calculations of measures of glycemia and glycemic variability

For the analyses, every other 5-minute CGM glucose measurement was paired with the corresponding 10-minute venous glucose measurement. Individual glucose measurements from CGM and venous blood sampling were first manually checked for unreliable measurements and technical errors and then processed as described below to derive measures of glycemia and glycemic variability.

Measures of glycemia were the 24h mean glucose level (09.00h – 09.00h), and the mean glucose level during daytime (09.00h – 23.00h) and nighttime (23.00h – 09.00h). The analyses during daytime and nighttime were conducted to validate in more detail the CGM during the day (when participants were awake, had food intake, and capillary glucose measurement for calibration were taken) and during the night (when participants were asleep, had no food intake, and no calibration was done).

Measures of glycemic variability were of two classes, namely (i)- indices based on glucose distribution and amplitude of glucose excursions, and (ii) indices based on risk of hypo-/hyperglycemia and quality of glycemic control (19). Indices of glycemic variability that were based on glucose distribution and amplitude of glucose excursions were the 24h standard deviation (SD), the standard deviation within series of 1 hour (SDws1) and of 4 hours (SDws4), the range (maximum – minimum), the interquartile range (IQR), the percentage coefficient of variation (% CV), the continuous overlapping net glycemic action over 1 hour (CONGA1) and over 4 hours (CONGA4) and the mean amplitude of glycemic excursions (MAGE). The SDws1 and SDws4 represent the average standard deviation of every 10-minute measurement over hourly (SDws1) and four- hourly (SDws4) periods of the glucose time series, and permit analysis of changes in variability by time of day (20). CONGA1 and CONGA4 are measures for assessing intra-day variability over hourly (CONGA1) and four- hourly (CONGA4) segments of the glucose time series (21). Except for

MAGE, which was calculated using a MAGE algorithm [22] that is based on the principle of gradual (successive) approximations of glucose peaks and troughs and IQR (75th percentile - 25th percentile), the other aforementioned indices were calculated using the Rodbard macro [23].

Indices based on risk of hypo-/hyperglycemia and quality of glycemic control were the J-index, hypoglycemia index and hyperglycemia index [20]. The J-index is a measure of quality of glycemic control based on mean and SD of all glucose values, and is calculated as J= 0.001 x (mean + SD)2. The hypoglycemia index is the weighted average of hypoglycemia values, calculated using the formula (∑ (LLTR - Glucose)b) / [N x d], where LLTR = Lower Limit of Target Range (we used the default value of 80mg/dL); b= exponent, generally in the range from 1.0 to 2.0 (we used the default value of 2.0); d= scaling factor to permit another form of differential weighting of hypoglycemic and hyperglycemic values (we used the default value of d=30); and N is the total number of observations including hypo-, eu, and hyperglycemic values. The summation for hypoglycemia index was performed for only the glucose values less than 80mg/dL. The hyperglycemia index is the weighted average of hyperglycemic values, calculated using the formula (∑ (Glucose – ULTR)a) / [N x c], where ULTR = Upper Limit of Target Range (we used the default value of 140mg/dL); a= exponent, generally in the range from 1.0 to 2.0 (we used the default value of 1.1); c= scaling factor (we used the default value of c=30); and N is the total number of observations. The summation for hyperglycemia index was performed for only the glucose values greater than 140mg/dL. The exponents a and b, and the scaling factors c and d in the formulas for hypoglycemia and hyperglycemia indices are constants that provide for differential weighting of hypo- and hyperglycemic values.

Statistical analysis

The accuracy of individual glucose measurements was studied by assessing the accuracy within a participant as well as for the whole study population, whereas the accuracy of the measures of glycemia and glycemic variability was assessed only for the study population.

For the analyses on accuracy of individual glucose measurements, we first calculated, per participant, a Pearson correlation coefficient between glucose measurements derived from CGM and venous blood sampling. From these individual Pearson correlation coefficients, we determined the median with the interquartile range. Secondly, we assessed the agreement between glucose measurements derived from CGM and venous blood sampling using Bland-Altman analysis [24]. The limits of agreement were studied by calculating the difference between the two methods ± 1.96 standard deviation of the difference. The Bland-Altman analyses were additionally stratified into daytime and nighttime. We additionally determined the mean absolute relative difference (MARD) of all paired points. MARD was calculated using the formula |CGM glucose - venous glucose|/ venous glucose, as has been previously done in other studies [8, 11]. Furthermore, to explore the MARD values across different glucose ranges within our dataset, we calculated the mean and median Absolute Relative Differences (ARD) after dividing the glucose values into tertiles based on venous glucose values.

The comparison of level of agreement of the per-participant estimates of glycemia and glycemic variability derived from CGM and venous blood sampling were conducted with paired t-tests.

Graphs of 24hour glucose trajectories and Bland-Altman plots were drawn using GraphPad Prism version 5 (GraphPad, San Diego, CA). All statistical analyses were performed using SPSS v.20 for Windows (SPPS Inc., Chicago, IL, U.S.A.). Two-sided p-values below 0.05 were considered statistically significant.

To determine whether the results and correlations obtained were modulated by the presence of one participant with a negative Pearson correlation, sub-analyses were also conducted after excluding this participant (in N=33).

RESULTS

Characteristics of the study population

Characteristics of the study population (N = 34) are presented in Table 1. Summarily, the study population had a mean age of 65.7 years, and comprised of 44% females. Participants had a mean BMI of 25.2 kg/m2, and mean fasted venous glucose of 4.9 mmol/L.

Accuracy of individual glucose measures obtained with CGM.

A total of 4,523 data points derived with CGM were paired with glucose levels from simultaneously obtained venous blood samples. A graphical representation of the average glucose level (CGM and venous blood glucose) per time point is visualized in Figure 1.

TABLE 2.1 | Characteristics of the study population

	N = 34
Female, n (%)	15 (44.1)
Age, years	65.7 (4.8)
Weight, kg	75.5 (13.3)
BMI, kg/m2	25.2 (3.9)
Waist circumference, cm	93.1 (12.2)
Waist: hip ratio	0.90 (0.09)
Fat mass, percentage	30.8 (8.04)
Total lean mass, kg	52.3 (11.6)
Fasted (venous) glucose, mmol/L	4.9 (0.6)

Data represent mean with standard deviation unless stated otherwise.

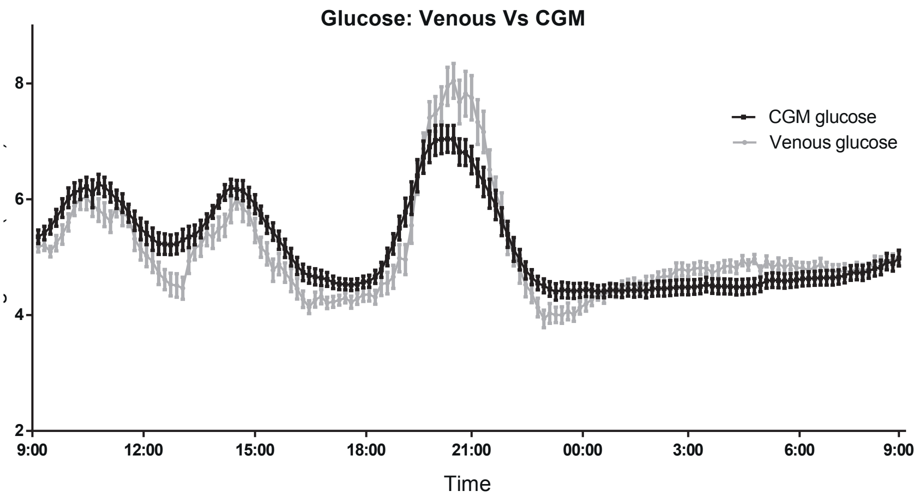

FIGURE 2.1 | Venous- and continuous glucose monitoring (CGM)- derived glucose during 24h period.

Data presented as the mean (SE) glucose level every 10 minutes. In red, the continuous glucose monitoring measurement data. In blue, the venous blood glucose measurement data.

Pearson correlation coefficients between glucose measurements derived with CGM and from venous blood samples are visualized per participant in Figure 2 (individual 24h graphs are presented in Supplementary Figure 1). These Pearson correlation coefficients ranged from -0.35 to 0.93 with a median Pearson correlation of 0.68 (interquartile range: 0.40 – 0.78).

Bland-Altman plots of all the individual glucose measurements are presented in Figure 3. Compared to venous glucose measurements, glucose levels derived with CGM were on average 0.10 mmol/L higher (95% of the individual data points between -2.21 and 2.41 mmol/L) during the 24-hour period. During the day, glucose levels were 0.23 mmol/L (95% of the individual data points between -2.36 – 2.82 mmol/L) higher with CGM, while during the night glucose levels were 0.09 mmol/L lower with CGM (95% of the individual data points between -1.85 – 1.67 mmol/L). The MARD was 17.6% (SD = 17.0%) throughout the 24-hour period, 19.3% (SD = 17.1%) during the day, and 15.3% (SD = 16.5%) during the night. Next, we divided the glucose values into tertiles based on venous glucose values to explore MARD values across different glucose ranges within our dataset. The 24-hour mean (and median) Absolute Relative Difference (ARD) were 22.8 (16.99), 14.45 (11.0) and 15.65 (13.29) for tertile 1 (lowest glucose values), 2 (intermediate glucose values) and 3 (highest glucose values) respectively, as described in supplementary Table 1. These results were similar after excluding the participant with a negative Pearson correlation.

Accuracy of estimates of glycemia and glycemic variability

Agreement between calculated estimates of glycemia and glycemic variability derived from CGM and venous blood data is presented in Table 2. The 24-hour mean glucose level was 0.08 mmol/L (standard error [SE]: 0.08) higher with CGM than with venous blood sampling, which was not statistically significantly different (p-value = 0.35). During daytime, the mean glucose level was 0.22 mmol/L (SE: 0.09) higher with CGM than with venous blood sampling, which was significantly different (p-value = 0.02). No significant difference (p-value = 0.33) in mean nighttime glucose was observed between CGM and venous blood (difference: -0.11 mmol/L; SE: 0.12).

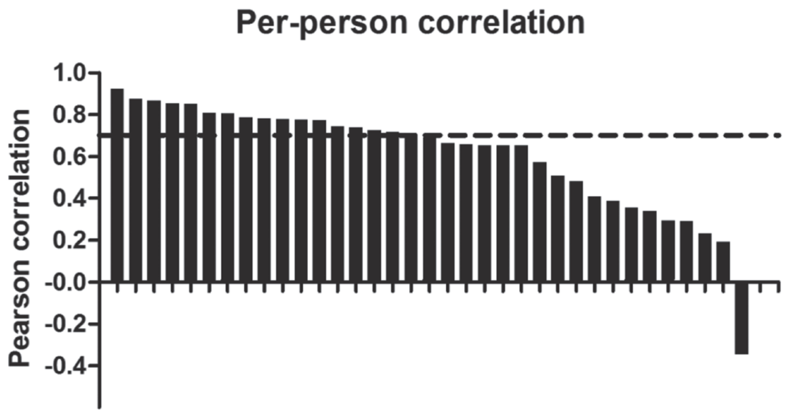

FIGURE 2.2 | Per-person Pearson correlations coefficients between venous- and continuous glucose monitoring (CGM)- derived glucose levels.

Bar chart showing the distribution of the Pearson correlations between paired CGM and venous glucose measurements determined for each of the 34 participants. Dashed line represents the median per-person Pearson correlation.

The 24-hour standard deviation of the glucose levels derived with CGM was 1.07, whereas it was 1.26 with venous blood sampling, which was statistically significantly different (difference: -0.19 [SE: 0.06]; p-value = 0.004). Similar significant results were observed for most other measures of glycemic variability that are based on glucose distribution and amplitude of glucose excursions, namely, SDw1, SDw4, range, % CV, MAGE, CONGA1 and CONGA4, but not for IQR. On the other hand, measures of glucose variability indices that are based on risk and quality of glycemic control did not significantly differ when derived from CGM compared to venous glucose, except for the hyperglycemia index (p-value < 0.001) (Table 2).

Results were similar after exclusion of the participant with a negative Pearson correlation.

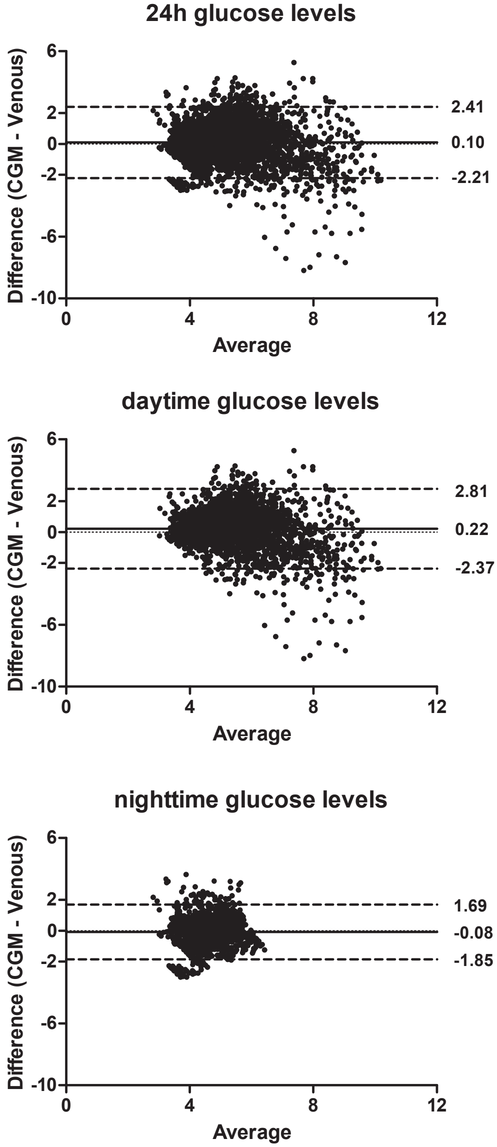

FIGURE 2.3 | Bland-Altman plots of individual glucose measurements

Each dot represents one paired (CGM and venous) glucose measurement (N = 4,523 data points derived from 34 participants). The bias of the measurements (represented as the solid lines) and the ± 1.96 SD (dotted lines) are presented for the measurements obtained (A) over 24 hours (B) during the day (09.00h – 23.00h), and (C) during the night (23.00h - 09.00h).

Table 2.2 | Comparison of estimates of glycemia and glycemic variability

	Mean CGM	Mean venous	Difference (SE)	P-value
Glycemia				
24h glucose	5.18 (0.46)	5.10 (0.35)	0.08 (0.08)	0.35
Daytime glucose (09.00h – 23.00h)	5.61 (0.52)	5.39 (0.43)	0.22 (0.09)	0.02
Nighttime glucose (23.00h - 09.00h)	4.57 (0.62)	4.68 (0.47)	-0.11 (0.12)	0.33
Glycemic variability: Glucose distributions/ excursions				
24h standard deviation	1.07 (0.29)	1.26 (0.36)	-0.19 (0.06)	0.004
SD*ws*1	0.47 (0.09)	0.68 (0.15)	-0.21 (0.02)	<0.001
SD*ws*4	0.72 (0.18)	0.95 (0.26)	-0.23 (0.04)	<0.001
Range	4.45 (1.19)	6.24 (1.72)	-1.79 (0.25)	<0.001
IQR (median (IQR))	1.24 (1.05-1.42)	1.27 (1.00-1.46)		0.354
% Coefficient of Variation	20.9 (6.04)	24.3 (6.67)	-3.39 (1.20)	0.008
MAGE	3.02 (1.02)	3.52 (1.36)	-0.50 (0.22)	0.034
CONGA1	1.50 (0.42)	1.97 (0.61)	-0.47 (0.07)	<0.001
CONGA4	1.57 (0.51)	2.07 (0.66)	-0.50 (0.11)	<0.001
Glycemic variability: Risk and quality of glycemic control				
J- index	0.039 (0.007)	0.041 (0.007)	0.002 (0.007)	0.341
Hypoglycemia index (median (IQR))	0.46 (0.07-2.0)	1.33 (0.35-2.15)		0.17
Hyperglycemia index (median (IQR))	0.003 (0.0-0.04)	0.031 (0.01-0.08)		<0.001

Values are mean (SD) unless otherwise indicated. Abbreviations: CGM, continuous glucose monitoring; SD, standard deviation; SE, standard error; SDws1and SDws4, standard deviation within time series of respectively 1 and 4 hours; CONGA1 and CONGA4, continuous overlapping net glycemic action over respectively 1 and 4 hours; and MAGE, mean amplitude of glycemic excursions.

DISCUSSION

In the present study we assessed the accuracy of CGM-derived glucose levels and of CGM-derived measures of glycemia and glycemic variability in a normo-glycemic study population. The findings were three-fold. First, we observed large variation in the per-person Pearson correlation coefficients of glucose measurements derived with CGM and venous blood glucose measurements. Second, we observed no significant systematic deviation in glucose measurements derived with CGM against glucose measurements derived with venous sampling. However, variation (as assessed by the 1.96 SD intervals in the Bland-Altman plots) was large. And third, we observed that of the calculated measures of glycemia and glycemic variability, the mean glucose level during daytime was higher with CGM, and that most measures of glycemic variability were lower with CGM, especially the glucose variability measures that were based on glucose excursions.

CGM has primarily been used for self-monitoring of blood glucose in patients with diabetes [(25, 26)], and only recently in a number of epidemiological studies [(12-14)]. Although repeated venous blood sampling could be considered as the gold standard to determine glucose rhythms over the day, this technique is too invasive to be used in larger cohort studies. Also, a large number of exclusion criteria need be considered before, for example, older participants (e.g., aged 65 and above) could undergo 24-hour venous blood collection[(17)]. These stringent selection criteria (e.g., lack of any significant chronic disease) will result in a highly selected study population, and increase the risk of selection bias, which decreases generalizability of potential research findings. On the other hand, the CGM device can be used with less stringent selection criteria, and can be used in a home-based setting for up to a week.

The assessment of the validity of the Enlite® sensor against frequently sampled venous blood has been studied before [(8-11)]. The MARD, which is indicative of the direction and extent of bias [(11)], has been previously reported to be 18.3% in subjects with diabetes over a 48-hour period [(11)] and 13.6% in another study over a 6-day period [(8)]. In line, we observed a MARD ranging from 15.25% – 19.15% depending on the time of the day. After dividing the glucose values into tertiles of venous glucose, we found that MARD values were highest in the lowest glucose range, suggesting that the MARD, as a relative error, weighs more errors at lower glucose levels. In addition, studies conducted on newer generation CGMs have reported lower MARD values. For example, a comparative study reported a MARD of

17.9 for Enlite® sensor (released 2010), whereas the FreeStyle Navigator (released 2012 by Abbott Diabetes Care) and G4 Platinum (released 2013 by Dexcom) had MARD values of 12.3 and 10.8 respectively. Thus, MARD values seem dependent on glucose ranges (normo-glycemic versus diabetic range), as well as on the type and generation of CGM sensor.

The accuracy of CGM-derived measures of glycemic variability has not been studied before. Currently, glycemic variability is often monitored, as diabetes complications may be associated with higher glycemic variability [26-28]. We observed that most measures of glycemic variability were lower when derived from CGM data than when derived from venous-blood data, suggesting that measures of glycemic variability were underestimated when calculated using CGM glucose values. Several probable sources of CGM underestimation have been put forth in literature [29-31]. One reason could be distortion due to blood- to-interstitium glucose kinetics, resulting in a time lag/ delay between interstitial fluid and venous blood. In our study, we used the Enlite® CGM sensor which was calibrated with glucose values from a self- monitored blood glucose (SMBG) meter (Contour® by Bayer). Of note, the glucometer measures capillary glucose, which is a compartment different from that from which glucose is measured both by the CGM (interstitial compartment) and by venous sampling (intravascular compartment). Thus, the existence of a physiological delay between blood glucose and interstitial glucose can hinder real- time accurate CGM glucose measurement [31].

A second possible reason could be due to inaccurate sensor calibration [29, 30], which may be affected by sample timing or level of self- monitored glucose used for calibration, or to a drift in time of sensor sensitivity. However, distortion by inaccuracy of the glucometer (Contour® by Bayer) is unlikely in our case, since this device has been previously validated against a reference laboratory glucose measuring instrument [32]. According to that study, the validity of the Contour® blood glucose monitoring system is above that required by the International Organization for Standardization's International standard (ISO 15197:2003) for blood glucose monitoring systems.

Thirdly, underestimation of CGM glucose could be attributed to random zero- mean measurement noise [29]. The measurement noise component appears to decrease day after day, causing inter-day sensor variability. The measurement noise of the CGM is highest in the first day of use and decreases thereafter. Hence, the CGM sensor was inserted the day before venous sampling was initiated in our study.

We observed a large variation in accuracy between individuals, which was reflected in a wide range in per-person Pearson correlation coefficients. In one extreme case, data showed a negative correlation between CGM and venous glucose values. No technical reason was found to explain this negative correlation. Although all participants received the same meals at approximately the same time, there were differences in individual responses, as measured by CGM or venous glucose. During the day, individual glucose values were higher when measured in the interstitial fluid using CGM than in serum (notably 0.23 mmol/L). A similar difference was observed when we calculated the mean glucose level during daytime. However, the variation in the per-person Pearson correlations is not unexpected, as individual differences may exist in how well the CGM calibration algorithm "fits" individual physiology [(4)]. Other reasons for the high variation in per-person Pearson correlation coefficients could include tissue reactions to the implanted sensors (e.g., inflammation, fibrosis, and vessel regression) [(33)]. Also, the implanted glucose sensor could have been placed close to a blood vessel, which has been previously associated with extended (average 7-15 minute) delay in interchange between interstitial fluid and venous blood [(33)]. These factors could contribute to a larger discordance in CGM and venous glucose values when matched based on time points. Nevertheless, despite the inclusion of one participant with a negative correlation in the analysis, our results (e.g. MARD, median Pearson correlation) are comparable to previously published studies [(8, 11)]. Furthermore, across the whole study population, we observed good agreement between individual glucose levels measured in serum and in interstitial fluid in normo-glycemic participants.

Compared to daytime venous glucose, we observed a higher mean CGM glucose during the day. This should be taken into account when the purpose of a study involves a cut-off determined on the basis of CGM data, as this could influence the results- the higher daytime glucose could result in a number of false-positives. Moreover, the higher standard deviation that we observed could affect the statistical power of a study. A consequence of a higher standard deviation with CGM is that CGM studies would need to be conducted with larger sample sizes than studies with venous blood sampling (figure 4). For example, when the expected differences between two groups is 0.25 mmol/L in 24-hour mean glucose level, a study using venous blood sampling would comprise 31 participants in each group, whereas a study using CGM would comprise 53 participants in each group.

A limitation of our study is that it has a limited sample size (N = 34), which is somewhat smaller than the other conducted validation studies in this field [(8-11)]. Another potential limitation is that venous glucose was measured in serum samples. However, the samples were centrifuged immediately after clotting, thus preventing glycolysis. The main strength is that the data with both sampling methods comprise glucose levels collected over a 24-hour period. This way, the validity of the sampling method could be studied in more detail. Furthermore, within the 24-hour study period, environment, physical activity, sleeping and feeding conditions were standardized. The study population was therefore more homogenous.

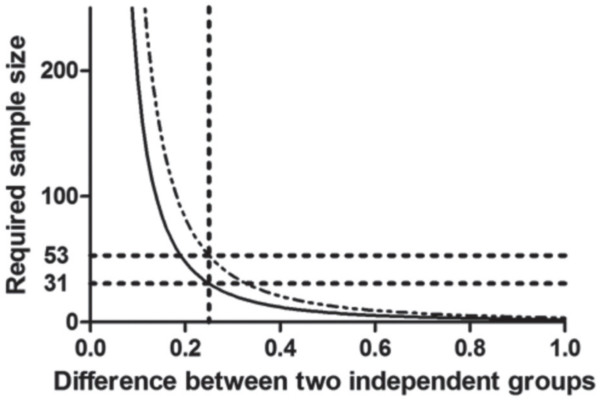

FIGURE 2.4 | Sample size calculations.

Figure depicts the sample sizes required to observe a statistically significantly difference between two study groups (alpha = 0.05; power = 0.8). The vertical dashed line depicts a hypothetical expected difference between two study groups. The horizontal dashed lines depict the number of participants required in both study groups to observe this difference. Dotted curved line represents CGM whereas the solid curved line represents venous blood sampling.

In conclusion, there is good agreement between individual glucose measurements derived with CGM and venous blood. However, the accuracy of measures of glycemia and most measures of glycemic variability deviated significantly, a fact that needs to be taken into account in future studies using CGM.

Supporting information

The Supplementary Material for this article can be found online at: http://journals.plos.org/plosone/article?id=10.1371/journal.pone.0139973#sec020

Supplementary Figure 1. Per- person graphs of 24-hour glucose rhythms. Supplementary Table 1. Mean and median absolute relative difference in tertiles of venous glucose.

REFERENCES

1. Standards of medical care in diabetes--2014. Diabetes Care. 2014;37 Suppl 1:S14-80.
2. Kerssen A, De Valk HW, Visser GH. Validation of the Continuous Glucose Monitoring System (CGMS) by the use of two CGMS simultaneously in pregnant women with type 1 diabetes mellitus. Diabetes technology & therapeutics. 2005;7(5):699-706; discussion 7-9.
3. Davison LJ, Slater LA, Herrtage ME, Church DB, Judge S, Ristic JM, et al. Evaluation of a continuous glucose monitoring system in diabetic dogs. The Journal of small animal practice. 2003;44(10):435-42.
4. Gross TM, Bode BW, Einhorn D, Kayne DM, Reed JH, White NH, et al. Performance evaluation of the MiniMed continuous glucose monitoring system during patient home use. Diabetes technology & therapeutics. 2000;2(1):49-56.
5. Dobson L, Sheldon CD, Hattersley AT. Validation of interstitial fluid continuous glucose monitoring in cystic fibrosis. Diabetes Care. 2003;26(6):1940-1.
6. Sachedina N, Pickup JC. Performance assessment of the Medtronic-MiniMed Continuous Glucose Monitoring System and its use for measurement of glycaemic control in Type 1 diabetic subjects. Diabetic medicine : a journal of the British Diabetic Association. 2003;20(12):1012-5.
7. Beardsall K, Vanhaesebrouck S, Ogilvy-Stuart AL, Vanhole C, VanWeissenbruch M, Midgley P, et al. Validation of the continuous glucose monitoring sensor in preterm infants. Archives of disease in childhood Fetal and neonatal edition. 2013;98(2):F136-40.
8. Bailey TS, Ahmann A, Brazg R, Christiansen M, Garg S, Watkins E, et al. Accuracy and acceptability of the 6-day Enlite continuous subcutaneous glucose sensor. Diabetes technology & therapeutics. 2014;16(5):277-83.
9. Bay C, Kristensen PL, Pedersen-Bjergaard U, Tarnow L, Thorsteinsson B. Nocturnal continuous glucose monitoring: accuracy and reliability of hypoglycemia detection in patients with type 1 diabetes at high risk of severe hypoglycemia. Diabetes technology & therapeutics. 2013;15(5):371-7.
10. Damiano ER, El-Khatib FH, Zheng H, Nathan DM, Russell SJ. A comparative effectiveness analysis of three continuous glucose monitors. Diabetes Care. 2013;36(2):251-9.
11. Damiano ER, McKeon K, El-Khatib FH, Zheng H, Nathan DM, Russell SJ. A comparative effectiveness analysis of three continuous glucose monitors: the navigator, g4 platinum, and enlite. Journal of diabetes science and technology. 2014;8(4):699-708.

12. Fabricatore AN, Ebbeling CB, Wadden TA, Ludwig DS. Continuous glucose monitoring to assess the ecologic validity of dietary glycemic index and glycemic load. The American journal of clinical nutrition. 2011;94(6):1519-24.
13. Pearce KL, Noakes M, Wilson C, Clifton PM. Continuous glucose monitoring and cognitive performance in type 2 diabetes. Diabetes technology & therapeutics. 2012;14(12):1126-33.
14. Wijsman CA, van Heemst D, Hoogeveen ES, Slagboom PE, Maier AB, de Craen AJ, et al. Ambulant 24-h glucose rhythms mark calendar and biological age in apparently healthy individuals. Aging Cell. 2013;12(2):207-13.
15. Jansen SW, Akintola AA, Roelfsema F, van der Spoel E, Cobbaert CM, Ballieux BE, et al. Human longevity is characterised by high thyroid stimulating hormone secretion without altered energy metabolism. Scientific reports. 2015;5:11525.
16. Westendorp RG, van Heemst D, Rozing MP, Frolich M, Mooijaart SP, Blauw GJ, et al. Nonagenarian siblings and their offspring display lower risk of mortality and morbidity than sporadic nonagenarians: The Leiden Longevity Study. Journal of the American Geriatrics Society. 2009;57(9):1634-7.
17. Akintola AA, Jansen SW, Wilde RBP, Hultzer G, Rodenburg R, van Heemst D. A simple and versatile method for frequent 24h blood sample collection in healthy older adults. MethodsX. 2015(0):33-8.
18. Medtronic. CGM sensor calibration. http://wwwmedtronicdiabetescom/customer-support/sensors-and-transmitters-support/calibration-sensor. site opened 30-04-2015.
19. Fabris C, Facchinetti A, Sparacino G, Zanon M, Guerra S, Maran A, et al. Glucose variability indices in type 1 diabetes: parsimonious set of indices revealed by sparse principal component analysis. Diabetes technology & therapeutics. 2014;16(10):644-52.
20. Rodbard D. Interpretation of continuous glucose monitoring data: glycemic variability and quality of glycemic control. Diabetes technology & therapeutics. 2009;11 Suppl 1:S55-67.
21. McDonnell CM, Donath SM, Vidmar SI, Werther GA, Cameron FJ. A novel approach to continuous glucose analysis utilizing glycemic variation. Diabetes technology & therapeutics. 2005;7(2):253-63.
22. the Institute of Diabetes GK, Karlsburg/Germany. KADIS® DCC Version 0.4.1.1. URL: http://wwwdiabetes-service-centerde/en/downloadsphp?lang=en, downloaded 13-08-2015.
23. Rodbard D. New and improved methods to characterize glycemic variability using continuous glucose monitoring. Diabetes technology & therapeutics. 2009;11(9):551-65.

24. Bland JM, Altman DG. Statistical methods for assessing agreement between two methods of clinical measurement. Lancet. 1986;1(8476):307-10.
25. Kohnert KD, Heinke P, Fritzsche G, Vogt L, Augstein P, Salzsieder E. Evaluation of the mean absolute glucose change as a measure of glycemic variability using continuous glucose monitoring data. Diabetes technology & therapeutics. 2013;15(6):448-54.
26. Tsang MW, Mok M, Kam G, Jung M, Tang A, Chan U, et al. Improvement in diabetes control with a monitoring system based on a hand-held, touch-screen electronic diary. Journal of telemedicine and telecare. 2001;7(1):47-50.
27. Sonksen PH, Judd SL, Lowy C. Home monitoring of blood-glucose. Method for improving diabetic control. Lancet. 1978;1(8067):729-32.
28. Wu JT. Review of diabetes: identification of markers for early detection, glycemic control, and monitoring clinical complications. Journal of clinical laboratory analysis. 1993;7(5):293-300.
29. Facchinetti A, Del Favero S, Sparacino G, Castle JR, Ward WK, Cobelli C. Modeling the glucose sensor error. IEEE transactions on bio-medical engineering. 2014;61(3):620-9.
30. Facchinetti A, Del Favero S, Sparacino G, Cobelli C. Model of glucose sensor error components: identification and assessment for new Dexcom G4 generation devices. Medical & biological engineering & computing. 2014.
31. Lunn DJ, Wei C, Hovorka R. Fitting dynamic models with forcing functions: application to continuous glucose monitoring in insulin therapy. Statistics in medicine. 2011;30(18):2234-50.
32. Harrison B, Leazenby C, Halldorsdottir S. Accuracy of the CONTOUR(R) blood glucose monitoring system. Journal of diabetes science and technology. 2011;5(4):1009-13.
33. Klueh U. Analysis: on the path to overcoming glucose-sensor-induced foreign body reactions. Journal of diabetes science and technology. 2013;7(2):452-4.

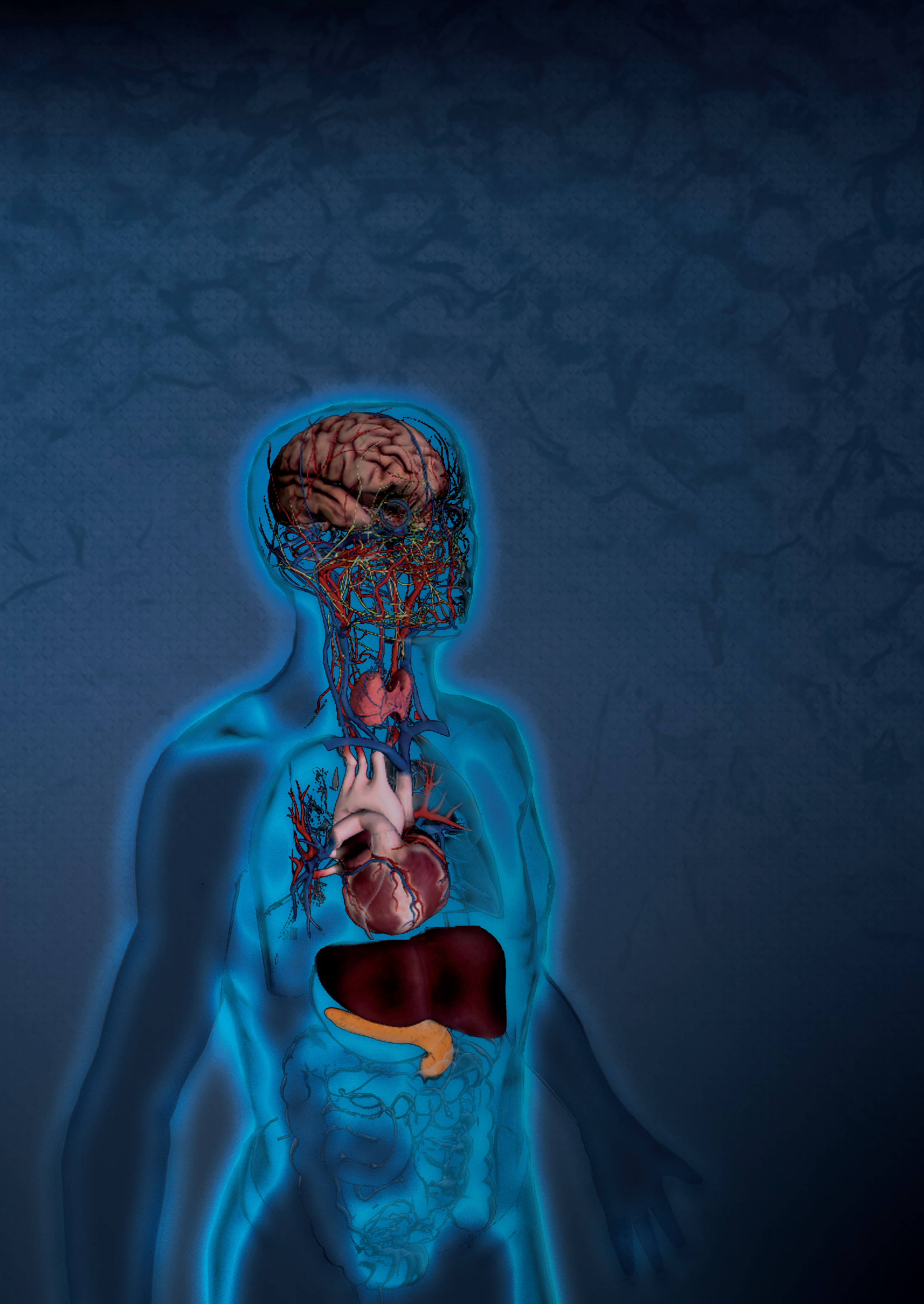

CHAPTER 3

PARAMETERS OF GLUCOSE METABOLISM AND THE AGING BRAIN: A MAGNETIZATION TRANSFER IMAGING STUDY OF BRAIN MACRO- AND MICRO-STRUCTURE IN OLDER ADULTS WITHOUT DIABETES

Abimbola A. Akintola
Annette van den Berg
Irmhild Altmann-Schneider
Steffy W. Jansen
Mark A. van Buchem
P. Eline Slagboom
Rudi G. Westendorp
Diana van Heemst
Jeroen van der Grond

PLoS One. 2015 Oct 7;10(10):e0139973.

ABSTRACT

Given the concurrent, escalating epidemic of Diabetes mellitus and neurodegenerative diseases, two age- related disorders, we aimed to understand the relation between parameters of glucose metabolism and indices of pathology in the aging brain. From the Leiden Longevity Study, 132 participants (mean age 66 years) underwent a 2-hour oral glucose tolerance test to assess glucose tolerance (fasted and area-under-the-curve (AUC) glucose), insulin sensitivity (fasted and AUC insulin, and homeostatic-model-assessment-of-insulin-sensitivity (HOMA-IS)) and insulin secretion (insulinogenic index). 3Tesla brain MRI was used to detect macro-structural damage (atrophy, white matter hyper intensities, infarcts and/or micro-bleeds), and Magnetization Transfer Imaging (MTI) to detect loss of micro-structural homogeneity that remain otherwise invisible on conventional MRI.

Macro-structurally, higher fasted glucose was significantly associated with white matter atrophy ($P=0.028$). Micro-structurally, decreased MTR peak height in gray matter was associated with higher fasted insulin ($P=0.010$), AUCinsulin ($P=0.001$), insulinogenic index ($P=0.008$) and lower HOMA-IS index ($P<0.001$). Similar significant associations were found for white matter. Thus, while higher glucose was associated with macro-structural damage, impaired insulin action was associated more strongly with reduced microstructural brain parenchymal homogeneity. These findings offer some insight into the association between different parameters of glucose metabolism (impairment of which is characteristic of Diabetes mellitus) and brain aging.

INTRODUCTION

The rising prevalence of type 2 Diabetes and neurodegenerative disease over the past several decades has made it of critical importance to understand the relation of glucose and insulin with the aging brain. The prevalence of type 2 Diabetes steadily increases with age, with estimates suggesting that more than half of individuals older than 65 years have either diabetes or pre-diabetes [(1)]. Diabetes and pre-diabetic states, characterized by impairments in glucose, insulin and insulin sensitivity, are known to be risk factors for cognitive decline, mild cognitive impairment and dementia [(1, 2)]. It is also known that higher glucose levels, in the absence of (pre) diabetes, are associated with increased risk of accelerated cognitive decline [(3)], or dementia [(4)] in older persons. Furthermore, there is a surge of new information pointing towards high circulating insulin and insulin resistance as mediators of neurodegenerative brain diseases [(5, 6)]. It however remains unclear what the association is of 'normal' glucose and insulin (glucose and insulin levels within the population reference range), with macro- and micro- structural brain changes in older persons without diabetes.

Existing literature has demonstrated a decrease in total brain volume in relation to diabetic and pre-diabetic states in late middle age [(7)]. Besides these macro-structural changes however, microstructural changes may possibly occur in normal appearing brain tissue in relation to glucose and insulin, serving as indices of brain pathology. These microstructural brain tissue changes, which are beyond the spatial resolution of the conventional MRI, can be detected with magnetization transfer (MT) imaging (MTI) [(8)]. MTI can also detect differences in the degree of tissue destruction in macro-structural lesions (cerebral atrophy, white matter hyper-intensities, lacunar infarcts or cerebral micro- bleeds in the white matter). MTI is based on the exchange of magnetization between protons bound to macromolecules and protons of free water molecules inside tissue. The MT ratio (MTR), which reflects the scale of this exchange, has been shown to decrease in the presence of brain tissue damage due to pathology or aging [(9, 10)]. MTR is calculated per voxel with subsequent generation of a histogram per region of interest, from which mean MTR and MTR peak height can be determined. The highest peak of each histogram is the MTR peak height, and is defined as the number of voxels with the most frequent MTR value. The mean MTR is defined as the average of the MTR value of all voxels in the region(s) of interest, as depicted in Figure 1. The peak height of a MTR histogram represents the uniformity within the region of interest. Both mean MTR and peak height reflect different aspects of MTR, and they may show different sensitivity in detecting structural changes in the brain. Specifically, MTR peak height has been suggested to be a relatively specific quantitative measure of microstructural brain parenchymal abnormalities, including myelin content and axonal numbers [(11)]. A lower brain tissue MTR peak height indicates loss of homogeneity of brain tissue [(12)] and is observed in brain parenchymal abnormalities that develop with aging or disease.

The aim of the present study was to investigate the association between parameters of glucose metabolism and three indices of brain pathology, namely- gray and white matter parenchymal volumes and atrophy, macroscopic brain damage, and micro-structural integrity. Parameters of glucose metabolism were derived from Oral Glucose Tolerance Test (OGTT) [(13)], and included measures of glucose tolerance, insulin sensitivity and of pancreatic β-cells secretory capacity. Macro-structural brain parameters were measured using MRI, and included presence and number of microbleeds, lacunar infarcts and/ or volume of white matter hyperintensities. Micro-structural parameters included quantification of homogeneity of brain parenchyma; including axonal and myelin integrity, as measured using MTI- derived mean MTR and peak height.

MATERIALS AND METHODS

Subjects were included from the Leiden Longevity Study (LLS), which was setup to investigate determinants and pathways associated with healthy aging and longevity, as previously described [(14)]. A total of 421 Caucasian families were included and regarded as enriched for familial longevity if at least two long-lived siblings were alive and fulfilled the age-criterion of ≥ 89 years for males or ≥ 91 years for females. Sex-specific age-criteria were used due to the higher life expectancy of females compared to males. No selection criteria on health or demographic characteristics were applied. Offspring of these long-lived nonagenarians were also included, having inherited on average 50% of the genetic propensity of their long-lived parent. Partners of these offspring, with whom they have shared the same socio-economic and geographical environment for decades and who are of a similar age, were also enrolled. In total, 2415 offspring and partners were included in LLS.

Of the 2415 subjects included in LLS, a random subset of 370 underwent an MRI scan of the brain, as had been previously described [15]. Of the 370 subjects, 132 non-diabetic subjects (75 offspring and 57 partners, comprising 49 couples) also underwent OGTT. Therefore, a total of 132 non-diabetic subjects with reliable, complete OGTT, brain MRI and MTI data were included in this study. These participants had no known history of dementia, were free of memory complaints, and had never visited a memory clinic. Furthermore, the participants underwent three cognitive tests- Stroop Color Word test (Stroop test), to test for cognitive flexibility and executive function; Digit Symbol Substitution Test (DSST), to evaluate attention and processing speed; and 15-Picture Word Learning Test (15- PLT), to test for immediate and delayed memory, as had been earlier described [16]. For Stroop test, subjects were asked to read a color name, which was displayed in a color different from the color that it actually names. The outcome parameter was the time (seconds) needed to complete the test; a higher score indicates worse performance. For the DSST, the participants had to match certain digits with letters according to a provided key. Outcome parameter was the number of correct digit-symbol combinations within 90s. For 15-PLT, fifteen pictures were successively presented at a rate of one per two seconds after which the subject was asked to recall as many pictures as possible. This procedure was carried out three times (PLT-1, PLT-2 and PLT-3). After 20 minutes, delayed recall was tested. Outcome parameters were the number of correct pictures after each trial for PLT-immediate (immediate recall) and after 20 min for PLT-delayed (delayed recall).

The Medical Ethical Committee of the Leiden University Medical Centre approved the study and written informed consent was obtained from all participants.

Ogtt- derived parameters of glucose metabolism

In the morning after an overnight fast of at least 10 hours, an OGTT was performed with a 75g glucose load per 300mL of water. Venous blood samples were withdrawn at 0, 30, 60, and 120 minutes after oral ingestion of the glucose load. Parameters derived from the OGTT included fasted glucose and area under the curve (AUC) for glucose (AUCglucose), which are measures of glucose tolerance; fasted insulin, AUCinsulin, and HOMA-IS, which are measures of insulin action and sensitivity [17]; and insulinogenic index [18] which is a measure of pancreatic Beta cell secretory capacity. AUC for glucose (AUCglucose) and insulin (AUCinsulin) were calculated using the trapezoid formula. The glucose and insulin curve was first divided into a number of strips of equal width. Then, the area of the trapezium formed approximated the area of each strip. The sum of these approximations gave the final numerical result of the area under the glucose (AUCglucose) and insulin (AUCinsulin) curves, taking into account the measurements themselves and the time distance between the measurements [(19)]. HOMA-IS was calculated by dividing 22.5 by the product of the fasting levels of serum insulin (in mU/L) and glucose (in mmol/L) (17). Insulogenic index was calculated by dividing increments of insulin at 30 minutes compared to fasting values by the corresponding increment at 30 minutes of glucose levels compared to fasted glucose values[(18)].

Biochemical analysis

All serum measurements were performed using fully automated equipment. For glucose, the Hitachi Modular P 800 from Roche (Almere, the Netherlands) was used, with coefficient of variation (CV) less than 5%. For insulin levels, the Immulite 2,500 from DPC (Los Angeles, CA) was used, with CV of less than 8%.

Brain MRI study

MRI acquisition

All imaging were performed on a whole body MR system operating at 3Tesla field strength (Philips Medical Systems, Best, The Netherlands). Three- dimensional (3D) T1-weighted (repetition time 9.7ms, voxel size 1.17×1.17×1.4 mm, covering the entire brain, acquisition time ≈5 minutes), T2-weighted (repetition time 4200ms, matrix size 448×320, 40 transverse slices with slice thickness of 3.6 mm, covering the entire brain), fluid attenuated inversion recovery (FLAIR, repetition time 11 000ms, matrix size 320×240, 25 transverse slices with slice thickness of 5 mm covering the entire brain) and T2*-weighted images (repetition time 45ms, field of view 250×175×112 mm) and MTI images were acquired. MTI was performed with the following parameters: TR = 100 ms, TE = 11 ms, FA = 9°, FOV = 224 × 180 × 144 mm, matrix size 224 × 169, and 20 slices with a 7 mm thickness.

Image processing and analysis

Using the Functional MRI of the Brain (FMIRB) Software Library (FSL) tools, the various analytical techniques and tools that were used for processing and analysis of the MRI scans are described below:

Brain volumes

Whole brain, gray matter and white matter volumes were calculated using the FSL-tool Structural Image Evaluation, using Normalization, of Atrophy (SIENAX) [(20)]. SIENAX extracted brain and skull images from the single whole-head input data [(21)]. Thereafter, tissue-type segmentation with partial volume estimation was performed using FMRIB's automated segmentation tool (FAST), and total volume of brain tissue, including separate estimates of volumes of gray matter and white matter were obtained. [(22)] Additionally, hippocampal volume was calculated using the FMRIB's Integration Registration and Segmentation Tool (FIRST), as has been previously described [(15)].

Brain atrophy

Atrophy was defined as the difference between intracranial and brain volume divided by intracranial volume multiplied by hundred percent. Using FSL, an estimate for the total intracranial volume was obtained by linearly aligning each subject brain to the MNI152 space and computing the inverse of the determinant of the affine matrix.

White matter hyper-intensities, lacunar infarcts and cerebral micro-bleeds

Medical Image Processing, Analysis, and Visualization (MIPAV) software was used to visualize the MRI scans. WMHs and lacunar infarcts were evaluated using FLAIR, T2-weighted, and 3-D T1-weighted images. Analysis was done blinded to age, sex and subject identity.

White matter hyper-intensities (WMHs) were defined as areas within the cerebral white matter with increased signal intensity on both FLAIR and T2-weighted images, without mass effect (i.e. the increased signal intensities were not secondary to pushing or displacing by surrounding tissue). Measurement of the WMH volume was carried out using the automated method, whereby 3DT1-weighted images were skull stripped [(23)] and the FLAIR and 3DT1 image were co-registered in order to create a brain extracted FLAIR image [(21)]. This brain extracted FLAIR image was subsequently affine-registered to MNI152 standard space using the FMRIB's Linear Image Registration Tool. A conservative MNI152 standard space white matter mask was used to extract the white matter from the FLAIR image. Finally, after excluding the cerebellum and brainstem, a threshold was set to identify which white matter voxels were hyperintense, followed by manually checking and editing for quality control.

Lacunar infarcts were defined as parenchymal defects within the cerebral white matter not extending into the cortical gray matter, with signal intensity centrally corresponding to that of cerebral spinal fluid on all three imaging sequences, surrounded by a rim of increased signal intensity on FLAIR [(24)]. Lacunar infarct diameter was defined to be >2 mm. To distinguish lacunar infarcts from normal dilated perivascular spaces (Virchow-Robin-Spaces), hyper- intensities within the lower one-third of the corpus striatum of the basal ganglia and a diameter of < 2 mm were excluded [(25)].

Cerebral micro-bleeds (CMBs) were defined as round focal areas of signal void on T2-weighted images, which increased in size on T2*-weighted images (blooming effect) [(26)]. Thus, CMBs can be distinguished from look-alikes such as vascular flow voids. Symmetric hypointensities in the basal ganglia were disregarded, as they are likely to represent calcifications or non-hemorrhagic iron deposition [(26)].

MTI data processing

The individual 3DT1-images were skull stripped using BET (brain extracting tool) and segmented using FAST (FMRIB's automated segmentation tool), resulting in individual brain masks for white matter and cortical gray matter. Subsequently non-saturated (M0) and saturated images were registered to the T1 image, using FMRIB's linear image registration tool (FLIRT). Registration matrices from the previous step were used to co-register the non-saturated M0 images and the individual brain masks for gray and white matter to create separate gray and white matter MTR maps. To correct for possible partial volume effects, an eroded mask of these segmentations was created by removing one voxel in plane for both volumes of interest (VOIs). Individual MTR maps were calculated voxel by voxel following the equation MTR = (M0-M1)/M0 and MTR histograms were generated for both VOIs. Mean MTR, MTR peak height, corrected for the size of the VOI, and MTR peak location were calculated from each MTR histogram. The mean of the MTR value of all voxels in the histogram is the mean MTR, and the highest peak of each histogram is the MTR peak height, as depicted in Figure 1.

For the voxel-based analysis of gray matter, the MTR GM maps were aligned to MNI standard space using non-linear transformation [(27)] and averaged to create a reference template for MTR images. Then, all individual gray matter MTR maps were non-linearly registered to this template, divided by the Jacobian of the warp field and smoothed with an isotropic Gaussian kernel with a sigma of 3 mm [(28)].

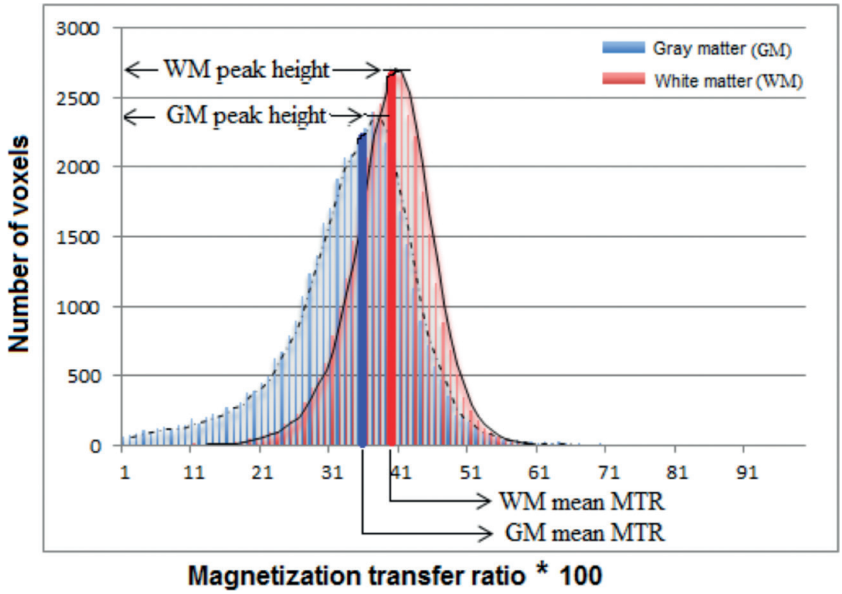

FIGURE 3.1 | MTR histogram of gray and white matter showing mean MTR and MTR peak height.

MTR histograms of both gray matter (in blue) and white matter (in red) with trend lines (moving averages). The MTR peak height, the highest peak of each histogram, is defined as the number of voxels with the most frequent MTR value. The mean MTR, shown as the thick vertical blue line (for gray matter) and red line (white matter) is defined as the average of the MTR value of all voxels in the region(s) of interest.

Statistical analyses

Analyses were conducted in a three-step approach. First, we assessed the association between OGTT- derived parameters of glucose metabolism and brain atrophy. Secondly, we investigated the association between OGTT- derived parameters and macroscopic brain damage (cerebral microbleeds, lacunar infarcts and volume of white matter hyperintensities). Thirdly, we assessed the relation between OGTT- derived parameters and brain micro-structural integrity.

Data analysis was done using Statistical Package for Social Sciences (SPSS) software for windows (version 20.0). Unless otherwise stated, data are presented as mean with standard deviation (SD). Distributions of continuous variables were examined for normality, logarithmically transformed when appropriate, and used in calculations. Serum insulin levels (fasted and AUCinsulin) and HOMA- IS were logarithmically transformed with resultant normalization of their skewed distribution. Geometric means are reported for transformed variables. Linear regression model was used to investigate the associations between OGTT- derived parameters, gray and white matter atrophy and MR brain tissue markers for microstructural integrity. The initial analyses were adjusted for age, sex and descent (Leiden longevity offspring/ partner status). Extended models further included smoking status, BMI, use of anti-hypertensive, and use of lipid lowering agents. Statistical significance was defined as $P < 0.05$.

For MRI data, voxel wise analysis statistics was carried out with FSL randomise using permutation-based non-parametric testing (5000 permutations). Threshold-Free Cluster Enhancement was used to optimize sensitivity to different shapes and sizes of MRI signals, to separate true signals from noise [(29)], with a significance level set at $P < 0.05$, controlled for Family Wise Error rate. Age and gender were inserted as covariates in the model.

RESULTS

Characteristics of the study subjects are summarized in table 1. The mean age of the subjects was 66 years (SD 6.6); 62 (47%) were males and 70 (53%) were females. Medical history showed that 29% had hypertension, 22% used anti- hypertensive medication(s), 14% used lipid-lowering drugs, 1% had had a previous CVA, and 1% had had a previous myocardial infarction. All OGTT- derived parameters were within normal reference range. Table 1 also shows the mean gray and white matter volumes and atrophy, and the mean MTI parameters of the subjects. The mean time needed to complete the Stroop test was 48 seconds, while there was an average of 47 correct answers for the DSST. Mean number of correct pictures for 15-PLT immediate and delayed recall were 10 and 11 respectively (Table 1). From the cross-sectional data, no significant correlation was found between the cognitive tests, which are a measure of functional brain integrity, and MTR peak height, which is a measure microstructural brain parenchymal tissue homogeneity; nor with white matter hyper-intensities, lacunar infarcts or cerebral micro-bleeds (data not shown).

TABLE 3.1 | Description of study subjects

Characteristics	N=132
Demographics	
Men, n (%)	62 (47)
Age in years	66 (6.6)
BMI in kg/m^2	26 (4)
Current smoking, n (%)	11 (8)
Medical History	
Myocardial infarct, n (%)	1 (0.8)
Hypertension, n (%)	29 (22)
Use of anti- hypertensive medications, n (%)	37 (28)
CVA, n (%)	1 (0.8)
Use of lipid lowering medications, n (%)	14 (11)
OGTT- derived characteristics	
Fasted glucose in mmol/L	5.1 (0.6)
AUC glucose in mmol/L	14 (4)
Fasted Insulin in pmol/L, median (25th , 75th percentile)	42 (28, 73)
AUC Insulin, median (25th , 75th percentile)	94 (64, 139)
HOMA-IS index, median (25th , 75th percentile)	-1.5 (-0.7, -2.4)
Insulinogenic Index, median (25th , 75th percentile)	13 (7, 20)
HbA1c in % (mmol/mol)	5.2 (33)
Cognitive tests results	
Digit Symbol Substitution Test, correct answers	46.5 (10)
Stroop test, seconds	48 (13)
15-PLTi, correct pictures	10 (2)
15-PLTd, correct pictures	11 (2)
Brain volumes in cm^3	
White matter	541 (57)
Gray matter	542 (36)
Brain atrophy in %	
Whole brain	24.1 (3.4)
White matter	2.8 (5.4)
Gray matter	20.9 (4.5)
Mean magnetization transfer ratio	
White matter	0.385 (0.010)
Gray matter	0.333 (0.097)
Peak height, pixel count x 10^3	
White matter	117 (24)
Gray matter	74 (12)
Macro-structural characteristics	
White matter hyper intensities n (%)	119 (90)
Lacunar infarcts n (%)	5 (3.8)
Cerebral micro-bleeds n (%)	14 (11)

Values are means (SD, standard deviation), unless otherwise stated. Age refers to age at MRI examination. BMI: body mass index; CVA: cerebrovascular accident; OGTT: Oral glucose tolerance test. AUC: area under the curve; HOMA-IS: Homeostatic model assessment of insulin sensitivity. 15-PLTi: 15- Picture Learning Test -immediate recall; 15-PLTd: 15- Picture Learning Test - delayed recall.

Parameters of glucose metabolism and atrophy

We assessed the association of OGTT- derived parameters of glucose metabolism with gray matter, white matter and hippocampal atrophy. Parameters of glucose metabolism included measures of glucose tolerance (fasted glucose and area under the glucose curve (AUCglucose)), measures of insulin sensitivity (fasted insulin, area under the insulin curve (AUCinsulin) and homeostatic model assessment of insulin sensitivity (HOMA-IS) index) and a measure of pancreatic β-cells secretory capacity (insulinogenic index). As shown in Table 2, higher fasted glucose was associated with white matter atrophy (β= -0.189, P= 0.028). No association was found between any of OGTT- derived parameters and hippocampal atrophy (data not shown) or gray matter atrophy (Table 2).

Parameters of glucose metabolism and macroscopic brain damage

The associations of measures of glucose tolerance, measures of insulin action and insulinogenic index with macroscopic brain damage were investigated (data not shown). Indices of macroscopic brain damage included presence and number of microbleeds, lacunar infarcts and/ or volume of the white matter hyperintensities, as measured using MRI. Fasted glucose was inversely associated with number of cerebral microbleeds (β= -0.214, R^2= 0.053, P= 0.045). None of the other OGTT- derived parameters (AUCglucose, fasted insulin AUCinsulin, HOMA-IS or insulinogenic index) were significantly associated with indices of macroscopic brain damage. Repetition of the analyses while adjusting for age, gender, descent, smoking status, use of anti-hypertensive, and use of lipid lowering agents did not materially change the results.

TABLE 3.2 | Association of gray and white matter atrophy with parameters of glucose metabolism

	Atrophy					
	Gray matter			White matter		
	Beta	P-value	R^2	Beta	P-value	R^2
Fasted glucose	0.007	0.924	0.336	-0.189	0.028	0.191
AUC glucose	-0.042	0.586	0.337	-0.148	0.084	0.179
Fasted insulin	0.002	0.983	0.336	-0.082	0.325	0.166
AUC insulin	-0.059	0.420	0.339	-0.076	0.361	0.165
HOMA-IS index	-0.003	0.968	0.336	0.105	0.213	0.170
Insulinogenic Index	-0.076	0.302	0.342	0.087	0.292	0.167

Atrophy is defined as the difference between intracranial and brain volume divided by intracranial volume multiplied by hundred percent. All insulin values were log-transformed. Associations are expressed as standardized Beta with corresponding P-values. Results are from linear regression analysis corrected for age, gender and offspring- partner status. AUC: area under the curve; HOMA-IS: Homeostatic model assessment of insulin sensitivity.

Parameters of glucose metabolism and brain microstructure

Table 3 shows the association of OGTT- derived glucose and insulin parameters with microstructural gray and white matter parenchymal integrity, measured via magnetization transfer imaging, and expressed in mean MTR and MTR peak height. A lower brain tissue mean MTR or peak height indicates loss of homogeneity of brain tissue or tissue damage. In the gray matter, parameters of reduced insulin action, namely, higher fasted insulin (β= -0.213, P= 0.010), AUCinsulin (β= -0.276, P= 0.001), insulinogenic index (β= -0.289, P<0.001) and decreased HOMA-IS (β= 0.220, P= 0.008) were significantly associated with lower gray matter MTR peak height. Similarly, higher AUCinsulin was associated with reduced mean gray matter MTR. Similar trends were seen between other OGTT derived parameters and mean MTR, but these did not reach statistical significance.

TABLE 3.3 | Association of Magnetization Transfer Imaging (MTI)- derived integrity of gray and white matter microstructure with parameters of glucose metabolism

	Gray matter						White matter					
	Mean MTR			Peak height			Mean MTR			Peak height		
	Beta	P -value	R^2	Beta	P -value	R^2	Beta	P- value	R^2	Beta	P -value	R^2
Fasted glucose	-0.124	0.166	0.159	-0.150	0.084	0.216	0.058	0.528	0.106	-0.050	0.572	0.181
AUC glucose	-0.165	0.063	0.170	-0.113	0.191	0.207	-0.031	0.737	0.103	-0.133	0.127	0.194
Fasted insulin	-0.068	0.432	0.150	-0.213	0.010	0.239	0.110	0.213	0.114	-0.189	0.024	0.213
AUC insulin	-0.181	0.033	0.177	-0.276	0.001	0.269	-0.033	0.709	0.104	-0.264	0.001	0.246
HOMA-IS index	0.081	0.351	0.152	0.220	0.008	0.241	-0.110	0.217	0.114	0.184	0.030	0.210
Insulinogenic Index	-0.151	0.075	0.168	-0.289	<0.001	0.277	0.018	0.833	0.103	-0.210	0.011	0.221

All insulin values were log- transformed. The standardized Beta and corresponding P-values are shown for analysis using individual brain volume corrected for head size. Results are from linear regression analysis corrected for age, gender and offspring- partner status. MTR: Magnetization transfer ratio; AUC: area under the curve; HOMA-IS: Homeostatic model assessment of insulin sensitivity.

In the white matter, increased fasted insulin (β= -0.189, P= 0.024), AUCinsulin (β= -0.264, P= 0.001), insulinogenic index (β= -0.210, P=0.011) and decreased HOMA-IS (β= 0.184, P= 0.030) were significantly associated with decreased white matter MTR peak height. In the white matter, increased fasted insulin (β= -0.189, P= 0.024), AUCinsulin (β= -0.264, P= 0.001), insulinogenic index (β= -0.210, P=0.011) and decreased HOMA-IS (β= 0.184, P= 0.030) were significantly associated with decreased white matter MTR peak height. These associations did not materially change after adjustment for age, gender, descent, smoking status, BMI, use of anti-hypertensive, and use of lipid lowering agents.

For visualization of the relations between reduced insulin action and brain microstructure, scatterplots were made as well as voxel based analysis, using area under the insulin curve (AUCinsulin). Figure 2 shows the inverse relation of AUCinsulin with gray matter peak height (Figure 2A) and white matter peak height (Figure 2B). Furthermore, via voxel based morphometric analysis, the association between cortical gray matter MTR with AUCinsulin are projected on T1 weighted images, as shown in Figure 3, where the corresponding decrease in cortical gray matter MTR with increasing AUCinsulin can be seen.

Sensitivity Analyses

To determine whether high 'normal' glucose levels i. e. glucose levels in the upper normal range (5.7-6.8 mmol/l) modulated the observed effects of glucose, sub-analyses were also conducted with lower fasting glucose levels (< 5.6mmol/l) and the findings of these were essentially similar to the results presented above.

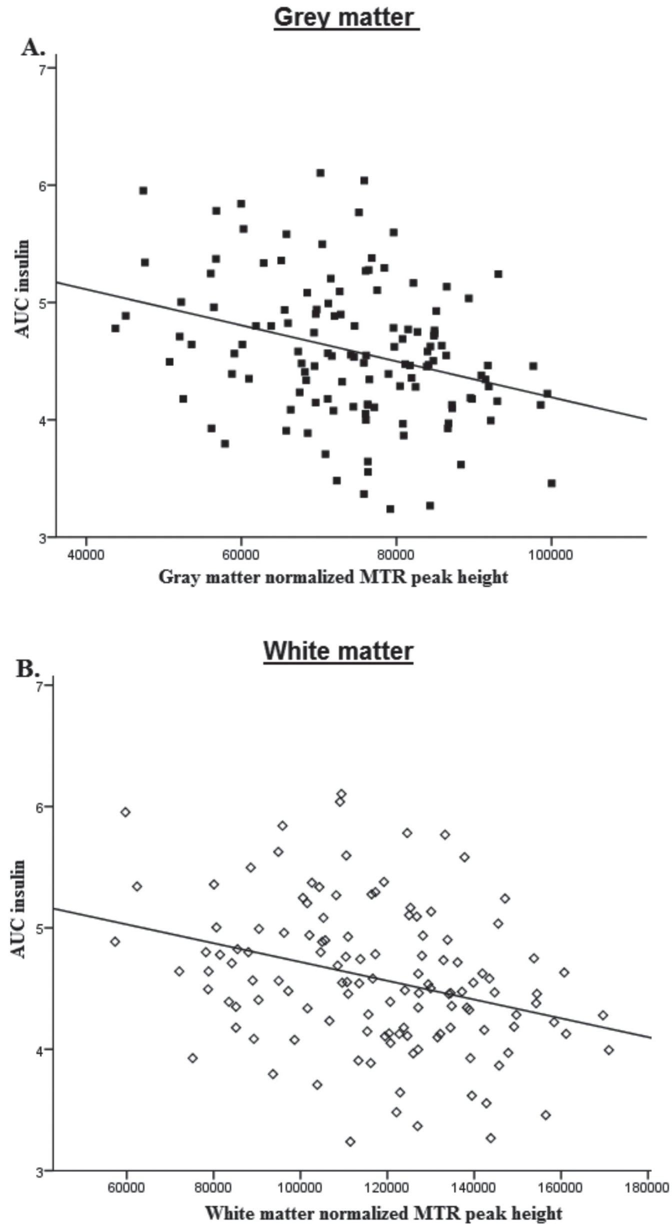

FIGURE 3.2 | Relation between the area under the insulin curve and MTR peak height in gray and white matter.

Scatterplots showing the inverse relation between area under the insulin curve (AUCinsulin) and A.) gray matter and B.) white matter MTR peak height. Lines of best fit were derived from bivariate Pearson's correlations.

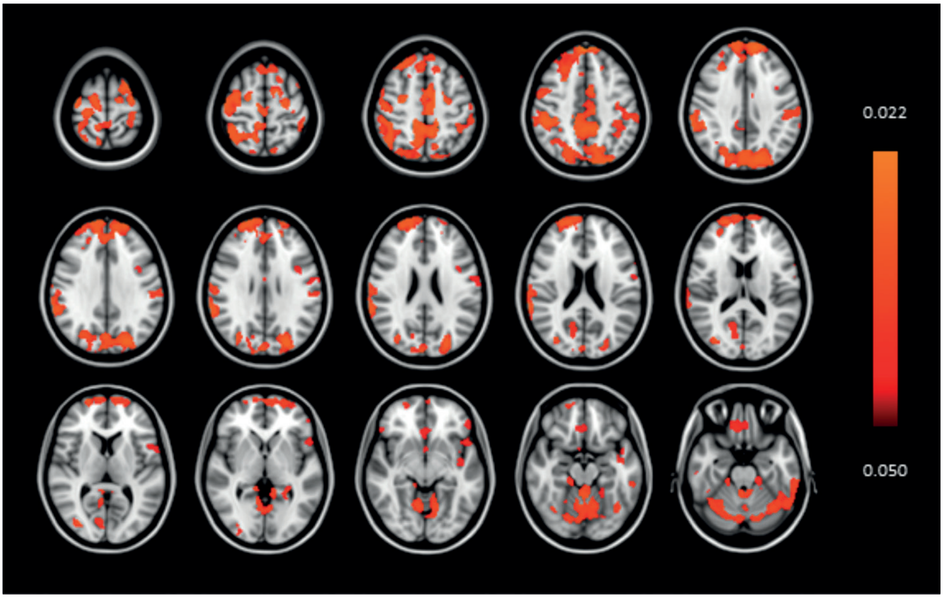

FIGURE 3.3 | Voxel- based analysis of relation between cortical gray matter magnetization transfer ratio and insulin.

Color scaling legend: Color (Red- Orange) represents voxels that are statistically significant for lower gray matter MTR in association with higher AUC insulin (area under the insulin curve). Results are from Voxel-based morphometric (VBM) analysis of cortical gray matter MTI- magnetization transfer ratio (MTR). Results are projected on the MNI152 space T1-weighted image provided by FSL. Statistical analysis was adjusted for sex, age and offspring-partner status. Threshold-Free Cluster Enhancement was applied with a significance level set at P< 0.05, corrected for Family Wise Error rate.

DISCUSSION

We report two main findings. The first is that subclinical variation in fasted glucose was associated with white matter atrophy. Secondly, in the absence of type 2 diabetes, higher insulin and reduced peripheral insulin action and sensitivity were associated with reduced microstructural brain integrity in older adults without diabetes.

The role of metabolic derangement associated with (pre) diabetic states in the decline in brain structure and function is an area of active investigation. Previous studies have shown relations between glucose levels (ranging from high normal to diabetic levels), with decreasing total brain volumes and cognition [30-33]. Associations between impairments in glucose regulation and smaller total brain volumes were found in a large cohort of middle-aged diabetic and non- diabetic subjects of the Framingham study, where inverse correlations were found between total cerebral brain volumes and HbA1c, HOMA- IR and fasted insulin levels [7]. In harmony with these studies, we found a significant association between indices of impairments in glucose regulation (fasted glucose, fasted insulin, AUCinsulin and HOMA-IS) and gray and white matter microstructure. Of note, there is an inverse relation between Homeostatic model assessment of insulin sensitivity (HOMA-IS) and Homeostatic model assessment of insulin resistance (HOMA-IR). The white matter atrophy observed in relation to fasted glucose in our study are consistent with previous research demonstrating high-'normal' blood glucose levels being associated with lower gray and white matter regional volumes [32]. Our findings thus suggest that the effect of plasma glucose on cerebral structural integrity in older people is not restricted to the upper normal range.

We describe here for the first time that increased fasted insulin, AUCinsulin and decreased HOMA-IS, insulinogenic index were significantly associated with decreased MTR histogram peak-height for both gray and white matter, indicating loss of homogeneity of brain tissue or tissue damage. Similar trends were found for mean MTR, but these are not statistically significant. Although mean MTR and histogram peak-height of MTR are both MTR measures, they reflect different aspects of MTR, and may show considerable difference in sensitivity with respect to demonstrating variations in structural brain integrity [9, 34-36]. Peak heights of MTR histograms are a sensitive measure of microstructural brain parenchymal abnormalities, loss of which has been associated with both aging and metabolic syndrome [9, 10]. Of note, previous population based, longitudinal studies have suggested insulin and insulin resistance as being a link between diabetes and neurodegenerative diseases [37, 38]. Interestingly, our findings showed lower MTR histogram peak heights in gray and white matter in relation with higher fasted insulin and decreasing sensitivity to insulin. We found an inverse association between fasted glucose and cerebral microbleeds, which was of borderline significance ($P= 0.045$). However, since the R2 was really low ($R2= 0.053$), we could not exclude the possibility that this could have been a chance finding. No other significant association was found between indices of disturbances in glucose or insulin parameters and macro-structural brain pathology (white matter hyper- intensities, lacunar infarcts, cerebral micro- bleeds).

Taken together, these findings suggest that metabolically related brain structural abnormalities is observable at a microscopic level, even in the presence of glucose and insulin levels that are considered normal by present standards. An inverse association was found between OGTT- derived insulin parameters (fasted insulin, AUCinsulin, HOMA-IS and insulinogenic index) and gray and white matter microstructural integrity. This suggests a link between reduced insulin action (evidenced by higher insulin and reduced peripheral insulin sensitivity) and loss of homogeneity of brain tissue (reflecting parenchymal abnormalities), even in older adults without diabetes. One possible mechanism that may underpin these findings is that with aging, the ability to maintain the delicate balance between the various gluco-regulatory mechanisms declines, leading to deleterious micro-structural changes in neuronal and thus brain tissue integrity. Such micro-structural brain changes may exist even without the appearance of overt macro-structural changes that are associated with clinically significant metabolic disease.

It is a limitation of this study that we only examined cross-sectional associations and did not examine the association of changes of these measures over time. Thus, our findings are descriptive, and no causal inference can be made. A strength of this study is that, in addition to using conventional MRI, magnetization transfer imaging (MTI) was used, which is an advanced MRI technique that has the discriminatory power to detect in vivo microstructural brain changes and quantitatively measure brain parenchyma abnormalities that are beyond the spatial resolution of conventional MRI.

In conclusion, using sensitive MRI techniques, we observed that subclinical differences glucose and insulin metabolism were associated with macro- and micro-structural brain changes in older adults, and these were detectable even with glucose and insulin levels within population reference ranges. These findings possibly offer more insight into the association between different parameters of glucose metabolism and brain aging. Sufficiently powered follow-up studies are needed to evaluate cause or consequence in the relation between parameters of glucose metabolism and brain integrity.

REFERENCES

1. Cowie CC, Rust KF, Byrd-Holt DD, Eberhardt MS, Flegal KM, Engelgau MM, et al. Prevalence of diabetes and impaired fasting glucose in adults in the U.S. population: National Health And Nutrition Examination Survey 1999-2002. Diabetes Care. 2006;29(6):1263-8.
2. Biessels GJ, Staekenborg S, Brunner E, Brayne C, Scheltens P. Risk of dementia in diabetes mellitus: a systematic review. Lancet Neurol. 2006;5(1):64-74.
3. Vagelatos NT, Eslick GD. Type 2 diabetes as a risk factor for Alzheimer's disease: the confounders, interactions, and neuropathology associated with this relationship. Epidemiologic reviews. 2013;35:152-60.
4. Crane PK, Walker R, Hubbard RA, Li G, Nathan DM, Zheng H, et al. Glucose levels and risk of dementia. The New England journal of medicine. 2013;369(6):540-8.
5. de la Monte SM, Wands JR. Alzheimer's disease is type 3 diabetes-evidence reviewed. JDiabetes SciTechnol. 2008;2(6):1101-13.
6. Steen E, Terry BM, Rivera EJ, Cannon JL, Neely TR, Tavares R, et al. Impaired insulin and insulin-like growth factor expression and signaling mechanisms in Alzheimer's disease--is this type 3 diabetes? JAlzheimersDis. 2005;7(1):63-80.
7. Tan ZS, Beiser AS, Fox CS, Au R, Himali JJ, Debette S, et al. Association of metabolic dysregulation with volumetric brain magnetic resonance imaging and cognitive markers of subclinical brain aging in middle-aged adults: the Framingham Offspring Study. Diabetes Care. 2011;34(8):1766-70.
8. Inglese M, Ge Y. Quantitative MRI: hidden age-related changes in brain tissue. Topics in magnetic resonance imaging : TMRI. 2004;15(6):355-63.
9. Benedetti B, Charil A, Rovaris M, Judica E, Valsasina P, Sormani MP, et al. Influence of aging on brain gray and white matter changes assessed by conventional, MT, and DT MRI. Neurology. 2006;66(4):535-9.
10. Sala M, de Roos A, van den Berg A, Altmann-Schneider I, Slagboom PE, Westendorp RG, et al. Microstructural brain tissue damage in metabolic syndrome. Diabetes Care. 2014;37(2):493-500.
11. Rademacher J, Engelbrecht V, Burgel U, Freund H, Zilles K. Measuring in vivo myelination of human white matter fiber tracts with magnetization transfer MR. NeuroImage. 1999;9(4):393-406.
12. van Buchem MA, Tofts PS. Magnetization transfer imaging. Neuroimaging clinics of North America. 2000;10(4):771-88 ,ix.

13. Takeuchi M, Kanazawa A, Suzuki M, Hasegawa M, Kimura Y, et al. Evaluation of factors during OGTT to correlate insulin resistance in non-diabetic subjects. Endocr J. 2000;47(5):535-42.
14. Schoenmaker M, de Craen AJ, de Meijer PH, Beekman M, Blauw GJ, Slagboom PE, et al. Evidence of genetic enrichment for exceptional survival using a family approach: the Leiden Longevity Study. EurJHumGenet. 2006;14(1):79-84.
15. Altmann-Schneider I, de Craen AJ, Slagboom PE, Westendorp RG, van Buchem MA, Maier AB, et al. Brain tissue volumes in familial longevity: the Leiden Longevity Study. Aging Cell. 2012;11(6):933-9.
16. Stijntjes M, de Craen AJ, van Heemst D, Meskers CG, van Buchem MA, Westendorp RG, et al. Familial longevity is marked by better cognitive performance at middle age: the Leiden Longevity Study. PloS one. 2013;8(3):e57962.
17. Matthews DR, Hosker JP, Rudenski AS, Naylor BA, Treacher DF, Turner RC. Homeostasis model assessment: insulin resistance and beta-cell function from fasting plasma glucose and insulin concentrations in man. Diabetologia. 1985;28(7):412-9.
18. Hanson RL, Pratley RE, Bogardus C, Narayan KM, Roumain JM, Imperatore G, et al. Evaluation of simple indices of insulin sensitivity and insulin secretion for use in epidemiologic studies. American journal of epidemiology. 2000;151(2):190-8.
19. Pruessner JC, Kirschbaum C, Meinlschmid G, Hellhammer DH. Two formulas for computation of the area under the curve represent measures of total hormone concentration versus time-dependent change. Psychoneuroendocrinology. 2003;28(7):916-31.
20. Smith SM. Fast robust automated brain extraction. Human brain mapping. 2002;17(3):143-55.
21. Jenkinson M, Bannister P, Brady M, Smith S. Improved optimization for the robust and accurate linear registration and motion correction of brain images. Neuroimage. 2002;17(2):825-41.
22. Zhang Y, Brady M, Smith S. Segmentation of brain MR images through a hidden Markov random field model and the expectation-maximization algorithm. IEEE TransMedImaging. 2001;20(1):45-57.
23. Smith SM, Zhang Y, Jenkinson M, Chen J, Matthews PM, et al. Accurate, robust, and automated longitudinal and cross-sectional brain change analysis. Neuroimage. 2002;17(1):479-89.
24. Longstreth WT, Jr., Bernick C, Manolio TA, Bryan N, Jungreis CA, Price TR. Lacunar infarcts defined by magnetic resonance imaging of 3660 elderly people: the Cardiovascular Health Study. Archives of neurology. 1998;55(9):1217-25.
25. Bokura H, Kobayashi S, Yamaguchi S. Distinguishing silent lacunar infarction from enlarged Virchow-Robin spaces: a magnetic resonance imaging and pathological study. JNeurol. 1998;245(2):116-22.

26. Greenberg SM, Vernooij MW, Cordonnier C, Viswanathan A, Al-Shahi et al. Cerebral microbleeds: a guide to detection and interpretation. The Lancet Neurology. 2009;8(2):165-74.
27. Andersson J, Jenkinson J, Smith S. Non-linear registration aka Spatial normalisation. FMRIB Technial Report TR07JA2. 2007; http://fmrib.medsci.ox.ac.uk/analysis/techrep/tr07ja2/tr07ja2.pdf.
28. Cosottini M, Pesaresi I, Piazza S, Diciotti S, Belmonte G, Battaglini M, et al. Magnetization transfer imaging demonstrates a distributed pattern of microstructural changes of the cerebral cortex in amyotrophic lateral sclerosis. AJNR American journal of neuroradiology. 2011;32(4):704-8.
29. Smith SM, Nichols TE. Threshold-free cluster enhancement: addressing problems of smoothing, threshold dependence and localisation in cluster inference. NeuroImage. 2009;44(1):83-98.
30. Cui X, Abduljalil A, Manor BD, Peng CK, Novak V. Multi-scale glycemic variability: a link to gray matter atrophy and cognitive decline in type 2 diabetes. PLoSOne. 2014;9(1):e86284.
31. Espeland MA, Bryan RN, Goveas JS, Robinson JG, Siddiqui MS, Liu S, et al. Influence of type 2 diabetes on brain volumes and changes in brain volumes: results from the Women's Health Initiative Magnetic Resonance Imaging studies. Diabetes Care. 2013;36(1):90-7.
32. Mortby ME, Janke AL, Anstey KJ, Sachdev PS, Cherbuin N. High "normal" blood glucose is associated with decreased brain volume and cognitive performance in the 60s: the PATH through life study. PLoSOne. 2013;8(9):e73697.
33. Samaras K, Lutgers HL, Kochan NA, Crawford JD, Campbell LV, Wen W, et al. The impact of glucose disorders on cognition and brain volumes in the elderly: the Sydney Memory and Ageing Study. Age (Dordrecht, Netherlands). 2014;36(2):977-93.
34. Ropele S, Enzinger C, Sollinger M, Langkammer C, et al. The impact of sex and vascular risk factors on brain tissue changes with aging: magnetization transfer imaging results of the Austrian stroke prevention study. AJNR American journal of neuroradiology. 2010;31(7):1297-301.
35. van den Bogaard SJ, Dumas EM, Milles J, Reilmann R, Stout JC, Craufurd D, et al. Magnetization transfer imaging in premanifest and manifest Huntington disease. AJNR American journal of neuroradiology. 2012;33(5):884-9.
36. Yamamoto A, Miki Y, Adachi S, Kanagaki M, Fushimi Y, Okada T, et al. Whole brain magnetization transfer histogram analysis of pediatric acute lymphoblastic leukemia patients receiving intrathecal methotrexate therapy. European journal of radiology. 2006;57(3):423-7.
37. Ronnemaa E, Zethelius B, Sundelof J, Sundstrom J, Degerman-Gunnarsson M, Berne C, et al. Impaired insulin secretion increases the risk of Alzheimer disease. Neurology. 2008;71(14):1065-71.

38. Schrijvers EM, Witteman JC, Sijbrands EJ, Hofman A, Koudstaal PJ, Breteler MM. Insulin metabolism and the risk of Alzheimer disease: the Rotterdam Study. Neurology. 2010;75(22):1982-7.

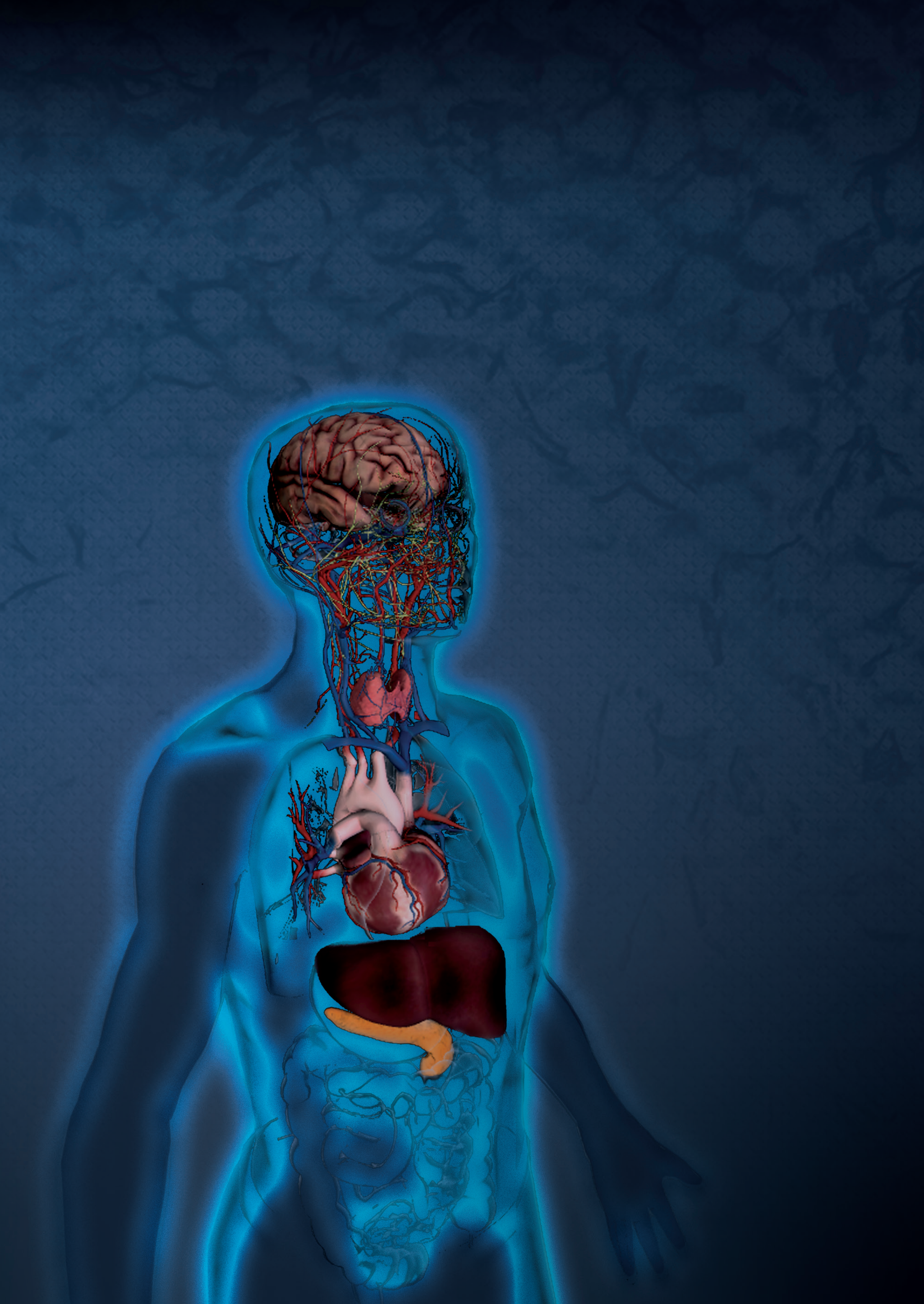

CHAPTER 4

ASSOCIATIONS BETWEEN INSULIN ACTION AND INTEGRITY OF BRAIN MICROSTRUCTURE DIFFER WITH AGE AND FAMILIAL LONGEVITY

Abimbola A. Akintola
Annette van den Berg
Mark A. van Buchem
Steffy W. Jansen
P. Eline Slagboom
Rudi G. Westendorp
Jeroen van der Grond
Diana van Heemst

Front Aging Neuroscience. 2015 May 28;7:92.

ABSTRACT

Impaired glucose metabolism and type 2 diabetes have been associated with cognitive decline, dementia, and with structural and functional brain features. However, it is unclear whether these associations differ in individuals that differ in familial longevity or age. Here, we investigated the association between parameters of glucose metabolism and microstructural brain integrity in offspring of long-lived families ("offspring") and controls; and age categories thereof.

From the Leiden Longevity Study, 132 participants underwent oral glucose tolerance test to assess glycemia (fasted glucose and glucose area-under-the-curve (AUC)), insulin resistance (fasted insulin, AUCinsulin, and homeostatic model assessment of insulin resistance (HOMA-IR)), and pancreatic Beta cell secretory capacity (insulinogenic index). 3Tesla MRI and Magnetization Transfer (MT) imaging MT-ratio peak-height was used to quantify differences in microstructural brain parenchymal tissue homogeneity that remain invisible on conventional MRI. Analyses were performed in offspring and age-matched controls, with and without stratification for age.

In the full offspring group only, reduced peak-height in gray and white matter was inversely associated with AUCinsulin, fasted insulin, HOMA-IR and insulinogenic-index (all $p<0.01$). When dichotomised for age (≤65 years & >65 years): in younger controls, significantly stronger inverse associations were observed between peak-height and fasted glucose, AUCglucose, fasted insulin, AUCinsulin and HOMA-IR in gray matter; and for AUCglucose, fasted insulin and HOMA-IR in white matter (all P-interaction<0.05). Although the strength of the associations tended to attenuate with age in the offspring group, the difference between age groups was not statistically significant.

Thus, associations between impaired insulin action and reduced microstructural brain parenchymal tissue homogeneity were stronger in offspring compared to controls, and seemed to diminish with age.

INTRODUCTION

There is increasing epidemiological evidence that metabolic disorders, including type 2 diabetes (T2D) and its risk factors, such as metabolic syndrome, are associated with risk of cognitive decline and dementia, and with structural and functional brain defects [1]. T2D has been associated with white matter lesions [2], atrophy [3, 4], infarcts [5], cognitive impairment [4] and risk of neurodegenerative diseases. Also in the absence of T2D, impaired glucose regulation and higher serum insulin concentrations were found to increase the risk of cognitive decline [6, 7]. Likewise, metabolic syndrome was found to be associated with cognitive impairment in middle-aged subjects [8]. There are however indications that in old age, the association between cognitive decline and metabolic syndrome, or its individual components, notably obesity and impaired glucose metabolism may be absent or even reverse [9].

Previously, the Leiden Longevity Study (LLS) [10] was set up to investigate factors associated with familial longevity. We recruited offspring of long- lived nonagenarian siblings, who are predisposed to become long-lived as well, and their partners as controls. We demonstrated that the propensity for longevity in the offspring of these families is marked by preserved insulin sensitivity and a lower prevalence of T2D, compared to controls of similar chronological age [11, 12]. In this relatively healthy and cognitively intact middle-aged to elderly population [13], we recently found that metabolic syndrome was specifically associated with microstructural loss of homogeneity of brain parenchymal tissue (assessed by magnetization transfer ratio (MTR) histogram peak height), but not with macrostructural brain damage [14]. It is unknown whether specific measures of glucose metabolism also associate with microstructural brain parenchymal tissue homogeneity and whether these associations are similar in offspring and controls.

In the current study of 132 participants, we aimed to investigate the association between parameters of glucose metabolism and microstructural brain parenchymal tissue homogeneity in offspring of long- lived families and controls; and with age. Parameters of glucose metabolism were derived from 2-hour oral glucose tolerance test (OGTT), and included fasted glucose and area under the glucose curve (AUCglucose), which are measures of glycemia; fasted insulin, area under the insulin curve (AUCinsulin), and HOMA index of insulin resistance, which are measures of insulin resistance; and insulinogenic index which is a measure of pancreatic Beta cell secretory capacity. Microstructural brain parenchymal tissue homogeneity was assessed using magnetization transfer imaging (MTI), which is an advanced, sensitive MRI technique that quantitatively measures microstructural brain parenchymal abnormalities, including reductions in myelin content and in axonal numbers [15] even in brain tissue that appears normal on conventional MR imaging.

MATERIALS AND METHODS

Ethics statement

The Medical Ethical Committee of Leiden University Medical Centre approved this study. All participants gave written informed consent to be included in the study.

Study subjects

Subjects were recruited from the Leiden Longevity Study (LLS), a family based study that was set up identify genetic factors and biomarkers of familial longevity [10]. The LLS consisted of 1,671 offspring of Caucasian, nonagenarian siblings (aged older than 89 years for men and 91 years for women, and having at least one sister or a brother fulfilling same age criteria). Also, 744 of the offspring's partners were included as controls. All eligible subjects were included without selection on health or demographic characteristics.

Of the 2415 subjects in the offspring/ partner group, a random subset of 370 underwent an MRI scan of the brain and another random subset of 234 subjects underwent an oral glucose tolerance test (OGTT) [16]. A total of 132 subjects without diabetes, and with complete datasets for OGTT, 3Tesla brain MRI and MTI were included for the analysis performed in this study. Furthermore, the participants underwent three cognitive tests-Stroop test, Digit Symbol Substitution Test (DSST) and 15-Picture Word Learning Test (15- PLT). Stroop test and DSST were used to evaluate attention and processing speed, while15-PLT was used for memory function. Outcome parameter for Stroop test was defined as the time needed to complete the test, while outcome parameter for the DSST was the number of correct digit-symbol combinations within 90s. For 15-PLT, fifteen pictures were successively presented at a rate of one per two seconds after which the subject was asked to recall as many pictures as possible. This procedure was carried out three times (PLT-1, PLT2 and PLT3). After 20 minutes, delayed recall was tested. Outcome parameters were the number of correct pictures after each trial (PLT-immediate) and after 20 min (PLT-delayed) [13].

Oral glucose tolerance test

In the morning after a 10-hour overnight fast, fasted glucose and insulin levels were measured after which subjects ingested a solution containing 75g anhydrous glucose in 5 minutes. Thereafter, venous blood samples were collected at 30, 60, and 120 minutes for determination of plasma glucose and insulin. Areas under the curves (AUCs) obtained in the OGTT were calculated using the trapezoid formula [17]. Homeostatic model assessment of insulin resistance (HOMA-IR) was calculated by the product of the fasting insulin level (mU/L) and the fasting glucose level (mmol/L) divided by 22.5. Insulogenic index was calculated by dividing increments of insulin at 30 minutes compared to fasting insulin values by the corresponding increment of 30 minutes glucose levels compared to fasted glucose values.

Biochemical Analysis

Plasma and serum aliquots were frozen at -80°C. All serum measurements were performed using fully automated equipment. Glucose levels were measured using Hitachi Modular P 800 from Roche (Almere, the Netherlands), with coefficient of variation (CV) for measurement less than 5%. Insulin levels were measured using the Immulite 2,500 from DPC (Los Angeles, CA). CV was less than 8%.

Brain MRI protocol

Image Acquisition

Subjects underwent imaging on a whole body MR system operating at field strength of 3 Tesla (Philips Medical Systems, Best, the Netherlands). 3D T1-weighted, T2-weighted FLAIR (fluid attenuated inversion recovery), T2*-weighted images, and MTI images were acquired. The dimensions of the images have been previously described in detail [18]. Image processing and analysis was done using the analytical techniques and tools of the Functional MRI of the Brain (FMRIB) Software Library (FSL).

Brain volumes

Gray and white matter volumes were calculated using FSL-tool Structural Image Evaluation Normalization of Atrophy (SIENAX). From the whole head input data, brain and skull images were extracted via SIENAX and affine registered to MNI (Montreal Neurological

Institute) 152 [19]. A volumetric scale factor was thus obtained for normalization of head size, after which total brain tissue volume with separate estimates of gray and white matter were obtained.

Magnetization transfer imaging (MTI)

Definitions: MTI

MTI is based in interactions between immobile protons (on macromolecular protons, probably contained in the cell walls) and free protons of tissue. Mean magnetization transfer ratio (MTR) reflects the average MTR value per structure. MTR peak location reflects the most common MTR value. The peak height of the MTR histogram indicates the number of voxels, which show the most common MTR value per structure, and is considered to be a measure of uniformity of the underlying voxels.

MTI Protocol

Raw magnetization transfer scans were split into M0-sequence (without saturation pulse) and the M1-sequence (acquired after application of a saturation pulse). Brain masks for white matter and cortical gray matter were created using FAST (FMRIB's automated segmentation tool) [20] and FIRST (FMRIB's integrated segmentation tool) on 3D T1 weighted images. To correct for possible partial volume effects, an eroded mask of these segmentations was created by removing one voxel in-plane for all mentioned volumes-of interest (VOIs) [21]. Then, the 3D T1- weighted images were registered to the M0 image using FMRIB's registration tool (FLIRT), and the transformation matrix of this registration was used to register all brain masks to the MTI volumes. Afterwards, individual MTR maps were calculated voxel by voxel following the equation MTR = (M0-M1)/M0. MTR histograms were generated for each VOI. Mean MTR as well as MTR peak height, normalized for the size of the VOI, and MTR peak location were calculated. All MTI measures below -3 or above 3 standard deviations were excluded from statistical analysis.

VBM (Voxel Based Morphometry) analysis was used to study the focal differences and spatial distribution of the changes in gray matter (GM). GM partial volume MTR maps were aligned to MNI152 standard space using the non-linear registration tool FNIRT (FMRIB's non-linear image registration tool). To improve the quality of normalization, averaging the obtained registered GM MTR maps of all subjects created a study-specific MTR template.

The native individual MTR maps were then non-linearly re-registered to this template, divided by the Jacobian of the warp field and smoothed with an isotropic Gaussian kernel with a sigma of 3 mm.

Statistical analysis

Distributions of continuous variables were examined for normality, logarithmically transformed when appropriate, and used in calculations. Median (interquartile range (25^{th}, 75^{th} percentile)) was reported for raw values of variables that were eventually logarithmically transformed (fasted insulin, AUCinsulin, HOMA-IR and insulogenic index). Differences in sex, smoking status, hypertension, cerebrovascular accident (CVA), myocardial infarction (MI), and use of lipid lowering drugs between the different groups were calculated using Pearson Chi-Square ($\chi 2$) test. Differences in age, BMI, glucose related characteristics, and MRI related characteristics were calculated using independent samples T-test for offspring/partner differences. Correlation between cognitive tests and gray and white matter MTR peak height were assessed using bivariate Pearson correlation analysis.

Z values were calculated for standardisation of variables. The relation between markers of glucose metabolism and brain structures was determined using linear regression and univariate analysis of variance, and presented as standardised Betas with corresponding p-values. Homogeneity of variance assumption was tested using Levene's test. Statistical significance was set as $p<0.05$. Analyses were performed in offspring and controls before and after stratification of offspring and controls into 2 groups based on age ($\leq$ 65 years, > 65 years). Initial analyses were adjusted for age and sex. Extended models further included smoking status, BMI, use of anti-hypertensive, and use of lipid lowering agents. To check for the effect sizes and interaction between the offspring and controls, an interaction term was added to the model while correcting for covariates. Similar analyses were performed to compare association between OGTT parameters and MRI markers of brain microstructure between age groups.

For statistical analyses, Statistical Package for Social Sciences (SPSS) software for windows (version 20.0) was used. Forest plots were made using GraphPad Prism version 5 (GraphPad, San Diego, CA).

For MRI data, The FSL randomize tool was used to perform permutation-based non-parametric testing (n=5000 permutations) for voxel-wise statistical analyses of the MTR data. Threshold-Free Cluster Enhancement (TFCE) was applied to correct for multiple comparisons. Significance was set at a TFCE corrected $p < 0.05$.

RESULTS

The current study was performed in a subgroup of 132 participants of the Leiden Longevity Study, with the aim of investigating the association between OGTT derived parameters and brain integrity in groups that differ in familial longevity and with age. After measurement of fasted glucose and insulin levels, participants underwent 2-hour oral glucose tolerance test (OGTT). Parameters derived from the OGTT included measures of glycemia (fasted glucose and AUCglucose); measures of insulin resistance (fasted and AUCinsulin, and HOMA index of insulin resistance); and a measure of pancreatic Beta cell secretory capacity (insulinogenic index). Thereafter, brain volumes were measured using MRI. Furthermore, Magnetization Transfer Ratio (MTR) histogram peak height (henceforth referred to as MTR peak height) was measured using magnetization transfer imaging (MTI). MTR peak height provides an estimate of microstructural brain parenchymal homogeneity, with lower MTR peak height being indicative of loss of homogeneity of the brain tissue. Characteristics of the study subjects are presented in Table 1, for the full study sample and stratified for offspring and controls. The study population from which both OGTT data as well as MTR and MTI data were available (N=132) consisted of 47% males, with mean age of 66.2±6.6 years. Mean BMI was 26.4±3.9 and mean fasted glucose was 5.08 mmol/L. Characteristics were similar between offspring (N=75) and controls (N=57), except for use of lipid lowering drugs, fasted glucose, and AUCglucose, which were significantly higher in the partner group.

Also, the outcomes of the cognitive tests were not significantly different in offspring and controls (Table 1). Furthermore, from the cross-sectional data, no significant correlation was found between the cognitive tests, which are a measure of functional brain integrity, and MTR peak height, which is a measure microstructural brain parenchymal tissue homogeneity, either in the whole group (n=132) or in offspring and controls (supplementary table S1).

TABLE 4.1 | Characteristics of study subjects

	Whole group	Familial longevity	
		Offspring	Controls
Number of participants	132	75	57
Demographics			
Age in years (range)	66.2 (49-84)	66 (52-84)	66 (49-81)
Men, n (%)	62 (47)	43 (57)	27 (47)
BMI in kg/m^2	26.4 (3.9)	26.6 (4.2)	26.3 (3.6)
Current smoking, n (%)	11 (8.3)	4 (5)	7 (12)
Medical History			
Hypertension, n (%)	29 (22)	15 (20)	14 (25)
CVA, n (%)	1 (0.8)	1 (1.3)	0 (0)
Myocardial infarct, n (%)	1 (0.8)	0 (0)	1 (1.8)
Lipid lowering medication use, n (%)	14 (10.6)	4 (5) *	10 (18)*
Glucose related characteristics			
Fasted glucose in mmol/L	5.08 (0.6)	4.97 (0.5)*	5.21 (0.6)*
AUC glucose	13.93 (3.5)	13 (3)*	15 (4)*
Fasted Insulin in pmol/L, median (IQR)	7 (4, 10)	7.0 (4.0, 10.0)	7.0 (3.5, 10.5)
AUC Insulin, median (IQR)	93.7 (64, 140)	93.7 (65, 139)	91.8 (60, 155)
Insulinogenic index, median (IQR)	13.7 (8, 20)	15 (9, 20)	10 (7, 18)
HOMA-IR index, median (IQR)	1.5 (0.9, 2.2)	1.4 (0.9, 2.2)	1.6 (0.8, 2.5)
Brain volumes in (cm^3)			
White matter	699 (38)	694 (41)	705 (34)
Gray matter	702 (40)	702 (36)	702 (45)
MTR peak height, pixel count x 10^3			
White matter	117 (24)	118 (25)	116 (23)
Gray matter	74.3 (1.2)	75 (13)	73 (10)
Cognitive tests			
DSST, correct answers	46.46 (9.5)	46.0 (13.2)	46.33 (12.4)
Stroop test, seconds	47.95 (12.5)	48.41 (13.2)	48.26 (11.4)
15-PLTi, correct pictures	10.38 (1.9)	10.27 (1.9)	10.54 (1.9)
15-PLTd, correct pictures	11.35 (2.0)	11.51 (2.1)	11.08 (1.9)

Unless otherwise stated, values are means (standard deviation). Age refers to age at MRI examination. Brain volumes are normalized for skull size. BMI: body mass index. CVA: cerebrovascular accident; AUC: area under the curve; IQR: interquartile range (25^{th}, 75^{th} percentile); DSST: Digit Symbol Substitution Test; 15- PLTi: 15- Picture Word Learning Test immediate recall; 15- PLTd: 15- Picture Word Learning Test delayed recall.

** p-value<0.05*

.

TABLE 4.2 | Association of MTR peak height with markers of glucose metabolism in offspring and controls.

	Offspring		Controls		*P*-interaction
	Beta	*p*-value	Beta	*p*-value	
Gray matter					
Fasted glucose	-0.166	0.289	-0.135	0.140	0.856
AUC glucose	-0.062	0.693	-0.145	0.119	0.733
Fasted insulin	-0.378	0.007	-0.079	0.384	0.070
AUC insulin	-0.473	<0.001	-0.107	0.245	0.021
HOMA-IR index	-0.382	0.007	-0.091	0.314	0.083
Insulinogenic index	-0.383	<0.001	-0.106	0.374	0.101
White matter					
Fasted glucose	-0.104	0.486	-0.014	0.896	0.745
AUC glucose	-0.097	0.518	-0.157	0.147	0.691
Fasted insulin	-0.371	0.005	-0.050	0.638	0.082
AUC insulin	-0.430	0.001	-0.129	0.225	0.086
HOMA-IR index	-0.366	0.006	-0.047	0.658	0.091
Insulinogenic index	-0.294	0.005	-0.038	0.785	0.150

MTR histogram peak MTR histogram peak height from magnetization transfer MRI was used as a measure of microstructural brain parenchymal tissue homogeneity. All insulin values were log-transformed. Univariate associations are from linear regression analysis, correcting for age and sex. Associations are presented as standardized Beta coefficients (per increase in SD) with corresponding P-values.

Familial longevity: markers of glucose metabolism and micro- structural brain parenchymal homogeneity

To investigate the association between markers of glucose metabolism and microstructural brain parenchymal tissue homogeneity (assessed using MTR peak height) in individuals that differ in familial longevity, analyses were done in the offspring of long- lived families and controls (Table 2). In the offspring, decreased gray matter MTR peak height was significantly associated with higher indices of reduced insulin action (fasted insulin (p=0.007), AUCinsulin (p<0.001), HOMA-IR (p=0.007)) and OGTT- derived measure of pancreatic Beta cell secretory capacity (insulinogenic-index (p<0.001)). Similar results were obtained for white matter. In the controls, similar trends were seen but the effects were smaller and did not reach statistical significance.

From voxel based morphometry analysis, statistically significant associations between gray matter MTR were observed with different OGTT derived insulin parameters ($p<0.05$) in offspring, spatial distributions of these focal differences are shown in Figure 1. Similar significant associations were not observed for the controls.

Chronological age: markers of glucose metabolism and micro- structural brain parenchymal homogeneity

With the aim of investigating the effect of age on the association between parameters of glucose metabolism and MTR peak height, the offspring and controls were stratified based on age into two groups: subjects ≤ 65 years and > 65 years. The results are presented in Table 3 and Figure 2.

Amongst the offspring, there were 35 subjects in the younger group (≤ 65 years), with mean age 61.3 (SD 3.2), age range 52-65 years. The older offspring consisted of 40 subjects with mean age 71.2 (SD 3.9), age range 66-84years. In the younger offspring, decreased MTR peak height in cortical gray matter, was significantly associated with higher fasted insulin ($p=0.038$), AUCinsulin ($p=0.005$), HOMA-IR ($p=0.033$) and insulinogenic-index ($p=0.007$). Likewise, in the white matter, decreased MTR peak height was significantly associated with OGTT derived measures of insulin resistance, namely, fasted insulin ($p=0.012$), AUCinsulin ($p=0.002$), HOMA-IR ($p=0.010$), and insulinogenic-index ($p=0.032$). Thus, in the younger offspring, parameters of reduced insulin action were significantly associated with decreased microstructural brain parenchymal homogeneity in both gray and white matter. Similar trends were seen in the older offspring (> 65 years), but the effects were smaller and did not reach statistical significance.

TABLE 4.3 | Association of MTR peak height with markers of glucose metabolism in 'younger' and 'older' offspring and controls.

	Offspring					Controls				
	≤ 65 years (n=35)		> 65 years (n=40)		*P* -interaction	≤ 65 years (n=30)		> 65 years (n=27)		*P* -interaction
	Beta	*P* -value	Beta	*P* -value		Beta	*P*- value	Beta	*P* -value	
Gray matter										
Fasted glucose	-0.379	0.203	-0.147	0.442	0.763	-0.350	0.020	-0.041	0.742	0.033
AUC glucose	-0.181	0.479	0.112	0.584	0.340	-0.487	0.001	0.114	0.341	0.002
Fasted insulin	-0.485	0.038	-0.291	0.107	0.567	-0.293	0.037	0.231	0.104	0.014
AUC insulin	-0.603	0.005	-0.322	0.069	0.293	-0.259	0.059	0.147	0.323	0.042
HOMA-IR	-0.512	0.033	-0.297	0.104	0.555	-0.325	0.022	0.209	0.129	0.009
Insulinogenic Index	-0.381	0.007	-0.442	0.014	0.623	0.003	0.986	-0.162	0.288	0.695
White matter										
Fasted glucose	-0.386	0.160	-0.025	0.893	0.628	-0.149	0.418	0.133	0.330	0.128
AUC glucose	-0.333	0.154	0.190	0.327	0.072	-0.444	0.013	0.055	0.686	0.033
Fasted insulin	-0.537	0.012	-0.213	0.218	0.362	-0.239	0.152	0.253	0.113	0.047
AUC insulin	-0.603	0.002	-0.239	0.158	0.150	-0.250	0.120	0.092	0.584	0.121
HOMA-IR	-0.562	0.010	-0.206	0.239	0.351	-0.248	0.146	0.246	0.110	0.038
Insulinogenic Index	-0.289	0.032	-0.360	0.037	0.557	0.124	0.601	-0.111	0.518	0.704

MTR histogram peak height from magnetization transfer MRI was used as a measure of microstructural brain parenchymal tissue homogeneity. All insulin values were log-transformed. Analyses were adjusted for age and sex, and associations are presented as standardized Beta coefficients (per increase in SD) with corresponding P-values.

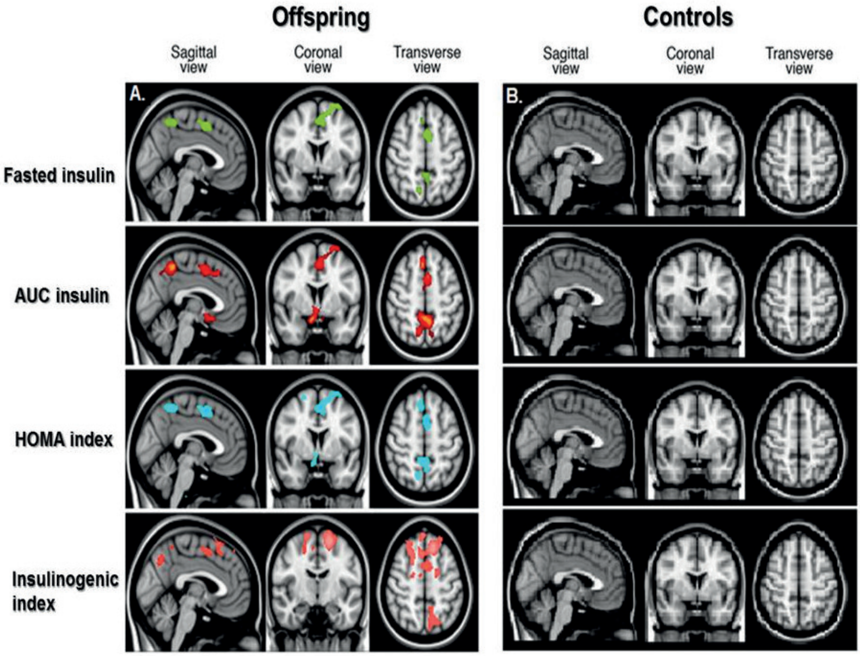

FIGURE 4.1 | Spatial distribution of associations between cortical gray matter MTR and insulin parameters in offspring and controls.

Voxel-based analysis of associations between cortical gray matter magnetization transfer ratio (MTR) and OGTT-derived insulin parameters in offspring (A.) and controls (B.). Colored areas in brain slices show statistically significant associations between gray matter MTR and OGTT derived insulin parameters, with the different colors indicating significant associations as follows: fasted insulin in green, insulin Area Under the Curve (AUC) in red, Homeostatic Model Assessment (HOMA index) of insulin resistance in blue, and insulinogenic index in pink. No colored areas are seen in the controls, because the associations were not significant in the controls.

Of the controls, there were 30 subjects in the younger control group, with mean age 60.4 (SD 4.6) years, and age range 49-65 years. The older controls consisted on 27 subjects, with mean age 71.7 (SD 4.5) years, age range 66-82 years. In the younger controls, higher fasted glucose (p=0.020), AUCglucose (p=0.001), fasted insulin (p=0.037), and HOMA-IR (p=0.022) were associated decreased MTR peak height in cortical gray matter. Similar trends were seen in the white matter, but these did not reach statistical significance, except for AUCglucose (p=0.013). In contrast, in the older controls, no significant associations were found between OGTT- derived parameters of glucose or insulin metabolism and MTR peak height in gray or white matter.

From the comparison of the age categories in offspring and controls, although the association between OGTT parameters and gray and white matter integrity were present in the offspring and controls ≤ 65 years, the differences in the strength of the observed associations between age categories were only significant in the controls, as indicated by the Pinteraction in Table 3. A visual representation of the associations according to age categories is shown in Figure 2.

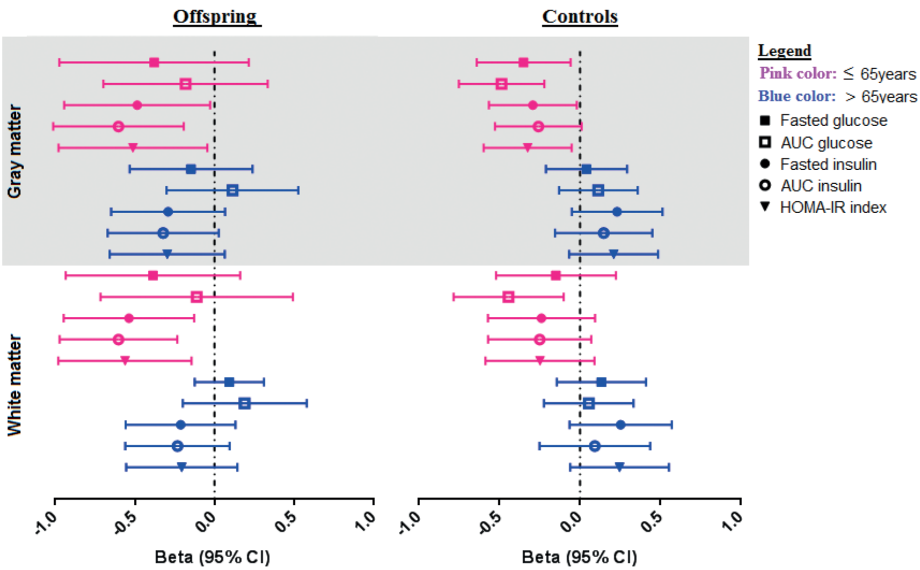

FIGURE 4.2 | Associations of OGTT parameters with gray and white matter peak height offspring and partner groups, stratified for age.

Forest plots showing the distribution of the association of OGTT parameters (fasted glucose, AUCglucose, fasted insulin, AUCinsulin, and HOMA-IR) with MTR peak height in gray and white matter in offspring and controls. The offspring and control groups were stratified into two age categories- ≤ 65 years old (shown in pink color), and > 65 years (shown in blue color). Associations are from linear regression analysis, correcting for age and sex. Associations are presented as standardized Beta coefficients with corresponding 95% CI.

Sensitivity analyses

The aforementioned associations in the offspring, controls, and in both age groups in the offspring and controls did not materially change after adjustment for age, gender, descent, smoking status, BMI and use of anti-hypertensive. In addition, since there was a significant difference between the offspring and controls in the use of lipid lowering drugs, all the analyses were repeated with adjustment for use of lipid lowering drugs. The results did not materially change. In the offspring group, decreased gray matter MTR peak height, an index of microstructural brain parenchymal homogeneity was significantly associated with higher indices of insulin resistance (fasted insulin, AUCinsulin and HOMA-IR, all $p<0.01$, see Table 2). After adjusting for use of lipid lowering drugs, decreased gray matter MTR peak height was still significantly associated with higher indices of insulin resistance (fasted insulin ($\beta = -0.411$, $p=0.018$), AUCinsulin ($\beta = -0.415$, $p=0.009$), HOMA-IR ($\beta = -0.436$, $p=0.013$), and insulinogenic index ($\beta = -0.410$, $p = 0.012$). Conversely, in the controls, gray matter MTR peak height was not significantly associated with indices of decreased insulin action, neither before nor after adjustment. Similarly, adjustment for lipid lowering medication did not materially change any of the results for white matter (Table 2) in offspring or controls (data not shown).

DISCUSSION

We report two main findings: Firstly, parameters of reduced peripheral insulin action were associated with reduced microstructural brain parenchymal homogeneity in the offspring group, but associations were less strong and did not reach statistical significance in the control group. Secondly, OGTT derived parameters of glucose metabolism were associated with reduced microstructural brain parenchymal homogeneity in 'younger' older adults, but associations seemed less strong in older age groups. Thus, the associations between reduced insulin action and reduced microstructural brain parenchymal homogeneity seemed to dampen with age and to be stronger in familial longevity.

Previous studies have shown inverse association between peripheral insulin action and brain structure and function. Inverse association between insulin parameters (fasted insulin, HOMA-IR) and brain volumes as well as executive brain function was reported in healthy older participants of the Framingham study. Furthermore, in another cohort of non- demented older adults, higher insulin levels (fasted insulin and AUCinsulin) and impairments in insulin sensitivity were found to be associated with increased rate of cognitive decline[1]. In line with these studies, we found an inverse association between parameters of peripheral insulin action (fasted and AUCinsulin, HOMA-IR and insulinogenic index) and brain microstructural integrity.

Changes in the direction and strength of associations with age have previously been observed between other metabolic risk factors and cognitive decline. While high blood pressure, high cholesterol, and overweight are associated with cognitive decline and risk of dementia in (advanced) middle-age [22-24], reversed associations were observed in very old persons, in which high blood pressure, high cholesterol and overweight seem to protect against cognitive decline [25, 26]. In our study population, we observed a weakening in the association between reduced insulin action and microstructural brain parenchymal homogeneity in advanced middle-age. Notably, in our study, we used MTI, which has the capacity of detecting microstructural changes in the aging brain. The aging brain is characterised by decline in total and segmental brain volumes, shrinkage of gray matter, loss of white matter, nerve fibres (axons), myelin and cells [27]. These subtle changes in microstructural brain parenchymal homogeneity, even in brain tissue that appears normal on conventional MR imaging sequences, can be detected and quantified using magnetization transfer imaging (MTI) [15]. MTI is a sensitive MRI technique that is based on the exchange of magnetization between protons bound to macromolecules and protons of free water molecules inside tissue. The scale of this exchange is reflected in the magnetization transfer ratio (MTR) and peak height. The MTR peak height is specifically a measure of microstructural brain parenchymal tissue homogeneity [28] that is sensitive to age-related and disease-related brain parenchymal abnormalities [14, 29], with a lower MTR peak height reflecting loss of homogeneity of the brain tissue, demyelination and axonal loss [15].

Due to the cross- sectional nature of our study, we cannot make any causal inference. Theoretically however, there are three possible interpretations for the inverse association between parameters of glucose metabolism and microstructural brain parenchymal homogeneity (brain integrity). The first theoretical explanation is that loss of brain integrity is a consequence of defects in glucose metabolism. Type 2 diabetes, characterised by hyperglycemia, insulin resistance and hyper-insulinemia, has been proposed to be involved in the pathogenesis of neurodegenerative diseases [30-32], hallmark of which are progressive loss of nerve fibres and cells. This may be due to direct damage to the brain from high circulating glucose levels. It may also be due to secondary effects, such as due to peripheral insulin resistance. A second theoretical possibility is that defects in glucose metabolism are a consequence of deficits in brain integrity. Emerging data from animal studies that show that the brain plays a physiologic role in glucose regulation [33-36] may support this possibility. The third possibility is that of the brain and metabolic dysregulation both being consequences of another common determinant. An example of a common pathway that may affect brain function as well as insulin resistance is oxidative stress [37].

Several theoretical explanations exist for the observed differences in the associations between insulin action and microstructural brain parenchymal homogeneity with age and familial longevity. It is becoming clearer that the brain plays an important role in the regulation of peripheral glucose and insulin action. Age related brain changes (reduced myelin and axons, and shrinkage of large neurons) are accompanied by reduction in brain volumes and function [27]. Brain control of glucose levels may also be affected, for which the body may compensate by higher peripheral insulin secretion. Our data show that higher insulin parameters are associated with decreased myelin and axonal integrity, and these are more pronounced in offspring and 'younger' older adults in whom glucose- regulatory compensatory mechanisms are probably more intact. Another hypothetical possibility is that in the elderly and controls, diseases may be more prevalent that could reverse the association between insulin action and microstructural brain parenchymal homogeneity. For example, diseases that are associated with weight loss might improve insulin sensitivity but decrease microstructural brain parenchymal homogeneity. Systemic diseases such as chronic kidney disease, chronic respiratory disease, diabetes mellitus, and malignancies are more prevalent in the older adults, and may cause weight loss, which in theory would be associated with improved insulin sensitivity. However, since these are systemic illnesses, the disease itself may also decrease the integrity of the brain. For example, chronic kidney disease is associated not only with weight loss, but also with microvascular damage in the brain [38].

This study is limited by its cross- sectional, observational nature. As such, the findings are purely correlative and descriptive. To clarify what is cause or consequence in the relation between insulin parameters and reduced brain integrity, intervention studies are required where insulin is specifically targeted to the brain (via the intranasal route) [39], in humans of different age categories. Another limitation is that although offspring of long-lived families are included, not all of them would carry the longevity phenotype, leading to dilution of the observed results.

Strengths of this study include the use of sensitive MRI techniques, which has the discriminatory power to detect in vivo microstructural brain changes even when peripheral glucose and insulin levels are still within normal ranges. Another strength is its unique design of investigating the relation of parameters of glucose regulation and microstructural brain parenchymal tissue homogeneity from two contrast points- familial longevity and age. The incorporation of contrasts based on familial longevity with the use of offspring and their partners' reduces the potential influence of environment, since the offspring share similar lifestyle and similar socio- economic and geographic background with their partners (age-matched controls), and so are highly comparable.

REFERENCES

1. Burns JM, Honea RA, Vidoni ED, Hutfles LJ, Brooks WM, Swerdlow RH. Insulin is differentially related to cognitive decline and atrophy in Alzheimer's disease and aging. Biochimica et biophysica acta. 2012;1822(3):333-9.
2. Devisser A, Yang C, Herring A, Martinez JA, Rosales-Hernandez A, Poliakov I, et al. Differential impact of diabetes and hypertension in the brain: adverse effects in grey matter. Neurobiology of disease. 2011;44(2):161-73.
3. den Heijer T, Vermeer SE, van Dijk EJ, Prins ND, Koudstaal PJ, Hofman A, et al. Type 2 diabetes and atrophy of medial temporal lobe structures on brain MRI. Diabetologia. 2003;46(12):1604-10.
4. Araki Y, Nomura M, Tanaka H, Yamamoto H, Yamamoto T, Tsukaguchi I, et al. MRI of the brain in diabetes mellitus. Neuroradiology. 1994;36(2):101-3.
5. Vermeer SE, Den Heijer T, Koudstaal PJ, Oudkerk M, Hofman A, Breteler MM. Incidence and risk factors of silent brain infarcts in the population-based Rotterdam Scan Study. Stroke. 2003;34(2):392-6.
6. Stolk RP, Breteler MM, Ott A, Pols HA, Lamberts SW, Grobbee DE, et al. Insulin and cognitive function in an elderly population. The Rotterdam Study. Diabetes Care. 1997;20(5):792-5.
7. Yaffe K, Blackwell T, Whitmer RA, Krueger K, Barrett Connor E. Glycosylated hemoglobin level and development of mild cognitive impairment or dementia in older women. The journal of nutrition, health & aging. 2006;10(4):293-5.
8. Wolf PA, Beiser A, Elias MF, Au R, Vasan RS, Seshadri S. Relation of obesity to cognitive function: importance of central obesity and synergistic influence of concomitant hypertension. The Framingham Heart Study. Current Alzheimer research. 2007;4(2):111-6.
9. van den Berg E, Biessels GJ, de Craen AJ, Gussekloo J, Westendorp RG. The metabolic syndrome is associated with decelerated cognitive decline in the oldest old. Neurology. 2007;69(10):979-85.
10. Schoenmaker M, de Craen AJ, de Meijer PH, Beekman M, Blauw GJ, Slagboom PE, et al. Evidence of genetic enrichment for exceptional survival using a family approach: the Leiden Longevity Study. EurJHumGenet. 2006;14(1):79-84.
11. Westendorp RG, van Heemst D, Rozing MP, Frolich M, Mooijaart SP, Blauw GJ, et al. Nonagenarian siblings and their offspring display lower risk of mortality and morbidity than sporadic nonagenarians: The Leiden Longevity Study. Journal of the American Geriatrics Society. 2009;57(9):1634-7.

12. Wijsman CA, Rozing MP, Streefland TC, le Cessie S, Mooijaart SP, Slagboom PE, et al. Familial longevity is marked by enhanced insulin sensitivity. Aging Cell. 2011;10(1):114-21.
13. Stijntjes M, de Craen AJ, van Heemst D, Meskers CG, van Buchem MA, Westendorp RG, et al. Familial longevity is marked by better cognitive performance at middle age: the Leiden Longevity Study. PloS one. 2013;8(3):e57962.
14. Sala M, de RA, van den Berg A, Altmann-Schneider I, Slagboom PE, Westendorp RG, et al. Microstructural brain tissue damage in metabolic syndrome. Diabetes Care. 2014;37(2):493-500.
15. Filippi M, Rocca MA. Magnetization transfer magnetic resonance imaging of the brain, spinal cord, and optic nerve. Neurotherapeutics : the journal of the American Society for Experimental NeuroTherapeutics. 2007;4(3):401-13.
16. Rozing MP, Westendorp RG, de Craen AJ, Frolich M, de Goeij MC, Heijmans BT, et al. Favorable glucose tolerance and lower prevalence of metabolic syndrome in offspring without diabetes mellitus of nonagenarian siblings: the Leiden longevity study. Journal of the American Geriatrics Society. 2010;58(3):564-9.
17. Pruessner JC, Kirschbaum C, Meinlschmid G, Hellhammer DH. Two formulas for computation of the area under the curve represent measures of total hormone concentration versus time-dependent change. Psychoneuroendocrinology. 2003;28(7):916-31.
18. Altmann-Schneider I, van der Grond J, Slagboom PE, Westendorp RG, Maier AB, van Buchem MA, et al. Lower susceptibility to cerebral small vessel disease in human familial longevity: the Leiden Longevity Study. Stroke; a journal of cerebral circulation. 2013;44(1):9-14.
19. Jenkinson M, Bannister P, Brady M, Smith S. Improved optimization for the robust and accurate linear registration and motion correction of brain images. Neuroimage. 2002;17(2):825-41.
20. Zhang Y, Brady M, Smith S. Segmentation of brain MR images through a hidden Markov random field model and the expectation-maximization algorithm. IEEE TransMedImaging. 2001;20(1):45-57.
21. van den Bogaard SJ, Dumas EM, Hart EP, Milles J, Reilmann R, Stout JC, et al. Magnetization transfer imaging in premanifest and manifest huntington disease: a 2-year follow-up. AJNR American journal of neuroradiology. 2013;34(2):317-22.
22. Kivipelto M, Helkala EL, Laakso MP, Hanninen T, Hallikainen M, Alhainen K, et al. Midlife vascular risk factors and Alzheimer's disease in later life: longitudinal, population based study. BMJ (Clinical research ed). 2001;322(7300):1447-51.

23. Whitmer RA, Gunderson EP, Barrett-Connor E, Quesenberry CP, Jr., Yaffe K. Obesity in middle age and future risk of dementia: a 27 year longitudinal population based study. BMJ (Clinical research ed). 2005;330(7504):1360.
24. Yaffe K, Kanaya A, Lindquist K, Simonsick EM, Harris T, Shorr RI, et al. The metabolic syndrome, inflammation, and risk of cognitive decline. JAMA. 2004;292(18):2237-42.
25. Elias MF, Elias PK, Sullivan LM, Wolf PA, D'Agostino RB. Lower cognitive function in the presence of obesity and hypertension: the Framingham heart study. International journal of obesity and related metabolic disorders : journal of the International Association for the Study of Obesity. 2003;27(2):260-8.
26. Weverling-Rijnsburger AW, Blauw GJ, Lagaay AM, Knook DL, Meinders AE, Westendorp RG. Total cholesterol and risk of mortality in the oldest old. Lancet. 1997;350(9085):1119-23.
27. Meier-Ruge W, Ulrich J, Bruhlmann M, Meier E. Age-related white matter atrophy in the human brain. AnnNYAcadSci. 1992;673:260-9.
28. Rademacher J, Engelbrecht V, Burgel U, Freund H, Zilles K. Measuring in vivo myelination of human white matter fiber tracts with magnetization transfer MR. NeuroImage. 1999;9(4):393-406.
29. Benedetti B, Charil A, Rovaris M, Judica E, Valsasina P, Sormani MP, et al. Influence of aging on brain gray and white matter changes assessed by conventional, MT, and DT MRI. Neurology. 2006;66(4):535-9.
30. de la Monte SM, Wands JR. Review of insulin and insulin-like growth factor expression, signaling, and malfunction in the central nervous system: relevance to Alzheimer's disease. Journal of Alzheimer's disease : JAD. 2005;7(1):45-61.
31. Luchsinger JA, Tang MX, Shea S, Mayeux R. Hyperinsulinemia and risk of Alzheimer disease. Neurology. 2004;63(7):1187-92.
32. Ott A, Stolk RP, van Harskamp F, Pols HA, Hofman A, Breteler MM. Diabetes mellitus and the risk of dementia: The Rotterdam Study. Neurology. 1999;53(9):1937-42.
33. Lin X, Taguchi A, Park S, Kushner JA, Li F, Li Y, et al. Dysregulation of insulin receptor substrate 2 in beta cells and brain causes obesity and diabetes. JClinInvest. 2004;114(7):908-16.
34. Lu M, Wan M, Leavens KF, Chu Q, Monks BR, Fernandez S, et al. Insulin regulates liver metabolism in vivo in the absence of hepatic Akt and Foxo1. Nature medicine. 2012;18(3):388-95.
35. Morton GJ, Matsen ME, Bracy DP, Meek TH, Nguyen HT, Stefanovski D, et al. FGF19 action in the brain induces insulin-independent glucose lowering. The Journal of clinical investigation. 2013;123(11):4799-808.

36. Schwartz MW, Seeley RJ, Tschop MH, Woods SC, Morton GJ, Myers MG, et al. Cooperation between brain and islet in glucose homeostasis and diabetes. Nature. 2013;503(7474):59-66.
37. Jayaraman A, Pike CJ. Alzheimer's disease and type 2 diabetes: multiple mechanisms contribute to interactions. Current diabetes reports. 2014;14(4):476.
38. O'Rourke MF, Safar ME. Relationship between aortic stiffening and microvascular disease in brain and kidney: cause and logic of therapy. Hypertension. 2005;46(1):200-4.
39. Chapman CD, Frey WH, 2nd, Craft S, Danielyan L, Hallschmid M, Schioth HB, et al. Intranasal treatment of central nervous system dysfunction in humans. Pharmaceutical research. 2013;30(10):2475-84.

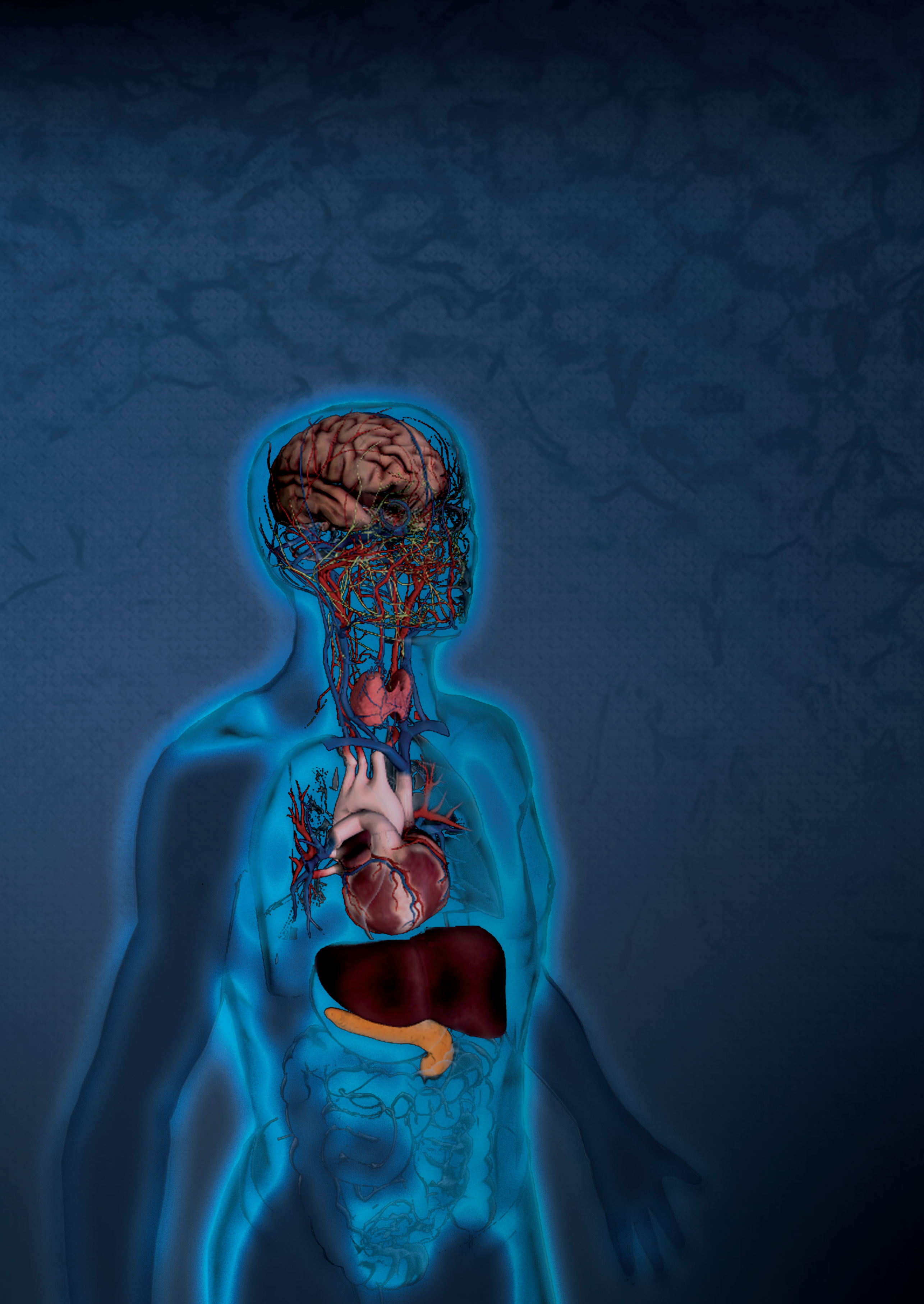

CHAPTER 5

EFFECT OF INTRANASALLY ADMINISTERED INSULIN ON CEREBRAL BLOOD FLOW AND PERFUSION; A RANDOMIZED EXPERIMENT IN YOUNG AND OLDER ADULTS

Abimbola A. Akintola*
Anna M. van Opstal*
Rudi Westendorp
Iris Postmus
Jeroen van der Grond
Diana van Heemst

*Equal contribution of authors

Submitted

ABSTRACT

Cerebral insulin acts as a vasoactive modulator regulating peripheral and cerebral blood flow. Insulin has been consistently linked to aging, lifespan and longevity. In this study, we assessed the effects of intranasally administered insulin on cerebral blood flow and perfusion in older and younger adults.

Eight healthy young men aged 20-26 years and eleven older men aged 60-69 years were intranasally administered insulin (40IU) or placebo after an overnight fast using a randomized, double-blinded, placebo-controlled crossover design. Changes in cerebral blood flow through three major cerebropetal arteries (basilar, left and right carotid arteries) were assessed by phase contrast MR angiography. Regional cortical tissue perfusion was assessed through pseudo continuous arterial spin labelling.

After intranasal administration of insulin as compared to placebo, total flow through the cerebropetal arteries was not changed, neither in young nor in older subjects. In young adults, intranasal insulin did not significantly change perfusion in any of the cortical regions tested. In older subjects, intranasal insulin compared to placebo increased perfusion through the occipital gray matter (65.2 ± 11.0 mL/100g/min vs 61.2 ± 10.1 mL/100g/min, P=0.001), the parietal gray matter (69.2 ± 11.5 mL/100g/min vs. 66.4 ± 10.9 mL/100g/min, P=0.034) and the thalamus (68.28 ± 6.75 versus 63.31 ± 6.84, P=0.003). Perfusion in the frontal and temporal gray matter was not changed.

Intranasal administration of insulin improved tissue perfusion of the parietal and occipital cortical brain regions and the thalamus in older adults. In younger adults, intranasal insulin had minimal effects, possibly because brain perfusion is not yet compromised.

INTRODUCTION

Cerebral blood flow is pivotal for providing oxygen and nutrients to the brain to maintain brain function. The brain is a highly metabolically active organ but has only limited possibilities for energy storage. Thus, cerebral blood flow is important because the brain depends on constant and regulated blood supply to function properly. With aging, pathophysiological changes occur in large arteries causing decreased ability of large arteries to absorb and dampen pulsatile blood flow, eventually leading to pulsatile stress and arterial stiffness [(1)]. Transmission of increased pulsatile stress to the brain microvasculature is thought to lead to increased microvascular brain damage via altered dampening of pulsatile blood flow in cerebral arteries, and is considered a contributing factor for some cerebrovascular diseases [(2)].

Insulin influences all aspects of human physiology, including central regulation of energy homeostasis, cognitive functions and neuronal activity [(3, 4)]. The central regulation of energy homeostasis involves a complex neuronal network, which comprises the hypothalamus, the thalamus as well as cortical brain structures. Insulin and its signaling have been consistently linked to aging, lifespan and longevity [(5)]. Aging is associated with reduced insulin action in peripheral tissues and possibly in the brain. Reduced insulin action in the aging brain may relate to age- associated cognitive defects and anomalies of metabolic homeostasis [(5-9)]. Recent data suggest that insulin is also a vasoactive modulator that regulates peripheral and cerebral blood flow, possibly via a direct vasodilatory effect [(10)]. Reduced insulin action has been associated with vascular impairment possibly via impaired insulin- mediated augmentation of endothelium- dependent vasodilation, enhanced generation of reactive oxygen species and/ or excessive free fatty acids release from adipose tissue [(11-15)].

When administered in humans via the nasal route, insulin has been shown to distinctly alter brain functions, without being absorbed into the blood stream or having direct systemic effects on peripheral blood glucose or insulin levels [(16)]. Thus, the nasal route provides a safe and effective way of conveying insulin to the brain to specifically modulate brain insulin action and exert beneficial effects.

In this randomized, placebo-controlled trial we investigated the effects of intranasal insulin administration on cerebral blood flow and perfusion in healthy young and elderly adults.

METHODS

Ethics statement

This study titled “Maintaining health in old age through homeostasis: Switchbox Phase II” was approved by the Medical Ethical Committee of Leiden University Medical Center under protocol P13.164. and the Dutch competent authority (Centrale Commissie Mensengebonden Onderzoek (CCMO)) with protocol code number NL45043.058.13. The study is registered in the European Clinical Trials Database under number 2012-005650-29. All investigations have been conducted according to the principles expressed in the Declaration of Helsinki. All participants provided written informed consent after written and verbal description of the study was given.

Trial design and participants

The design is a double-blinded, randomised, cross-over, placebo controlled trial in volunteers from the general population. This study was aimed at examining the effects of intranasal insulin on circulatory metabolic and endocrine parameters, as well as on resting and functional brain activities using MRI. Twenty-three (fourteen elderly and nine young) relatively healthy men aged 18-85 years (age criteria 18-35 years for young adults and 60-85 years for older adults), with a body mass index (BMI) between 20 kg/m2 and 27 kg/m2 were recruited from the general population. Exclusion criteria included fasting plasma glucose above 7 mmol/l, anemia (haemoglobin < 7.1 mmol/l), presence of anatomic deviations of the nose, any significant endocrine, neurological and cardiovascular diseases, or use of medication known to influence lipolysis, thyroid function, glucose metabolism, GH/IGF-1 secretion or any other hormonal axis. Furthermore, persons with a current smoking or alcohol addiction or history of substance abuse were excluded.

Of the 23 participants that were contacted via telephone, three (older) participants were excluded after screening. The reasons for exclusion were uncontrolled high blood pressure (n=1) and renal insufficiency (n=2). Of these, all participants except for one (young), successfully completed the study. The reason for drop-out was phobia for cannulas/ blood withdrawal.

Randomisation, masking and intervention

Randomisation was carried out by the pharmaceutical trial coordinator, while the researchers were blinded to what the participants received. Concealment of treatment allocation was ensured by delivery of trial medication in a standard plain vial (same for all treatment groups) that had been prepared and re-labelled by the hospital pharmacy. Deblinding was done at the end of the study.

The study interventions consisted of intranasal application of 40 IU insulin (Actrapid; Novo Nordisk, Mainz, Germany) or placebo (Sterile saline), delivered using the ViaNase Electronic Atomizer (Kurve Technology inc.). The ViaNase device had been specifically designed to deliver drugs to the olfactory region to maximize drug transport to the central nervous system. The device released a metered insulin (40 IU) or saline dose directly into the subject's nostrils. A total volume of 0.4 mL (0.2 ml per nostril) was administered, which was inhaled by breathing evenly over a 2-minute period. In both right and left nostril, two doses each were delivered resulting in a total insulin dose of 40 IU. This method allowed administration of smaller particle sizes to increase drug deposition in the upper nasal cavity without transporting the drug to the lungs [(17)].

For the current study, results from two study visits, spaced apart by a week, on one of which they received insulin and on the other placebo, in a randomised manner were compared. All participants underwent exactly the same protocol during both study visits.

Experimental protocol

In the morning after a 10-hour overnight fast, participants arrived at the MRI facilities at 08.00 in the morning. A catheter was placed in a vein of the forearm of the non-dominant hand. First, a baseline venous blood sample was collected in a serum-separator (SST)-tube thereafter, every 10 minutes, 4 ml of blood was collected into a SST-tube and 2 ml into K3-EDTA tube.

Ten minutes after the first blood withdrawal, the trial medication (placebo or 40 IU of insulin) was administered intranasally, under the supervision of the experimenter, with a ViaNase Electronic Atomizer. About 20 minutes after the intranasal application, participants were transferred into the MRI for the scanning procedure (figure 1). About 30 min after in the intranasal application, the CBF measurement was performed in the MRI scanner. This time interval was chosen to allow insulin to reach maximal concentrations in the CSF [(18)], since previous studies have shown that it takes insulin 30 minutes to reach maximal concentrations/effects in the CSF, and this approximate time window has been used in other studies where brain – related effects of intranasal insulin were studied [19-21].

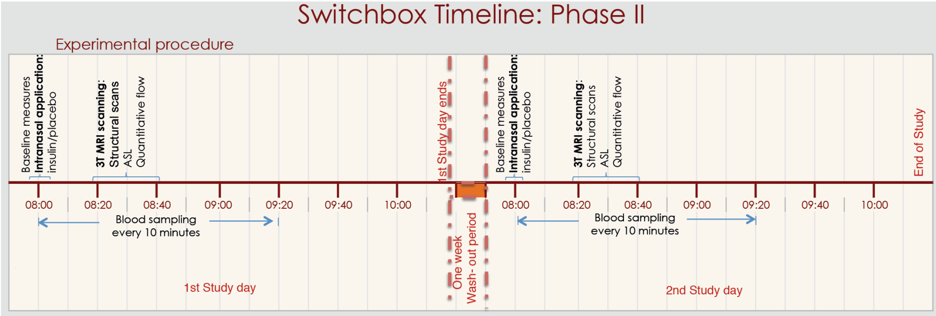

FIGURE 5.1 | Flowchart of experimental procedures related to cerebral blood flow and perfusion measurements.

After an overninght fast and baseline measures, the study day started at 08.00 with blood sample withdrawal for baseline measures, after which subjects received either the intranasal insulin or intranasal placebo treatment. MRI scanning began 20 mins later, including survey/structural MRI scans, flow and perfusion scans.

Anthropometrics.

During the first study day, height, weight, percentage of body fat, and waist and hip circumference of participants were measured. Weight (in kilograms) was divided by the squared height (in meters) to calculate the BMI.

Blood sampling and Chemical analysis of blood samples

After each withdrawal, the K3-EDTA tubes were immediately placed on ice before centrifugation, whereas the serum tubes were kept at room temperature and centrifuged when the samples were clotted, usually between 30–60 minutes. Samples were centrifuged at 3520 RPM at 4 °C for 10 minutes. The EDTA plasma and serum samples were stored in two aliquots of 500 µl during the rest of the sampling at – 20 °C. After the sampling they were transferred to a – 80 °C freezer and stored until analysis.

All laboratory measurements were performed with fully automated equipment and diagnostics from Roche Diagnostics (Almere, The Netherlands). Glucose levels were measured using Hitachi Modular P800 from Roche (Almere, the Netherlands), with coefficient of variation (CV) for measurement less than 1%. Insulin levels were measured using the Immulite 2500 from DPC (Los Angeles, CA). CV was less than 6%.

Brain MRI protocol

The perfusion measurement reported in the current study was part of a longer scanning protocol (48 minutes in young participants and 24 minutes in older participants) in which we aimed to successively assess several MRI endpoints. Scans were performed on a whole body magnetic resonance system with a 3 Tesla field strength (Philips Medical Systems, Best, the Netherlands). 3D T1-weighted images were acquired with the following imaging parameters: echo time (TE) 4.6ms, repetition time (TR) 9ms, Flip 8°, field of view (FOV) = 224 × 177 × 168mm, scan duration ~5minutes. The pseudo Continuous Arterial Spin Labeling (pCASL) with TE/TR/Flip: 14ms/4.0s/90°, FOV 240 x 133 x 240mm, matrix 80 x 80mm, slices 19, scan duration 6 minutes and the M0-scan with TE/TR/flip: 14ms/6.0s/90, FOV 240x133x240, Matrix 80 80, slices 19, scan duration 30sec. The phase-contrast quantitative flow (QF) scan was planned using 2 localizer angiograms in the sagittal and coronal planes and acquired with the following parameters: TR=11ms; TE 7.5ms; flip angle=10°; slice thickness=5mm; field of view 150x103mm; voxel size 1.17x1.17mm; velocity sensitivity=200cm/s, 20 signal averages. Time allocated to measure perfusion was 6 minutes.

Phase contrast MR Angiography

Quantitative flow measurements were performed using ungated phase-contrast MRA, based on 2 localizer MR angiograms in the sagittal and coronal orientation as shown in figure 2. A region of interest (ROI) was drawn around the vessel lumen on the magnitude images by an experienced rater using Philips Software on a PACS (Philips Medical Systems, Best, The Netherlands) workstation with ROI measurement tools. Flux was measured for basilar artery and both internal carotid arteries separately. Total flux was calculated for all three vessel together.

FIGURE 5.2 | MR images of the vasculature measured with phase contrast MR angiography imaging for Quantitive Flow (QF).

Typical placement of the QF phase-contrast slice (C) through the right internal carotid artery (RCAR), left internal carotid artery (LCAR) and the basilar artery (BAS) using the sagittal (A) and coronal (B) localizer angiograms. ROI's were drawn around the three arteries in slice C to measure flow.

pCASL quantitative analysis

MR images were analyzed using FMRIB Software Library (FSL) (Analysis Group, FMRIB, Oxford, UK). [22] pCASL cans were performed in a total time of 6 minutes. pCASL images were first corrected for slice timing, gradient nonlinearities and subject motion using in-house software and different tools of the FMRIB Software Library (FSL) version 5.0.6. Files were smoothed and after subtraction a mean CBF over the entire 6 minute pCASL scan was calculated, yielding one average perfusion map for the 6- minute scan. This map was then translated to MNI152 space using FLIRT and FNIRT with the conversion matrix based on the 3DT1 scans. The perfusion was measured in the corrected gray matter volume. This corrected gray matter was segmented in four cortical areas based on the Harvard Oxford probabilistic cortical atlas threshold 25 percent [23]. These ROI templates were subsequently used with each subject's gray matter mask to calculate the mean gray matter CBF in units of mL/100g/min for each anatomical region. Perfusion in the hypothalamus and thalamus was calculated in a similar way by measuring perfusion on the CBF maps in thalamic/hypothalamic ROI using Harvard oxford atlas ROI templates for these regions.

One participant was noticed to have extremely tortious blood vessels. For this participant, it was difficult to draw a consistent region of interest for phase contrast MR Angiography. For same reason, he also had strongly decreased ASL labelling efficiency. He was excluded from subsequent analyses.

Statistical analysis

Descriptive statistics were used to summarize the characteristics of both study groups. Homeostatic model assessment of insulin resistance (HOMA-IR) was calculated by the product of the fasting insulin level (mU/L) and the fasting glucose level (mmol/L) divided by 22.5.

The relation between intranasal insulin and cerebral blood flow was determined using paired t-tests, and presented as means with standard deviation with corresponding p-values. Homogeneity of variance assumption was tested using Levene's test. Correction for inter- individual and intra- individual differences in perfusion was done by calculating normalized gray matter volumes according to MNI standard space registration. For statistical analyses, Statistical Package for Social Sciences (SPSS) software for windows (version 20.0) was used. Statistical significance was set as $P<0.05$.

RESULTS

Characteristics of the study subjects are shown in table 1. The mean age of the younger adults was 22.3 years (range 20-26 years) while the mean age of the older adults was 65.2 (range 60-69) years. The average BMI was similar in both groups of adults. For the younger adults, mean systolic blood pressure (SBP) was 125 mmHg (SD 9.3) and diastolic blood pressure (DBP) 74.5 mmHg (SD 7.2). For the older adults, mean SBP was 156 mmHg (SD 22.7) and mean DBP was 90.4 mmHg (SD 7.9). Fasted glucose, fasted insulin and HOMA index of insulin resistance were all within normal reference ranges for both groups of adults.

Plasma glucose and insulin trajectories

We measured the peripheral (venous) glucose and insulin trajectories throughout an experimental period of 90 minutes, which comprised measurements before, during and after MRI scanning. As shown in figure 3, the trajectories of glucose and insulin values were similar and stable in insulin compared to placebo conditions throughout the experimental period, both in young and older adults. In the young adults, the mean (SD) glucose and insulin levels over the 90- minute period were 4.57 (0.3) mmol/L and 5.25 (2.7) mU/L respectively under placebo condition, while the mean (SD) glucose and insulin levels were

4.61 (0.5) mmol/L and 5.71 (2.6) mU/L respectively under insulin condition. Likewise, in the older adults, the mean (SD) glucose and insulin levels over the 90- minute period were 4.87 (0.5) mmol/L and 5.75 (3.4) mU/L respectively under placebo condition, while the mean (SD) glucose and insulin levels were 4.87 (0.5) mmol/L and 5.30 (3.6) mU/L respectively under insulin condition.

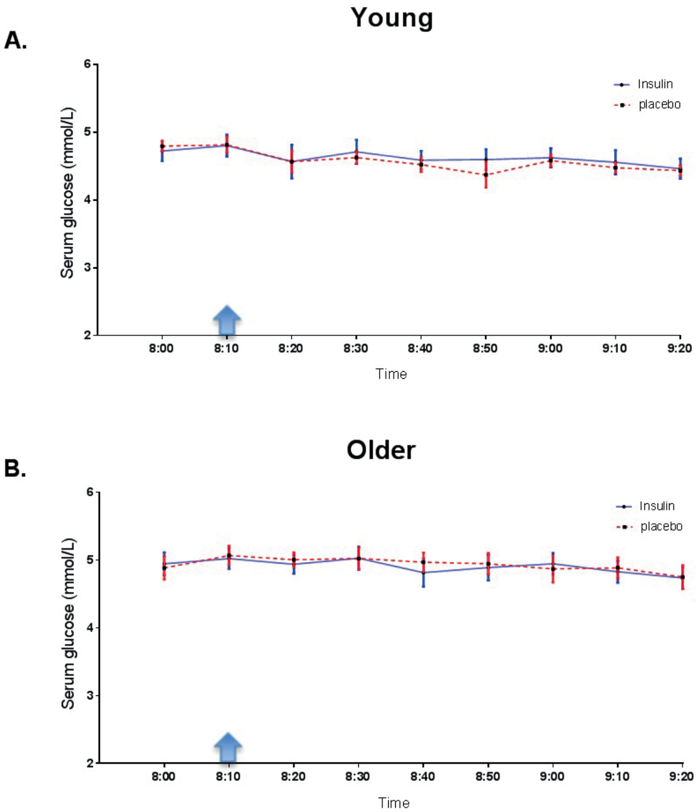

FIGURE 5.3 | Glucose trajectory during the experimental period.

Concentrations (every 10 minutes) of glucose in blood serum over a 90- minute period, comprising measurements before and after intranasal application of insulin (40IU in sulin Actrapid, blue line) or placebo (saline, red dotted line) using ViaNase nasal atomizer. Blue arrow indicate timing of intranasal insulin administration. Data is presented as mean with standard error in A.) younger and B.) older adults.

TABLE 5.1 | Characteristics of study subjects

	Young	Older
Demographics	N = 8	N = 11
Age in years (SD)	22.3 (1.8)	65.2 (3.3)
BMI in kg/m^2	23.6 (2.2)	24.1 (2.2)
Alcohol intake (units/week)	14.4 (2.2)	9.77 (1.7)
Systolic BP (mmHg)	125 (9.3)	156 (22.7)
Diastolic BP (mmHg)	74.5 (7.2)	90.4 (7.9)
Hypertension, n (%)	0 (0)	2 (18.2)
Metabolic		
Fasted glucose in mmol/L	4.83 (0.32)	5.31 (0.51)
Fasted Insulin in pmol/L, median (IQR)	5.3 (4.83, 6.58)	4.63 (2.9, 8.23)
HOMA-IR index, median (IQR)	1.21 (1.0, 1.49)	1.05 (0.65, 2.03)

Unless otherwise stated, values are means (standard deviation). BMI: body mass index.

Quantitative flow

The mean flow through the main cerebropetal arteries supplying the brain after intranasal application of insulin compared to placebo in both the young and older adults is presented in Table 2. Intranasal application of insulin did not significantly change mean blood flow through the cebebropetal arteries in either young nor in older adults. The mean difference in total quantitative flow under insulin minus placebo conditions in the younger adults was 0.35 ml/sec (SD 2.59), while that of the older adults was -0.24 ml/sec (SD 1.66).

The variance (standard deviations) around the mean flow were consistently lower after insulin administration. A Levene's test verified the inequality of the variances in total quantitative flow after intranasal application of insulin compared to placebo when data from young and old adults were combined (P=0.047). Similar trends towards lower variances in cerebral blood flow after intranasal insulin application were observed in young and older adults.

TABLE 5.2 | Quantitative flow through cerebropetal arteries

	Young			Older		
	Placebo Mean ± SD	**Insulin Mean ± SD**	***p*-value**	**Placebo Mean ± SD**	**Insulin Mean ± SD**	***p*-value**
Arterial Flow						
Basilar artery	3.36 ± 0.74	3.15 ± 0.42	0.376	2.91 ± 0.91	2.78 ± 0.63	0.313
Left carotid artery	4.44 ± 1.12	4.60 ± 0.78	0.745	4.48 ± 0.86	4.63 ± 0.69	0.537
Right carotid artery	4.24 ± 1.13	4.66 ± 0.81	0.263	4.64 ± 1.26	4.39 ± 0.75	0.532
Total flow	12.05 ± 2.73	12.40 ± 1.68	0.713	12.04 ± 2.26	11.8 ± 1.10	0.667

Cerebral blood flow (in ml/sec) ± Standard deviation (SD) through cerebropetal arteries in insulin conditions compared to placebo in young and older adults.

ASL perfusion

Perfusion through specific cortical regions of the gray matter is shown in Table 3. In addition to cortical regions, we also assessed perfusion in the thalamus and the hypothalamus. In younger adults, perfusion through the whole brain gray matter, frontal, parietal, temporal and occipital gray matter regions seemed slightly higher after intranasal administration of insulin, but were not significantly different when compared to placebo. In younger adults, intranasal administration of insulin did not change perfusion in the thalamus or in the hypothalamus.

In older adults, intranasal administration of insulin significantly increased perfusion through the occipital gray matter with 6.5% when compared to the administration of a placebo (Table 3, P=0.001). Perfusion through the parietal gray matter was 4.3% increased after intranasal administration of insulin (P=0.034). Perfusion in the frontal and the temporal gray matter regions was not significantly changed after intranasal administration of insulin (Table 3). In older adults, intranasal administration of insulin significantly increased perfusion in the thalamus (P=0.003), but no significant changes were found for perfusion in the hypothalamus. The change in perfusion after intranasal application of insulin for one representative participant is visualized in the gray matter perfusion map shown in figure 4.

TABLE 5.3 | ASL Perfusion through specific brain regions

	Young			Older		
	Placebo Mean ± SD	Insulin Mean ± SD	*p*-value	Placebo Mean ± SD	Insulin Mean ± SD	*p*-value
Brain regions						
Whole brain	65.79 ± 11.69	67.53 ± 5.58	0.488	57.53 ± 8.0	59.0 ± 9.77	0.292
Frontal GM	74.93 ± 13.67	76.64 ± 5.52	0.603	63.11 ± 8.19	63.90 ± 10.72	0.653
Temporal GM	62.48 ± 10.82	64.39 ± 7.47	0.405	55.83 ± 7.22	55.74 ± 9.22	0.959
Parietal GM	77.2 ± 14.87	78.66 ± 7.04	0.653	66.35 ± 10.95	69.22 ± 11.51	0.034
Occipital GM	67.67 ± 13.21	68.27 ± 8.97	0.837	61.20 ± 10.11	65.15 ± 11.0	0.001
Thalamus	65.43 ±10.27	65.84 ± 9.89	0.831	63.31 ± 6.84	68.28 ± 6.75	0.003
Hypothalamus	43.97 ± 8.64	42.31 ± 6.43	0.603	38.31 ± 5.25	42.51 ± 6.43	0.156

Perfusion through the four major cortical gray matter regions (ml/100g/min) ± Standard deviation (SD) in insulin conditions compared to placebo in young and older adults as measured by continuous arterial spin labelling. GM: gray matter.

In addition to the whole gray matter regions, we also looked at the perfusion through the right and left hemisphere of each ROI separately. The directions of observed effects in the left/right ROIs were comparable to those observed for the whole lobe ROIs. For example, in older participants perfusion in the right parietal region under placebo compared to insulin condition was 65.58 ± 11.70 compared to 68.31 ± 11.17 (p=0.061); and perfusion in the left parietal region under placebo compared to insulin condition was 67.12 ± 10.41compared to 70.12 ± 12.71 (p=0.221). Similarly, in older participants perfusion in the right occipital region under placebo compared to insulin condition was 60.92 ± 11.07 compared to 65.15 ± 10.97 (p=0.006); and perfusion in the left occipital region under placebo compared to insulin condition was 61.49 ± 9.35 compared to 65.13 ± 11.61 (p=0.005). Likewise, in older participants perfusion in the right thalamus under placebo compared to insulin condition was 63.79 ± 6.72 compared to 68.52 ± 6.14 (p=0.008); and perfusion in the left thalamus under placebo compared to insulin condition was 62.84 ± 7.11 compared to 68.03 ± 7.63 (p=0.005).

Figure 5 shows the paired gray matter perfusion in the parietal and occipital lobes and in the thalamus for every individual subject separately to illustrate individual differences between the placebo and insulin.

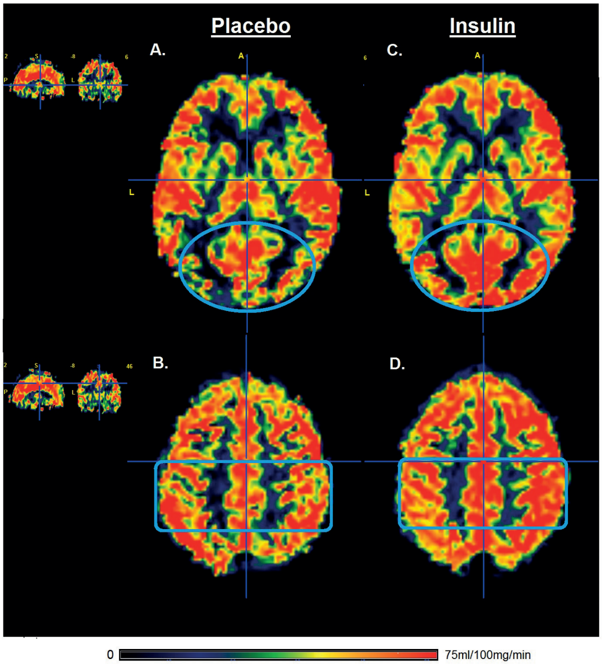

FIGURE 5.4 | Gray matter perfusion maps after intranasal administration of placebo and insulin.

Left panel (A. & B.) represents the gray matter perfusion map after intranasal placebo administration and the right panel (C. & D.) the perfusion map after intranasal insulin administration for one representative older participant. The top row shows an increase in the gray matter perfusion of occipital lobe (illustrated by blue oval) after intranasal administration of insulin compared to placebo. The bottom row shows an increase in gray matter perfusion in the parietal lobe (illustrated by blue rectangle) after intranasal administration of insulin compared to placebo. Only the gray matter was included for calculation of perfusion after intranasal administration of insulin compared to placebo.

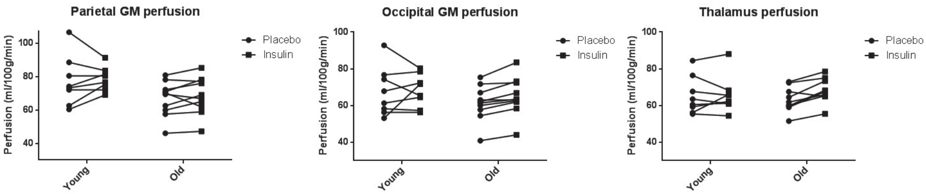

FIGURE 5.5 | Paired individual gray matter perfusion measurements for placebo and insulin conditions.

Left panel represents the gray matter perfusion in the parietal lobe as paired data for placebo and intranasal insulin per indivudual subject in the young and the older group. The right panel represents the gray matter perfusion in the occipital lobe.

DISCUSSION

This study was aimed at investigating the effects of intranasal application of insulin on cerebral blood flow and perfusion in healthy young and older adults. We found no effect of intranasal insulin application on total quantitative flow, or on flow in the basilar, left or right carotid arteries, in either young nor older adults. However, region specific analysis indicated that intranasal insulin application increased perfusion in parietal and occipital gray matter regions and in the thalamus in older but not in young adults.

Due to the presence of direct pathways from the nasal cavity to the CNS, insulin can be delivered non- invasively rapidly to the CNS through the intranasal route without spilling over to the periphery. The intranasal route of insulin administration thus bypasses uptake into the bloodstream and so circumvents the risk of systemic hypoglycemia that is associated with peripheral administration. We found that blood glucose and insulin levels did not change after intranasal administration. This is in line with previous studies that show that plasma glucose concentrations remain unchanged after intranasal application of 40 IU insulin [24, 25]. It further strengthens the fact that intranasal administration can safely be used for selectively increasing cerebral insulin levels.

One of the regions where insulin becomes readily available is the cerebral cortex, which is bathed by CSF, to which intranasally administered insulin has direct access [18]. There is evidence of bulk flow transport of peptides through extracellular pathways from the nasal cavity to the CNS, including cerebral cortex, gray matter and other parts of the CNS, via both olfactory and trigeminal pathways [26]. In the upper nasal cavity, olfactory neurons are exposed such that their axons project through the cribriform plate to the olfactory bulb. When inhaled, insulin accesses the CNS parenchyma either through the cribriform plate along the olfactory neurons through perivascular channels associated with the olfactory or trigeminal systems [27].

Very few studies have been performed to study the effect of intranasal application of insulin on regional blood flow in the brain. A recent study done in eight young healthy adults found no effect of intranasal insulin application on cerebral blood flow in the visual cortex, neither at baseline nor when cerebral blood flow was measured after specific tasks [19]. In line, we found no effect of intranasal insulin application on flux in the major vessels, neither in young healthy men, nor in older men.

While quantitative flow in the major arteries did not increase after intranasal application of insulin, we found that after intranasal insulin application tissue perfusion was increased by 6.5% in occipital cortex and 4.3% in parietal cortex in older but not in young adults. The occipital lobe is the visual processing center. It contains mainly the visual cortex and the ventral stream of vision that enables ability to focus on motor actions in response to outside stimuli. Next to the occipital lobe, the parietal lobe integrates sensory information among various modalities, including proprioception, mecano-reception, and visuo-spatial processing. The posterior parietal cortex, also referred to as the dorsal stream of vision, receives somatosensory and/or visual input that can be transmitted to motor signals. In line with the present data, another study found that perfusion was increased in the insular cortex, an area closely related to the parietal cortex, after intranasal insulin administration [(21)]. Somewhat similar to the parietal cortex, the insular cortex also integrates information from other sensory modalities and contains topographically organized visceral sensory representation. We also observed that intranasal insulin application increased perfusion of the thalamus. The thalamus receives information from almost all sensory systems and relays the information to associated cortical areas. From literature, increased cerebral blood flow has been linked to vasodilatation around the active area due to increased energy demand [(28)]. Also, insulin has been shown to be a vasoactive modulator that regulates peripheral and cerebral blood flow possibly via a direct vasodilatory effect [(10)]. Taken together, our finding of increased perfusion on the parietal and occipital cortex and in the thalamus in the older adults would support the hypothesis that intranasal insulin application might restore energy demand and neuronal activity in these regions in the older adults, possibly by overcoming age- induced deficits in local central insulin action [(5, 29)]. Similar finding was not demonstrated in the young men, probably because they already had optimal brain perfusion.

This is the first placebo-controlled, cross- over, study in young and older adults showing that intranasally administered insulin increased regional perfusion in the parietal and occipital brain regions and in the thalamus of older adults, as measured with a non-invasive ASL technique. A strength of our study is the cross-over design in which the adults were their own controls, thus minimizing the confounding effects of between- person differences. Moreover, both the young and older participant were included with strict in- and exclusion criteria. Thus, the characteristics of adults in both the young and older participant groups were homogenous, making them comparable within the group. On the other hand, this study has some limitations. It is limited by its sample size, and the inclusion of males only. Thus, we cannot rule out that insulin has effect on many other brain areas, since several previous studies have demonstrated that insulin had beneficial effects on brain function including, memory, cognition [30-32], and brain mediated functions such as postprandial thermogenesis and other metabolic profiles [29, 33-35]. Thus, other brain regions could have gone undetected because of the small sample size. We also cannot exclude the possibility that effects of intranasal administration of insulin may be sex specific. Indeed, sex-specific effects of intranasal administration of insulin have been observed for other endpoints, including reduction of body weight [34]. It is also a limitation that the clinical significance of the observed increases in CBF remains to be determined. Thus, larger sufficiently powered studies are needed to delineate the exact effects of insulin on cerebral blood flow and perfusion in both the cortical brain regions and in subcortical structures in both males and females and in both young and older adults and to relate these to clinically significant outcomes.

REFERENCES

1. Safar ME. Arterial aging--hemodynamic changes and therapeutic options. Nature reviews Cardiology. 2010;7(8):442-9.
2. Zarrinkoob L, Ambarki K, Wahlin A, Birgander R, Carlberg B, Eklund A, et al. Aging alters the dampening of pulsatile blood flow in cerebral arteries. Journal of cerebral blood flow and metabolism : official journal of the International Society of Cerebral Blood Flow and Metabolism. 2016.
3. Duarte AI, Moreira PI, Oliveira CR. Insulin in central nervous system: more than just a peripheral hormone. JAging Res. 2012;2012:384017.
4. Schwartz MW, Seeley RJ, Tschop MH, Woods SC, Morton GJ, Myers MG, et al. Cooperation between brain and islet in glucose homeostasis and diabetes. Nature. 2013;503(7474):59-66.
5. Akintola AA, D. vH. Insulin, aging and the brain: mechanisms and implications. frontiers in endocrinology. 2015;volume 6(article 13):1-13.
6. Krug R, Benedict C, Born J, Hallschmid M. Comparable sensitivity of postmenopausal and young women to the effects of intranasal insulin on food intake and working memory. The Journal of clinical endocrinology and metabolism. 2010;95(12):E468-72.
7. Scherer T, Lehnert H, Hallschmid M. Brain insulin and leptin signaling in metabolic control: from animal research to clinical application. Endocrinology and metabolism clinics of North America. 2013;42(1):109-25.
8. Schoenmaker M, de Craen AJ, de Meijer PH, Beekman M, Blauw GJ, Slagboom PE, et al. Evidence of genetic enrichment for exceptional survival using a family approach: the Leiden Longevity Study. European journal of human genetics : EJHG. 2006;14(1):79-84.
9. Akintola AA, van den Berg A, Van Buchem MA, Jansen S, Slagboom E, Westendorp R, et al. Associations between insulin action and integrity of brain microstructure differ with familial longevity and with age. Frontiers in Aging Neuroscience. 2015;7(92).
10. Hughes TM, Craft S. The role of insulin in the vascular contributions to age-related dementia. Biochimica et biophysica acta. 2015.
11. Barazzoni R, Zanetti M, Gortan Cappellari G, Semolic A, Boschelle M, Codarin E, et al. Fatty acids acutely enhance insulin-induced oxidative stress and cause insulin resistance by increasing mitochondrial reactive oxygen species (ROS) generation and nuclear factor-kappaB inhibitor (IkappaB)-nuclear factor-kappaB (NFkappaB) activation in rat muscle, in the absence of mitochondrial dysfunction. Diabetologia. 2012;55(3):773-82.

12. Cersosimo E, DeFronzo RA. Insulin resistance and endothelial dysfunction: the road map to cardiovascular diseases. Diabetes/metabolism research and reviews. 2006;22(6):423-36.
13. Kozakova M, Palombo C. Diabetes Mellitus, ArterialWall, and Cardiovascular Risk Assessment. International journal of environmental research and public health. 2016;13(2).
14. Nigro J, Osman N, Dart AM, Little PJ. Insulin resistance and atherosclerosis. Endocrine reviews. 2006;27(3):242-59.
15. Steinberg HO, Chaker H, Leaming R, Johnson A, Brechtel G, Baron AD. Obesity/insulin resistance is associated with endothelial dysfunction. Implications for the syndrome of insulin resistance. The Journal of clinical investigation. 1996;97(11):2601-10.
16. Hallschmid M, Benedict C, Schultes B, Perras B, Fehm HL, Kern W, et al. Towards the therapeutic use of intranasal neuropeptide administration in metabolic and cognitive disorders. Regulatory peptides. 2008;149(1-3):79-83.
17. Djupesland PG, Skretting A, Winderen M, Holand T. Bi-directional nasal delivery of aerosols can prevent lung deposition. Journal of aerosol medicine : the official journal of the International Society for Aerosols in Medicine. 2004;17(3):249-59.
18. Born J, Lange T, Kern W, McGregor GP, Bickel U, Fehm HL. Sniffing neuropeptides: a transnasal approach to the human brain. Nature neuroscience. 2002;5(6):514-6.
19. Grichisch Y, Cavusoglu M, Preissl H, Uludag K, Hallschmid M, Birbaumer N, et al. Differential effects of intranasal insulin and caffeine on cerebral blood flow. Human brain mapping. 2012;33(2):280-7.
20. Heni M, Kullmann S, Ketterer C, Guthoff M, Linder K, Wagner R, et al. Nasal insulin changes peripheral insulin sensitivity simultaneously with altered activity in homeostatic and reward-related human brain regions. Diabetologia. 2012;55(6):1773-82.
21. Schilling TM, Ferreira de Sa DS, Westerhausen R, Strelzyk F, Larra MF, Hallschmid M, et al. Intranasal insulin increases regional cerebral blood flow in the insular cortex in men independently of cortisol manipulation. Human brain mapping. 2014;35(5):1944-56.
22. Jenkinson M, Bannister P, Brady M, Smith S. Improved optimization for the robust and accurate linear registration and motion correction of brain images. Neuroimage. 2002;17(2):825-41.
23. Desikan RS, Segonne F, Fischl B, Quinn BT, Dickerson BC, Blacker D, et al. An automated labeling system for subdividing the human cerebral cortex on MRI scans into gyral based regions of interest. NeuroImage. 2006;31(3):968-80.
24. Novak V, Milberg W, Hao Y, Munshi M, Novak P, Galica A, et al. Enhancement of vasoreactivity and cognition by intranasal insulin in type 2 diabetes. Diabetes Care. 2014;37(3):751-9.

25. Reger MA, Watson GS, Green PS, Wilkinson CW, Baker LD, Cholerton B, et al. Intranasal insulin improves cognition and modulates beta-amyloid in early AD. Neurology. 2008;70(6):440-8.
26. Hanson LR, Frey WH, 2nd. Intranasal delivery bypasses the blood-brain barrier to target therapeutic agents to the central nervous system and treat neurodegenerative disease. BMC neuroscience. 2008;9 Suppl 3:S5.
27. Thorne RG, Frey WH, 2nd. Delivery of neurotrophic factors to the central nervous system: pharmacokinetic considerations. Clinical pharmacokinetics. 2001;40(12):907-46.
28. Attwell D, Iadecola C. The neural basis of functional brain imaging signals. Trends in neurosciences. 2002;25(12):621-5.
29. Jauch-Chara K, Friedrich A, Rezmer M, Melchert UH, H GS-E, Hallschmid M, et al. Intranasal insulin suppresses food intake via enhancement of brain energy levels in humans. Diabetes. 2012;61(9):2261-8.
30. Benedict C, Hallschmid M, Hatke A, Schultes B, Fehm HL, Born J, et al. Intranasal insulin improves memory in humans. Psychoneuroendocrinology. 2004;29(10):1326-34.
31. Guthoff M, Grichisch Y, Canova C, Tschritter O, Veit R, Hallschmid M, et al. Insulin modulates food-related activity in the central nervous system. The Journal of clinical endocrinology and metabolism. 2010;95(2):748-55.
32. Ott V, Benedict C, Schultes B, Born J, Hallschmid M. Intranasal administration of insulin to the brain impacts cognitive function and peripheral metabolism. Diabetes, obesity & metabolism. 2012;14(3):214-21.
33. Benedict C, Brede S, Schioth HB, Lehnert H, Schultes B, Born J, et al. Intranasal insulin enhances postprandial thermogenesis and lowers postprandial serum insulin levels in healthy men. Diabetes. 2011;60(1):114-8.
34. Hallschmid M, Benedict C, Schultes B, Fehm HL, Born J, Kern W. Intranasal insulin reduces body fat in men but not in women. Diabetes. 2004;53(11):3024-9.
35. Heni M, Wagner R, Kullmann S, Veit R, Mat Husin H, Linder K, et al. Central insulin administration improves whole-body insulin sensitivity via hypothalamus and parasympathetic outputs in men. Diabetes. 2014;63(12):4083-8.
36. Zhang R, Zuckerman JH, Levine BD. Spontaneous fluctuations in cerebral blood flow: insights from extended-duration recordings in humans. American journal of physiology Heart and circulatory physiology. 2000;278(6):H1848-55.

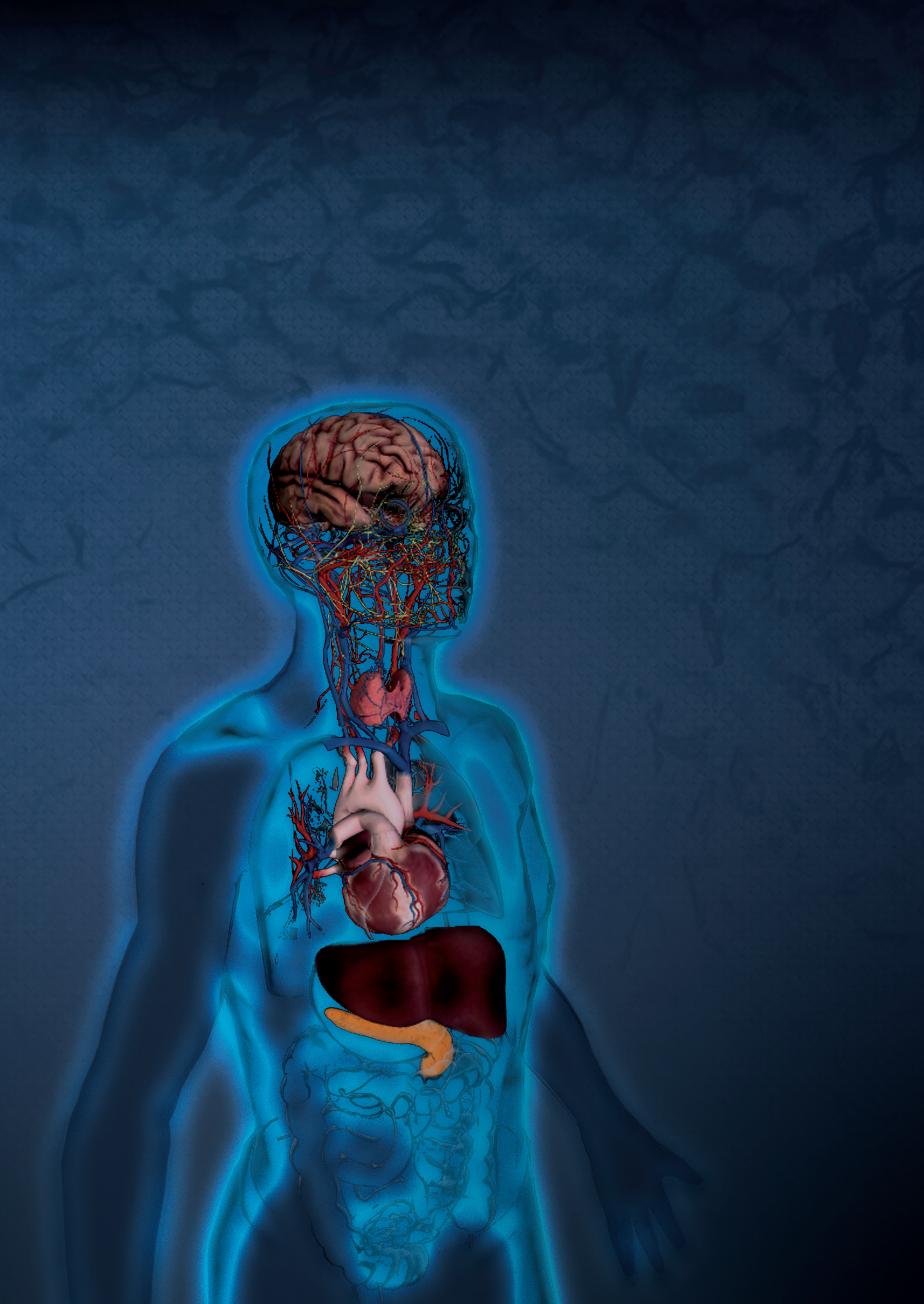

CHAPTER 6

INSULIN, AGING AND THE BRAIN: MECHANISMS AND IMPLICATIONS

Abimbola A. Akintola
Diana van Heemst

Front Endocrinol (Lausanne). 2015 Feb 6;6:13.

ABSTRACT

There is now an impressive body of literature implicating insulin and insulin signaling in successful aging and longevity. New information from in vivo and in vitro studies concerning insulin and insulin receptors has extended our understanding of the physiological role of insulin in the brain. However, the relevance of these to aging and longevity remains to be elucidated. Here, we review advances in our understanding of the physiological role of insulin in the brain, how insulin gets into the brain, and its relevance to aging and longevity. Furthermore, we examine possible future therapeutic applications and implications of insulin in the context of available models of delayed and accelerated aging.

INTRODUCTION

Pathways that orchestrate the responses of the organism to changes in its environment have been implicated in the genetic regulation of lifespan across different species. One of the key pathways identified by genetic analysis of long-lived Caenorhabditis elegans (C.elegans) mutants is insulin/insulin-like growth factor-1 (IGF-1) signaling (IIS) [1, 2]. In invertebrates, multiple insulin/IGF-1-like ligands signal via a common receptor, which shows homology to the mammalian insulin and IGF-1 receptors. Also in mammals, insulin/IGF-1 signaling has been linked to aging, lifespan and longevity [3]. Although in mammals insulin and IGF-1 act predominantly via distinct receptors, there is extensive overlap and interaction in their downstream signaling cascades, making it difficult to separate effects of insulin signaling from those of IGF-1 signaling. The long-lived phenotype of FIRKO mice, which were made by selective disruption of the insulin receptor in adipose tissue, supports a role of insulin signaling in longevity [4]. Moreover, many of the long-lived mouse mutants with disrupted GH/IGF-1 signaling display enhanced insulin sensitivity. In humans, a hallmark phenotype of healthy longevity is maintenance of insulin sensitivity [5, 6], which has been observed in familial human longevity [7, 8], as well as in centenarians [9-11]. Insulin influences all aspects of human physiology [12, 13]. Besides regulating peripheral glucose homeostasis, insulin is an important neuromodulator that contributes to neurobiological processes [14], with growing evidence that insulin supports behavioral, cellular, biochemical and molecular functions [15]. In literature, evidence linking aging and insulin signaling includes prolongation of life span in rodents via genetic mutations affecting insulin signaling pathways or via interventions that down-regulate nutrient sensing pathways such as caloric restriction. Further evidence includes data on the role of type 2 diabetes in accelerated aging syndromes, and the increased incidence of insulin resistance with age [16]. In model organisms (nematodes and fruit flies), specific neural manipulations of insulin signaling have also been linked to aging and lifespan [17, 18]. Insulin is produced in the brain of these organisms, making it undoubtedly a neuropeptide. In mammals and humans, insulin receptors are highly abundant in many brain areas and nuclei, but it remains unclear if insulin is produced in the brain. Furthermore, the physiological and pathophysiological mechanisms of insulin action in the brain in relation to aging and longevity remain to be elucidated.

With the global population aging, there has been an astonishing increase in the prevalence of obesity [19], metabolic syndrome [20], type 2 diabetes [21] and neurodegenerative diseases [22]. Insulin resistance is a shared feature in these diverse pathologies [13, 23-26]. It therefore becomes critical to understand the role of insulin in healthy longevity, as this may be relevant to combatting age related disorders that have been linked to disturbances in glucose metabolism. The aim of this article is to review advances in our knowledge about insulin, insulin signaling and the brain, and to present these in the context of available models of delayed and accelerated aging. Furthermore, we will examine the links between inflammation, metabolic health and brain health, and their effect on aging. Finally, we will review therapeutic options to enhance brain insulin action, including measures to enhance local brain insulin levels as well as measures to enhance the brain responses to insulin.

INSULIN AND THE BRAIN: A CENTURY OF DISCOVERIES

Insulin, after discovery in 1921, was initially considered a peripheral hormone and thus unable to cross the blood- brain barrier [27]. However, in 1967, Margolis and Altszuler demonstrated in dogs that the concentration of cerebrospinal fluid (CSF) insulin increased after an increase in plasma insulin [28], thus showing that insulin is able to cross the blood CSF barrier. In 1978, Havrankova et al. demonstrated the widespread presence of insulin receptors in the central nervous system of the rat [29]. Later that year, they further demonstrated that high levels of insulin were present in rat brain extracts, and found that the concentration of insulin in the central nervous system was considerably higher than its concentration in the circulation [30]. They thus proposed a physiological role for insulin in the central nervous system. In the 1980s, further evidence that insulin from peripheral circulation crosses the blood brain barrier (BBB) thus gaining access to the brain was provided. In 1983, Dorn et al. demonstrated that the human brain contains insulin in concentrations much higher than the blood, the highest being in the hypothalamus [31]. Furthermore, they showed the presence of high concentrations of insulin in the brains and spinal cords of human cadavers, mice and rats [32]. Baskin et al demonstrated uptake in the hypothalamus of [125I]iodoinsulin after the insulin had been stereotaxically injected into a lateral cerebral ventricle. Furthermore, they detected insulin-like immunoreactivity in the periventricular, supraoptic, suprachiasmatic, arcuate, and lateral hypothalamic nuclei of the rat hypothalamus [33, 34]. In 1992, Schechter et al delineated the ontogeny of rabbit brain insulin concentration and demonstrated that insulin availability is developmentally regulated [35]. In the past decade, studies of the effects of insulin in the brain have been enhanced after development of non-invasive methods of selective delivery of insulin into the brain, via the intranasal route, circumventing peripheral effects of systemic hypoglycemia [36]. This has advanced our understanding of potentially therapeutic effects of enhancing insulin concentrations in the brain. Furthermore, studies in recent years have brought forward the role of insulin signaling in the hypothalamus, as a key player in regulation of hepatic glucose production and food intake [37].

Brain insulin: is insulin a neuropeptide in humans?

In the rabbit, discordance was observed between insulin concentrations in serum and CSF [35]. Insulin was found to be present in high concentrations in brain micro-vessels [38], brain extracts [39], and immature nerve cell bodies [35, 40], despite that only 0.046% of peripheral insulin crosses the BBB in mice [12, 41]. Moreover, brain insulin concentrations were observed to vary according to developmental stages, with peak amounts being observed during the critical phases of brain growth and development [42]. Taken together, these results suggest that brain insulin availability is strictly regulated and can reach high levels in the CNS. This raises the question as to the source of brain insulin, does all of brain insulin derive from the periphery or is insulin also synthesized in the brain (Figure 1)?

There is unequivocal evidence for selective, regulated, time dependent, temperature sensitive, carrier mediated, and saturable insulin transport to the brain [43-50]. In mice, human insulin was shown to access the central nervous system (CNS) after crossing the BBB [51]. In rabbits, insulin infused into the carotid artery was shown to have crossed the BBB into the peri-capillary space and brain parenchyma with preservation of the peptide's integrity [45]. In dogs, studies using a three component mathematical model (plasma, intermediate component and CSF) have shown that insulin delivery to the CNS fits a receptor- mediated saturable process [43]. In healthy humans, during hyperinsulinemic, euglycemic clamp studies, increase in circulating insulin was demonstrated to rapidly affect brain activity, alongside rapid cerebral insulin signal transduction, independent of the systemic effects of the insulin[48].

Apart from passage through the BBB, direct access of insulin to the CSF has also been demonstrated (Figure 1). This alternative route occurs through circumventricular regions, such as the area postrema, that lack a BBB [34, 52-54]. Unlike the BBB that contains tight junctions, the capillaries in the circumventricular regions are porous, thereby allowing plasma solubles to diffuse freely and directly into these areas [55]. The route through which insulin accesses the brain has implications for the rate of convection and diffusion in the brain, and distribution of the insulin into the brain parenchyma. Following intraventricular administration of insulin/ peptides, insulin becomes distributed through the ventricular compartments and to the surface of the brain bathed by the subarachnoid space, with relatively slow rate of diffusion into the brain parenchyma, and is minimal at distances more than 1-2mm removed from the CSF surface [55, 56]. In addition, insulin delivered into the CSF undergoes relatively rapid bulk flow through the CSF flow tracks. For example, the entire CSF volume is turned over every 4-5 hours following production at the choroid plexus in the human brain [55].

In model organisms, insulin is biosynthesized by neurons in the brain and it exerts both local and remote actions, including regulation of homeostasis; making it undoubtedly a neuropeptide. In humans however, insulin is mainly produced in the pancreas, which raises the question as to whether insulin can be considered a neuropeptide in humans. Neuropeptides have been defined as 'small proteinaceous substances produced and released by neurons through the regulated secretory route and acting on neural substrates' [57]. Neuropeptides have been shown to have strict, cell specific expression patterns, on which the physiological or behavioral role of the peptides is based. Criteria for classification as a neuropeptide include gene expression and biosynthesis by neurons; storage, and regulated release upon demand and ability to modulate or mediate neural functioning directly through receptors [57]. Although insulin receptors are highly abundant in many brain areas and nuclei, it remains unclear if insulin is produced in the brain. Therefore, following the strict criteria for neuropeptide definition, it becomes debatable if mammalian insulin is a true neuropeptide.

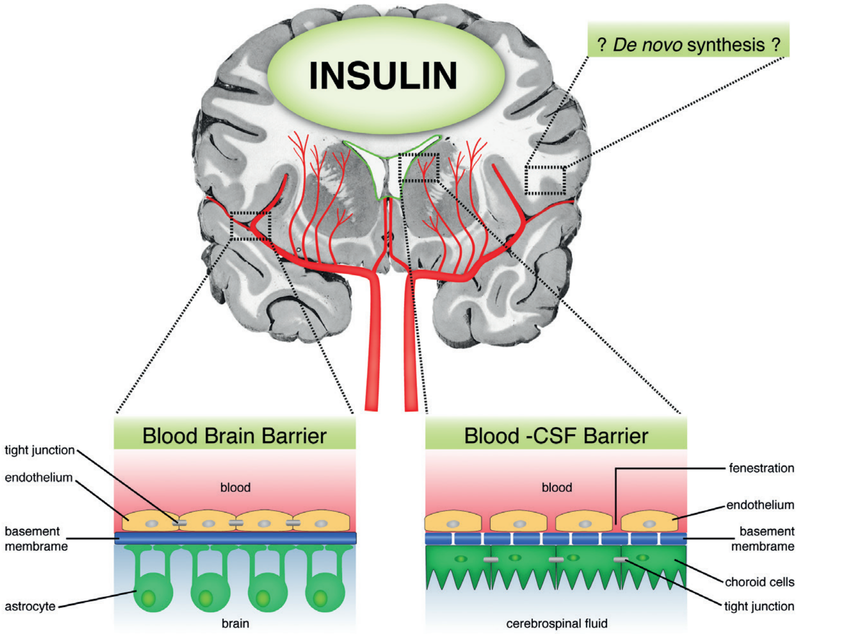

FIGURE 6.1 | Sources of brain insulin.

Schematic diagram showing the possible sources of brain insulin. Firstly, eripheral insulin can access the brain through the blood brain barrier (BBB) via a selective, carrier-mediated transport system. Secondly, insulin may diffuse through the blood CSF barrier in circumventricular regions, which are lacking in BBB. Thirdly, there is some limited evidence suggesting the possibility of ***de novo*** *insulin synthesis in the brain.*

Evidence in favor of insulin synthesis in the brain mostly derives from in vitro studies, including the study by Clarke et al in 1986, which demonstrated the synthesis of insulin by cultured rat brain neuronal and astrocyte glial cells and their release of insulin in primary culture. The insulin release after membrane depolarization of the neurons was biphasic, in a manner similar to that of pancreatic beta cells [(58)]. In 1990s, Schechter et al provided both in vivo and in vitro evidence from mammalian brains supporting the de novo synthesis of insulin. In-vitro evidence included the demonstration of preproinsulin I and II mRNA in neuron cell cultures of fetal rat brains [(59)]. From in vivo studies, presence of preproinsulin I and II mRNAs and insulin immunoreaction was detected within the rough endoplasmic reticulum, the Golgi apparatus, cytoplasm, axon, synapsis and dendrites of the rat fetal brain [(40)].

Summarily, as can be seen in figure 1, whether insulin is derived from the periphery, local sources or both, insulin is present in the CNS, where it subserves many functions and contributes to neurobiological processes.

Activation of insulin receptors in the brain

As in peripheral tissues, insulin signaling in the brain occurs mainly via the insulin receptor pathway (Figure 2), which contains several critical nodes of interaction with other signaling pathways [60].

Activation of the core insulin signaling cascade starts with binding of the insulin ligand to the insulin receptor (IR), which belongs to the family of tyrosine kinase receptors, auto phosphorylation of which is essential for their activation. Upon activation, the IR phosphorylates insulin receptor substrate (IRS) proteins. IRS proteins are also activated upon binding of the IGF-1 ligand to its cognate receptor. Thus, IRS proteins represent a critical node of conversion of the insulin and IGF-1 signaling cascades, and their crosstalk with other pathways, such as cytokine signaling. In addition to its activation of the Ras–mitogen-activated protein kinase (MAPK) pathway, activated IRS proteins serve as docking sites for the assembly and activation of, amongst others, phospho-inositol-3 kinase (PI3K) which generates the lipid second messenger phosphatidylinositol 3,4,5-triphosphate (PIP3). PI3K represents another critical node of crosstalk with other signaling pathways, including the c-Jun-N-terminal kinase (JNK) stress signaling pathway. Elevated levels of PIP3 activate phosphoinositide-dependent protein kinase-1 (PDK1) and AKT. AKT represents yet another critical node of interaction with the mammalian target of rapamycin (mTOR) nutrient signaling pathway. AKT targets include GSK3 (glycogen synthase kinase 3), AS160 (Akt substrate of 160 kD, phosphorylation of which is required for translocation of the glucose transporter GLUT4 to the plasma membrane) and forkhead transcription factors (FOXOs) (figure 2). Phosphorylation of FOXOs induces their translocation from the nucleus which causes profound changes in the transcription of key factors implicated in metabolism, cell cycle regulation, apoptosis and resistance to oxidative stress [61].

Distribution of insulin receptors in the brain

In higher mammals and humans, insulin receptors are widely distributed throughout peripheral tissues, with their main function being to transport glucose into cells, inhibit glucose production and increase glucose uptake by triggering signaling pathways in the liver, muscle and fat [62]. The insulin receptor consists of a tetramer, with two alfa subunits and two beta subunits. Brain IR subunits differ structurally from peripheral IR subunits in that they have a lower molecular weight [63] and can withstand exposure to high concentrations of insulin without undergoing down-regulation [64, 65].

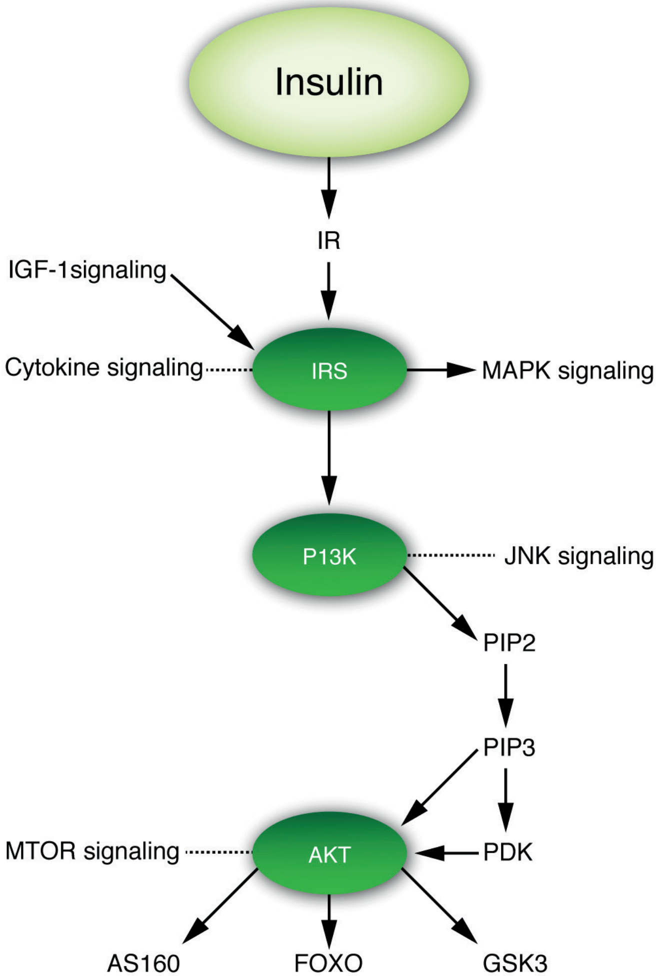

FIGURE 6.2 | Insulin-IRS-P13K-AKT signaling cascade and its crosstalk with other signaling pathways.

Figure denotes three critical nodes in insulin signaling that are important for the interaction of insulin signaling with other pathways relevant to this review.

The mammalian brain has specific insulin receptors [29, 66], which are of two types. One is the neuronal/ neuron- specific type, which are abundant in the neuron [67], while the second type are the non- neuronal/ peripheral- like type, with lower density in glial cells [38, 66, 68]. Insulin receptors are highly abundant in the neurons, with high protein concentrations in cell bodies and synapses, and less abundant in the glia. Brain insulin receptors are abundant in the brain, but are highly enriched in the olfactory bulb, hypothalamus, hippocampus, cerebellum, amygdala and cerebral cortex [12].

Growing but controversial evidence suggests that the specific regional concentrations of IR reflect different IR functions associated with particular brain regions. Insulin receptor enrichment in the hypothalamus and limbic system including the hippocampus, pyriform cortex and amygdala areas that reciprocally connect and communicate with each other has been proposed to be suggestive of a role in emotion and higher cognitive functions, particularly learning and memory [69, 70]. Higher IR concentrations are found in the hippocampus, which is critically involved in spatial memory processing, suggesting insulin's role in learning and declarative memory [69]. Evidence that synthesis of IR may be increased in these hippocampal areas as a result of learning is supported by the up-regulation and the changes in distribution patterns of IR mRNA in the hippocampus and dentate gyrus following water maze training in rats [70]. Insulin is involved in the regulation of food intake, which is consistent with the high concentrations of IR in the olfactory bulb and the hypothalamus. Furthermore, the high concentration of IR in the choroid plexus suggests that it may be required for transport of peripheral insulin across the blood CSF barrier [70].

Functional significance of insulin in the brain

As the most potent anabolic hormone yet identified, insulin has both metabolic and non-metabolic functions. Insulin regulates food intake, as well as glucose, lipid and energy homeostasis and stimulates synthesis (as well as inhibition of breakdown) of glycogen, triglycerides and most proteins. It is also involved in regulation of hedonic behavior, and non-homeostatic control of intake of food and other substances via reward processing.

Non- metabolic functions

The presence of insulin and insulin receptors in the brain indicates that the brain is a target organ for insulin. Insulin plays a key role in synaptic plasticity, apoptosis, mood, learning, reproduction and growth [37, 71-74]. Insulin and insulin receptor expression in the brain has been suggested to exert neurotrophic effects on CNS neurons [75]. Insulin has been considered to support neuronal protein synthesis and cytoskeletal protein expression [75], neurite outgrowth [76, 77], migration and differentiation in the absence of other growth factors [78, 79], and nascent synapse formation [75, 80]. It promotes growth and regeneration of axonal sprouts, especially small sized sensory neurons [81], neuronal survival, circuit development, synaptic plasticity [82] and postsynaptic neurotransmitter receptor trafficking [80]. Evidence in favor of insulin's role as a neurotransmitter in the CNS includes the observations that (i) insulin is present in neurons [67], (ii) neurons contain specific insulin receptors [64], and (iii) insulin affects neuronal firing and catecholamine metabolism [83-85]. Insulin also has effects on BBB function, including an ability to affect the transport of other substances. Binding sites for insulin have been described at both the choroid plexus and on brain endothelial cells [86, 87]. Insulin also has neuro-protective properties [88-90]. Central insulin plays a role in cognitive processes such as attention, executive functioning, learning and memory [91], and direct application of insulin to the CNS in humans has been shown to improve memory and cognition [92, 93]. Thus, insulin is involved in attributes that are essential for healthy aging.

Metabolic functions

The brain plays a key role in maintenance of homeostasis, or the ability to maintain vital parameters of the internal environment within narrow limits, despite fluctuations in the external environment. Metabolic homeostasis requires the integration of numerous cues reflecting energy availability by the hypothalamus and nearby brain structures, to mount a coordinated response to adapt fuel flux so as to maintain energy homeostasis. Insulin is one of the many cues informing the brain about energy status. Research on insulin signaling has primarily focused on insulin-mediated processes in the classical insulin target organs. These include glucose uptake into skeletal muscle, inhibition of glucose production by the liver and inhibition of lipolysis in adipose tissue. However, in 1979, a role for insulin in the central regulation of energy homeostasis was suggested based on the observations that insulin levels circulate in proportion to fat mass in most mammals and that intra-cerebroventricular insulin administration results in a dose dependent reduction in food intake and body weight in monkeys [94]. In line, insulin receptors are expressed throughout the mammalian brain[29]. Metabolic syndrome and diabetes have traditionally been considered as peripheral metabolic diseases. Recently, various non-invasive brain-imaging techniques have revealed structural and functional abnormalities that are associated with diabetes. Critical autonomic regulatory neurons in the hypothalamus and brainstem are responsible for maintenance of energy homeostasis and functional changes in these areas are associated with the development of diabetes [(95)]. It was also shown that after hepatic branch vagotomy the suppression of hepatic gluconeogenesis induced by increasing circulating insulin levels was reduced by half [(96)]. Mechanistically, binding of insulin to the IR and activation of the PI3K pathway in hypothalamic glucose-responsive neurons, which was shown to induce their hyperpolarization by opening of ATP-dependent potassium channels [(97)], has been implicated in the central effects of insulin on hepatic glucose production [(96)]. Recently, it was shown that ingestion of a glucose solution resulted in a prolonged and significant blood oxygen dependent decrease in activity in the hypothalamus of healthy subjects, but not in type 2 diabetic patients [(98)]. Insulin is also involved in regulation of energy homeostasis via IR in the ventromedial hypothalamus and acts on the brain to suppress feeding [(99)]. Thus, insulin acts as a satiety factor, a finding supported by the observation that the response of glucose- excited neurons in the ventrolateral and ventromedial hypothalamic nucleus to decreased glucose is blunted by insulin [(100)].

Taken together, these data indicate that, beside peripheral insulin resistance, reduced brain insulin action may also contribute to loss of maintenance of metabolic control. Indeed, brain specific deletion of the IR was shown to result in enhanced food intake in female mice; and in mild obesity, hyperleptinemia, insulin resistance, and hypertriglyceridemia in both male and female mice [(101)]. In line with these findings, in rats, decreasing hypothalamic insulin receptors caused overeating and insulin resistance and hypothalamic insulin signaling was shown to be required for inhibition of glucose production [(102)]. High-fat diet induced obesity is associated with reduced brain insulin transport and an impairment of insulin action when given directly into the CNS, suggesting a loss of the effectiveness of insulin in the CNS to provide feedback signaling in circumstances of chronic hyperinsulinemia [(103)]. Upon aging, peripheral insulin resistance progressively increases, inducing compensatory chronic elevations in circulating insulin levels. Therefore, central insulin action will be discussed in the context of models of delayed and accelerated aging.

INSULIN AND THE BRAIN: MODELS OF DELAYED AGING

Nematode models of delayed aging

There is an impressive body of literature implicating insulin/IGF-1 like ligands and insulin/IGF-1 signaling in the regulation of metabolism, development, and longevity in the roundworm C.elegans [104]. In response to unfavorable stressful environmental conditions, C. elegans larvae can transiently exit the cycle of growth and development to sexual maturity by transformation into developmentally arrested, non-feeding, stress resistant and long-lived dauer larvae [105, 106]. It was found that several dauer formation defective (daf) mutants are also long-lived, possibly because these mutants display specific key features of the dauer stage while developing in sexually mature adults, such as enhanced resistance to multiple stresses due to induction of cytoprotective pathways [107]. Of the many long-lived daf mutants in nematodes, the ones that are best characterized comprise the daf- 2, age- 1 (daf 23), daf-16 and daf- 18 mutants. Cloning and sequencing of the loci affected in long-lived daf mutants has revealed that these show strong sequence homology with evolutionarily conserved components of the mammalian insulin/insulin-like growth factor 1 signal transduction cascade [108-110]. For example, the daf- 2 gene that has been shown to regulate lifespan in C. elegans, and the related tyrosine kinase receptors InR in Drosophila melanogaster (D. melangogaster) encode components that are homologous to the mammalian insulin and insulin-like growth factor 1 receptors. In response to food or the perception of food, multiple insulin-like ligands are secreted from neurosecretory cells in the brain of C.elegans [111] and D. melanogaster [112], indicating that in these invertebrates, the central nervous system plays a key role in insulin signaling mediated regulation of physiology and lifespan in response to environmental cues. Moreover, more than 10 years ago, Wolkow et al [17] demonstrated that restoration of the daf-2 pathway of insulin-like signaling in neurons alone was sufficient to restore wildtype lifespan in C. elegans, and thus provided further evidence as to the role of insulin in the nervous system as a central regulator of animal longevity.

Mouse models of delayed aging

In mammals, the insulin/insulin-like growth factor 1 signaling cascade exhibits some striking differences compared to the insulin/insulin-like growth factor 1 signaling cascade in invertebrates [113]. These differences include the acquisition of GH as a main regulator of IGF-1 production by the liver, and the acquisition of separate receptors for insulin and IGF-1. Again, several of the existing long-lived mammalian mutants with defects in insulin/IGF-1 signaling point to a role of the central nervous system in the regulation of mammalian longevity. The mutations that have thus far been most consistently and most strongly associated with increases in lifespan in mice comprise the Prop-1 mutation displayed by Ames dwarf mice [114] and the Pit-1 mutation displayed by Snell dwarf mice [115]. These two mutations both confer a defect in the development of the anterior pituitary gland, which causes a lifelong combined hormonal deficiency in growth hormone, thyroid stimulating hormone and prolactin. In these as well as other long-lived mice, longevity has been strongly correlated with enhanced insulin sensitivity [116]. In addition to the Ames and Snell dwarf mice, many other mouse mutants with defects in insulin/IGF-1 signaling have been described to display a longevity phenotype, which strongly implicates the insulin/IGF-1 signaling pathway in the regulation of rodent longevity. Involvement of both insulin signaling as well as IGF-1 signaling in mouse longevity was suggested by the long-lived phenotypes displayed by mice with selective disruption of the insulin receptor in adipose tissue [4] and mice heterozygous for mutation of IGF-1R [1]. Summarily, improved insulin control (of carbohydrate homeostasis) has been identified as one of the pathways implicated in the remarkable extension of longevity in long- lived mouse mutants [117].

Human models of delayed aging

Also in humans, preserved insulin sensitivity has been associated with longevity. Insulin resistance has been shown to predict the development of age- related diseases, including hypertension, coronary heart disease, stroke, cancer and type 2 diabetes [118]. In the general population, the association between aging and decline in insulin sensitivity [119-123] has been demonstrated in several studies (Figure 3). Mechanisms suggested to contribute to decreased insulin sensitivity in the elderly include (i) age-related receptor and post-receptor defects in insulin action [124, 125], (ii) an age–related decrease in insulin stimulated whole body glucose oxidation [126], (iii) an age-related reduction in beta cell response to glucose [126], and (iv) impaired insulin mediated glucose uptake, and inability to suppress hepatic glucose output [127, 128]. In contrast, centenarians, that exhibit exceptional longevity, seem protected against the age-related decline in insulin sensitivity when compared to a group of advanced middle-aged individuals [11]. Of note, a methodological difficulty that is associated with the comparison of groups that differ in calendar age, is potential confounding by the changes that occur in body composition and endocrine function with advancing age. Moreover, differences may exist between different birth cohorts in environmental impacts, including differences in the availability vaccinations or medications (e.g. antibiotics).

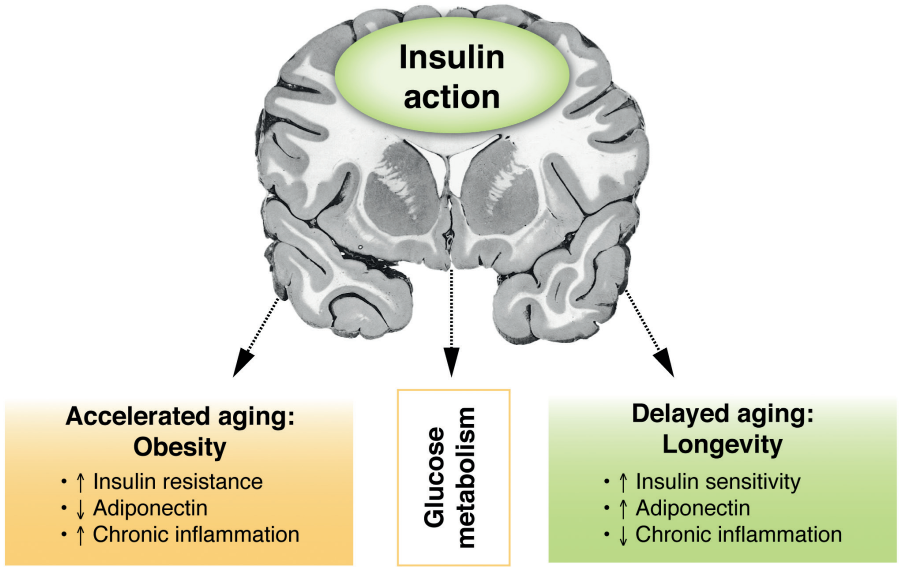

FIGURE 6.3 | Insulin and the brain: models of accelerated and delayed aging.

Figure showing the putative relationship between central insulin action and glucose metabolism in models of accelerated or delayed aging. Obesity as a model for accelerated aging is associated with peripheral insulin resistance, decreased adiponectin levels and enhanced chronic inflammation. Opposite features are observed in healthy longevity as a model of delayed aging.

The relationship between longevity and preserved insulin action has also been observed in studies of familial longevity. In the Leiden longevity study, offspring of long-lived nonagenarian siblings, having inherited on average 50% of the genetic propensity of their long-lived parent were included together with the partners of the offspring [129], with whom they have shared the same socio-economic and geographical environment for decades and who are of a similar age. We showed that already at middle age the offspring from these long-lived siblings displayed a decreased mortality risk suggesting that there is indeed evidence for genetic enrichment for longevity [130]. Moreover, human offspring of exceptionally long-lived siblings, when compared to their partners showed a remarkably lower prevalence of metabolic syndrome [131] and diabetes [132]. After exclusion of diabetic patients, the offspring of exceptionally long-lived siblings displayed lower circulating levels of glucose and slightly lower circulating insulin levels [7]. Using hyperinsulinemic euglycemic clamps studies, we could show that the offspring of long-lived siblings specifically displayed enhanced peripheral insulin sensitivity compared to age matched controls [8]. A study using high field (7-Tesla) MR spectroscopy of the tibialis anterior muscle indicated that the enhanced peripheral insulin sensitivity of offspring is associated with lower intramyocellular lipid content, which may be indicative of better mitochondrial capacity [133].

The mechanisms underlying the preserved insulin action in centenarians as well as in offspring of nonagenarian siblings remain unclear. However, suggested mechanisms include genetic enrichment for favorable features related to body fat and lipoprotein distribution, reduced plasma free radical concentrations, and enhanced cellular response to oxidative stress and immune function [11, 134, 135]. Taken together, these results suggest that maintenance of insulin sensitivity is a key feature of healthy longevity.

Insulin and the brain: models of accelerated aging

Obesity as a model for accelerated aging

The most common acquired factors causing insulin resistance are obesity and a sedentary lifestyle. Obesity and the associated increase in body fat are the consequences of chronic, long-term nutrient excess. In Western societies the prevalence of obesity continues to increase and numerous studies have demonstrated an association between obesity and enhanced mortality risk [136]. The relationship between obesity and excess mortality is consistent with evidence that obese individuals are at increased risk of essential hypertension, type 2 diabetes mellitus (DM2), and cardiovascular disease (CVD). It has been suggested that that insulin resistance is the major contributor to clinical outcomes associated with obesity [137].

It is not known why some obese individuals develop insulin resistance while others remain insulin sensitive [138]. A potential mechanism that might explain for the association between excess adiposity and peripheral insulin resistance is impaired adipogenesis and reduced lipogenesis in subcutaneous fat, which would lead to enhanced deposition of fat in the visceral depots and larger sizes of visceral adipocytes [138, 139]. Increased visceral adiposity is associated with enhanced secretion of inflammatory cytokines and induction of insulin resistance [140]. Nutrient excess results in enhanced exposure of cells and tissues to high levels of circulatory glucose and fatty acids. These exposures can activate various intracellular inflammatory pathways and lead to mitochondrial dysfunction, reactive oxygen species (ROS), ER stress and the associated unfolded protein response that induce resistance to both leptin and insulin [141]. ROS can have both stimulatory and inhibitory effects on insulin signaling. It was shown that under normal physiological conditions, optimal activation of the IR requires redox priming by IR mediated activation of NAD(P)H oxidase (NOX) in many cell types [142]. In addition, mild bursts in intracellular ROS can activate the IR receptor independent of insulin, allowing for ROS mediated ligand activation bypass of IR signaling [143]. In contrast, increased levels of ROS or prolonged exposure to oxidative stress have been shown to inhibit insulin signaling and to induce insulin resistance [144]. Enhanced exposure of skeletal muscle to high levels of fatty acids in circulation can result in enhanced levels of intraymocellular triglyceride storage. Because intramyocellular lipid droplets are stored in close vicinity to mitochondria, which constitute the main intracellular source of ROS, intraymocellular trigycerides are very vulnerable to oxidation. Upon peroxidation of intramyocellular trigycerides toxic lipid species are generated, including diacylglycerol (DAG), ceramide and long-chain fatty acyl-CoA, which impair insulin signaling [144]. Both enhanced influx, as a consequence of nutrient excess, as well as reduced efflux, as a result reduced oxidative capacity and mitochondrial dysfunction have been implicated in the accumulation of toxic intramyocellular lipids [145,146]. In support of a role of reduced efflux due to mitochondrial dysfunction, non-obese, insulin sensitive first degree relatives of patients with type 2 diabetes were shown to display impaired ability to switch to fat oxidation after high fat intake [147], as well as higher levels of intramyocellular lipids and reduced oxidative capacity [148]. These data implicate ROS and mitochondrial dysfunction in the development of insulin resistance.

It is unknown via which mechanisms insulin resistance is associated with a shortening of lifespan. If peripheral organs, such as skeletal muscle and adipose tissue become less responsive to insulin, euglycemia will be maintained by the capacity of the pancreas to hypersecrete insulin so as to overcome insulin resistance at peripheral organs. Exposure to continuous surges of hyperinsulinemia may overstimulate other tissues that have remained normally responsive to insulin, such as the liver, resulting in a pro-atherogenic lipid profile[149]. Other data implicate adiponectin in the association between insulin resistance and lifespan. Adiponectin, an anti-inflammatory adipokine secreted by adipose tissue [150] was found to be negatively correlated with adipocyte size and obesity [151]. Interestingly, elevated adiponectin levels have been observed in long-lived mice, such as the Ames dwarf mice [152] as well as in long-lived humans, such as centenarians [153-155]. Recently, effects of adiponectin on peripheral insulin sensitivity also implicate central effects on reduction of high fat diet induced hypothalamic inflammation and insulin resistance [156].

Inflammation and the brain

Inflammation and Aging: Inflammaging

Inflammaging is characterized by the increase in chronic, low-grade inflammation in the absence of overt infection that occurs with aging[157]. Inflammaging as well as the circulatory markers that characterize this state, including C-reactive protein (CRP), interleukine 6 (IL6), tumor necrosis factor alfa (TNF-alfa) and interleukine 1 beta (IL1beta) are strong risk factors for many age-related diseases and mortality. It is thought that part of these circulatory factors are produced locally, after which these leak into the circulation. Different sources that contribute to the state of inflammaging include the accumulation of cellular debris and organelle components, accumulation of senescent cells, immunosenescence, changes in the gut microbiome and deregulation of the coagulation system.

Macromolecules, cells and tissues are continuously damaged and repaired. Chronic inflammation is part of regular tissue remodeling as it facilitates tissue repair and turnover. However, a persistent inflammatory response can lead to tissue degeneration by activated leukocytes, cytokines, or collagen deposition. In literature, one key structure where links between inflammation and aging are emerging is the hypothalamus.

Hypothalamic inflammation

The hypothalamus is the seat of control of various metabolic and non- metabolic processes in the body, and is responsible for maintenance of homeostasis from early life through to aging. Besides its role in the synthesis and secretion of neurohormones, the hypothalamus regulates energy balance, stress responsiveness as well as lipid and glucose metabolism. Diet-induced obesity has been shown to be associated with central leptin and insulin resistanc [158]. High fat feeding has been shown to induce hypothalamic inflammation, which has been linked to the development of insulin resistance and obesity [158-160]. In 2005 De Souza et al demonstrated that 6 weeks of high fat feeding induced impaired functional and molecular activation of the insulin-signaling pathway, with accompanying expression of several proinflammatory cytokines (IL-1b, TNFa, and IL-6) and inflammatory responsive proteins in the hypothalamus [159]. Moreover, hypothalamic inflammation was shown to decrease the efficacy of central insulin administration to inhibit lipolysis, even before the onset of peripheral insulin resistance in white adipose tissue [161]. Recently, a series of experiments in mice has demonstrated that hypothalamic inflammation occurs rapidly after high fat feeding and is mediated by hyper activation of hypothalamic microglia which was associated with gliosis in the ARC nucleus and eventual reduction in the number of POMC neurons, which are key in the regulation of energy homeostasis and adiposity [162].

Microglia are resident macrophages that play an important role in the clearance of cell debris via phagocytosis and the release of pro-inflammatory cytokines to recruit other immune responsive cells to the sites of injury in the CNS, including blood borne macrophages. It is pivotal for tissue homeostasis and repair, that the initial inflammatory immune response is followed by an active phase of resolution of inflammation and scar tissue. Recently, it has been shown that after insult, monocyte-derived M2-like macrophages are recruited to the site of injury and that these have an essential role as inflammation-resolving cells in recovery from acute CNS injury. The anti-inflammatory activity displayed by M2-like macrophages, notably their IL10 expression, is required for regulation of the activated microglia [163, 164]. In addition, their expression of matrix degrading enzymes favors axonal regrowth by degradation of the glial scar [165]. CNS specific T cells facilitate recruitment of blood borne M2-like macrophages to the CNS through the choroid plexus within the blood-CSF barrier [166]. Age-related Th2 inflammation is associated with chronically elevated IL4 levels which can disrupt choroid plexus barrier functions and thus prevent the resolution of proinflammatory processes and induce a state of CNS inflammaging.

Therapeutic measures and future prospects

Since brain insulin has been linked with aging, two possible mechanisms can be proffered for enhancing brain insulin action (Figure 4). Enhanced insulin efficacy might occur through measures aimed at minimizing inflammation; and enhanced delivery might be promoted to the brain areas that are crucial for healthy longevity.

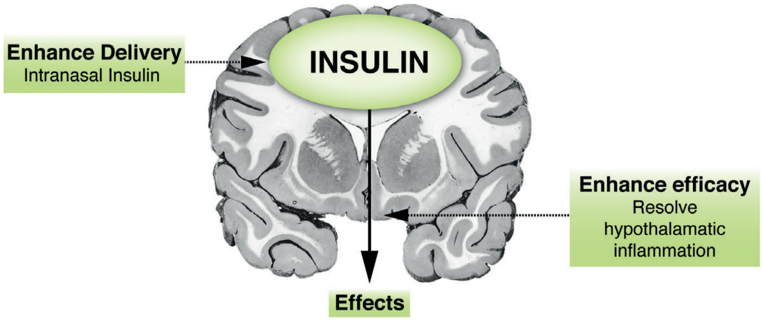

FIGURE 6.4 | Insulin and the brain: therapeutic implications.

Hypothetical figure presenting two possibilities of enhancing brain insulin action. First, a way of increasing insulin concentrations in the brain is via enhanced delivery, such as delivery via the intranasal route which has been shown to have some beneficial effects. Second, insulin action could probably also be augmented by enhancing its efficacy, for example via resolution of brain (hypothalamic) inflammation.

Inflammation, including that occurring in the hypothalamus, has been linked to age-related decline in insulin sensitivity. It has been shown that hypothalamic microglia hyperactivation is regulated by metabolic hormones (leptin, glucagon-like peptide 1 (GLP-1)) and diet but not by body weight per se [(167)]. Inflammaging may be treatable and preventable through changes in lifestyle. Interventions that are currently applied to reduce the state of low grade chronic inflammaging include low dosing of aspirin or statins, weight loss and exercise. Notably, a lower intake of calories and food that is rich in saturated fat and carbohydrates has been shown to reduce inflammaging [(168)]. In mice, it was shown that hypothalamic inflammation can be resolved by central administration of omega3 and omega9 fatty acids after which body weight regulation and food intake were normalized [(169)]. Physical exercise is known to be protective against numerous diseases and reduction of inflammation has been implicated in the health benefits conferred by exercise [(170)]. Recently, in mice exercise has also been shown to protect against hypothalamic inflammation induced by high fat diet [(171)]. Future research may focus on hypothalamic microglia as relevant targets for prevention and treatment of metabolic disorders.

The strong blood glucose lowering effects of intravenously administered insulin have hampered research on the role of insulin in the brain. These hypoglycemic effects can be circumvented by intranasal administration of insulin, which is an innovative way to enhance insulin concentration in the brain without affecting insulin concentration in the circulation [(172)]. Intranasal administration of insulin was shown to be safe and effective in numerous studies in healthy humans and in patients with metabolic disease or cognitive impairment [(173)]. Sub-chronic intranasal insulin application in humans was shown to decrease food intake and weight gain [(92)] in healthy young men, and to improve declarative memory and mood [(174)]. Moreover, sub-chronic intranasal insulin application in humans was also shown to decrease HPA activation in response to a social stress test. It was shown that insulin may also influence meal-induced thermogenesis and postprandial insulin levels [(175)]. Future research may focus on unravelling the effects of intranasal insulin on other aspects of energy and glucose metabolism in different age groups.

CONCLUSION

Insulin is the most powerful anabolic hormone discovered to date. Besides the well-established action of insulin in peripheral organs, such as liver, muscle and adipose tissue, it is becoming increasingly clear that insulin affects important features of glucose metabolism via central mechanisms. Insulin signaling has been linked to longevity in organisms ranging from nematodes to mammals. While insulin is clearly a neuropeptide in nematodes, it is not yet clear how central insulin contributes to the differences in glucose metabolism that are observed in the context of conditions that are associated with accelerated aging, such as obesity, and delayed aging, such as healthy human longevity. However, novel data indicate that obesity is associated with reduced brain insulin action. Potential mechanisms that contribute to deficits in brain insulin action are impaired transport of insulin from the periphery to the brain and reduced brain insulin sensitivity, due to hypothalamic inflammation. In contrast, we speculate that healthy longevity is associated with preserved brain insulin action, and discuss potential ways of enhancing brain insulin action in old age. Given the increasing prevalence of population aging, improving brain insulin action may represent an important therapeutic option to facilitate health in old age.

REFERENCES

1. Holzenberger M, Dupont J, Ducos B, et al. IGF-1 receptor regulates lifespan and resistance to oxidative stress in mice. Nature. 2003;421(6919):182-7.
2. Iser WB, Gami MS, Wolkow CA. Insulin signaling in Caenorhabditis elegans regulates both endocrine-like and cell-autonomous outputs. Developmental biology. 2007;303(2):434-47.
3. Bartke A, Chandrashekar V, Dominici F, et al. Insulin-like growth factor 1 (IGF-1) and aging: controversies and new insights. Biogerontology. 2003;4(1):1-8.
4. Bluher M, Kahn BB, Kahn CR. Extended longevity in mice lacking the insulin receptor in adipose tissue. Science. 2003;299(5606):572-4.
5. Fulop T, Larbi A, Douziech N. Insulin receptor and ageing. Pathologie-biologie. 2003;51(10):574-80.
6. Fulop T, Jr., Nagy JT, Worum I, et al. Glucose intolerance and insulin resistance with aging--studies on insulin receptors and post-receptor events. Archives of gerontology and geriatrics. 1987;6(2):107-15.
7. Rozing MP, Westendorp RG, Frolich M, et al. Human insulin/IGF-1 and familial longevity at middle age. Aging. 2009;1(8):714-22.
8. Wijsman CA, Rozing MP, Streefland TC, et al. Familial longevity is marked by enhanced insulin sensitivity. Aging Cell. 2011;10(1):114-21.
9. Barbieri M, Gambardella A, Paolisso G, et al. Metabolic aspects of the extreme longevity. Experimental gerontology. 2008;43(2):74-8.
10. Barbieri M, Rizzo MR, Manzella D, et al. Glucose regulation and oxidative stress in healthy centenarians. Experimental gerontology. 2003;38(1-2):137-43.
11. Paolisso G, Gambardella A, Ammendola S, et al. Glucose tolerance and insulin action in healty centenarians. The American journal of physiology. 1996;270(5 Pt 1):E890-4.
12. Duarte AI, Moreira PI, Oliveira CR. Insulin in central nervous system: more than just a peripheral hormone. JAging Res. 2012;2012:384017.
13. Schwartz MW, Seeley RJ, Tschop MH, et al. Cooperation between brain and islet in glucose homeostasis and diabetes. Nature. 2013;503(7474):59-66.
14. Gerozissis K. Brain insulin: regulation, mechanisms of action and functions. Cellular and molecular neurobiology. 2003;23(1):1-25.
15. Derakhshan F, Toth C. Insulin and the brain. Current diabetes reviews. 2013;9(2):102-16.
16. Anisimov VN. Insulin/IGF-1 signaling pathway driving aging and cancer as a target for pharmacological intervention. Experimental gerontology. 2003;38(10):1041-9.

17. Wolkow CA, Kimura KD, Lee MS, et al. Regulation of C. elegans life-span by insulinlike signaling in the nervous system. Science. 2000;290(5489):147-50.
18. Taguchi A, Wartschow LM, White MF. Brain IRS2 signaling coordinates life span and nutrient homeostasis. Science. 2007;317(5836):369-72.
19. Houston DK, Nicklas BJ, Zizza CA. Weighty concerns: the growing prevalence of obesity among older adults. Journal of the American Dietetic Association. 2009;109(11):1886-95.
20. Mozumdar A, Liguori G. Persistent increase of prevalence of metabolic syndrome among U.S. adults: NHANES III to NHANES 1999-2006. Diabetes Care. 2011;34(1):216-9.
21. CfDCa. P. National Estimates and General Information on Diabetes and Prediabetes int he United States, 2011. National Diabetes Fact Sheet:. 2011.
22. Alzheimer's disease facts and figures 2011. Alzheimer's & dementia : the journal of the Alzheimer's Association.7(2):208-44.
23. Schwartz MW, Porte D, Jr. Diabetes, obesity, and the brain. Science. 2005;307(5708):375-9.
24. Sherlock M, Toogood AA. Aging and the growth hormone/insulin like growth factor-I axis. Pituitary. 2007;10(2):189-203.
25. Frolich L, Blum-Degen D, Bernstein HG, et al. Brain insulin and insulin receptors in aging and sporadic Alzheimer's disease. Journal of neural transmission (Vienna, Austria : 1996). 1998;105(4-5):423-38.
26. Zeyda M, Stulnig TM. Obesity, inflammation, and insulin resistance--a mini-review. Gerontology. 2009;55(4):379-86.
27. Haugaard N, Vaughan M, Haugaard ES, et al. Studies of radioactive injected labeled insulin. The Journal of biological chemistry. 1954;208(2):549-63.
28. Margolis RU, Altszuler N. Insulin in the cerebrospinal fluid. Nature. 1967;215(5108):1375-6.
29. Havrankova J, Roth J, Brownstein M. Insulin receptors are widely distributed in the central nervous system of the rat. Nature. 1978;272(5656):827-9.
30. Havrankova J, Schmechel D, Roth J, et al. Identification of insulin in rat brain. Proceedings of the National Academy of Sciences of the United States of America. 1978;75(11):5737-41.
31. Dorn A, Rinne A, Bernstein HG, et al. Insulin and C-peptide in human brain neurons (insulin/C-peptide/brain peptides/immunohistochemistry/radioimmunoassay). Journal fur Hirnforschung. 1983;24(5):495-9.
32. Dorn A, Bernstein HG, Rinne A, et al. Insulin- and glucagonlike peptides in the brain. The Anatomical record. 1983;207(1):69-77.

33. Baskin DG, Woods SC, West DB, et al. Immunocytochemical detection of insulin in rat hypothalamus and its possible uptake from cerebrospinal fluid. Endocrinology. 1983;113(5):1818-25.
34. Wallum BJ, Taborsky GJ, Jr., Porte D, Jr., et al. Cerebrospinal fluid insulin levels increase during intravenous insulin infusions in man. The Journal of clinical endocrinology and metabolism. 1987;64(1):190-4.
35. Schechter R, Whitmire J, Holtzclaw L, et al. Developmental regulation of insulin in the mammalian central nervous system. Brain research. 1992;582(1):27-37.
36. Hallschmid M, Schultes B. Central nervous insulin resistance: a promising target in the treatment of metabolic and cognitive disorders? Diabetologia. 2009;52(11):2264-9.
37. Abraham MA, Filippi BM, Kang GM, et al. Insulin action in the hypothalamus and dorsal vagal complex. Experimental physiology. 2014;99(9):1104-9.
38. Frank HJ, Pardridge WM. A direct in vitro demonstration of insulin binding to isolated brain microvessels. Diabetes. 1981;30(9):757-61.
39. Havrankova J, Roth J, Brownstein MJ. Concentrations of insulin and insulin receptors in the brain are independent of peripheral insulin levels. Studies of obese and streptozotocin-treated rodents. The Journal of clinical investigation. 1979;64(2):636-42.
40. Schechter R, Beju D, Gaffney T, et al. Preproinsulin I and II mRNAs and insulin electron microscopic immunoreaction are present within the rat fetal nervous system. Brain research. 1996;736(1-2):16-27.
41. Banks WA, Kastin AJ. Differential permeability of the blood-brain barrier to two pancreatic peptides: insulin and amylin. Peptides. 1998;19(5):883-9.
42. Devaskar SU, Holekamp N, Karycki L, et al. Ontogenesis of the insulin receptor in the rabbit brain. Hormone research. 1986;24(4):319-27.
43. Banks WA. The source of cerebral insulin. European journal of pharmacology. 2004;490(1-3):5-12.
44. Baura GD, Foster DM, Porte D, Jr., et al. Saturable transport of insulin from plasma into the central nervous system of dogs in vivo. A mechanism for regulated insulin delivery to the brain. The Journal of clinical investigation. 1993;92(4):1824-30.
45. Duffy KR, Pardridge WM. Blood-brain barrier transcytosis of insulin in developing rabbits. Brain research. 1987;420(1):32-8.
46. Frank HJ, Jankovic-Vokes T, Pardridge WM, et al. Enhanced insulin binding to blood-brain barrier in vivo and to brain microvessels in vitro in newborn rabbits. Diabetes. 1985;34(8):728-33.

47. Frank HJ, Pardridge WM. Insulin binding to brain microvessels. Advances in metabolic disorders. 1983;10:291-302.
48. Freude S, Plum L, Schnitker J, et al. Peripheral hyperinsulinemia promotes tau phosphorylation in vivo. Diabetes. 2005;54(12):3343-8.
49. Pardridge WM. Receptor-mediated peptide transport through the blood-brain barrier. Endocrine reviews. 1986;7(3):314-30.
50. Pardridge WM, Eisenberg J, Yang J. Human blood-brain barrier insulin receptor. Journal of neurochemistry. 1985;44(6):1771-8.
51. Banks WA, Jaspan JB, Kastin AJ. Selective, physiological transport of insulin across the blood-brain barrier: novel demonstration by species-specific radioimmunoassays. Peptides. 1997;18(8):1257-62.
52. Porte D, Jr., Seeley RJ, Woods SC, et al. Obesity, diabetes and the central nervous system. Diabetologia. 1998;41(8):863-81.
53. Sankar R, Thamotharan S, Shin D, et al. Insulin-responsive glucose transporters-GLUT8 and GLUT4 are expressed in the developing mammalian brain. Brain research Molecular brain research. 2002;107(2):157-65.
54. Weindl A, Sofroniew MV. Relation of neuropeptides to mammalian circumventricular organs. Advances in biochemical psychopharmacology. 1981;28:303-20.
55. Pardridge WM. Transport of insulin-related peptides and glucose across the blood-brain barrier. Annals of the New York Academy of Sciences. 1993;692:126-37.
56. Blasberg RG, Patlak C, Fenstermacher JD. Intrathecal chemotherapy: brain tissue profiles after ventriculocisternal perfusion. The Journal of pharmacology and experimental therapeutics. 1975;195(1):73-83.
57. Burbach JP. Neuropeptides from concept to online database www.neuropeptides.nl. EurJPharmacol. 2010;626(1):27-48.
58. Clarke DW, Mudd L, Boyd FT, Jr., et al. Insulin is released from rat brain neuronal cells in culture. Journal of neurochemistry. 1986;47(3):831-6.
59. Schechter R, Yanovitch T, Abboud M, et al. Effects of brain endogenous insulin on neurofilament and MAPK in fetal rat neuron cell cultures. Brain research. 1998;808(2):270-8.
60. Taniguchi CM, Emanuelli B, Kahn CR. Critical nodes in signalling pathways: insights into insulin action. Nature reviews Molecular cell biology. 2006;7(2):85-96.
61. Eijkelenboom A, Burgering BM. FOXOs: signalling integrators for homeostasis maintenance. Nature reviews Molecular cell biology. 2013;14(2):83-97.

62. Saltiel AR, Kahn CR. Insulin signalling and the regulation of glucose and lipid metabolism. Nature. 2001;414(6865):799-806.
63. Heidenreich KA, Zahniser NR, Berhanu P, et al. Structural differences between insulin receptors in the brain and peripheral target tissues. The Journal of biological chemistry. 1983;258(14):8527-30.
64. Boyd FT, Jr., Raizada MK. Effects of insulin and tunicamycin on neuronal insulin receptors in culture. The American journal of physiology. 1983;245(3):C283-7.
65. Zahniser NR, Goens MB, Hanaway PJ, et al. Characterization and regulation of insulin receptors in rat brain. Journal of neurochemistry. 1984;42(5):1354-62.
66. van Houten M, Posner BI. Insulin binds to brain blood vessels in vivo. Nature. 1979;282(5739):623-5.
67. Raizada MK, Yang JW, Fellows RE. Binding of [125I]insulin to specific receptors and stimulation of nucleotide incorporation in cells cultured from rat brain. Brain research. 1980;200(2):389-400.
68. van Houten M, Posner BI, Kopriwa BM, et al. Insulin binding sites localized to nerve terminals in rat median eminence and arcuate nucleus. Science. 1980;207(4435):1081-3.
69. Wickelgren I. Tracking insulin to the mind. Science. 1998;280(5363):517-9.
70. Zhao W, Chen H, Xu H, et al. Brain insulin receptors and spatial memory. Correlated changes in gene expression, tyrosine phosphorylation, and signaling molecules in the hippocampus of water maze trained rats. The Journal of biological chemistry. 1999;274(49):34893-902.
71. Zhao WQ, Chen H, Quon MJ, et al. Insulin and the insulin receptor in experimental models of learning and memory. European journal of pharmacology. 2004;490(1-3):71-81.
72. de la Monte SM, Wands JR. Review of insulin and insulin-like growth factor expression, signaling, and malfunction in the central nervous system: relevance to Alzheimer's disease. Journal of Alzheimer's disease : JAD. 2005;7(1):45-61.
73. Avogaro A, de Kreutzenberg SV, Fadini GP. Insulin signaling and life span. Pflugers Archiv : European journal of physiology. 2010;459(2):301-14.
74. Plum L, Schubert M, Bruning JC. The role of insulin receptor signaling in the brain. Trends in endocrinology and metabolism: TEM. 2005;16(2):59-65.
75. Schulingkamp RJ, Pagano TC, Hung D, et al. Insulin receptors and insulin action in the brain: review and clinical implications. Neuroscience and biobehavioral reviews. 2000;24(8):855-72.
76. Dickson BJ. Development. Wiring the brain with insulin. Science. 2003;300(5618):440-1.
77. Song J, Wu L, Chen Z, et al. Axons guided by insulin receptor in Drosophila visual system. Science. 2003;300(5618):502-5.

78. Torres-Aleman I. Insulin-like growth factors as mediators of functional plasticity in the adult brain. Hormone and metabolic research = Hormon- und Stoffwechselforschung = Hormones et metabolisme. 1999;31(2-3):114-9.
79. Recio-Pinto E, Rechler MM, Ishii DN. Effects of insulin, insulin-like growth factor-II, and nerve growth factor on neurite formation and survival in cultured sympathetic and sensory neurons. The Journal of neuroscience : the official journal of the Society for Neuroscience. 1986;6(5):1211-9.
80. Puro DG, Agardh E. Insulin-mediated regulation of neuronal maturation. Science. 1984;225(4667):1170-2.
81. Sugimoto K, Baba M, Suda T, et al. Peripheral neuropathy and microangiopathy in rats with insulinoma: association with chronic hyperinsulinemia. Diabetes/metabolism research and reviews. 2003;19(5):392-400.
82. Kremerskothen J, Wendholt D, Teber I, et al. Insulin-induced expression of the activity-regulated cytoskeleton-associated gene (ARC) in human neuroblastoma cells requires p21(ras), mitogen-activated protein kinase/extracellular regulated kinase and src tyrosine kinases but is protein kinase C-independent. Neuroscience letters. 2002;321(3):153-6.
83. Palovcik RA, Phillips MI, Kappy MS, et al. Insulin inhibits pyramidal neurons in hippocampal slices. Brain research. 1984;309(1):187-91.
84. Barbaccia ML, Chuang DM, Costa E. Is insulin a neuromodulator? Advances in biochemical psychopharmacology. 1982;33:511-8.
85. Boyd FT, Jr., Clarke DW, Muther TF, et al. Insulin receptors and insulin modulation of norepinephrine uptake in neuronal cultures from rat brain. The Journal of biological chemistry. 1985;260(29):15880-4.
86. Baskin DG, Brewitt B, Davidson DA, et al. Quantitative autoradiographic evidence for insulin receptors in the choroid plexus of the rat brain. Diabetes. 1986;35(2):246-9.
87. Miller DW, Keller BT, Borchardt RT. Identification and distribution of insulin receptors on cultured bovine brain microvessel endothelial cells: possible function in insulin processing in the blood-brain barrier. Journal of cellular physiology. 1994;161(2):333-41.
88. Dudek H, Datta SR, Franke TF, et al. Regulation of neuronal survival by the serine-threonine protein kinase Akt. Science. 1997;275(5300):661-5.
89. Takadera T, Sakura N, Mohri T, et al. Toxic effect of a beta-amyloid peptide (beta 22-35) on the hippocampal neuron and its prevention. Neuroscience letters. 1993;161(1):41-4.
90. Tanaka M, Sawada M, Yoshida S, et al. Insulin prevents apoptosis of external granular layer neurons in rat cerebellar slice cultures. Neuroscience letters. 1995;199(1):37-40.

91. Kern W, Peters A, Fruehwald-Schultes B, et al. Improving influence of insulin on cognitive functions in humans. Neuroendocrinology. 2001;74(4):270-80.

92. Hallschmid M, Benedict C, Schultes B, et al. Intranasal insulin reduces body fat in men but not in women. Diabetes. 2004;53(11):3024-9.

93. Benedict C, Hallschmid M, Schultes B, et al. Intranasal insulin to improve memory function in humans. Neuroendocrinology. 2007;86(2):136-42.

94. Woods SC, Lotter EC, McKay LD, et al. Chronic intracerebroventricular infusion of insulin reduces food intake and body weight of baboons. Nature. 1979;282(5738):503-5.

95. Eikelis N, Esler M. The neurobiology of human obesity. Experimental physiology. 2005;90(5):673-82.

96. Pocai A, Lam TK, Gutierrez-Juarez R, et al. Hypothalamic K(ATP) channels control hepatic glucose production. Nature. 2005;434(7036):1026-31.

97. Spanswick D, Smith MA, Mirshamsi S, et al. Insulin activates ATP-sensitive K+ channels in hypothalamic neurons of lean, but not obese rats. Nature neuroscience. 2000;3(8):757-8.

98. Vidarsdottir S, Smeets PA, Eichelsheim DL, et al. Glucose ingestion fails to inhibit hypothalamic neuronal activity in patients with type 2 diabetes. Diabetes. 2007;56(10):2547-50.

99. Schwartz MW, Sipols AJ, Marks JL, et al. Inhibition of hypothalamic neuropeptide Y gene expression by insulin. Endocrinology. 1992;130(6):3608-16.

100. Cotero VE, Routh VH. Insulin blunts the response of glucose-excited neurons in the ventrolateral-ventromedial hypothalamic nucleus to decreased glucose. American journal of physiology Endocrinology and metabolism. 2009;296(5):E1101-9.

101. Bruning JC, Gautam D, Burks DJ, et al. Role of brain insulin receptor in control of body weight and reproduction. Science. 2000;289(5487):2122-5.

102. Obici S, Zhang BB, Karkanias G, et al. Hypothalamic insulin signaling is required for inhibition of glucose production. Nature medicine. 2002;8(12):1376-82.

103. Kaiyala KJ, Prigeon RL, Kahn SE, et al. Obesity induced by a high-fat diet is associated with reduced brain insulin transport in dogs. Diabetes. 2000;49(9):1525-33.

104. Kenyon CJ. The genetics of ageing. Nature. 2010;464(7288):504-12.

105. Braendle C, Milloz J, Felix MA. Mechanisms and evolution of environmental responses in Caenorhabditis elegans. Current topics in developmental biology. 2008;80:171-207.

106. Klass M, Hirsh D. Non-ageing developmental variant of Caenorhabditis elegans. Nature. 1976;260(5551):523-5.

107. Shore DE, Carr CE, Ruvkun G. Induction of cytoprotective pathways is central to the extension of lifespan conferred by multiple longevity pathways. PLoS genetics. 2012;8(7):e1002792.

108. Kimura KD, Tissenbaum HA, Liu Y, et al. daf-2, an insulin receptor-like gene that regulates longevity and diapause in Caenorhabditis elegans. Science. 1997;277(5328):942-6.
109. Lin K, Dorman JB, Rodan A, et al. daf-16: An HNF-3/forkhead family member that can function to double the life-span of Caenorhabditis elegans. Science. 1997;278(5341):1319-22.
110. Ogg S, Paradis S, Gottlieb S, et al. The Fork head transcription factor DAF-16 transduces insulin-like metabolic and longevity signals in C. elegans. Nature. 1997;389(6654):994-9.
111. Apfeld J, Kenyon C. Regulation of lifespan by sensory perception in Caenorhabditis elegans. Nature. 1999;402(6763):804-9.
112. Broughton SJ, Slack C, Alic N, et al. DILP-producing median neurosecretory cells in the Drosophila brain mediate the response of lifespan to nutrition. Aging Cell. 2010;9(3):336-46.
113. van Heemst D. Insulin, IGF-1 and longevity. Aging and disease. 2010;1(2):147-57.
114. Brown-Borg HM, Borg KE, Meliska CJ, et al. Dwarf mice and the ageing process. Nature. 1996;384(6604):33.
115. Flurkey K, Papaconstantinou J, Miller RA, et al. Lifespan extension and delayed immune and collagen aging in mutant mice with defects in growth hormone production. Proceedings of the National Academy of Sciences of the United States of America. 2001;98(12):6736-41.
116. Masternak MM, Panici JA, Bonkowski MS, et al. Insulin sensitivity as a key mediator of growth hormone actions on longevity. The journals of gerontology Series A, Biological sciences and medical sciences. 2009;64(5):516-21.
117. Bartke A, Westbrook R. Metabolic characteristics of long-lived mice. Frontiers in genetics. 2012;3:288.
118. Facchini FS, Hua N, Abbasi F, et al. Insulin resistance as a predictor of age-related diseases. The Journal of clinical endocrinology and metabolism. 2001;86(8):3574-8.
119. Paolisso G, Scheen A, Lefebvre P. Glucose handling, diabetes and ageing. Hormone research. 1995;43(1-3):52-7.
120. Bourey RE, Kohrt WM, Kirwan JP, et al. Relationship between glucose tolerance and glucose-stimulated insulin response in 65-year-olds. Journal of gerontology. 1993;48(4):M122-7.
121. Elahi D, Muller DC, McAloon-Dyke M, et al. The effect of age on insulin response and glucose utilization during four hyperglycemic plateaus. Experimental gerontology. 1993;28(4-5):393-409.
122. Pratley RE, Coon PJ, Muller DC, et al. The effects of single and sequential insulin infusions on glucose disposal in older men. Experimental gerontology. 1993;28(4-5):381-91.
123. Couet C, Delarue J, Constans T, et al. Age-related insulin resistance: a review. Hormone research. 1992;38(1-2):46-50.

124. Fink RI, Kolterman OG, Griffin J, et al. Mechanisms of insulin resistance in aging. The Journal of clinical investigation. 1983;71(6):1523-35.
125. Rowe JW, Minaker KL, Pallotta JA, et al. Characterization of the insulin resistance of aging. The Journal of clinical investigation. 1983;71(6):1581-7.
126. Gumbiner B, Thorburn AW, Ditzler TM, et al. Role of impaired intracellular glucose metabolism in the insulin resistance of aging. Metabolism: clinical and experimental. 1992;41(10):1115-21.
127. Meneilly GS, Elahi D, Minaker KL, et al. Impairment of noninsulin-mediated glucose disposal in the elderly. The Journal of clinical endocrinology and metabolism. 1989;68(3):566-71.
128. Paolisso G, Marrazzo G, de Riu S, et al. Effects of mild-to-moderate hyperglycaemia per se on glucose production and uptake in the elderly. The European journal of medicine. 1992;1(1):6-12.
129. Schoenmaker M, de Craen AJ, de Meijer PH, et al. Evidence of genetic enrichment for exceptional survival using a family approach: the Leiden Longevity Study. EurJHumGenet. 2006;14(1):79-84.
130. Schoenmaker M, de Craen AJ, de Meijer PH, et al. Evidence of genetic enrichment for exceptional survival using a family approach: the Leiden Longevity Study. European journal of human genetics : EJHG. 2006;14(1):79-84.
131. Rozing MP, Westendorp RG, de Craen AJ, et al. Favorable glucose tolerance and lower prevalence of metabolic syndrome in offspring without diabetes mellitus of nonagenarian siblings: the Leiden longevity study. Journal of the American Geriatrics Society. 2010;58(3):564-9.
132. Westendorp RG, van Heemst D, Rozing MP, et al. Nonagenarian siblings and their offspring display lower risk of mortality and morbidity than sporadic nonagenarians: The Leiden Longevity Study. Journal of the American Geriatrics Society. 2009;57(9):1634-7.
133. Wijsman CA, van Opstal AM, Kan HE, et al. Proton magnetic resonance spectroscopy shows lower intramyocellular lipid accumulation in middle-aged subjects predisposed to familial longevity. American journal of physiology Endocrinology and metabolism. 2012;302(3):E344-8.
134. Dekker P, Maier AB, van Heemst D, et al. Stress-induced responses of human skin fibroblasts in vitro reflect human longevity. Aging Cell. 2009;8(5):595-603.
135. Heijmans BT, Beekman M, Houwing-Duistermaat JJ, et al. Lipoprotein particle profiles mark familial and sporadic human longevity. PLoS medicine. 2006;3(12):e495.
136. Hu FB, Willett WC, Li T, et al. Adiposity as compared with physical activity in predicting mortality among women. The New England journal of medicine. 2004;351(26):2694-703.
137. McLaughlin T, Abbasi F, Lamendola C, et al. Heterogeneity in the prevalence of risk factors for cardiovascular disease and type 2 diabetes mellitus in obese individuals: effect of differences in insulin sensitivity. Archives of internal medicine. 2007;167(7):642-8.

138. McLaughlin T, Sherman A, Tsao P, et al. Enhanced proportion of small adipose cells in insulin-resistant vs insulin-sensitive obese individuals implicates impaired adipogenesis. Diabetologia. 2007;50(8):1707-15.
139. Salans LB, Knittle JL, Hirsch J. The role of adipose cell size and adipose tissue insulin sensitivity in the carbohydrate intolerance of human obesity. The Journal of clinical investigation. 1968;47(1):153-65.
140. Fontana L, Eagon JC, Trujillo ME, et al. Visceral fat adipokine secretion is associated with systemic inflammation in obese humans. Diabetes. 2007;56(4):1010-3.
141. Hotamisligil GS. Inflammation and metabolic disorders. Nature. 2006;444(7121):860-7.
142. Goldstein BJ, Mahadev K, Wu X. Redox paradox: insulin action is facilitated by insulin-stimulated reactive oxygen species with multiple potential signaling targets. Diabetes. 2005;54(2):311-21.
143. Papaconstantinou J. Insulin/IGF-1 and ROS signaling pathway cross-talk in aging and longevity determination. Molecular and cellular endocrinology. 2009;299(1):89-100.
144. Houstis N, Rosen ED, Lander ES. Reactive oxygen species have a causal role in multiple forms of insulin resistance. Nature. 2006;440(7086):944-8.
145. Samocha-Bonet D, Heilbronn LK, Lichtenberg D, et al. Does skeletal muscle oxidative stress initiate insulin resistance in genetically predisposed individuals? Trends in endocrinology and metabolism: TEM. 2010;21(2):83-8.
146. Moro C, Galgani JE, Luu L, et al. Influence of gender, obesity, and muscle lipase activity on intramyocellular lipids in sedentary individuals. The Journal of clinical endocrinology and metabolism. 2009;94(9):3440-7.
147. Heilbronn LK, Gregersen S, Shirkhedkar D, et al. Impaired fat oxidation after a single high-fat meal in insulin-sensitive nondiabetic individuals with a family history of type 2 diabetes. Diabetes. 2007;56(8):2046-53.
148. Petersen KF, Dufour S, Befroy D, et al. Impaired mitochondrial activity in the insulin-resistant offspring of patients with type 2 diabetes. The New England journal of medicine. 2004;350(7):664-71.
149. Reaven GM. Compensatory hyperinsulinemia and the development of an atherogenic lipoprotein profile: the price paid to maintain glucose homeostasis in insulin-resistant individuals. Endocrinology and metabolism clinics of North America. 2005;34(1):49-62.
150. Combs TP, Berg AH, Obici S, et al. Endogenous glucose production is inhibited by the adipose-derived protein Acrp30. The Journal of clinical investigation. 2001;108(12):1875-81.

151. Bahceci M, Gokalp D, Bahceci S, et al. The correlation between adiposity and adiponectin, tumor necrosis factor alpha, interleukin-6 and high sensitivity C-reactive protein levels. Is adipocyte size associated with inflammation in adults? Journal of endocrinological investigation. 2007;30(3):210-4.
152. Wang Z, Al-Regaiey KA, Masternak MM, et al. Adipocytokines and lipid levels in Ames dwarf and calorie-restricted mice. The journals of gerontology Series A, Biological sciences and medical sciences. 2006;61(4):323-31.
153. Atzmon G, Pollin TI, Crandall J, et al. Adiponectin levels and genotype: a potential regulator of life span in humans. The journals of gerontology Series A, Biological sciences and medical sciences. 2008;63(5):447-53.
154. Bik W, Baranowska-Bik A, Wolinska-Witort E, et al. The relationship between adiponectin levels and metabolic status in centenarian, early elderly, young and obese women. Neuro endocrinology letters. 2006;27(4):493-500.
155. Yasumichi Arai SN, Toshio Kojima, Michiyo Takayama, Yoshinori Ebihara, Ken-ichirou Shimizu, Ken Yamamura, Satoki Homma, Yasunori Osono, Yasuyuki Gondo, Yukie Masui, Hiroki Inagaki, Kohji Kitagawa and Nobuyoshi Hirose. High adiponectin concentration and its role for longevity in female centenarians. Geriatriatrics Gerontology International. 2006;6: 32-9.
156. Koch CE, Lowe C, Legler K, et al. Central adiponectin acutely improves glucose tolerance in male mice. Endocrinology. 2014;155(5):1806-16.
157. Franceschi C, Campisi J. Chronic inflammation (inflammaging) and its potential contribution to age-associated diseases. The journals of gerontology Series A, Biological sciences and medical sciences. 2014;69 Suppl 1:S4-9.
158. Zhang X, Zhang G, Zhang H, et al. Hypothalamic IKKbeta/NF-kappaB and ER stress link overnutrition to energy imbalance and obesity. Cell. 2008;135(1):61-73.
159. Cani PD, Amar J, Iglesias MA, et al. Metabolic endotoxemia initiates obesity and insulin resistance. Diabetes. 2007;56(7):1761-72.
160. Kleinridders A, Schenten D, Konner AC, et al. MyD88 signaling in the CNS is required for development of fatty acid-induced leptin resistance and diet-induced obesity. Cell Metab. 2009;10(4):249-59.
161. Scherer T, Lindtner C, Zielinski E, et al. Short term voluntary overfeeding disrupts brain insulin control of adipose tissue lipolysis. The Journal of biological chemistry. 2012;287(39):33061-9.
162. Thaler JP, Yi CX, Schur EA, et al. Obesity is associated with hypothalamic injury in rodents and humans. The Journal of clinical investigation. 2012;122(1):153-62.

163. Rapalino O, Lazarov-Spiegler O, Agranov E, et al. Implantation of stimulated homologous macrophages results in partial recovery of paraplegic rats. Nature medicine. 1998;4(7):814-21.
164. Shechter R, London A, Varol C, et al. Infiltrating blood-derived macrophages are vital cells playing an anti-inflammatory role in recovery from spinal cord injury in mice. PLoS medicine. 2009;6(7):e1000113.
165. Shechter R, Raposo C, London A, et al. The glial scar-monocyte interplay: a pivotal resolution phase in spinal cord repair. PloS one. 2011;6(12):e27969.
166. Kunis G, Baruch K, Rosenzweig N, et al. IFN-gamma-dependent activation of the brain's choroid plexus for CNS immune surveillance and repair. Brain : a journal of neurology. 2013;136(Pt 11):3427-40.
167. Gao Y, Ottaway N, Schriever SC, et al. Hormones and diet, but not body weight, control hypothalamic microglial activity. Glia. 2014;62(1):17-25.
168. Fontana L. Neuroendocrine factors in the regulation of inflammation: excessive adiposity and calorie restriction. Experimental gerontology. 2009;44(1-2):41-5.
169. Cintra DE, Ropelle ER, Moraes JC, et al. Unsaturated fatty acids revert diet-induced hypothalamic inflammation in obesity. PloS one. 2012;7(1):e30571.
170. Ford ES. Does exercise reduce inflammation? Physical activity and C-reactive protein among U.S. adults. Epidemiology (Cambridge, Mass). 2002;13(5):561-8.
171. Yi CX, Al-Massadi O, Donelan E, et al. Exercise protects against high-fat diet-induced hypothalamic inflammation. Physiology & behavior. 2012;106(4):485-90.
172. Born J, Lange T, Kern W, et al. Sniffing neuropeptides: a transnasal approach to the human brain. Nature neuroscience. 2002;5(6):514-6.
173. Benedict C, Dodt C, Hallschmid M, et al. Immediate but not long-term intranasal administration of insulin raises blood pressure in human beings. Metabolism: clinical and experimental. 2005;54(10):1356-61.
174. Benedict C, Hallschmid M, Hatke A, et al. Intranasal insulin improves memory in humans. Psychoneuroendocrinology. 2004;29(10):1326-34.
175. Benedict C, Brede S, Schioth HB, et al. Intranasal insulin enhances postprandial thermogenesis and lowers postprandial serum insulin levels in healthy men. Diabetes. 2011;60(1):114-8.

PART II:

CROSSTALK WITH THE THYROID AXIS

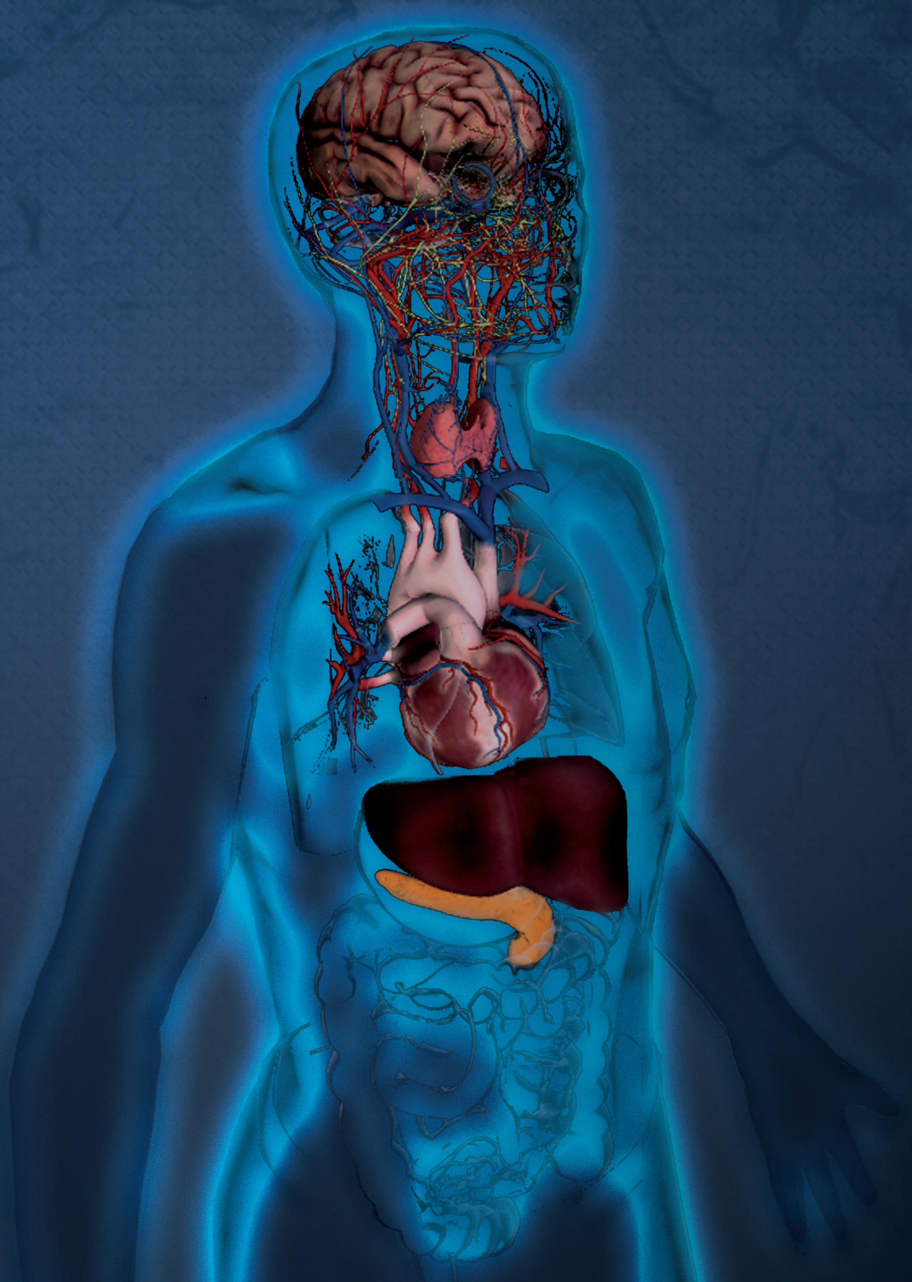

CHAPTER 7

A SIMPLE AND VERSATILE METHOD FOR FREQUENT 24 HOUR BLOOD SAMPLE COLLECTION IN OLDER ADULTS

Abimbola A. Akintola*
Steffy W. Jansen*
Rob B.P. Wilde
Gertjan Hultzer
Rene Rodenburg
Diana van Heemst

*Equal contribution of authors

MethodsX. 2014 Dec 26;2:33-8.

ABSTRACT

Repeated blood sampling, which is required for time series analyses of metabolites and/or hormones that show strong fluctuations in blood concentration over time, has a higher failure rate in older adults. We tailored existing venepuncture protocols towards use for 24 hour blood sampling (sampling frequency of 10 minutes) in older adults. The following modifications were made:

- Pre-sampling: evidence based risk assessment of older adults
- During sampling:
    - Ultrasound- guided identification and characterisation of veins
    - Use of 20-gauge arterial catheter with guide wire for venous access
    - Measures to prevent and/or reduce unidirectional blood flow (fluid flow into but not out of the vein) included:
        - Use of hot water bottles to dilate veins
        - Use of small gauge syringes, shortening of the extension line, and slowing of the blood withdrawal rate to reduce pressure on veins
        - Stimulation of movement of the arm or retraction of the IV cannula to relieve mechanical flow obstruction
- Post-sampling: prevention of bruising and prolonged bleeding

METHOD DETAILS

Repeated blood sampling, a frequently used method in research, is required for time series analyses of metabolites and/or hormones that show strong fluctuations in blood concentration over time. However repeated blood sampling has a higher failure rate in older adults due to difficulty in establishing and maintaining venous access due to age-induced changes in the integrity of the skin, venous vasculature and valves. Therefore we customized pre-sampling, sampling and post-sampling procedures for continuous sampling in older adults. In our laboratory, the customized protocol was used for 24 hour blood sampling with a sample frequency of 10 minutes in a group of 41 elderly mean (range) age of 66 (52-76) years. With the customized protocol, the mean (standard deviation) number of missing samples was 6.3 (7.0) out of 144 (4.4%) over the whole study period. Thus, the customized protocol that is discussed in more detail below represents a useful and successful method for high frequency sampling of blood in healthy older adults.

Standard protocols	Problems in older adults	Adaptations to existing protocols
Pre-sampling	***Pre-sampling***	***Pre-sampling***
1. Screening of participants	Guidelines are based on age range of 18-65 years	Evidence based systematic risk assessment of older adults
2. Determination of maximal amount of blood per sampling	Guidelines are based on age range of 18-65 years	The allowable maximal volume for blood withdrawal is calculated based on sex and weight in accordance with EU guidelines
During sampling	***During sampling***	***During sampling***
Venous cannulation: 3. Identification	Multiple failed attempts due to: Reduced skin tone and elasticity	Identification with Ultrasound (US) guidance: • Easier localization of the vessel and its relation to surrounding anatomical structures • Determination of vascular quality and tortious veins • Presence and location of intravascular valves.
Venous cannulation: 4. Access	Unstable, tortious veins	Cannulation with a 20-gauge guide wire catheter, 8 cm in length, inserted with Seldinger technique
5. Frequent blood withdrawal	No validated guidelines available	• Relaxed environment • Dilatation of veins: hot water bottles
6. Maintenance of IV access	Uni-directional flow due to reduced tone of the vessel wall, and/or age- induced fibrosis of the wall of the veins and valve leaflets	• Reduction of pressure on veins: - small gauge (e.g.2 ml instead of 5 ml) syringes - shortening of extension line - slow withdrawal of samples • Minimize mechanical obstruction of vessel lumen: - stimulate movement of the arm, retracting of IV cannula
Post-sampling	***Post-sampling***	***Post-sampling***
7. Processing of samples: use of heparinized saline to flush the extension line after blood withdrawal	Heparin in flushing fluid in combination with anti-coagulant use by participant may cause prolonged clotting times Re-clotting of pre- centrifuged samples	Use of saline only for flushing extension lines (limit use of heparinized saline to only the continuous infusion during blood sampling). Removal of clot and re-centrifuging
8. Removal of IV cannula	Bruising and prolonged bleeding	Application of gentle pressure for at least 3 minutes, use of pressure bandage

FIGURE | Graphical abstract

A. PRE-SAMPLING

1. Screening of participants

⚠ Maintenance of IV access and blood withdrawal proved to be most problematic in subjects older than 75 years of age, since venous capacitance and compliance reduces with age [(1)].

Standard protocols

According to the European guidelines [(2)], age range for blood donation is 18-65 years. Above the age of 65 years, blood donation is allowed only at the discretion of the responsible physician [(2)]. This medical discretion can be applied on an individual basis or through a systematic approach based on an appropriate risk assessment.

Adaptations made

A systematic risk assessment (Table 1) by a suitably qualified individual (physician) was done before inclusion of older subjects (≥ 65 years) for continuous/ repeated blood sampling.

TABLE 7.1 | Schematic overview of systematic assessment of older adults, to determine eligibility for frequent blood sampling.

Standard screening:	Pay attention to:	Reason for attention:
Medical history	Previous contra- indications to blood donation	Contra-indications of placement of IV cannula
	Previous difficulty with venepuncture	Frail veins, stiffened valves
	Previous mastectomy/ relevant surgery	
	Previous fistula or vascular graft	
	Severe arteriosclerosis	
	History of chemotherapy	
Medication use	Anti-coagulants	Increased bleeding risk causing bruises
	Medications relevant to hormone(s) of interest	
Tractus anamneses	Palpitations	These symptoms are indicators of underlying cardiac and brain hypo-perfusion, withdrawal of high amounts of blood can lead to damage to those tissue due to decreased oxygenation
	Chest pain	
	Signs of TIA (neurological paralysis)	
Medical examination	Appearance of blood vessels	Problems with insertion of IV cannula
	Extensive scaring on one or both hands	
	Pulse	To detect unknown cardiac problems
	Blood pressure	
	Cardiac sounds	

Risks assessed:

Medical status: assessed through medical history, medication use, physical examination and laboratory investigations. We assessed for:

- General state of health, presence of medical conditions and use of medications
    - Acceptable systolic blood pressure was ≤ 180 mmHg and diastolic blood pressure ≤100 mmHg [(2)]
    - Acceptable pulse of 50-100 (regular) beats per minute [(2)]
    - Acceptable BMI of 18-30 kg/m2
    - Absence of anaemia
- Assessment to exclude conditions that may interfere with maintenance of venous access such as:
    - Extensive scaring on one or both hands
    - Previous mastectomy
    - Previous fistula or vascular graft
    - Severe arteriosclerosis
    - Previous history of chemotherapy use

2. Determination of maximal amount of blood per sampling

⚠ There is presently no consensus as to the maximum amount of blood that can be withdrawn in older adults since blood donation guidelines are based on adults aged 18- 65 years.

Standard protocols

Based on the European guideline [(2)] the maximum amount of blood that can be taken is dependent on the weight and sex of the person, to a maximum of 500 ml over a 24 hour period. No more than 15% of the estimated blood volume is to be collected as whole blood, because of the risk of adverse reactions [(2)].

Adaptations made

We calculated maximum blood volume that can be withdrawn based on the weight, height, age and gender using a validated formula developed by the International Council of Standardisation in Haematology (ICHS) [(3)].

B. DURING SAMPLING

3. Venous cannulation: Identification

⚠ In older adults, skin loses tone and elasticity and becomes more fragile and prone to bruising. Upon finding a suitable blood withdrawal site, loss of subcutaneous tissue in older adults made their veins less stable, less visible, prone to receding and rolling under the skin thus reducing available IV access sites.

Standard protocols

Standard venepuncture and phlebotomy guideline involve visual identification of fore- arm veins (median cubittal and median veins) followed by venepuncture [(4,5)].

Adaptations made

Ultrasonography (US) was used for peripheral vein cannulation in subjects with difficult venous access to identify the peripheral vessels and guide the cannulation of the peripheral vein [(6,7)]. US guidance was used for:

- Easier localisation of the vessel and its relation to surrounding anatomical structures
- Determination of vascular quality and tortious veins
- Presence and location of intravascular valves

4. Venous cannulation: Access

⚠ In older adults more time is needed to find the most appropriate access site, since veins are more difficult to find, more tortious and veins have a tendency to collapse more due to degeneration of the vascular wall [(8)].

Standard protocols

Inspection of the antecubital fossa in preparation for cannulation, skin preparation with 2% chlorhexidine and insertion of appropriate cannula. Pressure is applied in cases of failed cannulation.

Adaptations made

In addition to the standard protocol, the following adaptations were implemented to improve success in older adults:

I. US- guided identification of the cephalic vein, basilica vein and median cubital vein.

II. Cannulation with a 20-gauge guide wire catheter, 8 cm in length, inserted with Seldinger technique (Arrow International, Reading, PA, USA).

- ! The choice to use arterial catheters is supported by recent literature reporting that the use of standard-length (3-5cm) catheters positioned in the deep brachial or basilica vein is frequently complicated by their dislodgment or dislocation [(7)]. Furthermore, the use of a longer IV-catheter provides freer arm movement and will increase comfort in individual subjects. Moreover, the amount of catheter failure and dislocation compared to standard-length IV catheters in the deep brachial and basilica vein is lower [(6,7)]. Keyes et al. [(6)] observed that the failure rate of peripherally inserted catheters was 8% within the first hour after venous cannulation. In a recent study, Elia et al. reported percentages of catheter failure of 45% vs 14%, [RR 3.2 (95% CI 1.4-7.3)], and dislocation of 42.5% vs 2.3% [RR 18.7 (95% CI 2.0-134.2)] when comparing standard-length to long IV catheters, inserted in the deep brachial and basilica vein [(7)].
- ! Nicking the skin with a scalpel or the use of a dilatator is not necessary.
- ◦ Venepuncture and catheter introduction is an aseptic procedure necessitating the use of sterile gloves. Finger guidance of the shaft of the exposed needle is not required.

III. In subjects with prominent veins, the basilica vein was the preferred access route because the basilica vein has a lager diameter compared with the cephalic vein, is easier to access and more suited for frequent blood sampling [(9)]. We cannulated with Arrow Catheterization Set (Product No. SAC 00820) without complications.

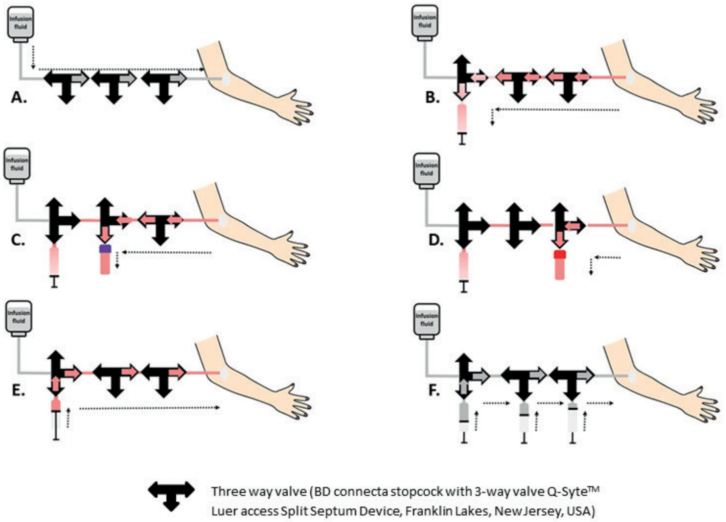

FIGURE 7.1 | Schematic overview of a closed method for frequent 24 hour blood sample collection.

A. Continuous infusion B. Turn the left three way valve 90°, withdraw 5 ml of saline/heparin mixed with blood C. Turn the middle three way valve 90°, withdraw EDTA sample and place it directly on ice D. Turn the right three way valve 90°, withdraw serum sample and let it clot for at least 30 minutes E. Turn the right and middle three way valve 90° and empty the syringe filled with the saline/heparin mixed with blood F. Flush with saline and turn the left three way valve 90° and continue with infusion (return to position A.).

5. Frequent blood withdrawal

Standard protocols

No published validated protocol was found for older adults. A previous study recommended addition of Heparin 100 IU/mL continuous saline infusion to prevent the IV system from clots and to reduce the number of catheter-related phlebitis/occlusions [10].

Adaptations made

For detailed hormonal and metabolic profiling of older adults aged 55-78 years, we aimed at total blood withdrawal of 432 ml over a 24-hour period. Serum (2 ml) and plasma (1.2 ml) samples were withdrawn every 10 minutes, with replacement by 480 ml of heparinized saline, using the following protocol (Figure 1):

I. Continuous infusion of heparinized saline (0.9% NaCl).
II. For the preparation of the heparinized saline, 500 IU of heparin was added to 500 ml of saline. This was infused over 24 hour via an infusion pump at a rate of 20 ml per hour.
III. Withdrawal of 5 ml of saline/heparin mixed with blood, without disconnecting the syringe from the blood withdrawal system.
IV. Placement of the 1.2 ml ethylenediaminetetraacetic acid (EDTA) Sarstedt S-monovette® (Nümbrecht, Germany) on the multiadaptor for S-monovette® (Nümbrecht, Germany) for blood sample withdrawal after which the blood is mixed gently with the EDTA and placed immediately on ice.
V. Placement of the 2 ml blood collection clotting tube BD (Franklin Lakes, USA) on the BD vacutainer®, (Franklin Lakes, USA). The sample was withdrawn and mixed with the clotting activator by gently turning the tube five times, after which it was allowed to clot for at least 30 minutes at room temperature.
VI. Flushing of the blood from the 5 ml syringe back into the subject, to reduce the total amount of blood that will be withdrawn.
VII. Flushing of the blood withdrawal system (including the extension line) to remove diluted blood, using 5 ml saline(0.9% NaCl).

6. Maintenance of IV access

⚠ In older adults, blood sampling was sometimes jeopardised by unidirectional blood flow (free flow of fluid into the vein but not out of the vein), with resultant impedance of sustained blood withdrawal. This is possibly due to reduced tone of the vessel wall, age- induced fibrosis of the wall of the veins and valve leaflets.

Standard protocols

No validated guidelines were available for older subjects.

Adaptations made

- Create a relaxing enviroment to reduce stress for the participant
- The particpant should be allowed to move their arm freely
- Application of hot water bottles to increase the diameter of the vessel

- Use of small gauge syringes (e.g. 2 ml syringes instead of 5 ml syringes) to reduce pressure on the vessel wall
- Obtaining blood samples very slowly e.g. using 1 ml/ 2 ml syringes
- Retraction of the IV cathether a few milimeters to change its position

C. POST SAMPLING

7. Processing of samples

⚠ Variable, sometimes prolonged clotting times in older adults

Standard protocols

There are different protocols depending on the hormone to be measured.

Adaptations made

For serum samples, blood was allowed to clot. Clotting time was very variable for older adults, ranging from approximately 15-70 minutes. Preferably within 60 minutes of sampling, tubes were centrifuged at 4000 rotations /min at 4°C for 10 minutes. Because of the clotting problems, re-clotting sometimes occurred in the serum samples after centrifuging. This was managed by manual removal of the clot from the sample tube followed by re-centrifuging.

After centrifuging, serum and plasma were pipetted into 500 µl Microvettes® Sarstedt (Nümbrecht, Germany), which were then stored first at -20°C and transferred to -80°C within 24 hours of blood withdrawal. Once frozen, samples were not allowed to thaw until laboratory analysis.

8. Removal of IV cannula

⚠ Prolonged bleeding, bruising

Standard protocols

The WHO guidelines on drawing blood recommend inspecting the puncture site and if bleeding occurs then applying gentle pressure on the puncture site until bleeding has stopped. If no bleeding occurred it is recommended to apply a bandage [4].

Adaptations made

For the prevention of bruising we applied gentle pressure to the puncture site for at least one minute. Thereafter participants were asked to apply gentle pressure for at least 2 minutes. A second inspection was made to check for bleeding, if bleeding occurred, gentle pressure was continued; if not then a bandage was placed. Extra attention was paid to older adults using anti-thrombotic medications.

REFERENCES

1. Greaney JL, Farquhar WB. Why do veins stiffen with advancing age? J Appl Physiol (1985). 2011;110(1):11-2.
2. European Committee (Partial Agreement) on Blood Transfusion (CD-P-TS), Guide to the Preparation, Use and Quality Assurance of Blood Components 16th Edition2010.
3. Pearson TC, Guthrie DL, Simpson J, Chinn S, Barosi G, Ferrant A, et al. Interpretation of measured red cell mass and plasma volume in adults: Expert Panel on Radionuclides of the International Council for Standardization in Haematology. British journal of haematology. 1995;89(4):748-56.
4. WHO Guidelines on Drawing Blood: Best Practices in Phlebotomy. Geneva: World Health Organization.; 2010.
5. Nikolac N, Supak-Smolcic V, Simundic AM, Celap I. Croatian Society of Medical Biochemistry and Laboratory Medicine: national recommendations for venous blood sampling. Biochemia medica. 2013;23(3):242-54.
6. Keyes LE, Frazee BW, Snoey ER, Simon BC, Christy D. Ultrasound-guided brachial and basilic vein cannulation in emergency department patients with difficult intravenous access. Annals of emergency medicine. 1999;34(6):711-4.
7. Elia F, Ferrari G, Molino P, Converso M, De Filippi G, Milan A, et al. Standard-length catheters vs long catheters in ultrasound-guided peripheral vein cannulation. The American journal of emergency medicine. 2012;30(5):712-6.
8. Moureau NL. Tips for inserting an I.V. device in an older adult. Nursing. 2008;38(12):12.
9. Stone BA. Re: Ultrasound-guided peripheral intravenous access. J Emerg Med. 2014;46(2):228.
10. Bertolino G, Pitassi A, Tinelli C, Staniscia A, Guglielmana B, Scudeller L, et al. Intermittent flushing with heparin versus saline for maintenance of peripheral intravenous catheters in a medical department: a pragmatic cluster-randomized controlled study. Worldviews Evid Based Nurs. 2012;9(4):221-6.

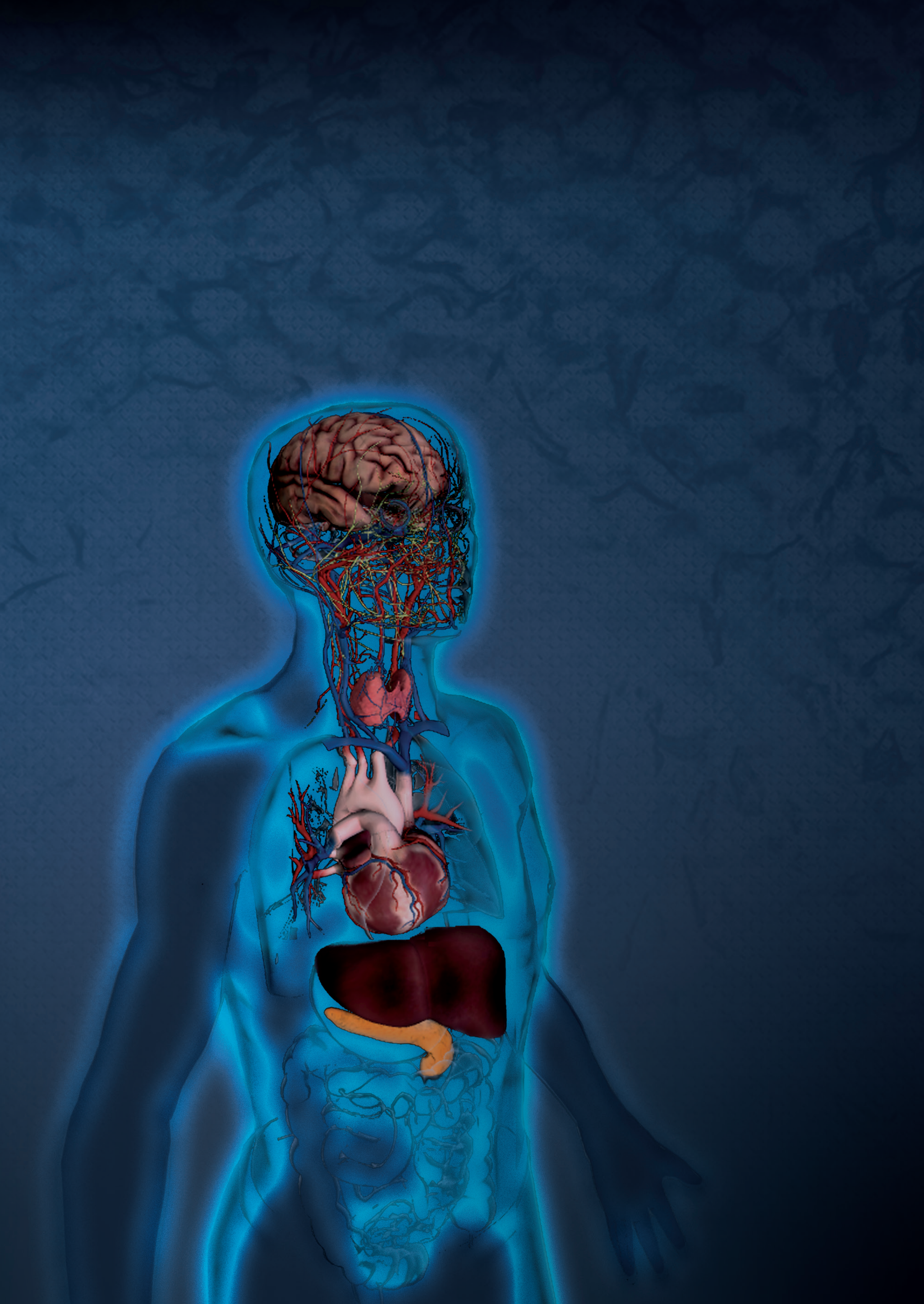

CHAPTER 8

HUMAN LONGEVITY IS CHARACTERIZED BY HIGH THYROID STIMULATING HORMONE SECRETION WITHOUT ALTERED WHOLE BODY ENERGY METABOLISM

Steffy W. Jansen*
Abimbola A Akintola*
Ferdinand Roelfsema
Evie van der Spoel
Christa M. Cobbaert
Bart E. Ballieux
Peter Egri
Zsuzsanna Kvarta-Papp
Balázs Gereben
Csaba Fekete
P. Eline Slagboom
Jeroen van der Grond
Barbara A. Demeneix
Hanno Pijl
Rudi G. J. Westendorp
Diana van Heemst

*Equal contribution of authors

Scientific reports 2015 Jun 19;5:11525.

ABSTRACT

Few studies have included subjects with the propensity to reach old age in good health, with the aim to disentangle mechanisms contributing to staying healthier for longer. The hypothalamic-pituitary-thyroid (HPT) axis maintains circulating levels of thyroid stimulating hormone (TSH) and thyroid hormone (TH) in an inverse relationship. Greater longevity has been associated with higher TSH and lower TH levels, but mechanisms underlying TSH/TH differences and longevity remain unknown. The HPT axis plays a pivotal role in growth, development and energy metabolism. We report that offspring of nonagenarians with at least one nonagenarian sibling have increased TSH secretion but similar bioactivity of TSH and similar TH levels compared to controls. Healthy offspring and spousal controls had similar resting metabolic rate and core body temperature. We propose that pleiotropic effects of the HPT axis may favour longevity without altering energy metabolism.

INTRODUCTION

Worldwide, the population of elderly is rapidly growing, with numbers expected to further increase in the coming decades. Although epidemiological studies have discovered specific lifestyle and genetic risk factors for cardiovascular disease, dementia and cancer, age is unequivocally the major common risk factor [(1)]. With the expansion of the aging population, the prevalence of all major age related diseases will increase, including cardiovascular disease, diabetes mellitus type 2 and dementia. Most studies have included diseased subjects with the aim to identify risk factors for specific diseases [(2)]. Only few studies have included subjects with a propensity to reach old age in good health, with the aim to disentangle mechanisms contributing to healthy human longevity and protection from disease. The Leiden Longevity Study (LLS) comprises nonagenarians with at least one nonagenarian sibling, their offspring and the offspring's partners [(3)]. Compared to their partners, offspring from nonagenarian siblings have a lower mortality rate, a lower prevalence of diabetes and cardiovascular disease [(3)] and are therefore well suited for studying the mechanisms underlying healthy human longevity.

Numerous theories of ageing link energy metabolism to the ageing process. The "rate of living theory" postulates that the positive correlation between lifespan and size implicates species differences in resting metabolic rate [(4)]. The mechanistically linked "free radical theory of ageing" proposes that free radicals generated as by-products of oxidative metabolism underpin the negative correlation between life span and resting metabolic rate [(5)]. Other theories propose ageing to involve precocious depletion of functional stem cell reserves[(6)] which might be retarded by slowing tissue turnover rates. One physiological integrator that influences metabolism, growth, development and tissue turnover is thyroid signalling. In previous studies, we found that when nonagenarians were stratified for their propensity to reach advanced age, those with the lowest family mortality history score had the highest TSH levels and slightly lower levels of free T4 (fT4) and free T3 (fT3) [(7)]. When offspring were compared to their partners, fT4 levels were similar, whereas TSH was higher and fT3 levels were slightly lower [(8, 9)]. Moreover studies in the oldest old from the general population also link increased levels of TSH with reduced old age mortality [(10)].

In this study, we are the first that make use of frequent blood sampling in relation with familial longevity to study TSH secretion and TH levels over 24 hours, because TSH and fT3 were shown to have circadian rhythms [(11)]. In addition, we investigate whether such differences in TSH and/or TH concur with differences in energy metabolism, a physiological process that has been associated with longevity in model organisms and is known to be responsive to TSH/TH action.

METHODS

Participants

Between 2002 and 2006, 421 families with at least two long-lived Caucasian siblings, 1671 of their offspring and 744 of the offspring's partners were recruited in the Leiden Longevity Study, without any selection on health. Males had to be aged 89 years or above and females 91 years or above [3, 12]. For the current study (Switchbox), between March 2012 and July 2013, 135 offspring and partners from the LLS were measured at the study centre of the Leiden University Medical Centre. Inclusion criteria included being middle-aged (55-77 years) and having a stable body mass index (BMI) between 19 kg/m2 and 33 kg/m2. Participants were excluded if their fasting plasma glucose was above 7 mmol/l, if they had any significant chronic, renal, hepatic or endocrine disease, or if they used any medication known to influence lipolysis, thyroid function, glucose metabolism, GH/IGF-1 secretion or any other hormonal axis. Moreover, participants were excluded if they had a recent trans meridian flight, smoking addiction, use of more than 20 units of alcohol per week and extreme diet therapies. Other exclusion criteria specific for the subgroup only, were difficulties to insert and maintain an intravenous catheter, anemia (hemoglobin < 7.1 mmol/l), and blood donation within the last two months. Based on information obtained via telephone questioning, controls with a nonagenarian parent who had one or more nonagenarian siblings were also excluded. All women in this study were postmenopausal. The Switchbox protocol was approved by the Medical Ethical Committee of the Leiden University Medical Centre and was performed according to the Helsinki declaration. All participants gave written informed consent for participation.

Of the 135 subjects included, we excluded from analysis 17 subjects due to incomplete indirect calorimetry data and 6 subjects due to incomplete core body temperature data (Supplementary Fig. 1). Thus, in total 112 subjects (61 offspring, 51 partners) were available for analysis (and are referred to as full study sample). Complete series of 24 hour blood samples were obtained for a subgroup of 38 participants (20 offspring, 18 partners).

Continuous blood sampling

Participants were sampled in the same research room and received standardized feeding at three fixed times during the day (between 09.00h-10.00h, 12.00h-13.00h and 18.00-19.00h), each consisting of 600 kcal Nutridrink (Nutricia Advanced Medical Nutrition, Zoetermeer, The Netherlands). No naps were allowed during the day and lights were turned off between 23.00h to 08.00h. A catheter was placed in a vein of the forearm of the non-dominant hand. Every 10 minutes, 1.2 ml of blood was collected in K3-EDTA tube and 2 ml in a serum-separator (SST)-tube. In total, 460.8 ml of blood was withdrawn from each participant.

Processing of the samples

After blood withdrawal, the K3-EDTA tubes were immediately placed on ice before centrifugation. Serum tubes were kept at room temperature and centrifuged when the samples were clotted, usually between 30-60 minutes. Samples were centrifuged at 3520 RPM at 4°C for 10 minutes. The EDTA plasma and serum samples were stored in two aliquots of 500µl during the rest of the sampling at -20°C. After the sampling they were transferred to a -80°C freezer until analysis.

Chemical analyses

All measurements were performed at the Department of Clinical Chemistry and Laboratory Medicine, Leiden University Medical Centre, The Netherlands. All laboratory measurements were performed with fully automated equipment and diagnostics from Roche Diagnostics (Almere, The Netherlands). Aspartate Aminotransferase (AST) (Catalog number 11876848216), Alanine Aminotransferase (ALT) (Catalog number 11876805216) and creatinine (Catalog numbers R1 11875566216, R2 11875582216) were measured from a fasted late morning serum sample using the Modular P800 clinical chemistry analyser. TSH (Catalog number 11731459122), fT4 (Catalog number 6437281190), fT3 (Catalog number 13051986190), and T3 (Catalog number 11731360122) were measured in serum by ElectroChemoLuminescence ImmunoAssay (ECLIA) using a Modular E170 Immunoanalyzer. The TSH method has been standardized against the 2nd IRP WHO Reference Standard 80/558. For each participant, all samples from one time series were measured with the same lot number in the same batch. For fT4 and fT3, all samples were measured in one batch. For TSH, measurements were divided over 10 batches. For each couple, offspring and partner were measured with the same lot number and preferentially also in the same batch. For this study, the precision and quality of all assayed analytes met or surpassed the level of desirable quality specifications [13]. The coefficients of variation (CVs) for AST, ALT, creatinine , and fT3 were all below their advised levels of 6.0% for AST, 12.2% for ALT, 2.2% for creatinine, and 4.4% for T3. For TSH, fT4 and fT3 Randox controls (catalog numbers IA 3109 and IA 3111) were used to determine the CVs. For TSH, the CV ranged in our study between 1.41-4.16, which was well below the desired CV of 9.9%. For fT4, the CV range in our study was 2.41-3.49 and for fT3 2.16-2.91, both well below the upper CV limits for desired precision of these assays (fT4 ≤ 3.8 and fT3≤ 4.0). In our laboratory, the reference values for TSH were 0.3-4.8 mU/l, for fT4 10-24 pmol/l, for fT3 3-8pmol/l and for T3 1.1-3.1 nmol/l.

rT3 measurements

All rT3 measurements were measured in the same batch for both the full study sample as well as for the subgroup. Serum rT3 levels were measured with in-house radioimmunoassays by the Laboratory of Endocrinology and Radiochemistry of the Academic Medical Centre in Amsterdam [14] with an intra-assay variation between 4-5% and an inter-assay variation between 5-9% and a detection limit of 0.03 nmol/l. The reference range of rT3 was 0.11-0.44 nmol/l.

Measurements of metabolism

On study day 1, between 12.00h and 13.00h, participants had a 30 minutes indirect calorimetry session using a ventilated hood system (Care Fusion Canopy Jaeger Oxycon Pro, Houten, The Netherlands) after 14 hours of fasting. Participants were kept under standardized conditions, lying awake and emotionally undisturbed, completely at rest and comfortably supine on a bed, their head under a transparent ventilated canopy, in a thermally neutral environment. From the VO2 and VCO2 measurements, resting metabolic rate (RMR) was calculated using the formula 3.91 VO2 + 1.10 VCO2 – 1.93N [15].

Body composition was measured using a Bioelectrical Impedance Analysis meter at a fixed frequency of 50kHz (Bodystat® 1500 Ltd, Isle of Man, British Isles) [16]. Participants wore the Equivital monitor (Equivital EQ02 SEM, Hidalgo, UK) for the measurements of core body temperature (CBT) for five consecutive days (Supplementary Fig. 2).

Data processing of the core body temperature

In order to assess core body temperature, each participant swallowed one Core Body Temperature Capsule (Capsule REF 500-0100-02, Respironics Inc., Murrysville, PA, USA) at each of three consecutive days, during dinner time (Supplementary Fig. 2). The capsule measured the core body temperature at a frequency of 250 ms and was connected with the Equivital device by radio emission, with a maximum range of one meter. The acceptable core body temperature sensing range of the capsule is from 32°C to 42°C, according to factory settings. After a variable number of hours or days the core temperature capsule was discarded with the faces.

Means per 5 minutes were calculated based on measurements every 15 seconds, temperature measurements ≤35°C or ≥41°C were excluded, and the first 5 hours after ingestion of the pill were removed to limit the influence of intake of food on the core body temperature measurements before passage through the stomach [17].

Single measurements of thyroid hormones

Fasted blood samples were taken in the late morning for measurement of TSH, fT4 and fT3.

TSH bioactivity

For the in vitro measurement of TSH bioactivity we used the 09.10h K3-EDTA-samples of the 38 participants who were frequently sampled over 24 hours. We measured the biological activity of TSH in vitro according to our established protocol based on the recommendation of the American Thyroid Association Guide by measuring intracellular cAMP production of cultured Chinese hamster ovary cells stably transfected with the human TSH receptor (kindly provided by Dr. AC Bianco, Chicago, USA) [18, 19]. The levels of cAMP were measured using a double-antibody radioimmunoassay kit (adenosine 3'5'cyclic monophosphate, PerkinElmer®, Massachusetts, USA).

Deconvolution analysis

The 24 hour TSH secretion was analyzed using a recently validated deconvolution method(20).

Approximate entropy (ApEn)

ApEn of TSH was used as a regularity statistic to quantify the regularity or orderliness of consecutive serum TSH concentration measurements over 24 hours. Mathematical models and feedback experiments establish that pattern orderliness monitors feedback and/or feed-forward interactions within an interlinked axis with high sensitivity and specificity, both greater than 90% (21). Reduced pattern regularity typifies hormone secretion in puberty and ageing, during diminished negative feedback or fixed exogenous stimulation, and by autonomous neuroendocrine tumours (22).

Statistical analysis

Descriptive statistics were used to summarize the characteristics of both study groups. Chi square test and t-test were used to describe differences between offspring and partners regarding sex, age, age of the parents, body composition, medical history, medication, creatinine clearance, liver function tests, smoking and alcohol use. To calculate differences in secretion between offspring and partner for the different thyroid status parameters, areas under the curves were calculated according to the trapezoid method using SigmaPlot for Windows Version 11.0 (Systat Software, GmbH, Erkrath, Germany). The areas under the curves were calculated over the 24 hours, during the day from 09.00h to 23.00h and during the night from 24.00h to 06.00h. Linear regression was used to compare total TSH secretion, levels of TH, T3, rT3, measurements of AUC's, levels of cAMP/TSH ratio, AUCfT4/total TSH secretion, fT4/TSH ratio, fT4xTSH product, fT3/fT4 ratio, T3/rT3 ratio, AUC fT3/AUC fT4 ratio and parameters of the energy metabolism between offspring and partners adjusted for age and sex. When not normally distributed parameters were log transformed for analysis, and data are presented as geometric mean with 95% confidence interval. Because ApEn of TSH was still not normally distributed after log transformation, a non-parametric test was used. For all above mentioned analyses the Statistical Package for the Social Sciences program for Windows, version 20 (SPSS, Chicago, IL) was used. Graphs were made using GraphPad Prism version 5 (GraphPad, San Diego, CA).

RESULTS

Baseline characteristics

Between 2002 and 2006, 421 families with at least two long-lived Caucasian siblings, were recruited in the Leiden Longevity Study, without any selection on health. Males had to be aged 89 years or above and females 91 years or above [3, 12]. For the current study (Switchbox) we included 61 offspring and 51 partners in which we measured energy metabolism (the full study sample) and 20 offspring and 18 partners (subgroup) in which we sampled blood continuously over 24 hours.

TABLE 8.1 | Baseline characteristics of full study sample and subgroup.

	Full study sample			Subgroup		
	Offspring n=61	Partner n=51	*P*-value	Offspring n= 20	Partner n= 18	*P*-value
Demographics						
Male n (%)	28 (45.9)	27 (52.9)	0.46	10 (50.0)	10 (55.6)	0.73
Age (years)	65.9 (6.4)	65.9 (6.1)	0.95	65.6 (5.4)	64.6 (4.9)	0.52
Age mother (years)†	89.7 (10.3)	77.5 (15.3)	<0.001	92.4 (7.9)	78.6 (13.9)	0.001
Age father (years)†	86.0 (15.1)	72.6 (11.5)	<0.001	82.5 (18.9)	76.8 (9.2)	0.25
BMI (kg/m^2)	25.6 (3.6)	26.5 (4.3)	0.22	25.4 (4.0)	25.5 (3.9)	0.91
Fat mass (kg)*	23.9 (6.6)	26.4 (9.8)	0.13	23.5 (7.1)	23.7 (7.8)	0.93
Fat free mass (kg)*	51.4 (11.8)	53.1 (10.4)	0.42	51.3 (12.0)	52.5 (11.4)	0.75
Medical history						
Cardiovascular disease n (%)	2 (3.2)	7(13.7)	0.04	0 (0)	1 (5.5)	0.29
Malignancies n (%)	7 (11.5)	2 (3.9)	0.14	3 (15.0)	0 (0)	0.09
Osteoporosis/arthritis n (%)	5 (8.2)	5 (9.8)	0.77	1 (5.0)	2 (11.1)	0.49
Medication						
Statins n (%)	4 (6.6)	9 (17.6)	0.07	0 (0)	1 (5.6)	0.29
Anti-hypertensive n (%)	11 (18.0)	17 (33.3)	0.06	3 (15.0)	2 (11.1)	0.72
Laboratory results						
Creatinine clearance (ml/min)	87.0 (21.2)	91.6 (27.1)	0.32	89.9 (18.7)	94.7 (22.0)	0.47
Aspartate Aminotransferase (U/l)	26.0 (8.9)	27.3 (13.1)	0.51	25.9 (6.2)	24.4 (6.9)	0.50
Alanine Aminotransferase (U/l)	25.0 (22.4)	24.4 (9.1)	0.86	23.4 (5.2)	23.1 (7.1)	0.88
Lifestyle						
Smoking current n (%)	1 (1.6)	1 (2.0)	0.90	0 (0)	1 (5.6)	0.29
Alcohol > 20 units/week n(%)	5 (8.2)	4 (7.8)	0.93	1 (5.0)	2 (11.1)	0.49

*Unless indicated otherwise, data are presented as mean (standard deviation). * Data were not available for 1 male partner due to technical problems. † missing data of 3 participants in the full study sample.*

The baseline characteristics of both the full study sample as well as the subgroup are presented in Table 1. In the full study sample as well as in the subgroup, the groups of offspring from long-lived families and partners were of similar age, sex and BMI. Participants were selected on the basis of the age of their parents. Consequently, in both groups mothers of offspring were significantly older (P < 0.001), and in the full study sample the age of the offspring's fathers was significantly higher as well (P < 0.001). In line with previous findings[3], offspring had less cardiovascular disease.

TSH and thyroid hormones

Offspring from long-lived siblings had on average 0.8 mU/l higher serum concentrations of TSH at all time points over a 24-hour period (Fig. 1a). We calculated the area under the curve (AUC) to estimate hormone production over the 24 hour period, during the day period (9.00h-23.00h) and during the night (24.00h-06.00h). The mean (95% CI) TSH AUC over the 24 hour period was significantly (P = 0.009) higher in the offspring (56.1 (45.7-66.5 mU/l)) compared to that of their partners (35.3 (24.4-46.3) mU/l) (Supplementary Table 1). Moreover, the mean (95% CI) TSH AUC was significantly higher during the day (P = 0.006) as well as during the night (P = 0.025) in the offspring compared to the partners thereof. The 24-hour profiles of fT4 (Fig. 1b) and fT3 (Fig. 1c) and the areas under the curves over the 24-hour period, during the day and night (Supplementary Table 1) did not differ between groups. We performed deconvolution analyses to quantify total TSH secretion over 24 hours on the basis of the TSH concentration profiles [20]. Geometric mean (95% CI) total TSH secretion over 24 hours was significantly (P = 0.007) higher in the offspring (55.0 (43.9-68.9) mU/l) compared to partners (34.4 (27.1-43.7) mU/l).

To ensure that the subgroup represented the full study sample, we replicated the TSH and TH measurements in a fasted single late morning sample for the 112 subjects from the full study sample (Table 2). Again, we found significantly increased (P = 0.01) geometric mean (95% CI) serum concentrations of TSH in offspring (2.1 (1.8-2.3) mU/l) compared to partners (1.6 (1.4-1.9) mU/l), but no difference in TH serum concentrations.

Regularity of consecutive serum tsh concentration measurements over 24 hours

ApEn was used as a regularity statistic to quantify the regularity or orderliness of consecutive serum TSH concentration measurements over 24 hours, with a higher ApEn indicating a greater irregularity [23, 24]. Geometric mean (95% CI) ApEn of TSH was similar between offspring and partners ((1.26 (1.13-1.41) versus (1.15 (1.02-1.29) P = 0.22)).

Relationship between circulating TSH and ft4

In the human population, the HPT axis maintains circulating TSH and thyroid hormone levels in a physiological inverse relationship. We calculated the fT4xTSH product and the fT4/TSH ratio as measures to further characterize the relationship between circulating TSH and fT4 in offspring and partners. In both the full study sample as in the subgroup we found a significantly higher fT4xTSH product in offspring compared to partners (Table 2). In the full study sample and subgroup, fT4/TSH ratio was significantly lower in the offspring compared to the partner group (Table 2). In addition, in the subgroup, offspring had a significantly lower (P = 0.01) geometric mean (95% CI) AUC fT4/total TSH production ratio (6.1 (4.8- 7.8)) compared to partners (9.7 (7.5- 12.7)).

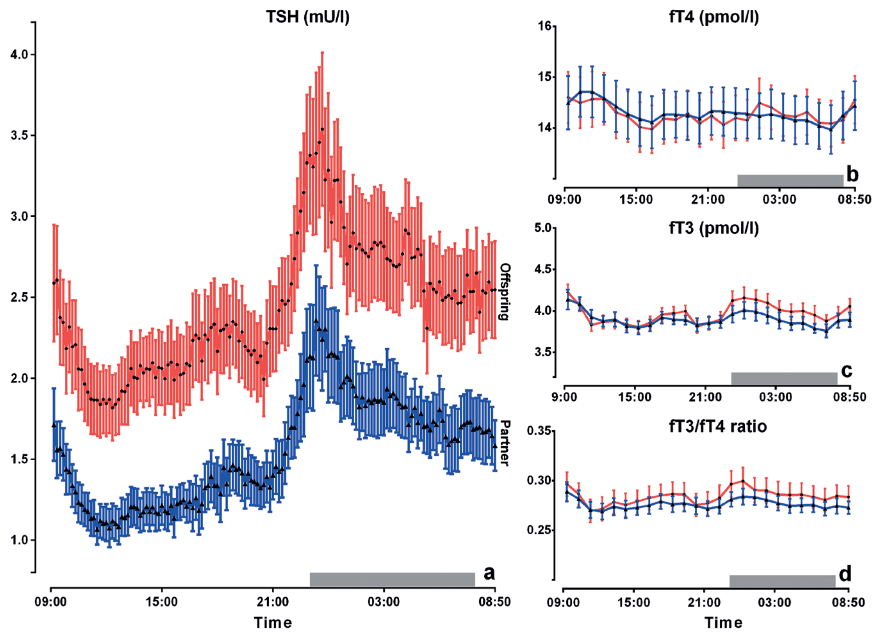

FIGURE 8.1 | Twenty-four hour profiles of TSH, fT4, fT3 and fT3/fT4 ratio in offspring from long-lived families and partners.

In all the panels, data points represent means with standard error of the mean. The red lines depict 20 offspring and the blue lines depict 18 the partners. (a) Ten minutes measurements of TSH. Hourly measurements of (b) fT4 (c) fT3 (d) fT3/ fT4 ratio. The grey bars represent lights off periods (from 23:00-08:00).

Estimates of peripheral deiodination

A possible mechanism that could underlie the offspring's increased TSH secretion is enhanced TH turnover due to increased uptake in tissues or hormone clearance. Amongst others, one process that could contribute to peripheral TH turnover is deiodination [25]. To estimate conversion of fT4 into fT3, we calculated the fT3/fT4 ratio in both the full study sample and the subgroup (table 2). In both the full study sample as in the subgroup no significant differences in fT3/fT4 ratio were found between offspring and partners thereof. Moreover, we calculated the AUCfT3/AUCfT4 ratio in the subgroup only, as a more precise measure of deiodination over the whole 24h period. However, no significant difference was observed in mean (95% CI) AUCfT3/AUCfT4 ratio between offspring and partners (6.8 (6.3-7.2) versus (6.6 (6.1-7.0), P = 0.56)). Deiodinase 1 and deiodinase 2 are responsible for the generation of T3 from T4, whereas deiodinase 3 is the major inactivating enzyme leading to an increase of reverse T3 (rT3). The ratio between T3 and rT3 (T3/rT3-ratio) is therefore regarded a more sensitive marker of the peripheral thyroid hormone metabolism [26-28]. No significant difference was observed in T3/rT3 ratio between offspring and partners in both the full study sample as well as in the subgroup (Table 2). After exclusion of 1 female partner, who had a rT3 measurement above the reference range, no difference was found between offspring and partners in the mean (95% CI) T3/rT3-ratio (6.8 (6.3-7.2) versus 6.5 (5.9-7.0) P = 0.39).

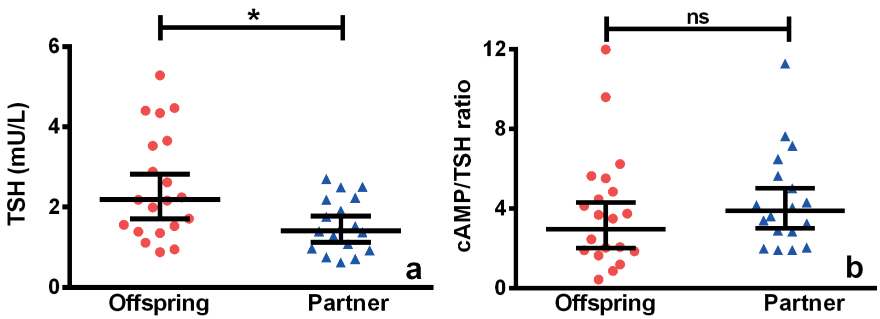

FIGURE 8.2 | *In vitro* TSH bioactivity in offspring from long-lived siblings and partners.

*Red circles represent 20 offspring, blue triangles represent 18 partners. Solid lines represent (a) geometric mean with 95% CI of TSH levels (mU/l) (b) geometric mean with 95% CI of cAMP/TSH-ratio. * P < 0.05; ns: not significant.*

TSH bioactivity

We determined TSH bioactivity in vitro to assess whether the offspring's increased TSH secretion was a compensatory mechanism for reduced TSH bioactivity. We first assessed if the TSH levels in the sample in which we wanted to measure TSH bioactivity were higher in the offspring (Fig. 2a). Again, we found a significant ($P < 0.02$) higher mean (95% CI) TSH level in offspring (2.2 (1.7-2.8) mU/l compared to partners thereof (1.4 (1.1-1.8) mU/l). To determine whether the bioactivity of TSH molecules was different between the groups, the total amount of cAMP produced was adjusted for sample TSH concentrations, by calculating the cAMP/TSH ratio which was similar for offspring and controls (Fig. 2b).

TABLE 8.2 | Thyroid status in offspring from long-lived siblings and partners.

	Full study sample*			Subgroup		
	Offspring (n=61)	**Partner (n=51)**	***P*-value**	**Offspring (n=20)**	**Partner (n=18)**	***P*-value**
Hormone levels (rv)						
TSH (0.3-4.8 mU/l)†	2.1 (1.8-2.3)	1.6 (1.4-1.9)	0.01	2.2 (1.7-2.8)	1.4 (1.1-1.8)	0.02
fT4 (10-24 pmol/l)	16.1 (15.5-16.7)	16.5(15.9-17.1)	0.36	14.7(13.7-15.7)	14.5 (13.5-15.5)	0.78
fT3 (4.7-8.2 pmol/l)	4.7 (4.6-4.8)	4.6 (4.5-4.8)	0.49	4.2 (4.10-4.4)	4.1 (3.9-4.3)	0.36
T3 (1.1-3.1 nmol/l)‡	1.66 (1.59-1.72)	1.62(1.55-1.68)	0.37	1.50(1.42-1.57)	1.48 (1.40-1.56)	0.72
rT3(0.11-0.44nmol/l)‡	0.26 (0.24-0.28)	0.27(0.25-0.29)	0.30	0.18(0.16-0.20)	0.17 (0.15-0.19)	0.57
fT4xTSH product †	33.0 (29.0-37.4)	26.4(23.0-30.3)	0.02	31.7(25.0-40.0)	20.4 (15.9-26.2)	0.01
fT4/TSH ratio †	6.7 (5.2-8.6)	10.1 (7.7-13.2)	0.03	7.7 (6.7-8.8)	10.1 (8.7-11.8)	0.01
fT3/fT4 ratio	0.30 (0.29-0.31)	0.29(0.27-0.30)	0.20	0.30(0.28-0.32)	0.29 (0.27-0.31)	0.55
T3/rT3 ratio‡	6.77 (6.28-7.25)	6.36(5.84-6.88)	0.26	8.84(7.80-9.88)	9.24(8.13-10.34)	0.60

*Unless otherwise indicated data are displayed as means with 95% (CI) adjusted for age and sex. *data were not available in the full study sample for 2 offspring and 2 partners for analyses of fT4, fT3, TSHxfT4 product, fT4/TSH ratio and fT3/fT4 ratio; †geometric mean with 95% CI. ‡ data were not available for 4 offspring and 1 partner for analysis due to limited amount of blood. rv: reference values.*

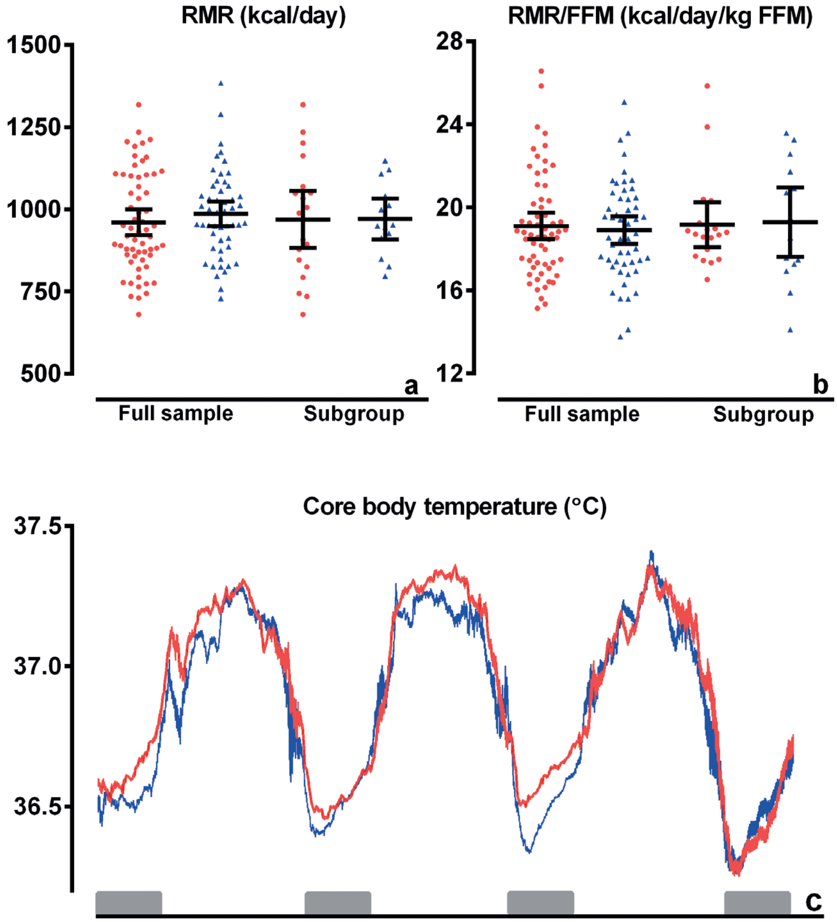

FIGURE 8.3 | Parameters of energy metabolism in offspring from long-lived siblings and partners.

Red circles represent offspring (n=61 for full study sample; n=20 for subgroup) and blue triangles represent partners (n=51 for full study sample; n=18 for subgroup). (a) Mean (95% CI) resting metabolic rate (kcal/day). (b) Mean (95% CI) resting metabolic rate per kg fat free mass (c) Mean (SEM) core body temperature per 5 minutes over 3 days in full study sample offspring (red line) and partners (blue line). Grey blocks are the dark periods (24.00h - 07.00h). RMR: resting metabolic rate; FFM: fat free mass. P ≤ 0.05; ** P ≤ 0.01; ns: not significant.*

Metabolism

Mean (95% CI) resting metabolic rate did not significantly differ between offspring and partners in the full study sample (960 (924-997) kcal/day versus (987 (947-1026) kcal/day, P = 0.34)) nor in the subgroup (Fig. 3a). Adjustments for age and sex did not materially change the results. Moreover, resting metabolic rate per kg fat free mass (FFM) did not differ between offspring and partners in both groups (Fig. 3b). There was no difference in core body temperature over the 3 day period between offspring and partners in the full study sample (Fig. 3c) or in the subgroup.

DISCUSSION

In this study, we investigated if human longevity is associated with differences in TSH and/or TH and whether these concur with differences in energy metabolism because this process is responsive to TSH/TH action and has been associated with longevity in model organisms. The main findings of this article are that familial longevity is characterized by higher TSH secretion, in the absence of differences in TH levels and metabolism.

The association of higher TSH with familial longevity is in line with our earlier observations in nonagenarians from the Leiden Longevity Study [7] and their offspring [9] as well as with earlier observations in Ashkenazi centenarians and their offspring [29]. In line with the data described in this article, higher TSH in Ashkenazi centenarians and their offspring was not associated with lower concentrations of circulating thyroid hormone levels [29]. In contrast, previously we did find slightly lower levels of thyroid hormones in offspring from long-lived siblings [8] and we also found that nonagenarians from families with the lowest family mortality history score had relatively lower levels of thyroid hormones [7]. However, these previous studies were performed using non-fasted single blood samples randomly taken over the day and there were no [7] or less stringent [8] selection criteria on health status of the participants, which both can influence TH levels. In addition, the observed differences between offspring and partners with respect to the thyroid hormones were very small [8]. In the current study, to reduce confounding by health status, we used more strict inclusion criteria (as described in the methods) and to reduce confounding by sampling time, all comparisons of serum TSH and thyroid hormone measurements between groups were standardized for sampling time.

The observation that despite increased levels of TSH, levels of TH were similar between groups aligns with the observation that energy metabolism was not different between groups. Metabolic rate is inversely associated with longevity in different animals and metabolism plays a central role in several ageing theories. In turn, administration of TH is well known to increase metabolic rate in diverse species, including humans. Recent studies in animals have also implicated central mechanisms in the effects of T3 on increased metabolism [30]. We did not find differences in resting metabolic rate or core body temperature between the offspring and the partners in the full study sample nor in the subgroup. This is remarkable, since many ageing theories and longevity models in animals are related to changes in energy metabolism. These findings align with the observation that despite increased levels of TSH, levels of TH were similar between groups. Also the fT3/fT4 ratio, as a proxy for conversion of fT4 into fT3 was comparable between offspring and partners both in the full study sample and in the subgroup. Moreover in the subgroup the AUCfT3/AUCfT4 ratio over the 24h period did not significantly differ between offspring and partners.

Several possible mechanisms can contribute to the observed increase in TSH in the offspring group, including (i) reduced bioactivity of circulating TSH, (ii) diminished sensitivity of thyrotrophs to negative feedback by thyroid hormones, (iii) diminished responsiveness of the thyroid gland to TSH, and (iv) enhanced thyroid hormone turnover in peripheral tissues and (v) enhanced clearance of thyroid hormones from the circulation.

The bioactivity of circulating TSH is known to differ depending on the degree of glycosylation and sialylation. A lower TSH bioactivity in the offspring would require higher concentrations of circulating TSH to maintain circulating thyroid hormone levels. In our study sample, TSH bioactivity, as reflected by the cAMP/TSH ratio in an in vitro activity assay, was similar in the offspring and partners.

To explore the possibility that the offspring might have higher TSH because of diminished sensitivity of thyrotrophs to negative feedback by thyroid hormones, we calculated the fT4xTSH product and found that it was higher in the offspring group. Previously, the fT4xTSH product has been used to quantitate the sensitivity of the thyroptrophs to feedback regulation by thyroid hormone and the degree of inherited thyroid hormone resistance [31]. Although all subjects with inherited thyroid hormone resistance had higher serum concentrations of fT4 for corresponding TSH concentrations, the degree of thyroid hormone resistance differed depending on the type of mutation, which was reflected by the fT4xTSH product [31]. Thus, a higher thyrotroph T4 resistance index in the offspring might be indicative of reduced sensitivity of the thyrotrophs to feedback regulation by thyroid hormone. However, there are two observations that might argue against this interpretation. First, one would expect the increased TSH secretion to result in an increase in fT4 concentrations. However, in contrast to subjects with thyroid hormone resistance [31], circulating thyroid hormone levels were not higher in the offspring. Second, the ApEn of TSH secretion was not significantly different in the subgroup between offspring and partners. ApEn of TSH was used as a regularity statistic to quantify the regularity or orderliness of TSH secretion, with a higher ApEn indicating a greater irregularity. Mathematical models and feedback experiments have established that pattern orderliness monitors feedback and/or feedforward interactions within different hypothalamo-pituitary target-organ systems with high sensitivity and specificity [23]. With regard to TSH secretion, previous studies have shown that the ApEn of TSH secretion is greatly increased in patients with severe hypothyroidism, but not in subjects with subclinical hypothyroidism or in controls [24]. Thus, in severe hypothyroid patients, the failure of the thyroid gland to produce sufficient amounts of thyroid hormone will lead to loss of thyroid hormone mediated feedback on TRH and TSH secretion, and this was reflected by an increase in the irregularity of TSH secretion (higher ApEn of TSH secretion). In contrast, in patients with subclinical hypothyroidism, thyroid hormone levels are within the normal range, and the ApEn of TSH secretion was unchanged, reflecting intact thyroid hormone mediated feedback on TRH and TSH secretion [32].

An alternative interpretation for the increased fT4xTSH product in offspring is that it reflects higher serum concentrations of TSH for corresponding fT4 concentrations. This finding may thus hint more towards reduced responsiveness of the thyroid gland to TSH, driving production of TSH to maintain sufficient circulating fT4 and fT3 levels. We further explored the possibility that TSH secretion could compensate for reduced responsiveness of the thyroid gland by calculating the fT4/TSH ratio in the full study sample and the AUC fT4/total TSH production ratio. We found that these ratio's were significantly lower in the offspring lending support to the possibility that their thyroid gland is likely to be less responsive to TSH than the thyroid gland of their partners.

A fourth possible mechanism underlying increased TSH secretion is enhanced TH turnover. The fT3/fT4 ratio, a proxy for conversion of fT4 into fT3 did not differ between offspring and partners. However, while circulating levels of fT4 and fT3 are kept within narrow ranges, TH levels exhibit much wider variation within target tissues due to intense and highly regulated control of tissue- specific TH action by deiodinases, transporters and transcriptional co-regulators. Thus, we cannot exclude the possibility that TSH levels are increased in familial longevity due to increased TH turnover in target tissues. Although we did not have data on deiodinase activity in specific target tissues, circulating T3/rT3 ratio was shown to exhibit a strong and positive correlation with liver deiodinase 1 activity [26]. In our study, no differences were found between offspring and partners in the T3/rT3 ratio. Taken together, enhanced TH turnover by increased peripheral turnover of TH is less likely to be an underlying mechanism of the increased TSH secretion.

It should be noted that the sample size of the current study is relatively small and that differences that did not reach statistical significance in our study sample might be clinically significant. The families included in the Leiden Longevity Study are genetically heterogeneous, and thus different mechanisms may be at play in different families and/or in different individuals.

A fifth possible mechanism underlying increased TSH secretion is that the offspring may have an enhanced rate of thyroid hormone clearance from the circulation, which would trigger the pituitary to secrete more TSH, stimulating the production of thyroid hormones to ensure appropriate circulating TH concentrations. Unfortunately, we did not have data on thyroid hormone clearance by the liver and kidneys to evaluate this possibility.

Thus, our data cannot discriminate which mechanism is responsible for the altered thyroid status in familial longevity and what the physiological consequences are of the observed increased TSH secretion. Future studies should aim to disentangle the causes and consequences of the altered thyroid status by TSH and TH challenges.

Moreover, this study did not investigate other processes that might be influenced by differences in TSH and/or TH and that might be relevant for longevity. One such key process is tissue turnover. In adult mammalian tissues, damaged and worn-out mature cells are continuously being replaced during normal tissue homeostasis and in response to stresses and injury, a process that is critically dependent on the differentiation of self-renewing, tissue-specific stem cells. Various theories propose that ageing implicates either depletion or failed differentiation of stem cells [6]. The TSH receptor (TSHR), a G-protein coupled hormone receptor, plays an important role in growth and differentiation of thyroid follicular cells. However, TSHR expression is not limited to the thyroid. TSHR is also expressed on bone cells [33, 34] and other cells, including adipocytes, hepatocytes, skeletal muscle cells, neuronal cells, astrocytes and mesenchymal stem cells [35-37]. In mesenchymal stem cells TSH induces gene expression patterns that have been implicated in functions related to stem cell fate, including self-renewal, differentiation and maintenance [35]. TSH is also involved in cellular differentiation in other cells with effects depending on the stage of differentiation, e.g. TSH stimulated early differentiation of preadipocytes but inhibited their proliferation and terminal differentiation [38]. However, because of the physiological inverse relationship between TSH and thyroid hormones, and the critical role of thyroid hormone in development, the extrathyroidal effects of TSH in the skeleton and other tissues remain controversial [33].

A strength of our study is that we frequently measured hormone levels over a 24 hour period. Therefore, we were able to standardize comparison of hormone levels between groups for clock time and were able to explore differences in total TSH secretion using deconvolution analysis. Another strength is that we simultaneously measured several physiological parameters known to be affected by thyroid hormones. Since we included offspring enriched for longevity and compared them with their their partners, we had a matched control group. One of the weaknesses of the study is that not all offspring are enriched for longevity causing us to underestimate actual effects. Moreover, the invasive nature and the high costs of hormone rhythm studies make it impossible to perform such studies using a large sample size and relative small but clinically significant differences between groups may not be detected.

The principal findings of this study are that familial longevity is characterized by higher TSH secretion, in the absence of differences in TH concentration and in whole body energy metabolism. Taken together, these observations suggest that pleiotropic effects of the HPT axis protect long-lived families. Further in depth mechanistic studies should focus on disentangling these underlying mechanisms.

Supporting information

The Supplementary Material for this article can be found online at:
http://www.nature.com/srep
Supplementary Figure 1. Switchbox study sample selection process.
Supplementary Figure 2. Study time table for full study sample and the subgroup.
Supplementary Table 1. Thyroid status in offspring and partners.

REFERENCES

1. Rae MJ, Butler RN, Campisi J, de Grey AD, Finch CE, Gough M, et al. The demographic and biomedical case for late-life interventions in aging. Science translational medicine. 2010;2(40):40cm21.
2. Abbott A. Ageing: growing old gracefully. Nature. 2004;428(6979):116-8.
3. Westendorp RG, van Heemst D, Rozing MP, Frolich M, Mooijaart SP, Blauw GJ, et al. Nonagenarian siblings and their offspring display lower risk of mortality and morbidity than sporadic nonagenarians: The Leiden Longevity Study. Journal of the American Geriatrics Society. 2009;57(9):1634-7.
4. Pearl R. The Rate of Living. New York: Knopf. 1928.
5. Harman D. Free radical theory of aging. Triangle; the Sandoz journal of medical science. 1973;12(4):153-8.
6. Campisi J. Cancer and ageing: rival demons? Nature reviews Cancer. 2003;3(5):339-49.
7. Rozing MP, Houwing-Duistermaat JJ, Slagboom PE, Beekman M, Frolich M, de Craen AJ, et al. Familial longevity is associated with decreased thyroid function. The Journal of clinical endocrinology and metabolism. 2010;95(11):4979-84.
8. Rozing MP, Westendorp RG, de Craen AJ, Frolich M, Heijmans BT, Beekman M, et al. Low serum free triiodothyronine levels mark familial longevity: the Leiden Longevity Study. The journals of gerontology Series A, Biological sciences and medical sciences. 2010;65(4):365-8.
9. Bowers J, Terrien J, Clerget-Froidevaux MS, Gothie JD, Rozing MP, Westendorp RG, et al. Thyroid hormone signaling and homeostasis during aging. Endocrine reviews. 2013;34(4):556-89.
10. Gussekloo J, van Exel E, de Craen AJ, Meinders AE, Frolich M, Westendorp RG. Thyroid status, disability and cognitive function, and survival in old age. JAMA : the journal of the American Medical Association. 2004;292(21):2591-9.
11. Russell W, Harrison RF, Smith N, Darzy K, Shalet S, Weetman AP, et al. Free triiodothyronine has a distinct circadian rhythm that is delayed but parallels thyrotropin levels. The Journal of clinical endocrinology and metabolism. 2008;93(6):2300-6.
12. Schoenmaker M, de Craen AJ, de Meijer PH, Beekman M, Blauw GJ, Slagboom PE, et al. Evidence of genetic enrichment for exceptional survival using a family approach: the Leiden Longevity Study. European journal of human genetics : EJHG. 2006;14(1):79-84.
13. Fraser CG. Biological Variation: From Principles to Practice. Washington, DC: AACC Press; 2001.

14. Wiersinga WM, Chopra IJ. Radioimmunoassay of thyroxine (T4), 3,5,3'-triiodothyronine (T3), 3,3',5'-triiodothyronine (reverse T3, rT3), and 3,3'-diiodothyronine (T2). Methods in enzymology. 1982;84:272-303.
15. Simonson DC, DeFronzo RA. Indirect calorimetry: methodological and interpretative problems. The American journal of physiology. 1990;258(3 Pt 1):E399-412.
16. Kyle UG, Bosaeus I, De Lorenzo AD, Deurenberg P, Elia M, Gomez JM, et al. Bioelectrical impedance analysis--part I: review of principles and methods. Clinical nutrition. 2004;23(5):1226-43.
17. Byrne C, Lim CL. The ingestible telemetric body core temperature sensor: a review of validity and exercise applications. British journal of sports medicine. 2007;41(3):126-33.
18. Bianco AC, Anderson G, Forrest D, Galton VA, Gereben B, Kim BW, et al. American thyroid association guide to investigating thyroid hormone economy and action in rodent and cell models. Thyroid : official journal of the American Thyroid Association. 2014;24(1):88-168.
19. Nagayama Y, Kaufman KD, Seto P, Rapoport B. Molecular cloning, sequence and functional expression of the cDNA for the human thyrotropin receptor. Biochemical and biophysical research communications. 1989;165(3):1184-90.
20. Keenan DM, Roelfsema F, Biermasz N, Veldhuis JD. Physiological control of pituitary hormone secretory-burst mass, frequency, and waveform: a statistical formulation and analysis. American journal of physiology Regulatory, integrative and comparative physiology. 2003;285(3):R664-73.
21. Veldhuis JD, Keenan DM, Pincus SM. Motivations and methods for analyzing pulsatile hormone secretion. Endocrine reviews. 2008;29(7):823-64.
22. Pincus SM. Irregularity and asynchrony in biologic network signals. Methods in enzymology. 2000;321:149-82.
23. Veldhuis JD, Straume M, Iranmanesh A, Mulligan T, Jaffe C, Barkan A, et al. Secretory process regularity monitors neuroendocrine feedback and feedforward signaling strength in humans. American journal of physiology Regulatory, integrative and comparative physiology. 2001;280(3):R721-9.
24. Roelfsema F, Pereira AM, Adriaanse R, Endert E, Fliers E, Romijn JA, et al. Thyrotropin secretion in mild and severe primary hypothyroidism is distinguished by amplified burst mass and Basal secretion with increased spikiness and approximate entropy. The Journal of clinical endocrinology and metabolism. 2010;95(2):928-34.
25. Gereben B, Zavacki AM, Ribich S, Kim BW, Huang SA, Simonides WS, et al. Cellular and molecular basis of deiodinase-regulated thyroid hormone signaling. Endocrine reviews. 2008;29(7):898-938.

26. Peeters RP, Wouters PJ, van Toor H, Kaptein E, Visser TJ, Van den Berghe G. Serum 3,3',5'-triiodothyronine (rT3) and 3,5,3'-triiodothyronine/rT3 are prognostic markers in critically ill patients and are associated with postmortem tissue deiodinase activities. The Journal of clinical endocrinology and metabolism. 2005;90(8):4559-65.
27. Peeters RP, van der Deure WM, Visser TJ. Genetic variation in thyroid hormone pathway genes; polymorphisms in the TSH receptor and the iodothyronine deiodinases. European journal of endocrinology / European Federation of Endocrine Societies. 2006;155(5):655-62.
28. de Jong FJ, Peeters RP, den Heijer T, van der Deure WM, Hofman A, Uitterlinden AG, et al. The association of polymorphisms in the type 1 and 2 deiodinase genes with circulating thyroid hormone parameters and atrophy of the medial temporal lobe. The Journal of clinical endocrinology and metabolism. 2007;92(2):636-40.
29. Atzmon G, Barzilai N, Surks MI, Gabriely I. Genetic predisposition to elevated serum thyrotropin is associated with exceptional longevity. The Journal of clinical endocrinology and metabolism. 2009;94(12):4768-75.
30. Lopez M, Varela L, Vazquez MJ, Rodriguez-Cuenca S, Gonzalez CR, Velagapudi VR, et al. Hypothalamic AMPK and fatty acid metabolism mediate thyroid regulation of energy balance. Nature medicine. 2010;16(9):1001-8.
31. Yagi H, Pohlenz J, Hayashi Y, Sakurai A, Refetoff S. Resistance to thyroid hormone caused by two mutant thyroid hormone receptors beta, R243Q and R243W, with marked impairment of function that cannot be explained by altered in vitro 3,5,3'-triiodothyroinine binding affinity. The Journal of clinical endocrinology and metabolism. 1997;82(5):1608-14.
32. Roelfsema F, Veldhuis JD. Thyrotropin secretion patterns in health and disease. Endocrine reviews. 2013;34(5):619-57.
33. Bassett JH, Williams GR. Critical role of the hypothalamic-pituitary-thyroid axis in bone. Bone. 2008;43(3):418-26.
34. Zhang W, Zhang Y, Liu Y, Wang J, Gao L, Yu C, et al. Thyroid-stimulating hormone maintains bone mass and strength by suppressing osteoclast differentiation. Journal of biomechanics. 2014;47(6):1307-14.
35. Bagriacik EU, Yaman M, Haznedar R, Sucak G, Delibasi T. TSH-induced gene expression involves regulation of self-renewal and differentiation-related genes in human bone marrow-derived mesenchymal stem cells. The Journal of endocrinology. 2012;212(2):169-78.
36. Crisanti P, Omri B, Hughes E, Meduri G, Hery C, Clauser E, et al. The expression of thyrotropin receptor in the brain. Endocrinology. 2001;142(2):812-22.

37. Endo T, Kobayashi T. Expression of functional TSH receptor in white adipose tissues of hyt/hyt mice induces lipolysis in vivo. American journal of physiology Endocrinology and metabolism. 2012;302(12):E1569-75.
38. Zhang L, Baker G, Janus D, Paddon CA, Fuhrer D, Ludgate M. Biological effects of thyrotropin receptor activation on human orbital preadipocytes. Investigative ophthalmology & visual science. 2006;47(12):5197-203.

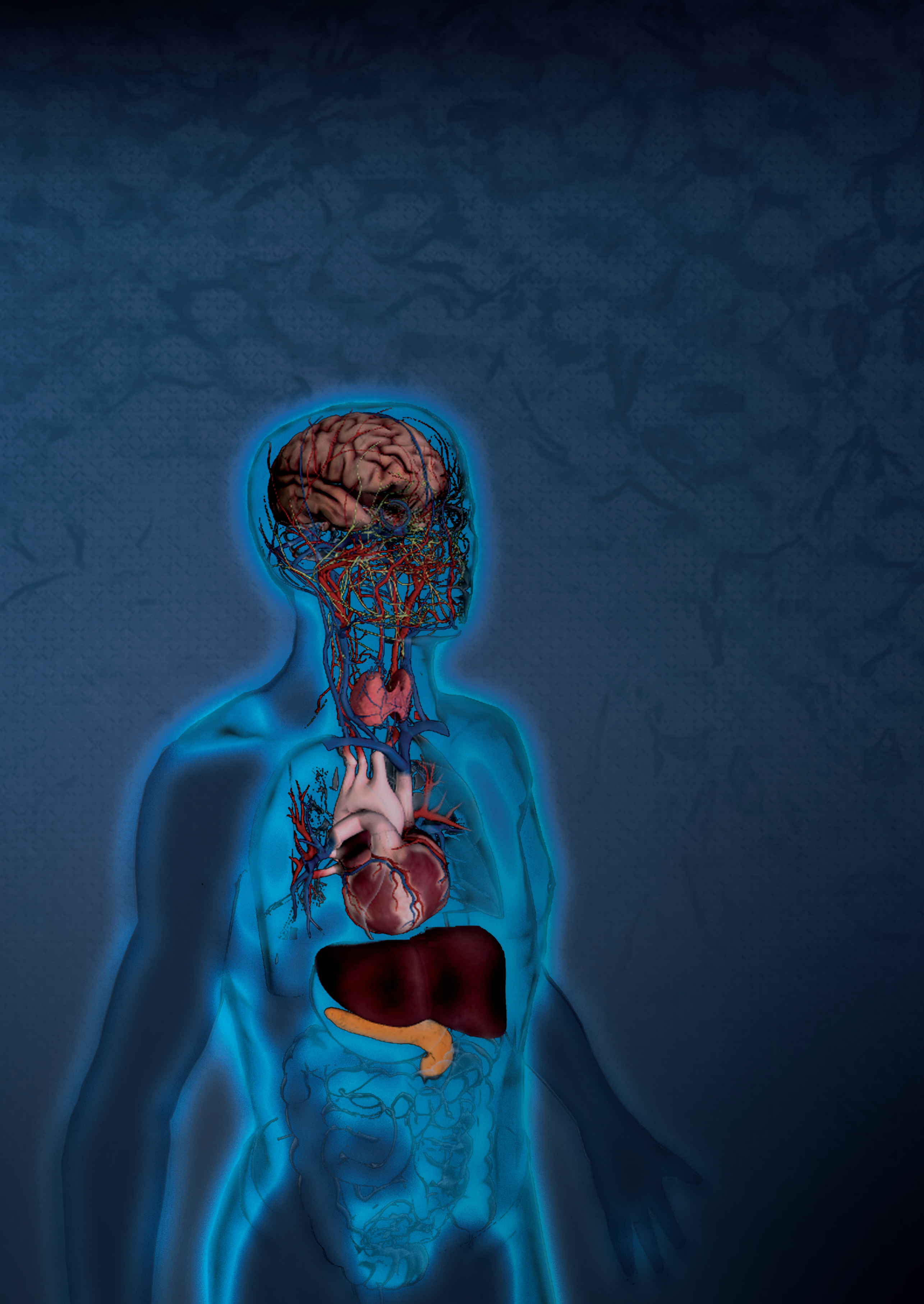

CHAPTER 9

SUBCLINICAL HYPOTHYROIDISM AND COGNITIVE FUNCTION IN PEOPLE OVER 60 YEARS: A SYSTEMATIC REVIEW AND META- ANALYSIS.

Abimbola A. Akintola
Steffy W. Jansen
David van Bodegom
Jeroen van der Grond
Rudi G. Westendorp
Anton J.M. de Craen
Diana van Heemst

Front Aging Neurosci. 2015 Aug 11;7:150.

ABSTRACT

Subclinical hypothyroidism (SCH), defined as elevated thyroid stimulating hormone and normal thyroid hormone levels, and cognitive impairment are both common in older people. While the relation between overt hypothyroidism and cognitive impairment is well established, data on the association between SCH and cognitive impairment are conflicting. This systematic review and meta-analysis was performed to assess available evidence on the association of SCH with cognition in community dwelling, relatively healthy older adults.

PubMed, EMBASE, Web of Science, COCHRANE, CINAHL, PsycINFO and Academic Search Premier (January 1966 to April 1, 2015) were searched without language restrictions, as were references of key articles, for studies on the association between SCH and cognition in older adults (> 60 years). These studies were reviewed by two independent reviewers according to predefined criteria for eligibility and methodological quality, and data extracted using standardized forms.

Of the 844 reports initially identified, 270 remained after exclusion of duplicates. Of the 270, fifteen studies comprising 19,944 subjects, of whom 1,199 had subclinical hypothyroidism were included. Data from the 15 studies was pooled, and meta- analyzed cross-sectionally for global cognition (MMSE), executive function, and memory, using random effects models. Pooled effect size (ES) for MMSE was -0.01 (95% CI -0.09, 0.08), with heterogeneity (I^2) of 55.1%. Pooled ES was <0.001 (95% CI -0.10, 0.09) for executive function (I^2 = 13.5%), and 0.01 (95% CI -0.12, 0.14) for memory (I^2 = 46.9%). In addition, prospective analysis including four studies showed pooled ES of 0.033 (95% CI -0.001-0.067) for MMSE (I^2 <0.001%), indicating that subclinical hypothyroidism was not significantly associated with accelerated cognitive decline.

This systematic review and meta-analysis provides no evidence that supports an association between SCH and cognitive impairment in relatively healthy older adults.

INTRODUCTION

Overt adult onset hypothyroidism, which is marked by elevated thyroid stimulating hormone (TSH) levels and reduced levels of circulating thyroid hormones, has been associated with increased risk of deficits in specific cognitive domains including attention, concentration, memory, perceptual function, language, executive function and psychomotor speed [1-4]. However, controversies persists as to whether subclinical hypothyroidism (SCH), defined as mild elevation of TSH in the presence of normal free thyroxine (fT4), is associated with these specific cognitive domains. This is especially relevant in the older adults, as the prevalence of subclinical hypothyroidism increases with age and is estimated to be up to 22% in women aged more than 60 years and somewhat lower in men [5, 6].

Many studies have investigated whether subclinical hypothyroidism is associated with increased risk of cognitive impairment [7-21]. However, the data are conflicting, and epidemiological studies that investigated this relationship have reported inconsistent findings. Furthermore, due to use of different TSH cut- off values, methodological differences, application of varying cognitive tests for different cognitive domains, and diverse reporting of results by these studies, the interpretability and comparability of their findings are hindered.

Here, we performed a systematic review of available evidence from both cross-sectional and prospective studies on the association between subclinical hypothyroidism and cognition in the older adults. Furthermore, we performed a meta- analysis to quantify the magnitude of the associations between subclinical hypothyroidism and both global cognition as well as two specific cognitive domains, namely executive function and memory.

METHODS

Data sources and search strategy

A systematic literature search was conducted of articles published from January 1966 to April 1, 2015 on the association between subclinical hypothyroidism and cognition in the elderly. PubMed, EMBASE, Web of Science, COCHRANE, CINAHL, PsycINFO and Academic Search Premier were searched (Datasheet 1). The design of the electronic search strategy was done in consultation with an expert information specialist. A thorough search was conducted on the bibliographies of key articles in the field and these were included in this review. To avoid missing any relevant study in the search, broadly defined terms were used (Datasheet 1). Reference lists of key articles were also searched for relevant articles that could have been missed.

Study selection

Two independent reviewers (AAA and SWJ) screened the extracted citations for eligibility. To maximize the quality and comparability of the studies, general inclusion and exclusion criteria were defined a priori (Table 1). The titles, abstracts and later the full- texts of the search results were screened- the studies included were those that assessed the cognitive status of relatively healthy (community dwelling, and considered healthy by the authors of the original articles) elderly (aged 60 years and above) participants with subclinical hypothyroidism.

Subclinical hypothyroidism is defined as elevated TSH and normal fT4 [22]. However, controversies exist as to the upper limit of the TSH reference range. Several reviews suggest a TSH upper limit of 4.5 to 5.0 mU/L (22, 23), but some authors suggest that the upper limit of the TSH range should be reduced to 2.5 to 3.0 mU/L, based on a higher risk of progression to overt hypothyroidism and a higher prevalence of anti-thyroid antibodies than in euthyroid participants (24). In the absence of a consensus, the use of a specific TSH upper limit was not pre-specified in this systematic review to define subclinical hypothyroidism. Furthermore, fT4 values were considered normal if indicated as normal by the authors, even if data on fT4 were not presented.

Studies done on participants with depression (according to the Diagnostic and Statistical Manual of Mental Disorders (DSM) criteria), dementia, psychiatric symptoms, neurological disorders e.g. Parkinson's disease, and other chronic systemic illnesses were excluded. Furthermore, participants using thyroid medications were excluded. Three relatively large studies that measured health status of participants with an elevated TSH were initially included. However, they were later excluded because assessment of mood, general and mental health status was done qualitatively, without specifying whether global cognition or specific cognitive domains were measured [25-27].

TABLE 9.1 | Selection criteria for eligibility for inclusion or exclusion

Inclusion criteria	**Exclusion criteria**
Human studies	Animal studies
Median/mean age 60 or above	Younger than 60
Subclinical hypothyroidism (SCH)- • Elevated TSH and normal fT4; • All self-defined subclinical hypothyroidism - Elevated serum TSH in association with normal total or free T4 and T3 values - High-normal TSH and abnormal response to TRH - Elevated serum TSH with normal thyroid hormone levels, without symptoms that could be explained by overt hypothyroidism	SCH not defined
Relatively healthy elderly participants: Healthy as determined by the authors of the original articles	Full blown depression, psychiatric symptoms, neurological disorders as Parkinson's disease or predefined dementia, substance abuse
Free living/ community dwelling	Hospitalized patients
Original research articles Including prospective studies, randomized-controlled trials, etc. that provide baseline data	Systematic reviews, meta- analyses, reviews, conference abstracts, web pages.
Cognitive measure and domain specified	Cognitive domain not well defined, e.g. 'mood', 'quality of life', 'mental health' etc.
All languages	
	Duplicates

Data extraction and quality assessment

From each study that met the eligibility criteria, information was extracted about study design (prospective or cross-sectional), participant characteristics, criteria used to define subclinical hypothyroidism, cognitive tests applied and domains tested, and study results (effect estimates, variables included for adjustments, or matching procedures) using a standardized data- collection form.

The two reviewers (AAA and SWJ) independently assessed the methodological quality of included studies using a pre- defined list of criteria [28, 29] (Datasheet 2). In total, 11 key indicators were used to systematically assess study quality. These were 1) clarity of hypothesis, 2) population studied (convenience sample versus population-based, defined as a random sample of the general population, 3) clear definition of subclinical hypothyroidism (indication of TSH cut-off and fT4 values that were used in the study), 4) detailed description of study materials and methods, 5) validity of measurements and cognitive tests, 6) number of cognitive domains tested (global cognition, executive function and/ or memory), 7) clear description of statistical methods, 8) adjustments/ correction for potential confounders, 9) clear presentation of results, 10) generalizability to other populations, and 11) method of outcome adjudication (use of formal adjudication procedures, defined as having clear criteria for the outcome (cognitive impairment). A score of “0” (lacking), “1”(incomplete) or “2” (complete) was assigned to each of the key indicators per study, with a maximum total score of 22.

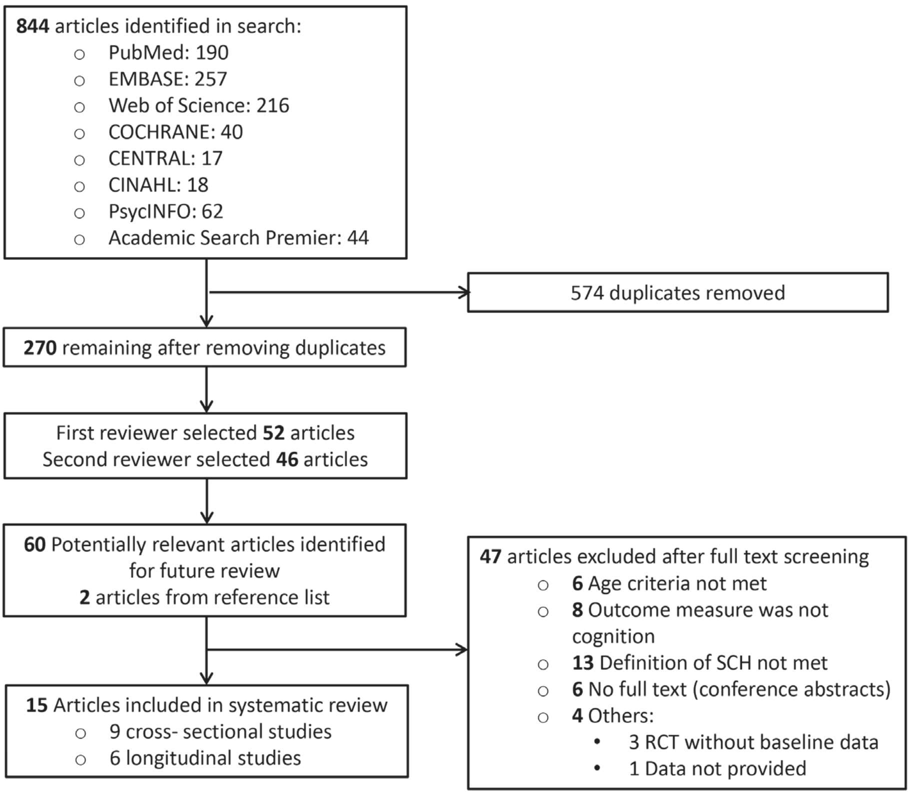

FIGURE 9.1 | Flowchart showing the literature search for the systematic review.

Data synthesis and statistical analysis

Authors were contacted when necessary to request more detailed data on the association between subclinical hypothyroidism and cognition in older adults [10-12]. The most adjusted estimates and SD/SE were used for analysis, where available. In instances where participants were divided into groups based on TSH values (tertiles/ quartiles), the mean TSH value for the whole group was used.

Data was qualitatively synthesized and assessed for the number of participants that were included, the definition of subclinical hypothyroidism applied, the cognitive tests that were used and the cognitive domains that were measured. Meta-analysis was done by comparing estimates from participants with subclinical hypothyroidism with those from euthyroid participants, using data from both cross- sectional studies and baseline data from prospective studies for the cross- sectional analysis. Thus, only studies that provided these estimates were included in the meta- analysis. Using Hedges method [30], pooled estimates with standard error were calculated first from cross- sectional analysis of available studies, and then for the prospective data, using the same approach.

To make effect estimates comparable between studies, effect sizes (ES) were calculated from calculated means with standard deviation of participants with subclinical hypothyroidism compared to euthyroid participants. For studies that used > 1 cognitive test [9, 12, 14, 16, 17, 20], a pooled ES was calculated for each study. After calculating an ES for each study, a meta- analysis was performed using a random effects model. The random effects model was applied, because it takes into account the heterogeneity between the studies. All statistical analyses were performed using STATA version 10. Cochrane Q test and I^2 index with a conservative p-value of 0.10 was used to evaluate the heterogeneity across individual studies. I^2 values of < 25% was considered reflective of low, between 25 and 50% of moderate and > 50% of high heterogeneity between studies.

RESULTS

Study selection

Of the 844 reports initially identified, 270 remained after exclusion of duplicates. Of the 270 reports, 210 were excluded that were unrelated to the association between subclinical hypothyroidism and cognition in the elderly (Figure 1), leaving 60 articles for full text analysis. Two more articles were selected from reference lists of relevant articles. Of the 62 articles that were selected for detailed (full text) evaluation, full texts were not available for six studies. Additionally, ten studies were excluded because the participants were not considered healthy, another thirteen because the definition of subclinical hypothyroidism (high TSH and normal fT4) was not met and four because data was not available for systematic review (three were randomized controlled trials (RCTs) without baseline data, and one study that reported qualitative results). Furthermore, eight studies that did not measure cognition as endpoint were excluded- these either measured mental health by means of questionnaires, or studied depression. Six other studies were excluded because the mean/ median age of the participants was less than 60 years (Figure 1).

Two studies each were reported in Spanish and Dutch respectively, one in Italian and another in Czech. The researchers (AAA and SWJ) themselves translated the two Dutch articles into English. Another article was translated from Czech to English by the author himself [(31)]. The other foreign language articles were translated to English by the researchers' colleagues that spoke the language. These articles were all later excluded after full- text analysis. When similar data were published more than once [(12, 32, 33)], the article with the most definitive and extractable data was included [(12)]. A study was later dropped because it studied the effect of subclinical hypothyroidism on demented and non-demented elderly using only clinical dementia rating, thus was incomparable with the other selected studies in terms of results [(34)]. Fifteen observational studies met the eligibility criteria.

Study characteristics

Table 2 shows the characteristics of the nine cross- sectional and six prospective studies that were included in the review. In total, the 15 studies comprised 19, 944 participants, of whom 1,199 had subclinical hypothyroidism. The upper reference limit of TSH (TSH cut-off) to define subclinical hypothyroidism ranged from 3.6 mU/L to 10 mU/L. A total of 13 out of the 15 studies also reported fT4 measurement. The studies used varying cognitive tests to measure a wide range of cognitive domains. The cognitive domains that were covered included global cognition, executive function, memory, general intelligence, attention and concentration, visio- spatial organization, language, and cognitive or psychomotor speed. These cognitive domains were merged into three main domains, namely global cognition, executive function and memory, as shown in Table 3. The cognitive tests that were used for each of these cognitive domains are also presented in Table 3.

TABLE 9.2 | Characteristics of studies included in the systematic review on the association between subclinical hypothyroidism (SCH) and cognitive impairment in older adults.

	First author	Type of study	Study (Follow-up in years)	N Total	N with SCH	Mean Age (Years)	Cut off TSH (ref. range) mIU/l	fT4 pmol/l	Cognition tests	Study Quality
1	Roberts et al, 2006	Cross- sectional	N/A*	5865	168	73.6	>5.5	9.0-20.0	MMSE, MEAMS	21
2	Wijsman et al, 2013	Prospective	Prosper study (3y)	5.154	161	75	>4.5 (0.45– 4.5)	12-22	MMSE, Stroop, LDCT, WLT. (Immediate and delayed)	22
3	Parsaik et al, 2014	Cross- sectional	N/A*	1904	141	81	>10	12.87-12.04	WAIS-R: TMT, DSST; BNT, CFT, PCBD, WMS (logical memory I & visual reproduction II)	21
4	Park et al, 2010	Cross- sectional	N/A*	918	164	76	>4.1 (0.4-4.1)	9.0-23.2	MMSE, DS, FAB, CERAD-K-N including CFT, BNT-modified, CPT, WLMT, WLRT, WRLRcT, CRT	19
5	De Jongh et al, 2011	Prospective	Longitudinal aging study, Amsterdam, (10.7y)	1219	64	75.5	>4.5 (0.3-4.5)	11-22	MMSE, RPM and the coding task	20
6	Hogervorst et al, 2008	Prospective	MRC cognitive function and aging study (2 y)	1047	33	73.6	>4.8	13-23	MMSE, WMS- revised	20
7	Gussekloo et al, 2004	Prospective	Leiden 85+ study (3.7y)	558	30	85	> 4.8	13-23	MMSE, Stroop, LDCT, WLT (immediate and delayed).	21#
8	S$_T$. John et al, 2009	Cross- sectional	N/A*	489	286	>60	>10.0 (0.3-10.0)	Not indicated	SILS, TMT-b, SDMT, JLO, BD and LNS from WAIS, AN, BNT-modified, CVLT, EBMT, Faces I& II from WMS	17
9	Resta et al, 2012	Cross- sectional	N/A*	391	42	74.3	>3.6 (8.0-17.0 pg/mL)	8.1-15.43	MMSE, PMT and MT	16
10	Ceresini et al, 2009	Cross- sectional	N/A*	1117	25	77	> 4.7	9.9-28.2	MMSE	18
11	Formiga et al, 2014	Prospective	OCTABAIX study (3y)	328	20	85	> 5	10-26	MMSE (MEC, Spanish version)	19#
12	Manciet et al, 1995	Cross- sectional	N/A*	425	26	74.4	>4.5 (0.5-4.5)	16-29	MMSE, WAIS, BVRT, ZBT, IT	16
13	Yamamoto et al, 2010	Prospective	Japanese study (1y)	229	15	80.9	Not indicated	Not indicated	MMSE, revised hasegawa dementia scale	16
14	Cook et al, 2002	Cross- sectional	N/A*	97	15	74	4.0 (0.4-4)	Not indicated	MMSE, AVLT, DSCT from WAIS, N Back test, backward DS	16
15	Cardenas- Ibarra et al, 2007	Cross- sectional	N/A*	253	9	80	> 4.5	Not indicated	MMSE	12

AN: Animal naming; AVLT: Auditory verbal learning test; BD: block design; BNT: Boston naming test; CFT: category fluency test; CPT: constructional praxis test; CRT: constructional recall test.; CVLT: California Verbal Learning Test; CVMT: continuous visual memory test; DS: digit spans forward and backward of WAIS-R; DSCT Digit symbol coding test (from WAIS); DSST: Digit symbol substation test; EBMT: East Boston Memory Test; FAB: Frontal assessment battery; IT: Isaacs set test of verbal fluency; JLO: Judgement of line orientation; LDCT: letter digit coding test; LNS: Letter- number sequencing; LW: list of words; MEAMS: Middlesex elderly assessment of mental state (12 scores); MEC: Mini mental state examination (35 scores); MMSE: Mini-Mental State Examination(30 scores); MMMSE: Modified Mini-Mental State Examination; MT: Matrix test; PMT: Prose memory test; PCBD: Picture completion and block design; RPM: raven progressive matrices test; RW: Rey's words immediate and delayed recall; SDMT: symbol digit modalities test; SILS: Shipley Institute of Living scale; Stroop: Stroop colour word test; TMTA&B: trail making test A and B; WAIS: Wechsler adult intelligence scale; WAIS-R: Wechsler adult intelligence scale-revised; WFT: word fluency test; WLMT: word list memory test; WLRT: Word list recall test; WRLRcT: Word list recognition test; WLT: word learning task; WMS: Wechsler memory scale; ZBT: Zazzos barring test.
** N/A: Not applicable*
 # Score based on published and unpublished data provided by the author.

Systematic review

In total, 1,199 participants with subclinical hypothyroidism were included in the systematic review. From the 15 studies in our systematic review, 12 studies indicated a lack of significant association between subclinical hypothyroidism and cognitive impairment in the elderly. These studies comprised 1,109 participants with subclinical hypothyroidism and therefore contributed 92.5% of the population sampled and to the outcome of the systematic review. Of the remaining three studies, two found an association, and one was inconclusive [(13)]. The inconclusive study demonstrated an association between log transformed TSH levels with decreasing MMSE performance in hypothyroid participants, but it was not specified whether the observed association was with overt hypothyroidism or with subclinical hypothyroidism. This study was included in the systematic review but excluded from meta- analysis.

A total of two studies found an association between subclinical hypothyroidism and cognition in the elderly. The first study found (in 15 participants with subclinical hypothyroidism) that high TSH levels were associated with worse verbal memory and MMSE scores but not speed of performance [(9)]. The second study found (in 42 participants with subclinical hypothyroidism) that performance in MMSE and Prose memory test were lower in participants with subclinical hypothyroidism compared to euthyroid participants [(18)]. Performance in matrix test was also slightly lower in subclinical hypothyroidism, but this was not significant. Summarily, from the studies that observed a significant association between subclinical hypothyroidism and cognitive impairment, the cognitive domains affected were global cognition as assessed via MMSE; executive function as assessed via matrix test; and memory as assessed via auditory verbal learning test, prose memory test, and verbal fluency. The two studies combined comprised 57 participants with subclinical hypothyroidism and contributed only 4.75% to the overall population with subclinical hypothyroidism and to the outcome of the systematic review.

Meta- analysis

To assess whether subclinical hypothyroidism was associated with impairment of various cognitive domains, we analyzed MMSE separately as a measure of global cognition. Ten out of the 15 studies provided MMSE results either at baseline or at follow- up. The rest of the cognitive tests were categorized into tests of executive function or of memory, as shown in Table 3. Data from the 15 studies was pooled first for cross- sectional analysis, and meta- analyzed separately for global cognition (MMSE), executive function, and memory. The pooled effect size (ES) for MMSE was -0.01 (95% CI -0.09, 0.08), with heterogeneity (I^2) of 55.1% (Figure 2A). Pooled ES was < 0.001 (95% CI -0.10, 0.09) for executive function (I^2 = 13.5%) (Figure 2B), and 0.01 (95% CI -0.12, 0.14) for memory (I^2 = 46.9%) (Figure 2C). These analyses indicated that available evidence does not support an association of subclinical hypothyroidism with worse performance in MMSE, executive function or global cognition.

Prospective analysis was done for MMSE in four studies from which prospective data was available (Figure 3). The pooled ES was 0.03 (95% CI -0.001-0.07) P = 0.055, with heterogeneity (I^2) of <0.001%. Thus, subclinical hypothyroidism was not significantly associated with accelerated decline of global cognition, as assessed by MMSE. Due to the small number of available studies, prospective analysis was not done for executive function or memory.

Subgroup and sensitivity analyses

Subgroup analyses were performed on studies with similar TSH cut- off values, and in studies with similar study design (cross- sectional or prospective). The effect sizes of these different subgroups were essentially similar, indicating that in this meta- analysis, subclinical hypothyroidism was not significantly associated with cognitive impairment.

TABLE 9.3 | Cognitive tests and domains used for meta- analysis

Cognitive domain	Measures and cognitive tests
Global cognition	MEAMS, MMSE, MMMSE, 3MSE
Memory (including tests for language)	AN, AVLT, CRT, CVMT, DS, EBMT, FMT, IPALT, LDCT, LW, N-back test, PMT, PWLT, RCFT, SRT, WLT, RBP, RW, WLMT, WLRT, WMS, WRLRcT, Language: AN, BNT, CFT, CVLT, COWAT, IT, OR, RW, WFT, WD, ZBT
Executive function	BD, FAB, DSST, GNG, LMN, MT, PM, RPM, SILS, TMT, WAIS, WFT,
	Attention and concentration: CST, DS, LNS, PASAT, SDMT, Stroop, TMTA&B
	Visuo- spatial organization: CC, CoS, CPT, FR, JLO, HT, PCBD, ScT, SDMT, TMT(Part A), WAIS-R
	Cognitive or psychomotor speed: DSCT, WAIS-R, TMT(Part A), WFT

AN: animal naming; AVLT: Auditory verbal learning test; BD: block design; BNT: Boston naming test; CFT: category verbal fluency test; COWAT: Controlled oral word; CPT: constructional praxis test; CRT: constructional recall test.; CST: concept shifting test; CVLT: California Verbal Learning Test; CVMT: continuous visual memory test; DS: digit spans forward and backward of WAIS-R; DSCT: Digit symbol coding test (from WAIS); DSST: Digit symbol substitution test; FMT: Milner facial memory test; EBMT: East Boston Memory Test; FAB: Frontal assessment battery; FR: figure rotation from the Schaie-Thurstone adult mental abilities test; GNG: Go-No-Go; HT: Hooper test; IPALT: Inglis paired associates learning test; IT: Isaacs set test of verbal fluency; JLO: Judgement of line orientation; LDCT: letter digit coding test; LMN: Luria m's and n's; LNS: Letter- number sequencing; LW: list of words; 3MSE: Modified MMSE (100 scores); MEAMS: Middlesex elderly assessment of mental state (12 scores); MMSE: Mini mental state examination (30 scores); MMMSE: Modified Mini-Mental State Examination; MT: Matrix test; OR: oral reading; PASAT: paced auditory serial addition task; PM: Porteus maze; PMT: Prose memory test; PCBD: Picture completion and block design; PWLT: picture word learning test; RBP: Rivermead behavioral profile; RCFT: Rey-Osterrieth complex figure test; RPM: raven progressive matrices test; RW: Rey's words immediate and delayed recall; ScT: scribble test; SDMT: symbol digit modalities test; SILS: Shipley Institute of Living scale; SRT: selective reminding test (Buschke); TMTA&B: trail making test A and B; WAIS: Wechsler adult intelligence scale; WAIS-R: Wechsler adult intelligence scale-revised; WD: word discrimination; WFT: word fluency test; WLMT: word list memory test; WLRT: Word list recall test; WRLRcT: Word list recognition test; WLT: word learning task; WMS: Wechsler memory scale; ZBT: Zazzos barring test.

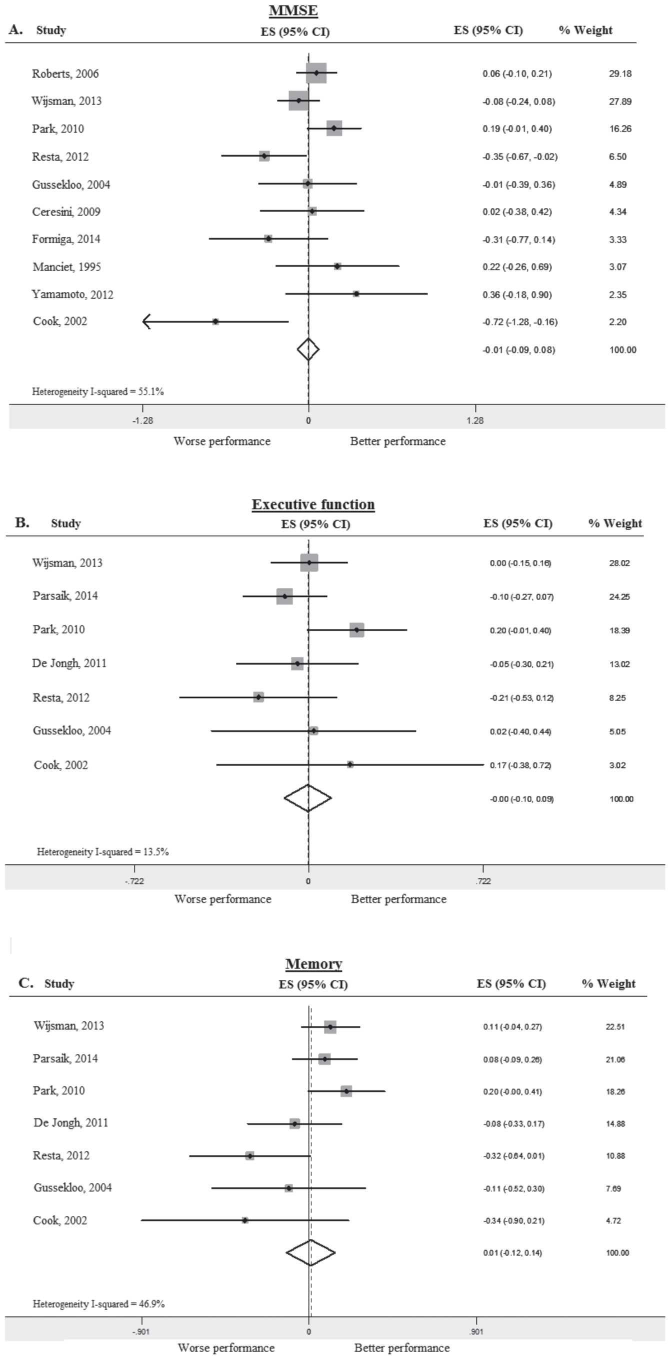

FIGURE 9.2 | Forest plots depicting the cross-sectional associations observed between subclinical hypothyroidism (compared to controls) and cognitive performance in 10 studies, arranged according to the weight of the studies.

Data was pooled from cross-sectional studies and baseline data of prospective studies A.) Association between subclinical hypothyroidism and global cognition as measured by MMSE, B.) Association between subclinical hypothyroidism and executive function, and C.) Association between subclinical hypothyroidism and memory. The pooled effect sizes are displayed as diamonds. MMSE: Mini-mental state examination.

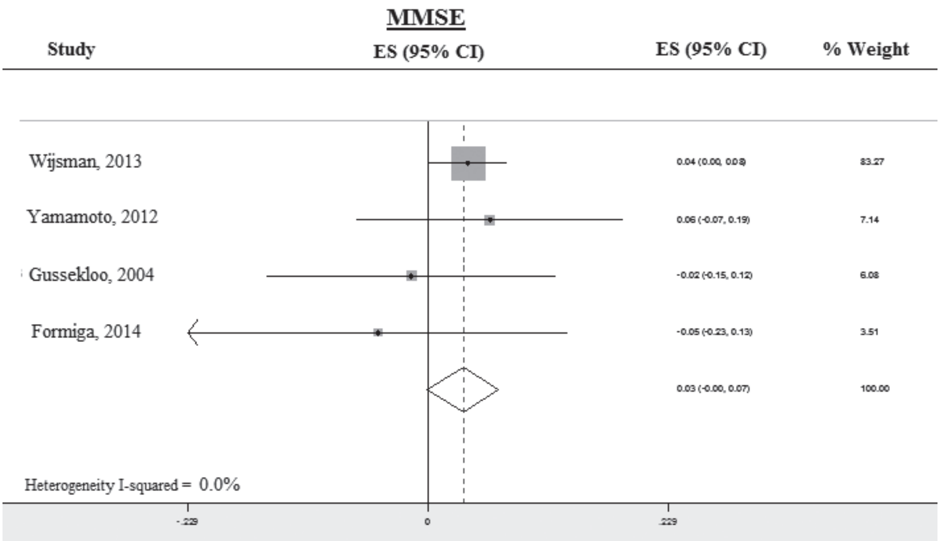

FIGURE 9.3 | Forest plots depicting the prospective analysis of associations observed between subclinical hypothyroidism and decline in global cognition as measured by MMSE, arranged according to the weight of the studies.

The pooled effect sizes are displayed as diamonds. MMSE: Mini-mental state examination.

DISCUSSION

On the basis of the findings of this systematic review and meta- analysis we did not find evidence supporting an association of subclinical hypothyroidism with cognitive impairment in relatively healthy, community- dwelling elderly. Out of 15 observational studies, only two small cross-sectional studies [9, 18] observed statistically significant associations between subclinical hypothyroidism and cognitive impairment, namely global cognition (MMSE), and memory. All other studies indicated a lack of association. No evidence was found that the lack of association between subclinical hypothyroidism and cognitive impairment was limited to unadjusted studies, or to studies of lower methodological quality. Meta-analysis of studies from which data for cross sectional analysis could be retrieved, revealed lack of association between subclinical hypothyroidism and global cognition (assessed by MMSE) as well as lack of association of subclinical hypothyroidism with memory and executive function. Subgroup analyses by type of study design showed a similar trend in the prospective cohort studies group compared with the cross-sectional studies. We also did not find evidence supporting an association of subclinical hypothyroidism with cognitive impairment in a prospective analysis. However, the number of studies retrieved for prospective analysis was low and the study quality (assessed by scoring based on key indicators) varied.

Our results are in line with previous focused reviews [35, 36] supporting a lack of association between subclinical hypothyroidism and cognitive impairment that largely drew upon the results from large population based studies [37]. In contrast, another review conducted on the association between TSH and cognitive impairment in community dwelling and hospitalized elderly [38] reported some evidence supporting the association between subclinical hypothyroidism and cognitive impairment, which was driven by studies showing an association between thyroid hormones and dementia. Thus, previous observational studies on the association of cognition impairment and subclinical hypothyroidism have yielded conflicting results. Our finding of lack association between subclinical hypothyroidism and cognitive impairment is also in line with the results of two placebo controlled randomized clinical trials [36, 39] that showed no effect of treatment with T4 on cognitive endpoints in participants with subclinical hypothyroidism.

To our knowledge, this is the first meta- analysis to examine the cross- sectional and prospective associations between subclinical hypothyroidism and cognitive impairment using available evidence. By pooling the data from the 15 studies, a total of 19, 944 participants, of whom 1, 199 had subclinical hypothyroidism were analyzed. This increased the power to detect potential associations and reduced the probability of false-negative results [18]. Case-control and cross-sectional studies are more susceptible to bias, particularly selection bias for case-control studies [40]. Although bias cannot be excluded, almost all the cross-sectional studies that fulfilled our quality criteria demonstrated the absence of a statistically significant association between subclinical hypothyroidism and cognitive impairment [13, 16].

Overt hypothyroidism has been associated with global cognitive impairment as well as with impairments in various cognitive domains, notably in memory and executive function. Because thyroid dysfunction can be seen as a continuum, it has been hypothesized that subclinical hypothyroidism might also be associated with mild cognitive impairment. The inverse physiological relationship between circulatory levels of TSH and thyroid hormones implies that in subclinical hypothyroidism, thyroid hormone action may be slightly reduced (even though circulatory thyroid hormones are still in the normal range), which might be associated with subtle defects in specific cognitive domains, including memory and executive function. Moreover, one might speculate that potential associations between subclinical hypothyroidism and cognitive impairment are stronger when TSH is markedly increased (TSH > 10 mIU/L) as compared to mild or moderate increases. Similarly, it was found previously that associations between subclinical hypothyroidism and risk for coronary heart disease and mortality were strongest with a TSH concentration of 10 mIU/L or greater [41].

This analysis has four main limitations. Firstly, all data were obtained from observational studies, many of which are cross- sectional studies. There is a possibility of bias in the selection of included studies, bias and quality problems in the original studies, publication bias, heterogeneity, and confounding [29]. To limit bias in the selection of included studies, broad inclusion criteria were used for studies that provided quantitative data on the risk of cognitive impairment in elderly participants with subclinical hypothyroidism. Furthermore, sensitivity analyses were performed according to differences between the studies and methodological study quality, as recommended [29, 42]. Many of the original studies did not have statistically significant results, thus a meta- analysis was conducted to increase the power to find an association. Still, the negative conclusion of this systematic review and meta- analysis may be limited by inherent biases and differences in study designs [43]. However, the sensitivity analyses performed did not suggest that the presented results meaningfully depended on differences in study designs or other study characteristics.

Secondly, the possibility of misclassification of subjects as having subclinical hypothyroidism cannot be ruled out [43]. In most of the studies, the diagnosis of subclinical hypothyroidism was based on single assessment of TSH, without repeated confirmatory TSH measurement. This could have resulted in inclusion of individuals with only transiently elevated TSH levels. Furthermore, none of the included studies used age-adjusted TSH reference ranges to enroll the subjects. Since increased age has been associated with an increase in the upper limit of the TSH reference range [44], the use of unadjusted reference ranges may have resulted in misclassification of some elderly participants as having subclinical hypothyroidism. This misclassification may have resulted in underestimation of the association between subclinical hypothyroidism and cognition. However, since the 95% CI around the estimates are quite narrow and the misclassification is likely to be small, a large effect of subclinical hypothyroidism on cognition can be confidently ruled out.

Thirdly, the definitions of subclinical hypothyroidism and cognitive decline were slightly different between the studies. The use of different TSH cut-offs reflects the absence of consensus to define subclinical hypothyroidism [22, 23]. Some studies used a TSH upper limit of less than 4.5 mU/L [9, 16], and the inclusion of those participants may have blunted the effect of any observed associations, since they may not have had subclinical hypothyroidism [23]. However, the sensitivity analyses pooling more homogeneous studies gave similar results indicating a lack of evidence supporting an association of subclinical hypothyroidism with cognitive impairment. However, one might speculate that potential associations between subclinical hypothyroidism and cognitive impairment might only be present when TSH is markedly increased (TSH > 10m IU/L). Future studies using individual participant data should be directed at analyzing available evidence for an association between subclinical hypothyroidism and cognition on based TSH categories, as was done previously for associations between subclinical hypothyroidism and coronary heart disease [41].

Fourthly, there were several differences in methodologies and choice of cognitive domains that were tested in the studies in this systematic review and meta- analysis. Thus, we cannot exclude the possibility that subclinical hypothyroidism might be associated with subtle defects in specific domains that can only be identified using highly specific cognitive tests and measures. Indeed, functional neuro- imaging studies in participants with subclinical hypothyroidism and markedly elevated TSH levels has revealed impairments in working memory and brain areas associated with executive function that reversed by treatment with T4 [44]. However, the clinical relevance of such specific measures remains unclear. Moreover, different laboratory methods were used for the measurements of TSH and fT4. In addition, TSH has a distinct circadian rhythm and time of the measurements of TSH was not reported in the articles, which may have affected the results.

In conclusion, this systematic review and meta- analysis provides no evidence that supports an association between subclinical hypothyroidism and cognitive impairment in relatively healthy, community dwelling elderly. However, available prospective studies were limited. Thus, additional large, high- quality studies are needed that will allow for more extended analyses.

Supporting information

The Supplementary Materials for this article can be found online at: http://journal.frontiersin.org/article/10.3389/fnagi.2015.00150

Appendix 1. Search strategy

Appendix 2: Quality assessment of included studies

REFERENCES

1. Constant EL, Adam S, Seron X, et al. Anxiety and depression, attention, and executive functions in hypothyroidism. Journal of the International Neuropsychological Society. 2005;11(5):535-44.
2. Correia N, Mullally S, Cooke G, et al. Evidence for a specific defect in hippocampal memory in overt and subclinical hypothyroidism. JClinEndocrinolMetab. 2009;94(10):3789-97.
3. Davis JD, Tremont G. Neuropsychiatric aspects of hypothyroidism and treatment reversibility. Minerva Endocrinol. 2007;32(1):49-65.
4. Samuels MH. Cognitive function in untreated hypothyroidism and hyperthyroidism. Current opinion in endocrinology, diabetes, and obesity. 2008;15(5):429-33.
5. Canaris GJ, Manowitz NR, Mayor G, et al. The Colorado thyroid disease prevalence study. Archives of internal medicine. 2000;160(4):526-34.
6. Sawin CT, Castelli WP, Hershman JM, et al. The aging thyroid. Thyroid deficiency in the Framingham Study. Archives of internal medicine. 1985;145(8):1386-8.
7. Cardenas-Ibarra L, Solano-Velazquez JA, Salinas-Martinez R, et al. Cross-sectional observations of thyroid function in geriatric Mexican outpatients with and without dementia. ArchGerontolGeriatr. 2008;46(2):173-80.
8. Ceresini G, Lauretani F, Maggio M, et al. Thyroid function abnormalities and cognitive impairment in elderly people: results of the Invecchiare in Chianti study. JAmGeriatrSoc. 2009;57(1):89-93.
9. Cook SE, Nebes RD, Halligan EM, et al. Memory impairment in elderly individuals with a mildly elevated serum TSH: The role of processing resources, depression and cerebrovascular disease. Aging Neuropsychology and Cognition. 2002;9(3):175-83.
10. de Jongh RT, Lips P, van Schoor NM, et al. Endogenous subclinical thyroid disorders, physical and cognitive function, depression, and mortality in older individuals. Eur J Endocrinol. 2011;165(4):545-54.
11. Formiga F, Ferrer A, Padros G, et al. Thyroid status and functional and cognitive status at baseline and survival after 3 years of follow-up: the OCTABAIX study. Eur J Endocrinol. 2014;170(1):69-75.
12. Gussekloo J, van EE, de Craen AJ, et al. Thyroid status, disability and cognitive function, and survival in old age. JAMA. 2004;292(21):2591-9.
13. Hogervorst E, Huppert F, Matthews FE, et al. Thyroid function and cognitive decline in the MRC Cognitive Function and Ageing Study. Psychoneuroendocrinology. 2008;33(7):1013-22.
14. John JAS, Henderson VW, Gatto NM, et al. Mildly Elevated TSH and Cognition in Middle-Aged and Older Adults. Thyroid. 2009;19(2):111-7.

15. Manciet G, Dartigues JF, Decamps A, et al. The PAQUID survey and correlates of subclinical hypothyroidism in elderly community residents in the southwest of France. Age Ageing. 1995;24(3):235-41.
16. Park YJ, Lee EJ, Lee YJ, et al. Subclinical hypothyroidism (SCH) is not associated with metabolic derangement, cognitive impairment, depression or poor quality of life (QoL) in elderly subjects. ArchGerontolGeriatr. 2010;50(3):e68-e73.
17. Parsaik AK, Singh B, Roberts RO, et al. Hypothyroidism and risk of mild cognitive impairment in elderly persons: a population-based study. JAMA Neurol. 2014;71(2):201-7.
18. Resta F, Triggiani V, Barile G, et al. Subclinical Hypothyroidism and Cognitive Dysfunction in the Elderly. EndocrMetab Immune Disord Drug Targets. 2012.
19. Roberts LM, Pattison H, Roalfe A, et al. Is subclinical thyroid dysfunction in the elderly associated with depression or cognitive dysfunction? AnnInternMed. 2006;145(8):573-81.
20. Wijsman LW, de Craen AJ, Trompet S, et al. Subclinical thyroid dysfunction and cognitive decline in old age. PLoS One. 2013;8(3):e59199.
21. Yamamoto N, Ishizawa K, Ishikawa M, et al. Cognitive function with subclinical hypothyroidism in elderly people without dementia: one year follow up. GeriatrGerontolInt. 2012;12(1):164-5.
22. Helfand M. Screening for subclinical thyroid dysfunction in nonpregnant adults: a summary of the evidence for the U.S. Preventive Services Task Force. Ann Intern Med. 2004;140(2):128-41.
23. Surks MI, Ortiz E, Daniels GH, et al. Subclinical thyroid disease: scientific review and guidelines for diagnosis and management. JAMA. 2004;291(2):228-38.
24. Vanderpump MP, Tunbridge WM, French JM, et al. The incidence of thyroid disorders in the community: a twenty-year follow-up of the Whickham Survey. Clin Endocrinol (Oxf). 1995;43(1):55-68.
25. Gulseren S, Gulseren L, Hekimsoy Z, et al. Depression, anxiety, health-related quality of life, and disability in patients with overt and subclinical thyroid dysfunction. Archives of medical research. 2006;37(1):133-9.
26. Razvi S, Ingoe LE, McMillan CV, et al. Health status in patients with sub-clinical hypothyroidism. Eur J Endocrinol. 2005;152(5):713-7.
27. Vigario P, Teixeira P, Reuters V, et al. Perceived health status of women with overt and subclinical hypothyroidism. Medical principles and practice : international journal of the Kuwait University, Health Science Centre. 2009;18(4):317-22.
28. Egger M, Davey Smith G, Schneider M, et al. Bias in meta-analysis detected by a simple, graphical test. BMJ (Clinical research ed). 1997;315(7109):629-34.

29. Stroup DF, Berlin JA, Morton SC, et al. Meta-analysis of observational studies in epidemiology: a proposal for reporting. Meta-analysis Of Observational Studies in Epidemiology (MOOSE) group. JAMA. 2000;283(15):2008-12.
30. Hedges LV, Vevea JL. Fixed-and random-effects models in meta-analysis. Psychological methods. 1998;3(4):486.
31. Jensovsky J, Spackova N, Hejdukova B, et al. [Effect of normalization of an isolated increase in TSH on the neuropsychological profile of patients]. CasLekCesk. 2000;139(10):313-6.
32. Gussekloo J, van EE, de Craen AJ, et al. [Thyroid function, activities of daily living and survival in extreme old age: the 'Leiden 85-plus Study']. NedTijdschrGeneeskd. 2006;150(2):90-6.
33. Wiersinga WM. [Uncertainties about the benefit of treatment in subclinical thyroid dysfunction]. NedTijdschrGeneeskd. 2006;150(2):71-4.
34. Ganguli M, Burmeister LA, Seaberg EC, et al. Association between dementia and elevated TSH: a community-based study. Biol Psychiatry. 1996;40(8):714-25.
35. Joffe RT, Pearce EN, Hennessey JV, et al. Subclinical hypothyroidism, mood, and cognition in older adults: a review. Int J Geriatr Psychiatry. 2013;28(2):111-8.
36. Parle J, Roberts L, Wilson S, et al. A randomized controlled trial of the effect of thyroxine replacement on cognitive function in community-living elderly subjects with subclinical hypothyroidism: the Birmingham Elderly Thyroid study. The Journal of clinical endocrinology and metabolism. 2010;95(8):3623-32.
37. Roberts LM, Pattison H, Roalfe A, et al. Is subclinical thyroid dysfunction in the elderly associated with depression or cognitive dysfunction? Ann Intern Med. 2006;145(8):573-81.
38. Annerbo S, Lokk J. A Clinical Review of the Association of Thyroid Stimulating Hormone and Cognitive Impairment. ISRN Endocrinol. 2013;2013:856017.
39. Jorde R, Waterloo K, Storhaug H, et al. Neuropsychological function and symptoms in subjects with subclinical hypothyroidism and the effect of thyroxine treatment. The Journal of clinical endocrinology and metabolism. 2006;91(1):145-53.
40. S.B. Hulley, S.R. Cummings, W.S. Browner, et al. Designing Clinical Research: an epidemiologic approach. Lippincott Williams & Wilkins, Philadelphia 2001.
41. Rodondi N, den Elzen WP, Bauer DC, et al. Subclinical hypothyroidism and the risk of coronary heart disease and mortality. JAMA. 2010;304(12):1365-74.
42. Berlin JA. Invited commentary: benefits of heterogeneity in meta-analysis of data from epidemiologic studies. American journal of epidemiology. 1995;142(4):383-7.

43. Huston P, Naylor CD. Health services research: reporting on studies using secondary data sources. CMAJ : Canadian Medical Association journal = journal de l'Association medicale canadienne. 1996;155(12):1697-709.
44. Zhu DF, Wang ZX, Zhang DR, et al. fMRI revealed neural substrate for reversible working memory dysfunction in subclinical hypothyroidism. Brain. 2006;129(Pt 11):2923-30.

PART III:

CONTRIBUTIONS OF THE AUTONOMIC NERVOUS SYSTEM

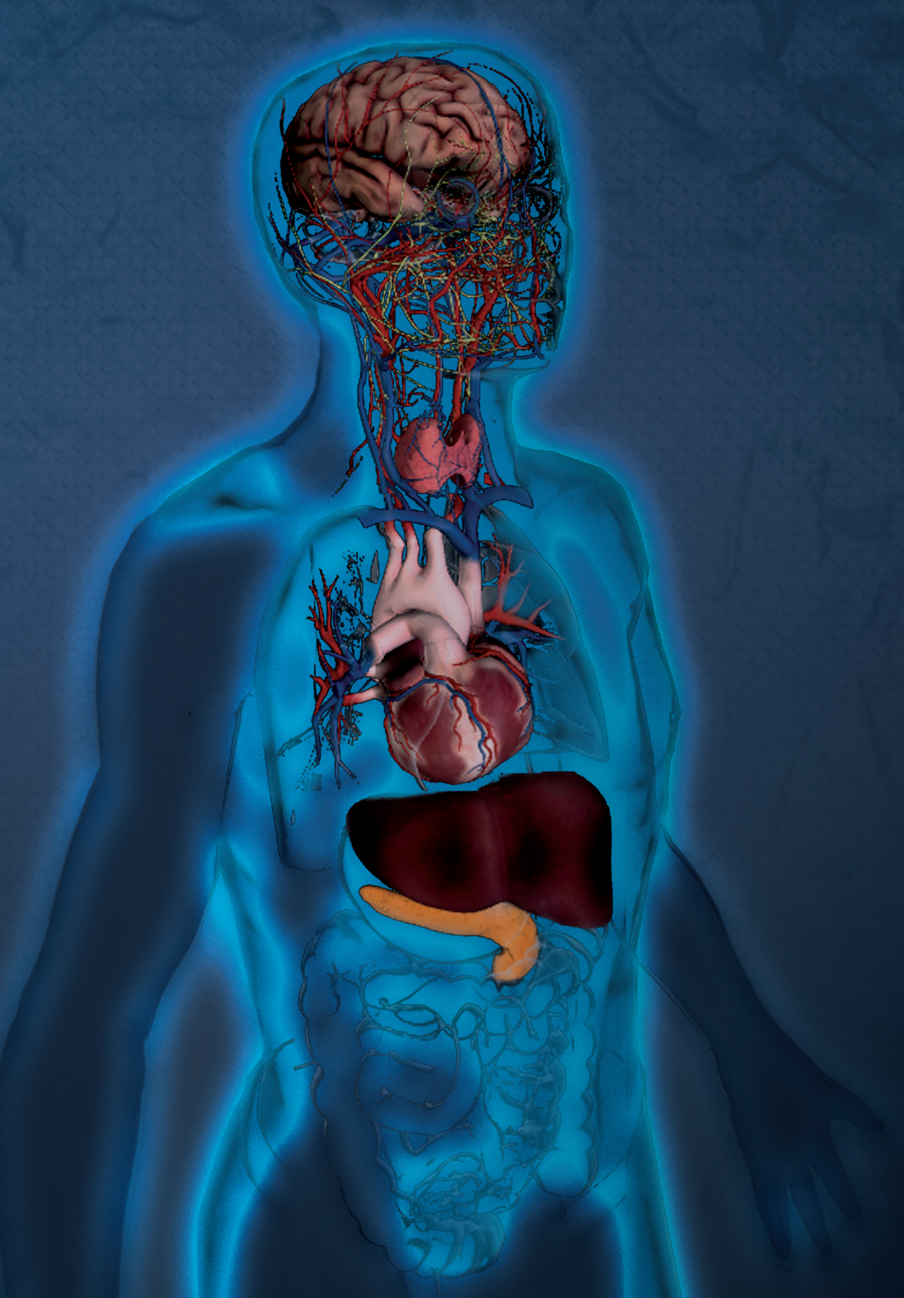

CHAPTER 10

COMPARATIVE ANALYSIS OF THE EQUIVITAL EQ02 LIFEMONITOR WITH HOLTER AMBULATORY ECG DEVICE FOR CONTINUOUS MEASUREMENT OF ECG, HEART RATE AND HEART RATE VARIABILITY: A VALIDATION STUDY FOR PRECISION AND ACCURACY.

Abimbola Akintola
Vera van de Pol
Daniel Bimmel
Arie Maan
Diana van Heemst

Front. Physiol. (cardiac electrophysiology) 7:391. doi: 10.3389/fphys.2016.00391.

ABSTRACT

The Equivital (EQ02) is a multi-parameter telemetric device offering both real-time and/or retrospective, synchronized monitoring of ECG, HR and HRV, respiration, activity and temperature. Unlike the Holter, which is the gold standard for continuous ECG measurement, EQO2 continuously monitors ECG via electrodes interwoven in the textile of a wearable belt. We aimed to compare EQ02 with the Holter for continuous home measurement of ECG, heart rate (HR) and heart rate variability (HRV).

Eighteen healthy participants wore, simultaneously for 24 hours, the Holter and EQ02 monitors. Per participant, averaged HR and HRV per 5 minutes from the two devices were compared using Pearson correlation, paired T-test and Blant-Altman analyses. Accuracy and precision metrics included mean absolute relative difference (MARD).

Artefact content of EQ02 data varied widely between (range 1.93% to 56.45%) and within (range 0.75% to 99.61%) participants. Comparing the EQ02 to the Holter, the Pearson correlations were respectively 0.724, 0.955 and 0.997 for datasets containing all data and data with <50% or <20% artefacts respectively. For datasets containing respectively all data, data with <50% or <20% artefacts, bias estimated by Bland-Altman analysis was -2.8, -1.0 and -0.8 beats per minute and 24h MARD was 7.08, 3.01 and 1.5. After selecting a three-hour stretch of data containing 1.15% artefacts, Pearson correlation was 0.786 for HRV measured as standard deviation of NN intervals (SDNN).

Although the EQ02 can accurately measure ECG and HRV, its accuracy and precision is highly dependent on artefact content. This is a limitation for clinical use in individual patients. However, the advantages of the EQ02 (ability to simultaneously monitor several physiologic parameters) may outweigh its disadvantages (higher artefact load) for research purposes and/ or for home monitoring in larger groups of study participants. Further studies can be aimed at minimizing the artefacts.

INTRODUCTION

With cardiovascular diseases still representing a leading cause of death globally, continuous electrocardiography (ECG) measurement is becoming increasingly important. Continuous ECG measurements yields valuable information on heart rate (HR) and its variability (HRV) that can be measured at a beat-to-beat level. Their direct clinical importance has been demonstrated in numerous studies. HR is a major risk factor for morbidity and mortality in cardiovascular diseases [(1, 2)]. Even in apparently healthy individuals, HR has predictive value for sudden cardiac death [(3)]. Furthermore, control of HR has become the focus of drug development for cardiovascular diseases [(4)]. In addition to HR, continuous measurement heart rate variability (HRV) serves as an index of cardiac sympathetic and parasympathetic activity [(5)]. HR and HRV associates with cardiac [(3)], physiological [(6)], psychological [(7, 8)] and sleep- related disorders [(9)]; and are being used as prognostic indicators for cardiac and non-cardiac diseases, such as idiopathic dilated myopathy [(10)], myocardial infarction [(11)], renal failure [(12)], end stage renal disease [(13)] and cancer [(14)].

ECG signals can be obtained from varying sources, such as Holter monitoring, bedside monitoring of vital parameters, systems for surface ECG, ergometric stress tests and systems for telemetry [(15)]. Of these, the Holter monitor (Holter) is the gold standard for continuous ECG measurement. The Holter records ECG signals via electrodes attached to the chest. However, over the years different innovative devices that are able to comfortably monitor ECG simultaneously with other physiological parameters for a prolonged period of time in freely moving subjects have become available. The Equivital EQ02 Lifemonitor (EQ02,) is a convenient and safe wireless ambulatory device that continuously measures ECG, HR and HRV via a chest-worn sensor belt embedding textile-based electrodes. In addition to cardiac parameters, EQ02 also measure breathing rate, body position and movement (accelerometry), and skin and core body temperature, all synchronized and time- stamped to provide contextual significance for possible diagnostic, therapeutic or research purposes. Although EQ02 has been used in several studies, e.g. for ambulatory monitoring of pilots, athletes and military personnel, both under physiological and extreme environmental conditions [(16-20)], EQ02 has not yet been validated against the gold standard for measurement of cardiac parameters.

Here for the first time, we compared the accuracy of EQ02 and Holter for continuous ECG, HR and HRV monitoring. The EQ02 and Holter were worn simultaneously for 24hours in home setting by an heterogeneous group of healthy male and female volunteers. Results were analyzed in point accuracy (including absolute and relative differences), monitor reliability and precision metrics for both devices.

METHODS

Ethics statement

This study was approved by the institutional review board of Leiden University Medical Center (LUMC) under protocol P11.116. All study participants gave written informed consent.

Study participants

The present study was embedded in the Switchbox Study, which was a sub-study of the Leiden Longevity Study (LLS). The LLS was originally designed to investigate genetic and phenotypic biomarkers associated with human longevity. A more detailed description of the study design and recruitment strategy for switchbox study [21] and the LLS [22] has been described elsewhere. The present study population consisted of 18 healthy adult male and female volunteers from the local population. The only exclusion criterion was presence of obvious chest deformity, which would impair lifemonitor belt fitting.

Apart from the 18 subjects, artefact percentage was determined in all raw Holter recordings that were collected in the department of cardiology of the LUMC in 2014. In total, artefact data from ECG recording of 4143 persons were used. Apart from the percentage of artefacts contained in the recordings, no other data from these individuals were used. Furthermore, similar raw artefact data were extracted from EQ02 recordings from 200 switchbox participants.

Experimental protocol

After body mass index and waist: hip ratio was measured, participants wore, simultaneously, the EQ02 monitor, a Holter and a Fitbit one™. These were turned on approximately concurrently. Participants undertook their usual daily activities, except swimming. They additionally kept a detailed diary of type and timing of all their activities.

Study devices

EQ02 monitoring

The EQ02 (Equivital EQ02, Hidalgo, UK) continuously measured ECG on two channels via three electrodes (table 1). The EQ02 monitoring system consists of a LM 1000 Lifemonitor sensor electronic module (SEM), Lifemonitor belts of varying sizes, a SEM lead and charging dock, a blue tooth USB dongle for laptop/ PC, and an Equivital Manager to configure SEMs and to download and export data. For this study, SEMs were configured in clinical mode, and data reported retrospectively at local time. Bluetooth connectivity was disabled and data transmission was at partial disclosure.

An appropriately sized lifemonitor belt held the SEM onto the subject's body. Its textile-based electrodes were moistened with water before making contact with the participant's skin. SEMs were charged for approximately one hour after 12 hours of recording. Upon study completion, SEM data was uploaded onto the Equivital manager; from where date- and time- stamped ECG, inter-beat interval and summary data of vital signs were extracted and exported.

Holter ECG monitoring

The Holter (SEER MC Holter monitor, GE Healthcare, USA) measured ECG on three channels. The Holter consisted of seven electrodes; color- coded lead wires and a battery operated, digital ECG recorder. Before placement of electrodes, participants' skin were prepared with alcohol and 3M red dot 2236 trace prep (3M Healthcare, Canada) to remove nonconductive skin layer and reduce skin impedance and eventual artefacts. Color- coded leads were clipped on to 3M electrodes (type 2271, 3M Healthcare, Canada) and placed as shown in figure 1.

TABLE 10.1 | Technical characteristics of the EQ02 and Holter monitors

	Holter	Equivital (EQ02) lifemonitor
Acceptance	Gold standard	Relatively new device
Parameters measured	ECG only	ECG, breathing rate, tri-axial accelerometry, skin temperature, core body temperature and energy expenditure, all fully synchronized.
Data presentation	Retrospective	Real- time (live) and retrospective (date- and time- stamped).
Recording modes	Ambulatory	Ambulatory and Clinical
Recording time	Usually 24- 48 hours	Fully charged battery lasts 24- 48 hours*. The internal memory of the recorder stores up to 50 days of data.
Channels	3	2
Electrodes	7	3
Type of Electrodes	Stick- on	Textile electrodes
Skin preparation	Necessary	
(Removal of non-conductive skin layer)	None	
Convenience	Can be cumbersome due to multiple lead wires, sensor pads, clips and/or re- enforcing tapes, carry-case	Easy to wear belt
Analysis software	MARS	Vivosense

**For this study, the monitors were charged after 12 hours of use*

Fitbit oneTM wireless activity and sleep tracker

The Fitbit oneTM (Fitbit, San Franscisco, USA) was worn on the waist (belt) during the day for tracking activity (step-counts) and on the sleep wrist- band at night for tracking sleep length and number and durations of awakenings. Upon study completion, data was downloaded via Fitbit dashboard. Sleep efficiency was extracted as a composite of time to fall asleep, number of awakenings and restless periods, total time in bed and the actual sleep time [23].

Data management

While data extracted from EQ02 were automatically time- and date stamped (date, time in hr., min., sec. & ms.), Holter data were not. Data from both devices were synchronized based on the Equivital time stamp, by selecting aberrations (non-sinus beats) in two consecutive heart beats from the Holter that corresponded to those from EQ02, mostly around the start of the recording. Five-minute trends (averages) of HR, RR and HRV parameters from synchronized data were then extracted for analysis.

Data management: Holter monitor

Holter ECG data were analysed using MARS ambulatory Holter ECG analysis system (GE Healthcare, Milwaukee, WI, USA). After extraction, an exportable file was visible on MARS, which contained the annotations 'N' (normal sinus-rhythm), 'V' (ventricular-beat), 'S' (supraventricular-beat) or 'X' (artefact) (figure 1A). The software recognized and grouped QRS complexes on similarity. This process was manually checked and corrected when the recognition of QRS-location was faulty or the sinus/non-sinus labeling was wrong.

EQ02 data management: Vivosense

Raw ECG data from EQ02 was analyzed using Vivosense modular physiological monitoring and analysis platform (Vivonoetics, San Diego, USA). EQ02 data were visualized with Cardiac layout (figure 1B), for inspecting each ECG channel and derived R- wave markings, and artefact identification. This layout also contains accelerometer data channels for contextual interpretation.

The EQ02 unit provided two leads of ECG measurements that shared a common reference. These were denoted as SEM_ecg1 (primary raw ECG signal) and SEM_ecg2 (secondary raw ECG signal) respectively. Vivosense processed and performed QRS detection on both channels to generate two sets of R- wave markings. We chose SEM_ecg1, which was then scaled and filtered by Vivosense, as primary source ECG for derivation of RR, HR, and HRV parameters.

Artefacts in the ECG signals were identified and annotated. Artefacts were defined as (i) distorted signals and/ or (ii) segments of signal in which the different waves of the ECG complex could not be clearly identified. Vivosense offers an algorithm that automatically marks and calculates artefact percentage (figure 1B), and no-, low-, medium- and high-artefact cleaning/ noise reduction options. The automatic artefact-marking algorithm takes into account the minimum and maximum allowable heart rates, presence of ectopic beats, maximal interpolation length and signal noise. After removal of charging times, Vivosense automatic cleaning of the data in this study was performed by selecting the timeframe to be cleaned, setting the sensitivity level of the automatic cleaning algorithm at medium noise filtering, and setting the minimal and maximal allowable HR limits to 30 and 220 beats per minutes respectively.

In addition, complete manual cleaning of EQ02 data was done for one participant, involving the time- intensive process of relocating incorrectly automatically recognized QRS-complexes to correct locations, and manually identifying and excluding artefacts.

Furthermore, Vivosense software calculated and displayed eight HRV indices, namely, average of NN-intervals (ANN), standard deviation of NN-intervals (SDNN), standard deviation of 5-minute averages of NN-intervals (SDANN), standard deviation of successive differences of NN-intervals (SDSD), square root of the mean squared differences of successive intervals (RMSSD), mean of the standard deviation of 5-minute NN-intervals (SDNNi), number of adjacent NN-intervals with a difference less than 50ms (NN50) and ratio of NN50 to total number of NN-intervals (pNN50).

Accuracy, precision and reliability metrics

The point accuracy of EQ02 was measured in terms of the relative difference (RD) and absolute relative difference (ARD) of HR measurements to assess respectively the bias (relative to the Holter) and the average error. The RD was calculated using the formula [(EQ02 HR – Holter HR)/Holter HR]. The ARD was calculated using the formula [|EQ02 HR – Holter HR|/Holter HR]. We additionally determined the mean absolute relative difference (MARD) of all paired points. The mean and standard deviation (SD) of MARDs from all 18 participants were computed for each synchronized 24h HR measurement, to assess respectively the accuracy and precision of EQ02 HR measurements.

Statistical analysis

Of the original 5182 paired data points of 5- minute HR averages from 18 participants, 4736 (91.4%) remained after exclusion of charging times. From these, three datasets were made containing: 1) raw data (all 4736 data points) 2) filtered data containing <50% artefacts (4059 (85.5%) data points) 3) filtered data containing <20% artefacts (3677 (77.6%) data points).

To analyze the strength of the linear relationship and agreement between both devices, synchronized data from both devices were analyzed with Pearson correlation analysis and Bland-Altman plots for all three datasets. To explore possible determinants of artefacts, we stratified data based on sex, day and night, and tertiles of waist: hip ratios, tertiles of activity. The artefact distribution in strata was compared using Chi-square (X2) test. The association between BMI and artefact load was assessed using linear regression.

The per-participant estimates of HR and HRV derived from EQ02 and Holter monitors were compared with paired t-tests. For all paired points, RD, ARD and MARD were determined using aforementioned formulae.

Graphs were drawn using GraphPad Prism version 5 (GraphPad, San Diego, CA). All statistical analyses were performed using SPSS v.20 (SPPS Inc., Chicago, U.S.A.). Two-sided p-values below 0.05 were considered statistically significant.

RESULTS

Heart rate

Characteristics of study participants are summarized in table 2 and described in details per-person in supplementary table 1. The mean age of the participants was 27.6 years (range 19-57 years); 10 (55%) were males. The activity pattern of the participants was variable, ranging from 5,017 to 14,265 steps taken in 24 hours. Medical history showed that none of the participants had persistent chest pain, tiredness, dyspnea, lightheadedness, palpitations, cardiovascular diseases, hypertension, endocrine or other diseases. Two participants had hypothyroidism, for which they used levothyroxine (data not shown).

Different components of the cardiac cycle, including p-waves were clearly identifiable in the ECG tracings from both the EQ02 and Holter (figure 1).

TABLE 10.2 | Subject characteristics

Demographics	N=18
Male n(%)	10(55)
Age, years	27.6(9.4)
Weight, kg	72(10.2)
BMI, kg/m2	22.5(2.4)
Waist: hip ratio	0.81(0.1)
Sleep (total hours)	580.2(156)
Step counts (total (mins) in 24 hours)	9635(2916)
% artefacts in raw EQ02 data*	19.0(14.7)

Data represent mean with standard deviation unless stated otherwise.

A. Holter ECG monitor

Holter data, analysed using MARS system

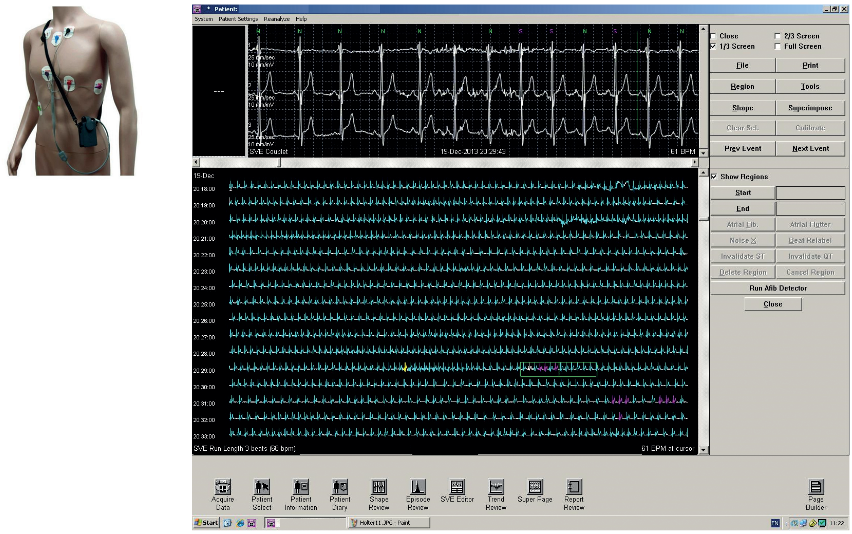

B. Equivital EQ02 lifemonitor

EQ02 data, analysed using Vivosense system

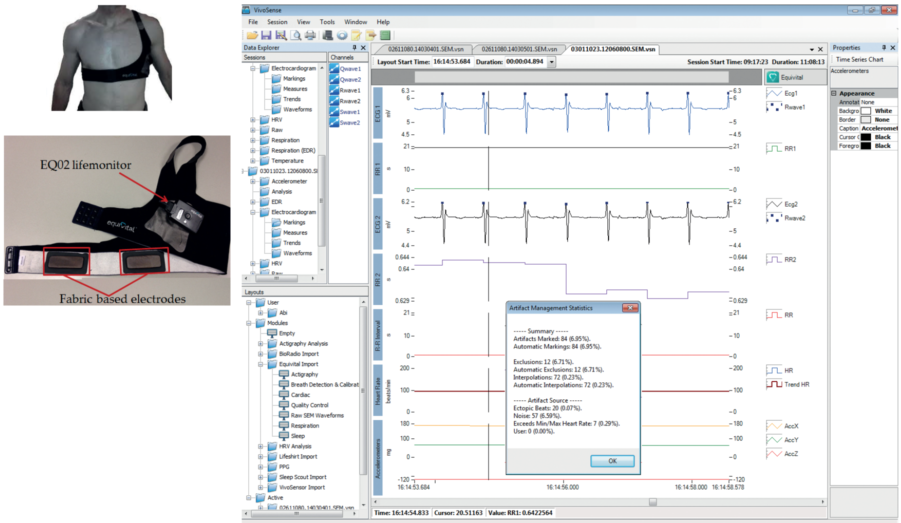

FIGURE 10.1 | Analysis software for Holter and EQ02 data management.

Figure 1A. shows the Holter monitor including its electrodes, lead wires, and its analytical software. Annotated tracings from the Holter can be seen on the MARS software. Figure 1B shows the EQ02 unit, consisting of the lifemonitor belt on which are three textile- based electrodes. ECG tracings are visualized on the cardiac layout of Vivosense software.

Artefact management

As shown in table 2, the average artefact percentage of the 24h EQ02 data was 19% (SD 14.7). However, marked differences existed in data quality (supplementary table 1) between participants (range 1.93% to 56.45%) and within participants (range 0.75% to 99.61%). Individual 24h graphs of Holter and EQ02 heart rate measurements of each of the 18 participants are shown in supplementary figure 1.

Figure 2 shows hourly averages of HR from the Holter, and EQ02 before cleaning, and after medium and high sensitivity cleaning for three representative participants with average artefact percentages over 24 hours of 1.93%, 56.45% and 22.15% respectively. Artefact percentages were variable throughout the day, but higher just around charging times, and lowest at night. At lower artefact percentages, there was good concordance between the EQ02 and Holter HR. In contrast, at higher artefacts percentages, there was discordance between the EQ02 and Holter HR values that persisted after applying the Vivosense automatic cleaning methods.

In addition, 24h EQ02 data for the participant in figure 2C was cleaned manually, which took 24 hours. Manual cleaning did not eliminate the discordance between Holter and EQ02 data at high artefacts percentages.

EQ02 sensor performance

Figure 3 display the Pearson correlation coefficients of HR measured using EQ02 and Holter for the three datasets sorted on artefact percentage. Pearson correlations were 0.724 for all data, and 0.955 and 0.997 for the datasets containing <50% and <20% artefacts respectively.

EQ02 point accuracy, mean accuracy and precision metrics

The point accuracy for EQ02 across the three datasets of varying artefact percentages are shown as RD and ARD distributions in figure 4A and B. For all data, 2246 of 4542 (49%) paired RD points had negative RD values. From the datasets containing <50% artefacts and <20% artefacts, respectively, 1802 of the 3882 (46%) and 1359 of the 3118 (43.6%) paired RD points had negative RD values. From the distribution of RD and ARD values shown in figure 4, the distribution of the underestimation extended over a broader range of HR values at higher artefact percentages.

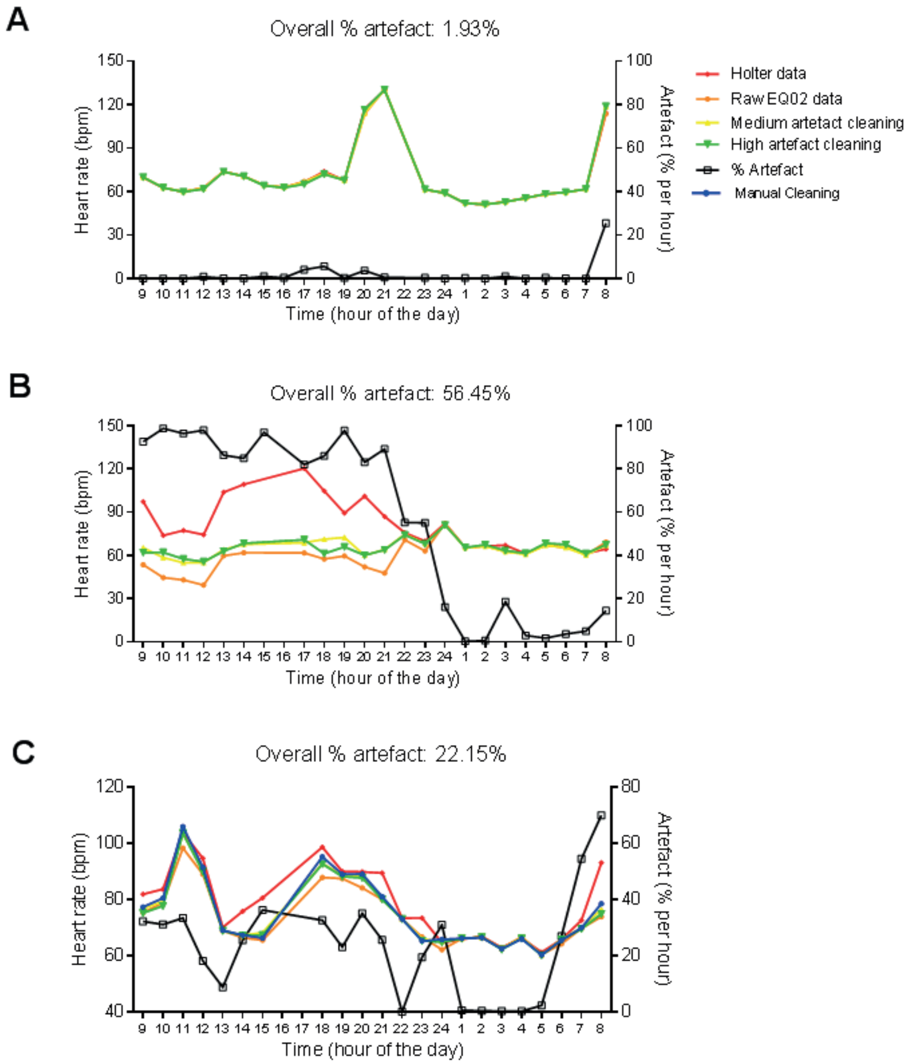

FIGURE 10.2 | 24h HR measurements by EQ02 and Holter.

Hourly averages of HR measured simultaneously using the EQ02 and Holter monitors for three participants (A, B and C). Raw EQ02 and automatically cleaned EQ02 data using the medium and high artefact sensitivity options of the Vivosense software are displayed. Artefact percentages over 24hours (above each graph) and per hour (right y-axis) are presented.

As an indicator of mean accuracy and precision of the EQ02, the MARD in EQ02 HR data relative to Holter HR over 24h are presented for the three data sets in figure 4C. The 24h MARD was 7.08±17% for all data, 3.01±10.55% for data containing <50% artefacts and 1.5±10.51% for data containing <20% artefacts. As depicted by the SD of the MARD, while the precision did not markedly differ between <20% (SD 10.51) or <50% artefacts (SD 10.55), precision decreased at >50% artefacts (SD 17).

Agreement between devices

Bland- Altman plots of paired HR values from both devices are presented in figure 5, for the three datasets. Compared to the Holter, HR was on average lower when derived from EQ02, with respectively a mean (95% CI) difference of -2.8 (-29.8 to 24.3) beats per minute (bpm) for all data, -1.0 (-16.1 to 14.14) bpm for data <50% artefact and -0.8 (-13.5 to 11.8) bpm for data <20% artefacts.

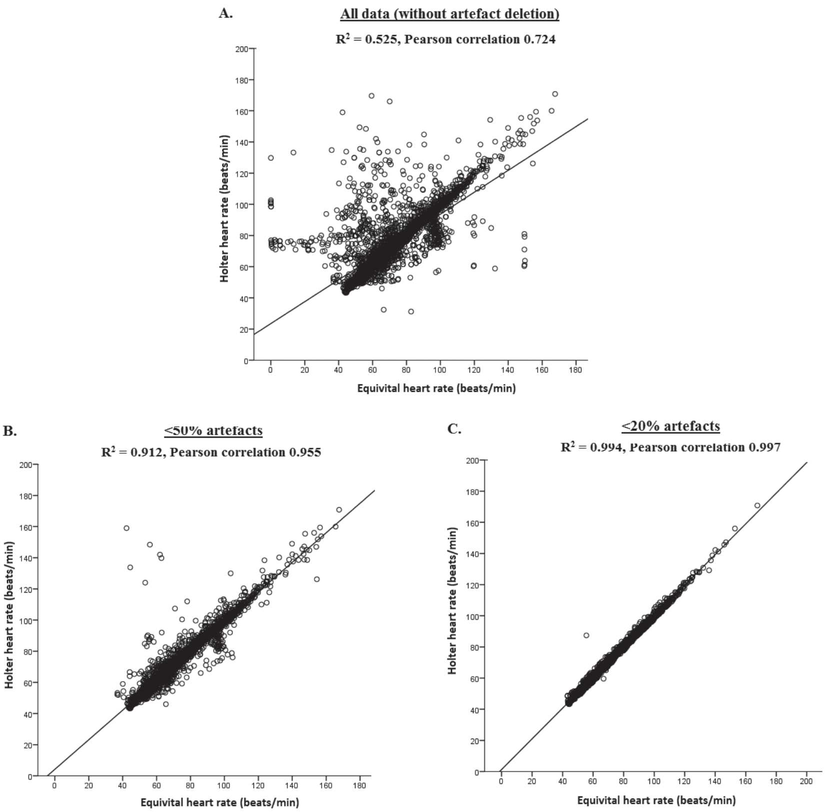

FIGURE 10.3 | Pearson correlations of HR measured by EQ02 and Holter.

Both R2 and Pearson correlation coefficients are shown for (A) all data, and filtered data containing (B) <50% artefacts and (C) < 20% artefacts.

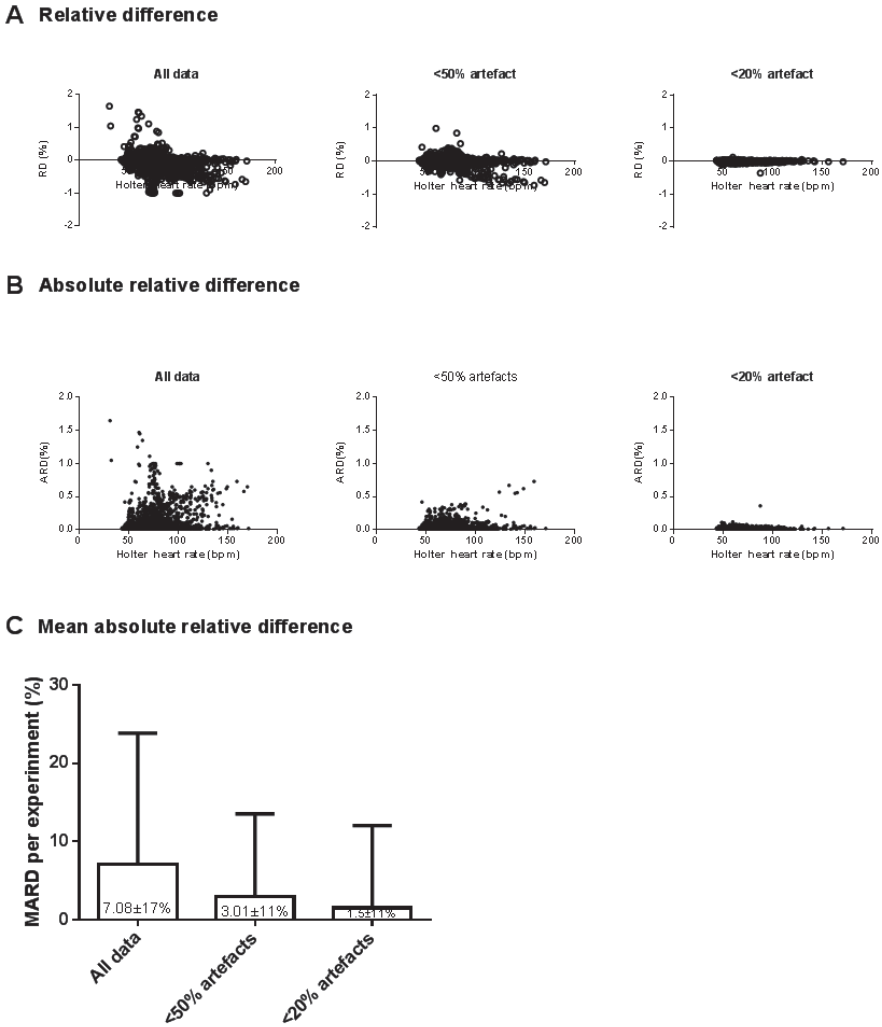

FIGURE 10.4 | Accuracy, precision and reliability of the EQ02 HR measurements.

The distribution, as a function of Holter values, of the relative difference (RD, panel A) and absolute RD (panel B) between each EQ02 HR measurement and its corresponding Holter HR value, for all data, and filtered data containing <50% and < 20% artefacts respectively. Panel C: MARD between EQ02- and Holter- derived HR values.

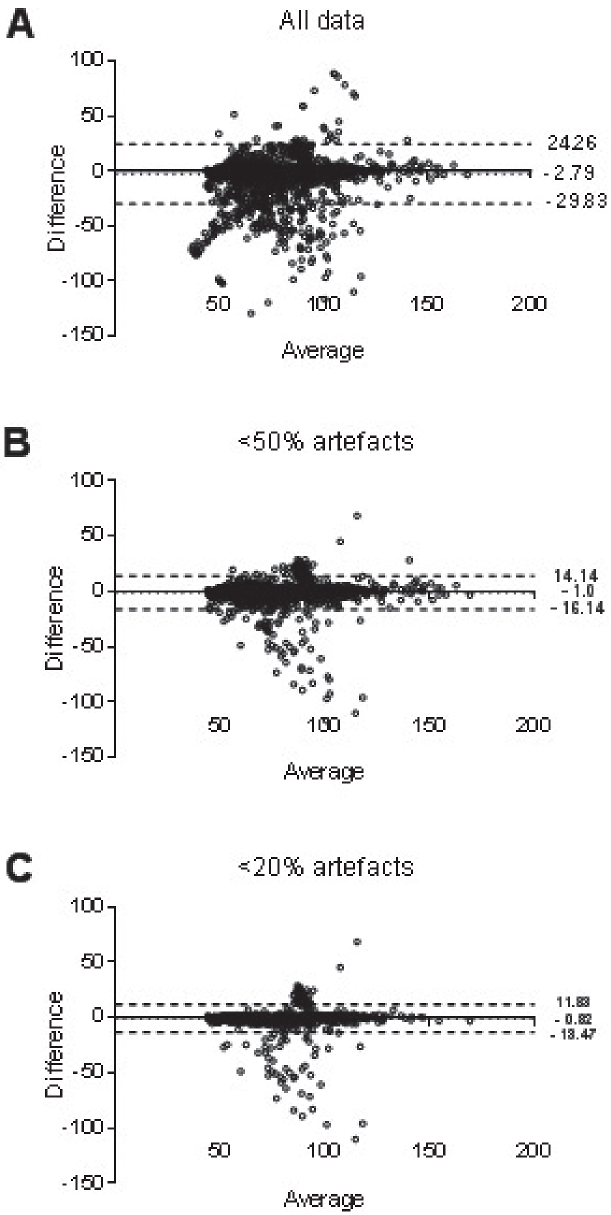

FIGURE 10.5 | Bland- Altman plots of HR measured by EQ02 and Holter.

Each dot represent paired (EQ02- Holter) HR values derived from all participants. The bias of the measurements (represented as solid lines) and the ± 1.96 SD (dotted lines) are presented for the measurements obtained for all data (A), filtered data containing <50% (B) artefacts and < 20% artefacts (C).

Evaluation of artefacts

In order to evaluate the artefact burden of the EQ02, we compared the artefact content of 24h Holter ECG recordings from 4,143 subjects with raw EQ02 data from 200 subjects. The average artefact percentage from the 4143 holter recordings was 2.95%, whereas the average artefact percentage from the 200 EQ02 recordings was 12.76%. Thus, the mean difference in artefact percentage in raw EQ02 compared to raw holter ECG was 10%. For the Holter, 77.9% of the 4,143 raw Holter ECG recordings had artefact percentage of ≤ 5%, whereas 65.5% of the 200 raw EQ02 ECG recordings had artefact percentage of ≤ 5%. The distribution of the artefacts is presented in figure 6.

Next, we evaluated possible sources of artefacts for the EQ02 recordings, including sex, waist: hip ratio, daytime versus nighttime (during which participants were asleep), activity (step counts) and BMI. The mean (SD) artefact percentages of male participants (19.4% (11.4)) was not significantly different (P=0.348) from that of females (15.9 (17.9)). When participants were divided into tertiles based on waist: hip ratio (w:h), tertile 1 (w:h range 0.71-0.76) had mean (SD) artefact percentage of 7.5 (3.5); tertile 2 (w:h range 0.77-0.83) had mean (SD) artefact percentage of 16.4 (6.0) while tertile 3 (w:h range 0.87-0.92) had mean (SD) artefact percentage of 29.7 (18.5) (P=0.014).

During the day, 62.9% of the data contained <20% artefacts, 17.15% contained 20-50% artefacts and 19.9% had 50-100% artefacts. In contrast, during the night, 82.7% of the data contained <20% artefacts, 12.4% contained 20-50% artefacts whereas 4.9% had 50-100% artefacts. Thus, there was considerably more artefacts during daytime compared to nighttime (p<0.001).

Furthermore, we also evaluated if activity of the participants, as measured using number of step counts taken during the study, had a bearing on artefacts percentage. Participants were divided into tertiles based on step counts, representing low activity (tertile 1, with 5017-8228 steps), medium activity (tertile 2 with 8229-11439 steps) and high activity (tertile 3 with 11440-14265 steps) respectively. For tertile 1 (least active), 73.3% of the data contained <20% artefacts, 11.8% contained 20-50% artefacts, and 14.9% of the data from the least active people contained 50-100% artefacts. For tertile 2 (medium active), 66.2% of the data contained <20% artefacts, 14.7% contained 20-50% artefacts, and 19.0% of the data contained 50-100% artefacts. Thus, there was comparatively more artefact in tertile 2 compared to tertile 1 (p<0.001). Similar significant result was obtained for comparison of tertile 3 (most active) to tertile 1 (p<0.001).

Finally, we assessed the association between BMI and artefact percentage. No significant association was found between BMI and artefact content of the EQ02 ECG recordings (P=0.256), data not shown.

Heart rate variability

Figure 7 graphically displays 10-minute averages of different HRV parameters for one participant (serial number 11, with overall average artefact percentage of 5.23%). Comparing HRV parameters from the two devices, the Pearson correlations were 0.967 for ANN, 0.393 for SDNN, 0.285 for rMSSD, 0.680 for SDANN and 0.982 for pNN50 for the 24-hour data. However, after selecting a three-hour stretch of data containing minimal artefacts (1.15% artefacts), the Pearson correlation for ANN remained the same. Except for pNN50 with Pearson correlation of 0.967 for 3- hour data, the Pearson correlation coefficients of the other HRV parameters improved to 0.786 for SDNN, 0.868 for rMSSD and 0.991 for SDANN for the 3 hour data with minimal artefacts (figure 8).

DISCUSSION

The EQ02 is a wireless device which can be used for monitoring multiple parameters, either real-time/live or offline/retrospectively. This is the first study to investigate the accuracy of EQ02 for continuous ECG measurement by comparing EQ02 with the gold standard (Holter). The major findings of this study are: 1) EQ02 is a convenient device for continuous measurement of ECG and its derivatives; 2) marked differences were observed in data quality between and within participants; 3) at lower artefacts percentages, HR and HRV measurements from EQ02 and Holter measurements were highly correlated; 4) artefacts percentages were lower during nighttime, when waist: hip ratio was lower, and at lower activity/ movement levels, as measured by step counts taken during the study.

EQ02 is relatively easy to wear in a home setting during habitual activities due to the design of the belt system with textile electrodes (the absence of wires). The use of wireless fabric electrodes in the a wearable belt provides comfort that makes the system suitable for prolonged and/ or frequent recordings [(24)]. However, this also imposes a limitation because textile electrodes are more prone to motion artefacts which interfere with R-wave detection [(25)]. Since textile– based electrodes do not have adhesives or clips, the instability and misplacement of the electrodes can be a possible source of the relatively higher artefact percentages that we observed for the ECG recording from the EQ02 monitor. This validation study found marked differences in EQ02 data quality between and within participants, as determined by the percentage of artefacts. We found more artefacts just before EQ02 charging times. For this study, the EQ02 was charged for one hour for every 12 hours of use. Removal and replacement of the monitor around charging times is a possible reason for the increased artefacts around charging times. Known sources of artefacts for cardiac telemetric devices include electrode movement with respect to the skin interface (disrupting electrochemical equilibrium); muscle contraction resulting in unwanted electromyographic contamination that may share the desired signal frequency band; vocalizations; temperature changes; sensor-cross-talk; optical path length changes and electromagnetic induction [25, 26]. In literature, artefact load of cardiac telemetric devices have also been attributed to body movement, temporary impairment of skin electrode contact, loose electrode connections, broken leads, skeletal myopotentials, and ambient noise [27]. In line, we also found that higher artefacts were found at higher activity levels, since this involves increased body movement.

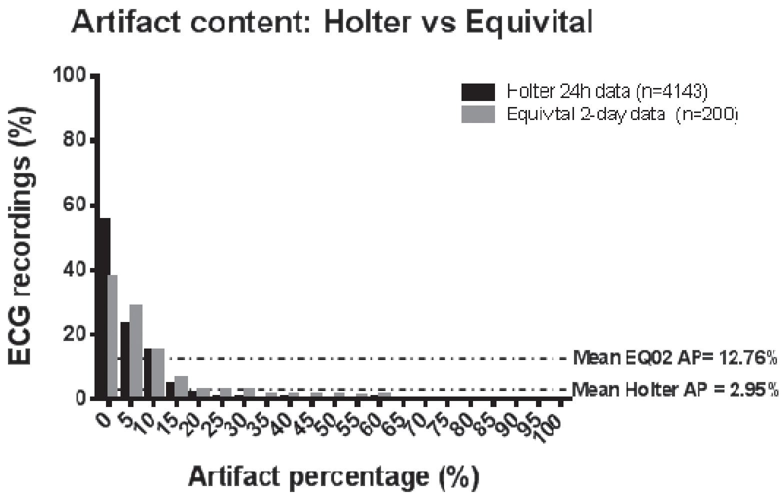

FIGURE 10.6 | Comparison of artefact content of raw Holter data to raw EQ02 data.

Bar chart showing content and distribution of artefact in raw (uncleaned) 24h Holter ECG recordings from 4,143 subjects with raw EQ02 data from 200 subjects. The average artefact percentage from the holter recordings was 2.95%, whereas the average artefact percentage from that 200 EQ02 recordings was 12.76%. AP: artefact percentage.

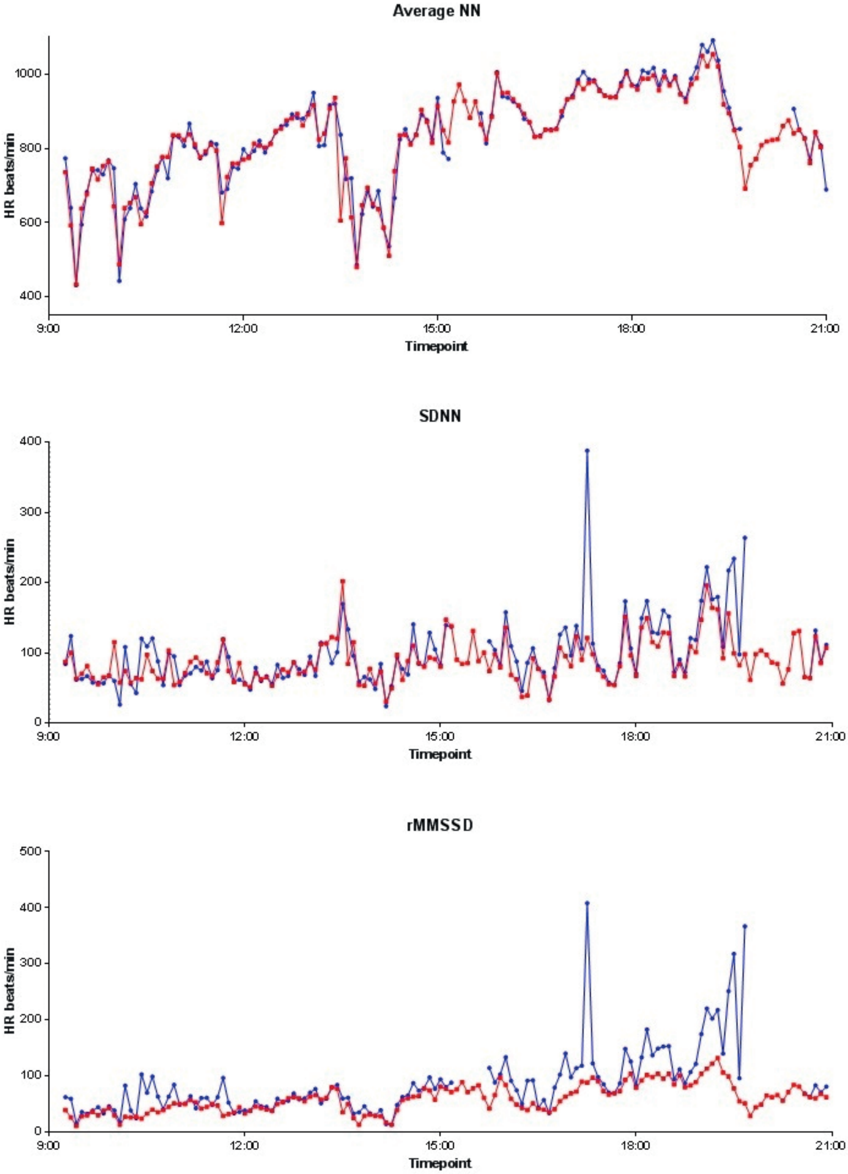

FIGURE 10.7 | 24- hour EQ02 and Holter HRV profile.

Average NN, SDNN and rMMSD of a participant over 24h, as recorded by the Holter (red) and EQ02 (blue).

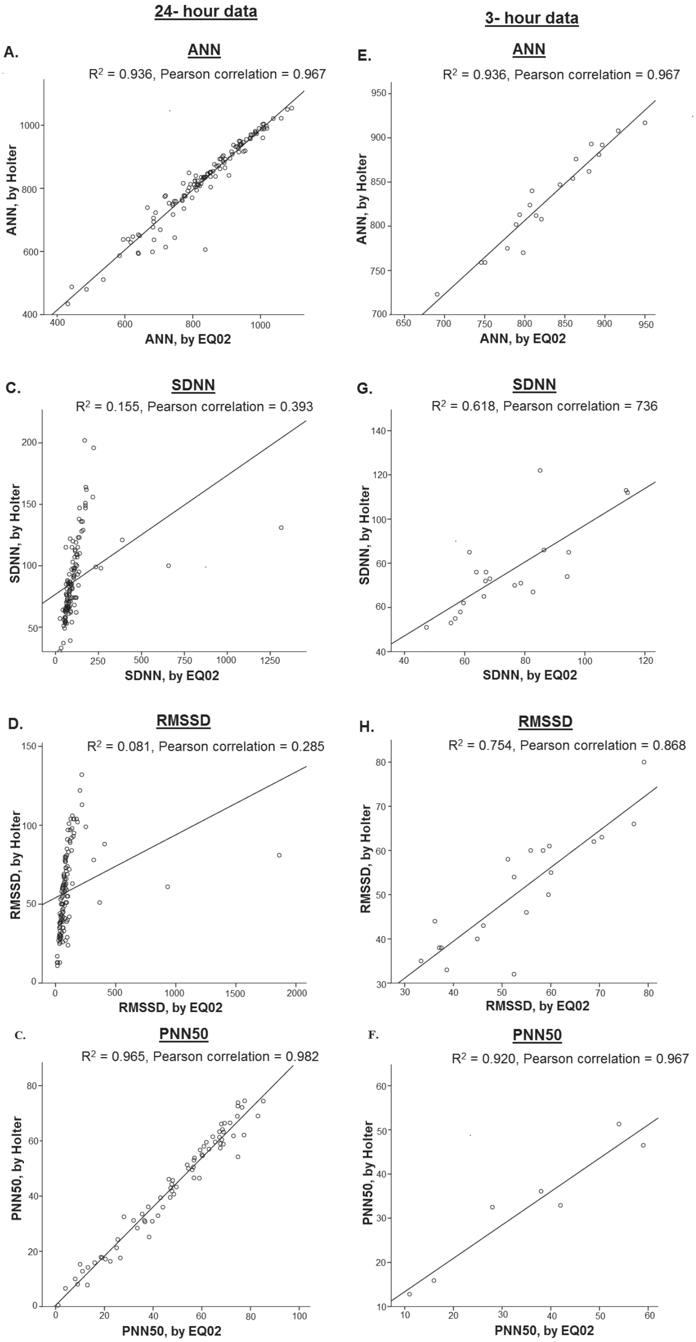

FIGURE 10.8 | Comparison between HRV parameters measured by EQ02 and Holter.

Correlation between ANN, SDNN, RMSSD and pNN50 in a participant from both devised over 24hr (A,B, C, D) and in a sub- selection of 3-hour data with artefact percentage 1.15% (E, F, G and H).

We demonstrated that at low artefact percentages, EQ02 can be used to reliably monitor ECG and its derivatives (HR, HRV) in relatively healthy participants. This is in accordance with a previous study [(19)] that compared HR derived from EQ02 and Polar S810i HR monitors under 10 minutes each of standing, lying and sitting. However, at higher artefact percentages (50% and higher), we found discordance between the EQ02 and Holter, which did not improve after application of the automatic cleaning options provided by Vivosense. Correlations improved by selecting data with <50% artefact or <20% artefacts. Similarly, HRV parameters (SDNN, RMSSD and pNN50) also showed markedly improved correlations after selection on a three- hour stretch of data with minimal artefacts. This further strengthens the finding that the quality of EQ02 is best at low artefact percentages. This agrees well with observations made by investigations into other mobile devices [(28, 29)]. For example, a validation study of the Actiheart found that HR values from Actiheart were in good agreement with those of other HR monitors during rest, but errors increased during exercises of higher intensity [(28)]. During high intensity movements, mobile devices are more prone to artefacts, in comparison to during rest. In line, whilst investigating potential determinants of artefacts, we found that artefact percentages were lower at lower activity levels (fewer step counts), at night, in subjects with lower waist: hip ratio and also somewhat lower in females. At night, participants were lying supine and mostly asleep which might result in better contact with electrodes and/ or decreased movement. Participants with lower waist: hip ratio also had significantly lower artefact percentages possibly because of better fitting of the Equivital belt. This could also have been the case in females, since female participants wore an extra layer of underwear over the Equivital belt, which might have potentially reduced belt displacements. This suggest that the artefact content of the EQ02 would most likely be attributable to motion artefacts and/or impaired skin- electrode contact.

One main limitation of our study is that it was conducted in eighteen relatively healthy participants without overt cardiac disease. A strength was that ECG was measured continuously and simultaneously using both devices over 24hours. More studies are needed to validate the EQ02 in specific groups, such as in the elderly, in large population studies and in patients with known cardiac disease. However, the susceptibility of the EQ02 to artefacts should be taken into account in such studies. Before application of Holter monitors, skin preparation is normally done with alcohol/KCl and red dot to remove nonconductive skin layer and reduce skin impedance to minimize artefacts. Perhaps employing skin preparation techniques could also aid in minimizing artefacts with EQ02 recordings.

Summarily, we compared continuous ECG from EQ02 to the Holter over 24hours. Skin preparation, as well as clips used before application of the Holter electrodes prevents artefacts, whereas artefact management of EQ02 was done after data acquisition. We found that there was, on average, good agreement between HR and HRV values derived from EQ02 and Holter. However, its accuracy and reliability depended on the presence and quantity of artefacts. Presently, the artefact load of EQ02's ECG recordings exceeds that of the Holter. This would pose a serious limitation to its clinical use in individual patients, especially for measurements that are especially sensitive to artefacts. On the other hand, if artefacts can be properly managed, the EQ02's ability to monitor (live and/or retrospective), synchronize and store cardiac and other physiological parameters may offer potential benefits for home monitoring and/ or research purposes, as it could be useful for extensive continuous recording of ECG, HR, HRV and other physiologic data in large population studies.

Supporting information

The Supplementary Material for this article can be found online at:
http://journal.frontiersin.org/article/10.3389/fphys.2016.00391/full

Supplementary Table 1. Detailed characteristics of the study participants

Supplementary figure 1. 24h graphs of Holter and EQ02 heart rate measurements of individual study participants

REFERENCES

1. Diaz A, Bourassa MG, Guertin MC, Tardif JC. Long-term prognostic value of resting heart rate in patients with suspected or proven coronary artery disease. European heart journal. 2005;26(10):967-74.
2. Hjalmarson A. Heart rate: an independent risk factor in cardiovascular disease. European Heart Journal Supplements. 2007;9(Supplement F):F3–F7.
3. Molgaard H, Sorensen KE, Bjerregaard P. Attenuated 24-h heart rate variability in apparently healthy subjects, subsequently suffering sudden cardiac death. Clinical autonomic research : official journal of the Clinical Autonomic Research Society. 1991;1(3):233-7.
4. Routledge HC, Chowdhary S, Townend JN. Heart rate variability--a therapeutic target? Journal of clinical pharmacy and therapeutics. 2002;27(2):85-92.
5. Thayer JF, Yamamoto SS, Brosschot JF. The relationship of autonomic imbalance, heart rate variability and cardiovascular disease risk factors. Int J Cardiol. 2010;141(2):122-31.
6. Tsuji H, Venditti FJ, Jr., Manders ES, Evans JC, Larson MG, Feldman CL, et al. Reduced heart rate variability and mortality risk in an elderly cohort. The Framingham Heart Study. Circulation. 1994;90(2):878-83.
7. Dishman RK, Nakamura Y, Garcia ME, Thompson RW, Dunn AL, Blair SN. Heart rate variability, trait anxiety, and perceived stress among physically fit men and women. International journal of psychophysiology : official journal of the International Organization of Psychophysiology. 2000;37(2):121-33.
8. Friedman BH, Thayer JF. Autonomic balance revisited: panic anxiety and heart rate variability. J Psychosom Res. 1998;44(1):133-51.
9. Stein PK, Pu Y. Heart rate variability, sleep and sleep disorders. Sleep medicine reviews. 2012;16(1):47-66.
10. Fauchier L, Babuty D, Cosnay P, Autret ML, Fauchier JP. Heart rate variability in idiopathic dilated cardiomyopathy: characteristics and prognostic value. J Am Coll Cardiol. 1997;30(4):1009-14.
11. La Rovere MT, Bigger JT, Jr., Marcus FI, Mortara A, Schwartz PJ. Baroreflex sensitivity and heart-rate variability in prediction of total cardiac mortality after myocardial infarction. ATRAMI (Autonomic Tone and Reflexes After Myocardial Infarction) Investigators. Lancet. 1998;351(9101):478-84.
12. Oikawa K, Ishihara R, Maeda T, Yamaguchi K, Koike A, Kawaguchi H, et al. Prognostic value of heart rate variability in patients with renal failure on hemodialysis. Int J Cardiol. 2009;131(3):370-7.

13. Hayano J, Takahashi H, Toriyama T, Mukai S, Okada A, Sakata S, et al. Prognostic value of heart rate variability during long-term follow-up in chronic haemodialysis patients with end-stage renal disease. Nephrology, dialysis, transplantation : official publication of the European Dialysis and Transplant Association - European Renal Association. 1999;14(6):1480-8.
14. Guo Y, Koshy S, Hui D, Palmer JL, Shin K, Bozkurt M, et al. Prognostic Value of Heart Rate Variability in Patients With Cancer. Journal of clinical neurophysiology : official publication of the American Electroencephalographic Society. 2015;32(6):516-20.
15. Gulizia MM, Casolo G, Zuin G, Morichelli L, Calcagnini G, Ventimiglia V, et al. [ANMCO/AIIC/SIT Consensus document: Definition, precision and appropriateness of the electrocardiographic signal of electrocardiographic recorders, ergometry systems, Holter systems, telemetry and bedside monitors]. Giornale italiano di cardiologia (2006). 2016;17(6):393-415.
16. Bizzini M, Impellizzeri FM, Dvorak J, Bortolan L, Schena F, Modena R, et al. Physiological and performance responses to the “FIFA 11+” (part 1): is it an appropriate warm-up? Journal of sports sciences. 2013;31(13):1481-90.
17. Karlen W, Cardin S, Thalmann D, Floreano D. Enhancing pilot performance with a SymBodic system. Conference proceedings : Annual International Conference of the IEEE Engineering in Medicine and Biology Society IEEE Engineering in Medicine and Biology Society Annual Conference. 2010;2010:6599-602.
18. Tharion WJ, Buller MJ, Potter AW, Karis AJ, Goetz V, Hoyt RW. Acceptability and Usability of an Ambulatory Health Monitoring System for Use by Military Personnel. IIE Transactions on Occupational Ergonomics and Human Factors. 2013;1(4):203-14.
19. Liu Y, Zhu SH, Wang GH, Ye F, Li PZ. Validity and reliability of multiparameter physiological measurements recorded by the Equivital LifeMonitor during activities of various intensities. Journal of occupational and environmental hygiene. 2013;10(2):78-85.
20. Matthis Weippert, Dagmar Arndt, Steffi Kreuzfeld, Stoll R. Validity of a mobile multi-sensor system for RR interval measurement and HRV analysis in psychophysiologi-specific issues. Edition Czwalina. 2012:1-5.
21. Jansen SW, Akintola AA, Roelfsema F, van der Spoel E, Cobbaert CM, Ballieux BE, et al. Human longevity is characterised by high thyroid stimulating hormone secretion without altered energy metabolism. Scientific reports. 2015;5:11525.
22. Schoenmaker M, de Craen AJ, de Meijer PH, Beekman M, Blauw GJ, Slagboom PE, et al. Evidence of genetic enrichment for exceptional survival using a family approach: the Leiden Longevity Study. EurJHumGenet. 2006;14(1):79-84.

23. Fitbit. https://www.fitbit.com/sleep/2013/10/10. Site last accessed 06-01-2016.
24. Di Rienzo M, Racca V, Rizzo F, Bordoni B, Parati G, Castiglioni P, et al. Evaluation of a textile-based wearable system for the electrocardiogram monitoring in cardiac patients. Europace : European pacing, arrhythmias, and cardiac electrophysiology : journal of the working groups on cardiac pacing, arrhythmias, and cardiac cellular electrophysiology of the European Society of Cardiology. 2013;15(4):607-12.
25. Yu-Hong; S, ; ZJ-W, ; ZZ-B, Chen-Ming L. Design and implementation of a wearable, multiparameter physiological monitoring system for the study of human heat stress, cold stress, and thermal comfort. Instrumentation Science & Technology. 2012;40(4):290-304.
26. Nangalia V, Prytherch DR, Smith GB. Health technology assessment review: remote monitoring of vital signs--current status and future challenges. Critical care (London, England). 2010;14(5):233.
27. El-Sherif N, Turitto G. Ambulatory electrocardiographic monitoring between artifacts and misinterpretation, management errors of commission and errors of omission. Annals of noninvasive electrocardiology : the official journal of the International Society for Holter and Noninvasive Electrocardiology, Inc. 2015;20(3):282-9.
28. Brage S, Brage N, Franks PW, Ekelund U, Wareham NJ. Reliability and validity of the combined heart rate and movement sensor Actiheart. European journal of clinical nutrition. 2005;59(4):561-70.
29. Haberman ZC, Jahn RT, Bose R, Tun H, Shinbane JS, Doshi RN, et al. Wireless Smartphone ECG Enables Large-Scale Screening in Diverse Populations. Journal of cardiovascular electrophysiology. 2015;26(5):520-6.

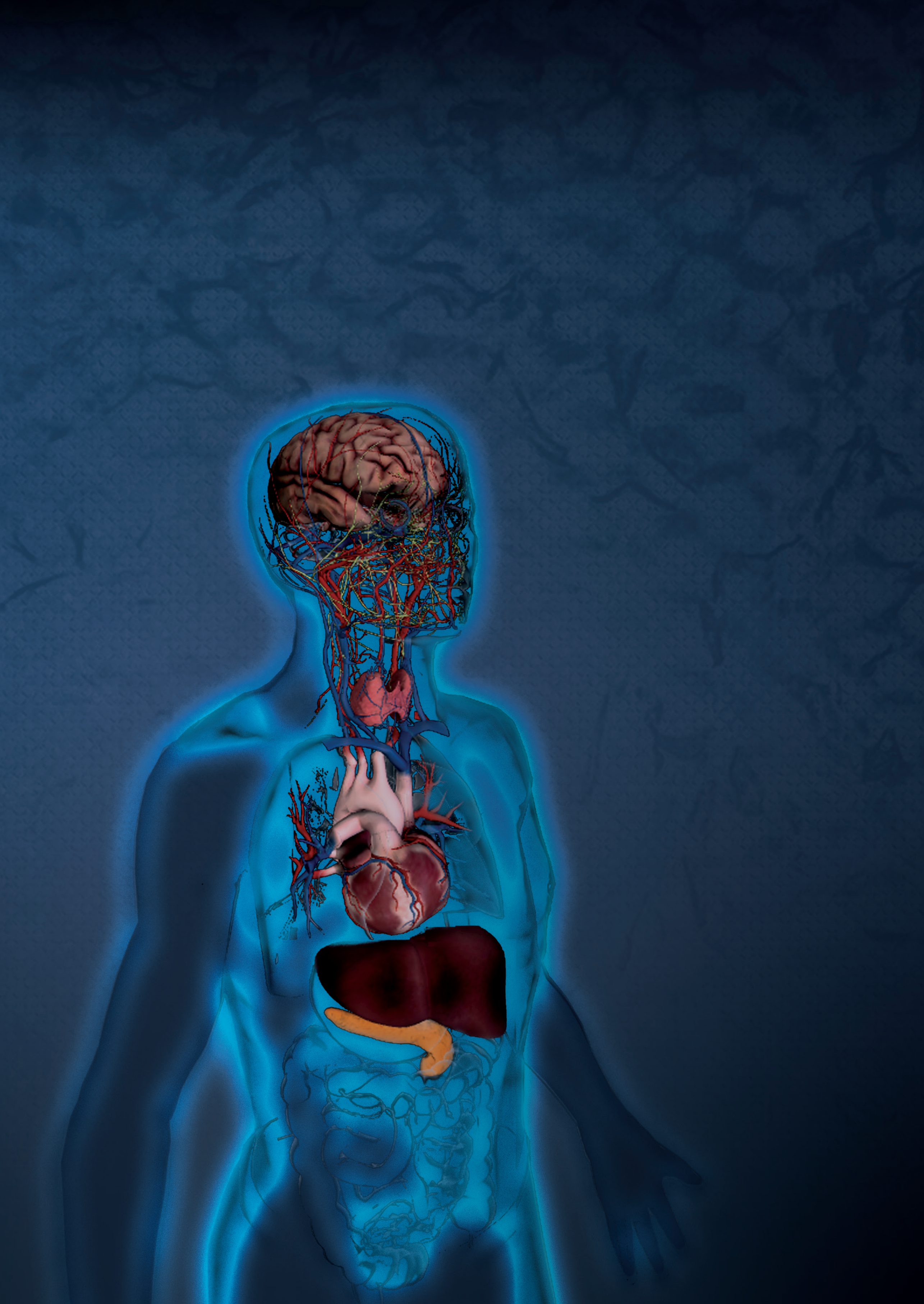

CHAPTER 11

CHARACTERISATION OF HEART RATE RHYTHMS AND THEIR VARIABILITY IN AGEING AND FAMILIAL LONGEVITY

Abimbola A. Akintola
Steffy W. Jansen
Eline Smith
Hanno Pijl
P. Eline Slagboom
Jeroen van der Grond
Rudi G. Westendorp
Arie C. Maan
Diana van Heemst

ABSTRACT

Age related cardiac changes occur in everyone, but not at the same rate. Here, we compared heart rate rhythms and their variability in offspring from long-lived siblings enriched for familial longevity (offspring) versus age-matched controls, and in young versus older adults. Heart rate (HR) and heart rate variability (HRV) were continuously measured over three consecutive days in a total of 28 offspring, 23 age-matched aged controls and 19 young controls (mean age 65, 66 and 23 years respectively). To take the differences in the awake/ sleep rhythms into account, HR and HRV were calculated during 24h, and also during awake and self- reported sleep periods separately.

Heart rate rhythms and HRV were not different in offspring compared to middle- aged controls. While the difference between HR during awake and sleep periods (HR_{awake} – HR_{sleep}), was not different between offspring and controls, the young participants had a higher difference compared to middle- aged controls ($P<0.001$). The mean (standard error (SE)) standard deviation of NN intervals (SDNN) over 24- hours was higher in young (108.5 (6.3)) compared to the older adults (83.7 (6.3)) ($P=0.01$). Similar results were obtained for NN50 and pNN50 over 24h and also during awake and sleep periods.

Thus, we observed beat-to-beat heart rate variability were increased with age but not with familial longevity.

INTRODUCTION

Cardiovascular health, like many other biologic processes, is modified by time. Age-associated changes in cardiac autonomic function (autonomic dysfunction) (1) have been linked with increased risk for a number of cardiac outcomes, including left ventricular hypertrophy, hypertension, heart failure, ventricular arrhythmias and sudden cardiac death (2-6). Autonomic dysfunction has been suggested as a common pathway leading to increased morbidity and mortality from cardiovascular diseases (7). Changes in cardiac autonomic function can be non- invasively estimated by quantifying sympathetic and parasympathetic inputs by measuring beat-to-beat changes in heart rate (heart rate variability (HRV)).

Existing literature show that HRV is believed to decline with age (8, 9). Although age related changes occur in everyone, these do not occur at the same rate (10). Since cardiovascular ageing is influenced by genetic, lifestyle and environmental factors, it thus would be imperative to investigate heart rate rhythms in relation to ageing and longevity, since longevity has a genetic component. Epidemiological studies in both model organisms and humans have focused on identifying mechanisms of healthy longevity, and the autonomic nervous system has been identified as playing a role, since it has been implicated in the onset of many adverse cardiovascular events.

The Leiden Longevity Study (LLS) was designed to investigate factors associated with human longevity (11). Offspring of long- lived nonagenarian siblings, who are predisposed to become long-lived were included. Their partners with whom most have had a relationship and shared environment for decades, were included as age- and, environment- matched controls. These offspring carry 50% of the genetic advantage of their long- lived parent and were shown to have a 35% lower mortality rate compared to their birth cohort (11), and thus are genetically enriched for exceptional longevity. Offspring were observed to have a lower prevalence of cardiovascular diseases, myocardial infarctions, hypertension, type 2 diabetes, as well as preserved insulin sensitivity and resistance to cellular stress, compared to controls of similar chronological age (11-13). Most studies of the association between heart rate variability and age have included subjects based on calendar age. We aimed to decipher whether heart rate and its variability is also modified by familial longevity as well as calendar age.

Here for the first time, we investigated associations of continuously measured 72- hour heart rate rhythms and HRV with propensity for longevity, and (chronological) age.

METHODS

Ethics statement

The present study was approved by the Medical Ethical Committee of Leiden University Medical Center under protocol P11.116. All investigations were conducted according to the principles of the Declaration of Helsinki. All study participants gave written informed consent.

Study participants

Participants for the current study were derived from the Switchbox study, which is a satellite study of the Leiden Longevity Study (LLS). The LLS is a family based study consisting of 421 families with at least two long-lived siblings (men ≥ 89 years, women ≥ 91 years) of Dutch descent, without any selection on demographics or health (14).

For the present study, 28 offspring from long-lived siblings and 23 middle- aged controls (partners from offspring) from the LLS were included. Inclusion criteria for Switchbox study included being aged 55–77 years, having a stable body mass index (BMI) between 19 and 33 kg/m2 and having no significant chronic disease or medication use known to influence any hormonal axis. To enhance the contrast in familial longevity between groups, controls with a nonagenarian parent who had one or more nonagenarian siblings were excluded (based on telephone questioning). Exclusion criteria have been described in details elsewhere (15). Additional inclusion criteria specific for this study were being free- living during the 5- day study period, and having good quality ECG recordings. Good quality ECQ recordings was defined as having ≤ 20% average artefacts on 5-day ambulatory ECG recording.

Additionally, we further recruited 19 young healthy volunteers from the general population via advertisement, using the same exclusion criteria that were used for the middle- aged participants, except for age, which was set at 18 – 30 years.

Experimental protocol

At the study center, height, weight, body composition, and waist and hip circumference were measured, and body mass index (BMI) was calculated. Body composition was measured using a bioelectrical impedance analysis (BIA) meter at a fixed frequency of 50kHz (Bodystat® 1500 Ltd, Isle of Man, British Isles). Timing and duration of sleep was assessed using detailed diaries that were filled in by the participants, as well via the Pittsburg sleep quality index (PSQI) questionnaire (16) that was filled in by the participants during the study.

Fasted blood samples were collected for baseline measurement of glucose, HbA1c, cholesterol and HDL cholesterol. After blood withdrawal, the serum tubes were kept at room temperature to clot and immediately centrifuged when the samples were clotted. Serum was aliquoted into 500µl tubes and promptly stored at -80°C. HbA1c was measured on a Primus Ultra 2 HPLC analyzer (Trinity Biotech, Bray, Ireland), using Boronate affinity separation. Glucose levels were measured using fully automated equipment with the Hitachi Modular P800 from Roche Diagnostics (Almere, the Netherlands). Coefficient of variation for measurements ranged between 0.9–3.0%.

ECG monitoring

Each participant was assigned to an Equivital EQ02 lifemonitor, which was worn over five consecutive days. The EQ02 (Equivital EQ02, Hidalgo, UK) continuously measures ECG, as well as breathing rate, skin and core body temperature, and tri- axial accelerometry. ECG was measured on two channels via three electrodes. The EQ02 monitoring system consisted of an LM 1000 Life monitor sensor electronic module ((SEM), Life monitor belts of varying sizes, a SEM lead and a charging dock, and an Equivital Manager to configure SEMs and to download and export data. For this study, SEMs were configured in clinical mode, and data reported retrospectively at local time. A lifemonitor belt, whose size was chosen based on the participant's body size and fit held the SEM onto the participant's body. It's fabric (lycra) -based electrodes were moistened with water before making contact with the participant's skin (14). SEMs were disconnected from the belt after 12 hours of recording, for charging for approximately one hour, after which SEMs were reconnected. Upon study completion, SEM data was uploaded onto the Equivital manager; from where date- and time- stamped ECG data (raw and in mV), inter-beat interval (in sample period and in milliseconds), and summary data of all vital signs were extracted and exported. Circadian HR and HRV were calculated from the ECG.

Data and artefact management

Raw data from EQ02, which were automatically time- and date stamped (date, time in hr., min., sec. & ms.), was extracted from the EQ02 using the Equivital manager and uploaded to the Vivosense modular physiological monitoring and analysis platform (Vivonoetics, San Diego, USA). Via the cardiac layout, EQ02 data were visualized for inspection of each ECG channel and derived R- wave markings. This layout also contained accelerometer data channels for contextual interpretation and artefact identification, raw SEM waveforms and quality control.

After removal of charging times, the ECG data was cleaned using automatic cleaning methods in Vivosense, by selecting the timeframe to be cleaned, and the automatic cleaning module and setting the lower HR limit to 30 and the upper limit to 220. For the analysis contained in this study, only files containing less than 20% artefacts were selected for HR analysis and files with less than 2% artefacts were used for HRV analysis. Thus, data from days 2-5 was used for the HR analysis, whereas the 24- hour data with than 2% artefacts were used for HRV analysis.

Five-minute trends (averages) of HR, RR and HRV parameters in time domain were extracted for analysis. Five- minute HR averages of less than 30 beats per minutes were considered non- physiological (probably caused by undetected artefacts) and excluded from analyses. Furthermore, eight HRV indices, namely, average of NN intervals (ANN), standard deviation of NN intervals (SDNN), standard deviation of 5 minute averages of NN intervals (SDANN), standard deviation of successive differences of NN intervals (SDSD), square root of the mean squared differences of successive intervals (RMSSD), mean of the standard deviation of 5 minute NN intervals (SDNNi), number of adjacent NN intervals with a difference less than 50ms (NN50) and ratio of a NN50 to total number of NN intervals (pNN50) were extracted from Vivosense for analysis .

Statistical analysis

All data are presented as mean with standard errors (SE). Groups were compared using linear mixed effects models, with adjustment for sex. To take the differences in awake/ sleep rhythms into account, we studied first the continuous rhythm over three days and then the rhythms during awake periods and sleep periods separately, based on the self-reported sleep data provided by the participants. Differences between HR on awake and sleep periods were compared between offspring, partner and young using unpaired

T-tests with Welch's correction. All statistical analyses were performed using SPSS v.20 for Windows (SPPS Inc., Chicago, IL, U.S.A.). Graphs of 24h HR and HRV trajectories were drawn using GraphPad Prism version 5 (GraphPad, San Diego, CA). Two-sided p-values below 0.05 were considered statistically significant.

RESULTS

Characteristics of the young individuals from the general population and middle- aged individuals with propensity for longevity and their age-matched controls from the Leiden Longevity Study are summarized in table 1. To study the relation between heart rate rhythms and familial longevity, participants were selected on the basis of the age of their parents. Thus the parents of the offspring were significantly older than those of the middle- aged controls ($P<0.001$) and those of the young controls of whom most parents are still alive ($P<0.001$). The mean age and cardiovascular risk factors were not significantly different between the middle aged controls and the middle aged participants with propensity for longevity.

The number of females was lower in the middle aged with propensity for longevity (46%) compared to middle aged controls (56.5%) and to the young group (63.2%). All subsequent analyses were therefore adjusted for sex. In all groups, BMI and serum parameters were all within the normal range.

Heart rate rhythms

The heart rate rhythms were measured continuously over three consecutive days. Figure 1 shows the 3-day heart rate rhythms for one representative offspring enriched for familial longevity (Figure 1A), one representative middle-aged control (Figure 1B), and one representative young participant (Figure 1C).

TABLE 11.1 | Description of study subjects

	Leiden Longevity Study		General population
	Middle- aged Offspring N=28	**Middle- aged Controls N=23**	**Young Controls N=19**
Age of parents*			
Age of father	90.0 (9.2)	72.8 (12.6)	57.1 (6.4)
Age of mother	88.25 (10.0)	76.7(17.6)	54.7 (3.4)
Anthrometrics			
Age, years	65.38 (6.7)	65.7 (6.9)	22.9 (2.1)
BMI kg/m^2	25.65 (3.9)	26.4 (4.4)	23.2 (2.4)
Lean mass	52.9 (10.9)	51.1 (9.4)	58.1 (11.0)
Fat, kg	23.3 (7.0)	26.6 (10.1)	14.6 (4.9)
Female (%)	13 (46.4)	13 (56.5)	12 (63.2)
Serum parameters			
Glucose, mmol/l	5.5 (0.4)	5.5 (0.5)	4.9 (0.4)
HbA1c, mmol/mol	34.8 (2.0)	35.6 (39)	
Cholesterol, mmol/l	5.9 (0.9)	5.7 (0.9)	4.7 (0.9)
HDL cholesterol	1.8 (0.6)	1.7 (0.6)	1.7 (0.5)
Cardiovascular risk			
Alcohol n(%)	1 (3.6)	1 (4.3)	2 (10.5)
Systolic BP	151.3 (18.5)	155.7 (19.9)	119.2 (13.0)
Diastolic BP	91.3 (10.7)	91.0 (10.8)	75.5 (8.73)
Anti-hypertensives	4 (14.3)	5 (22.7)	0 (0)
CVD n(%)	1 (3.6)	2 (8.7)	0 (0)
Activity			
Working full time n(%)	16 (57.1)	16 (69.6)	19 (100)
Hours worked per day	5.7 (8.2)	4.4 (2.1)	8 (1.3)
Sleep duration(hours)	7.58 (0.93)	7.28 (0.96)	7.82 (1.19)
Motion**	36.7 (66.8)	36.7 (52.7)	37.6 (58.9)

Data presented as mean (standard deviation) unless otherwise stated. BMI: Body mass index. CVD: cardiovascular disease.

** Age of parents indicate age at death or age at moment the questionnaire was taken.*

***Motion indicate mean tri-axial body movement per five minutes as measured by the equivital monitor.*

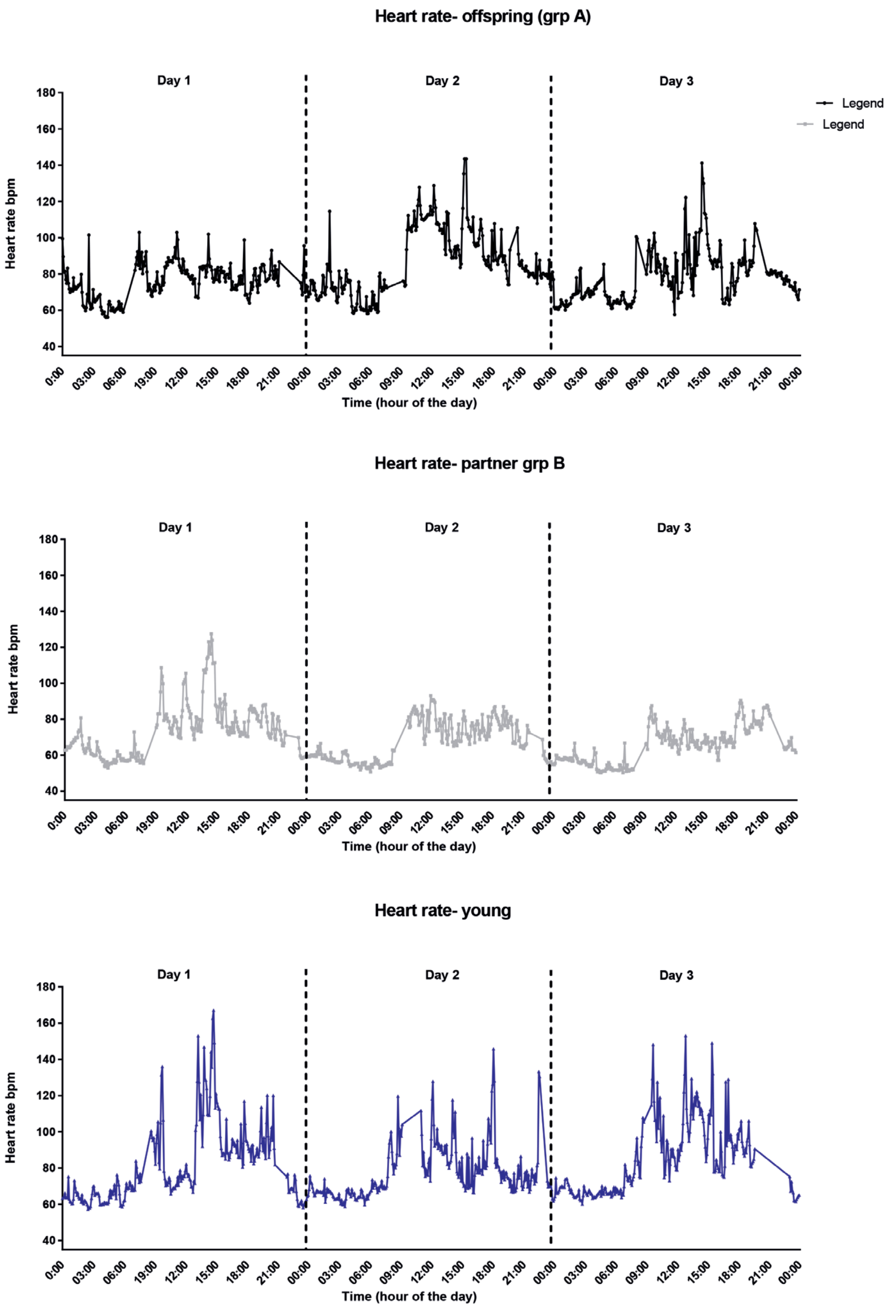

FIGURE 11.1 | 3-day heart rate rhythm of one representative participant each from the offspring, middle- aged controls, and the young.

Heart rate: familial longevity

To test if heart rate rhythm is modified by familial longevity, we compared the continuously-measured 5- minute HR averages in offspring enriched for longevity to those of age-matched controls. As shown in table 2, the mean HR for the three- day period, and during awake and sleep periods was not significantly different in offspring compared to age-matched controls. The mean HR over the entire three days and when stratified to awake and sleep periods was 70.8, 76.1 and 62.6 beats per minute (bpm) respectively for the offspring and 71.4, 75.2 and 62.6 bpm respectively for the middle- aged controls. We further measured the difference between HR during awake and sleep periods, as a measure of fitness and adaptability. The mean (HR_{awake} – HR_{sleep}) difference in HR did not significantly differ in offspring compared to controls (P=0.150).

TABLE 11.2 | Mean heart rate in groups that differ in familial longevity or calendar age.

	Leiden Longevity Study		General population	*P*-value*	*P*-value**
	Middle- aged Offspring N=28	Middle aged controls N=23	Young controls N=19		
Heart rate (HR)					
Over 3- days	70.80 (1.4)	71.43 (1.8)	70.15 (2.0)	0.760	0.633
Awake	76.13 (1.7)	75.22 (1.9)	78.03 (2.2)	0.803	0.335
Sleep	62.56 (1.2)	62.61 (1.6)	59.72 (1.8)	0.798	0.229
HR_{awake} – HR_{sleep}	13.57 (2.1)	12.61 (2.5)	18.31 (2.7)	0.150	<0.001

Data presented as mean with standard error.
** P-value for difference between offspring with propensity for longevity and middle aged controls.*
***P-value for difference between young and middle aged controls.*
All analyses were adjustment for gender.

Heart rate: Chronological age

Table 2 also shows the result of the comparison of continuously- measured 5- minute HR averages in young participants and middle aged control participants, to assess if heart rate rhythm is modified by chronological age. The mean HR for the three- day period, during awake and during self- reported sleep periods was not significantly different in young compared to middle aged controls. The mean HR over the entire three days and when stratified to awake and sleep periods was 71.4, 75.2 and 62.6 bpm respectively for the middle- aged controls and 70.2, 78.0 and 59.7 bpm respectively for the young controls. However, when the difference between HR during awake and sleep periods was compared in young versus middle aged controls, the mean (HRawake – HRsleep) difference in young was significantly higher in young compared to middle aged controls (P<0.001).

Heart rate variability

The differences in variability in 24h heart rate between offspring compared to middle- aged controls and middle- aged controls compared to young was assessed using five parameters of heart rate variability, namely SDNN, RMSSD, SDNNi, NN50 and pNN50. The results are presented in table 3.

Heart rate variability: familial longevity

To assess which parameters of heart rate variability associated with familial longevity, we compared HRV parameters between offspring and middle- aged controls, as shown in table 3. For the whole 24- hour period, the mean SDNN, RMSSD SDNNi and SDANN were consistently but not statistically significantly lower in the offspring compared to middle- aged controls. Conversely, NN50 and pNN50 seemed to be higher in the offspring, although not statistically significant. SDNN, RMSSD, NN50 and pNN50 showed a trend of increased variability during self- reported sleep- time compared to awake periods, in both offspring and middle- aged controls.

Heart rate variability: Chronological age

We also compared parameters of heart rate variability in middle- aged controls to young controls in order to test which parameters of 24- hour HRV associated with chronological age. As depicted in table 3, there were no significant differences in RMSSD, SDNNi and SDANN in middle- aged controls compared to young controls, neither during the full 24- hour period, nor during awake or sleep- time. On the other hand, after adjustment for sex, younger participants had higher mean (standard error (SE)) SDNN compared to the older adults (108.5 (6.3) versus 83.7 (6.3), P=0.011. Similar difference was seen in SDNN during awake periods but not during sleep.

TABLE 11.3 | Parameters of 24- hour heart rate variability in groups of different calendar age and familial longevity

	Leiden Longevity Study		General population	*P*-value*	*P*-value**
	Middle- aged Offspring N=10	**Middle aged Controls N=12**	**Young Controls N=12**		
Measure of total HRV					
SDNN					
24hr	76.8 (8.1)	83.7 (6.3)	108.5 (6.3)	0.634	**0.011**
Awake	72.7 (7.6)	78.2 (6.6)	104.3 (6.7)	0.685	**0.011**
Sleep	81.1 (12.5)	95.5 (1.5)	112.0 (11.3)	0.511	0.307
Measures of short- term HRV					
SDNNi					
24hr	276.6 (99.5)	403.5 (213)	575.9 (238)	0.438	0.598
Awake	207.0 (133)	486.9 (131)	196.5 (160)	0.137	0.157
Sleep	403.8 (146)	248.0 (516)	1054.2 (513)	0.336	0.265
SDANN					
24hr	124.5 (65.2)	235.5 (66.2)	171.9 (71.5)	0.329	0.542
Awake	72.5 (77.0)	279.2 (76.0)	122.2 (86.5)	0.120	0.103
Sleep	220.6 (106)	93.6 (117.3)	270.2 (116)	0.399	0.291
Measures of vagal activity					
RMSSD					
24hr	68.5 (11.6)	83.6 (9.2)	95.4 (9.2)	0.427	0.368
Awake	61.7 (11.3)	78.0 (10.0)	90.0 (10.1)	0.367	0.406
Sleep	76.8 (17.2)	95.9 (15.4)	98.5 (15.1)	0.482	0.905
NN50					
24hr	96.1 (25.7)	79.4 (21.7)	192.8 (21.9)	0.652	**0.002**
Awake	84.2 (25.7)	78.9 (27.7)	181.3 (24.7)	0.887	**0.009**
Sleep	110.0 (32.2)	82.3 (27.2)	200.8 (27.4)	0.553	**0.007**
pNN50					
24hr	0.160 (0.042)	0.112 (0.036)	0.297 (0.037)	0.422	**0.002**
Awake	0.122 (0.039)	0.109 (0.039)	0.255 (0.040)	0.808	**0.018**
Sleep	0.207 (0.054)	0.121 (0.045)	0.340 (0.045)	0.276	**0.003**

*Data presented as mean with standard error. *P-value for difference between young and middle aged from the general population, with adjustment for gender. ** P-value for difference between middle aged from the general population and middle- aged with propensity for longevity. All analyses were adjustment for gender.*

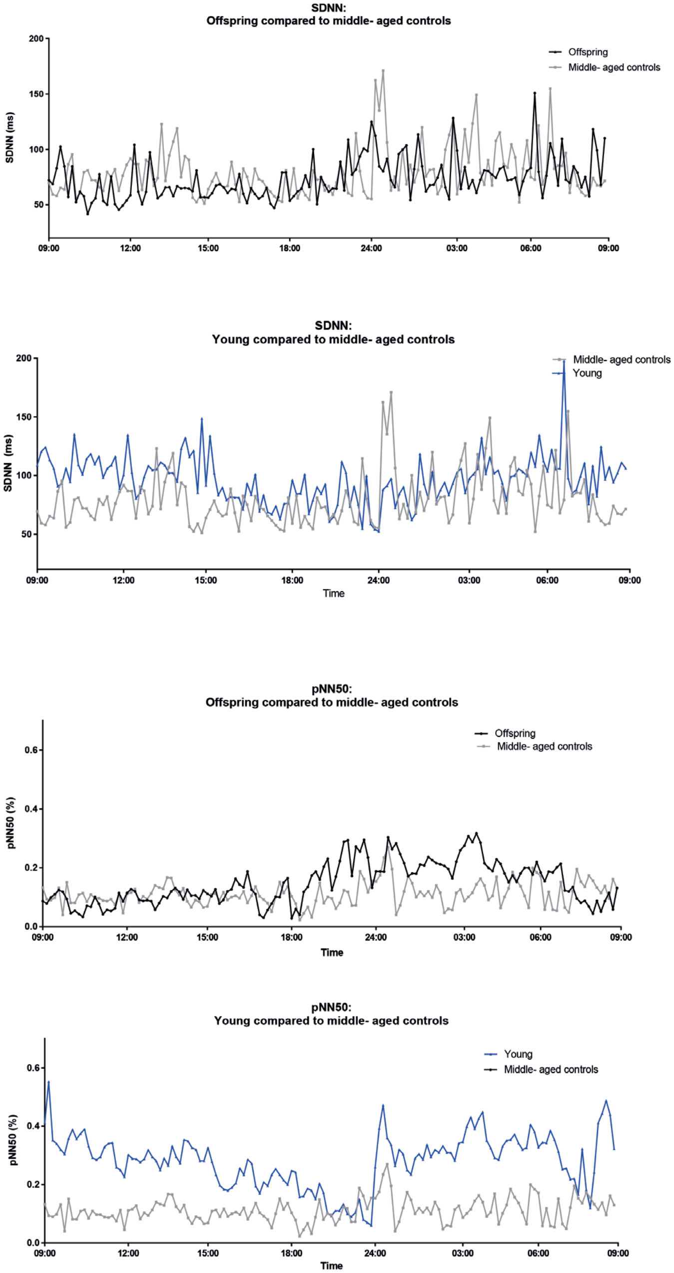

FIGURE 11.2 | 24h HRV parameters (SDNN and pNN50) in offspring, middle aged controls and the young.

Also, younger participants showed higher NN50 and pNN50 values, which was found from the 24hr analysis and also when stratified for awake and sleep period. The mean (SE) pNN50 in young compared to older adults was 0.297 (0.037) versus 0.112 (0.036), P= 0.002 during the 24h period, 0.255 (0.040) versus 0.109 (0.039), P=0.018 during awake periods, and 0.340 (0.045) versus 0.121 (0.045), P= 0.003 during self- reported sleep time. The differences in SDNN and pNN50 in young compared to older adults are visualized in figure 2.

DISCUSSION

We report two main findings. First, mean 3- day heart rate was not different in offspring compared to middle- aged controls, or in middle- aged controls compared to younger participants. However, difference between HR during awake and sleep periods (HR_{awake} – HR_{sleep}), as a measure of fitness and adaptability, was higher in young compared to middle- aged controls. Secondly, we observed significantly higher values of SDNN, NN50 and pNN50 in young compared to older adults, and the difference in the latter two HRV parameters were consistent both during awake and sleep periods.

Cardiovascular events are known to increase with age. It is well established that the autonomic nervous system, which acts as control system for the body's visceral system, associates with cardiovascular mortality, including sudden cardiac death [3, 8, 9, 17]. Heart rate is controlled on a beat- to- beat basis by the combined effects of the sympathetic and parasympathetic system. Continuous measurement of HR and its variability provides a non- invasive way to measure autonomic activity. In our study, we measured HRV in the time domain. In young compared to older adults, we found that increased variability in SDNN, NN50 and pNN50. The SDNN is considered as the most global measure of HRV because it captures total HRV while being insensitive to small measurement errors [17, 18]. Since the SDNN is a measure of total HRV, it is not surprising that we found higher SDNN in younger compared to older participants. This is in line with previous studies that show that HRV decreases with increasing age [3, 8, 17]. The differences have been ascribed to a decline in parasympathetic activity and possible sympathetic nervous system [8]. In line, we found differences also on NN50 and pNN50, which are measures of vagal activity.

Concerning heart rate, we did not find significant differences in heart rate in the main study sample, neither in offspring compared to controls, or in the controls compared to young. While the difference between HR during awake and sleep periods ($HR_{awake} – HR_{sleep}$), was not different between offspring and controls, the young participants had a higher difference compared to middle- aged controls. This could be a reflection of the difference in behaviour and activity patterns, since young participants worked longer hours per day, and moved more, in comparison with the offspring and middle aged controls. The ability to maintain comparatively higher heart rate during the day and lower heart rate during sleep periods could thus suggest that the young had comparatively more adaptable day- night heart rate rhythms, or more preserved global autonomic nervous system [1].

To our knowledge, this is the first study where continuously measured heart rate and its variability were compared in offspring enriched for familial longevity and age- matched controls. Previously, offspring have been shown to differ from partners in many cardio-metabolic parameters compared to controls of similar calendar age [12, 13, 19] However, in both the main and full study samples, we found no difference in HRV parameters in offspring enriched for familial longevity and controls. In a previous study in which healthy participants aged 10 – 99 years were included, HRV parameters were found to decrease with age, and it was concluded that persistently high HRV could be predictive of longevity [20]. In line, we also found that HRV was lower in older compared younger participants. However, this was not the case in offspring enriched for longevity and age- matched controls. Thus, our findings that heart rate and its variability did not differ would suggest that familial longevity may not be characterized by changes in the autonomic nervous system. This may be in line with previous arguments that HRV studies in older adults could be confounded by increasing erratic rhythms, and so, difference found in previous studies may not be due to longevity [21,22].

A strength of this study is that the heart rate and its variability was continuously recorded over 5 consecutive days, during the home setting of the participants. A limitation of this study is that we only examined cross-sectional associations and so, our findings are only descriptive. Another limitation is the small sample size. Using continuous ECG measurement, we observed beat-to-beat heart rate variability were increased with age but not with familial longevity. These findings possibly offer more insight into the association between different parameters of heart rate variability and aging. Sufficiently powered follow-up studies are needed to evaluate cause or consequence in the relation between parameters of heart rate variability and aging.

REFERENCES

1. Almeida-Santos MA, Barreto-Filho JA, Oliveira JL, Reis FP, da Cunha Oliveira CC, Sousa AC. Aging, heart rate variability and patterns of autonomic regulation of the heart. Archives of gerontology and geriatrics. 2016;63:1-8.
2. Lakatta EG, Levy D. Arterial and cardiac aging: major shareholders in cardiovascular disease enterprises: Part II: the aging heart in health: links to heart disease. Circulation. 2003;107(2):346-54.
3. Jandackova VK, Scholes S, Britton A, Steptoe A. Are Changes in Heart Rate Variability in Middle-Aged and Older People Normative or Caused by Pathological Conditions? Findings From a Large Population-Based Longitudinal Cohort Study. Journal of the American Heart Association. 2016;5(2).
4. Nicolini P, Ciulla MM, De Asmundis C, Magrini F, Brugada P. The prognostic value of heart rate variability in the elderly, changing the perspective: from sympathovagal balance to chaos theory. Pacing and clinical electrophysiology : PACE. 2012;35(5):622-38.
5. La Rovere MT, Bigger JT, Jr., Marcus FI, Mortara A, Schwartz PJ. Baroreflex sensitivity and heart-rate variability in prediction of total cardiac mortality after myocardial infarction. ATRAMI (Autonomic Tone and Reflexes After Myocardial Infarction) Investigators. Lancet. 1998;351(9101):478-84.
6. Molgaard H, Sorensen KE, Bjerregaard P. Attenuated 24-h heart rate variability in apparently healthy subjects, subsequently suffering sudden cardiac death. Clinical autonomic research : official journal of the Clinical Autonomic Research Society. 1991;1(3):233-7.
7. Thayer JF, Yamamoto SS, Brosschot JF. The relationship of autonomic imbalance, heart rate variability and cardiovascular disease risk factors. Int J Cardiol. 2010;141(2):122-31.
8. Reardon M, Malik M. Changes in heart rate variability with age. Pacing and clinical electrophysiology : PACE. 1996;19(11 Pt 2):1863-6.
9. Zhang J. Effect of age and sex on heart rate variability in healthy subjects. Journal of manipulative and physiological therapeutics. 2007;30(5):374-9.
10. Nakou ES, Parthenakis FI, Kallergis EM, Marketou ME, Nakos KS, Vardas PE. Healthy aging and myocardium: A complicated process with various effects in cardiac structure and physiology. Int J Cardiol. 2016;209:167-75.
11. Schoenmaker M, de Craen AJ, de Meijer PH, Beekman M, Blauw GJ, Slagboom PE, et al. Evidence of genetic enrichment for exceptional survival using a family approach: the Leiden Longevity Study. EurJHumGenet. 2006;14(1):79-84.

12. Westendorp RG, van Heemst D, Rozing MP, Frolich M, Mooijaart SP, Blauw GJ, et al. Nonagenarian siblings and their offspring display lower risk of mortality and morbidity than sporadic nonagenarians: The Leiden Longevity Study. Journal of the American Geriatrics Society. 2009;57(9):1634-7.
13. Wijsman CA, Rozing MP, Streefland TC, le Cessie S, Mooijaart SP, Slagboom PE, et al. Familial longevity is marked by enhanced insulin sensitivity. Aging Cell. 2011;10(1):114-21.
14. Schoenmaker M, de Craen AJ, de Meijer PH, Beekman M, Blauw GJ, Slagboom PE, et al. Evidence of genetic enrichment for exceptional survival using a family approach: the Leiden Longevity Study. European journal of human genetics : EJHG. 2006;14(1):79-84.
15. Jansen SW, Akintola AA, Roelfsema F, van der Spoel E, Cobbaert CM, Ballieux BE, et al. Human longevity is characterised by high thyroid stimulating hormone secretion without altered energy metabolism. Scientific reports. 2015;5:11525.
16. Buysse DJ, Reynolds CF, 3rd, Monk TH, Berman SR, Kupfer DJ. The Pittsburgh Sleep Quality Index: a new instrument for psychiatric practice and research. Psychiatry Res. 1989;28(2):193-213.
17. Felber Dietrich D, Schindler C, Schwartz J, Barthelemy JC, Tschopp JM, Roche F, et al. Heart rate variability in an ageing population and its association with lifestyle and cardiovascular risk factors: results of the SAPALDIA study. Europace : European pacing, arrhythmias, and cardiac electrophysiology : journal of the working groups on cardiac pacing, arrhythmias, and cardiac cellular electrophysiology of the European Society of Cardiology. 2006;8(7):521-9.
18. Stein PK, Pu Y. Heart rate variability, sleep and sleep disorders. Sleep medicine reviews. 2012;16(1):47-66.
19. Akintola AA, van den Berg A, Van Buchem MA, Jansen S, Slagboom E, Westendorp R, et al. Associations between insulin action and integrity of brain microstructure differ with familial longevity and with age. Frontiers in Aging Neuroscience. 2015;7(92).
20. Zulfiqar U, Jurivich DA, Gao W, Singer DH. Relation of high heart rate variability to healthy longevity. The American journal of cardiology. 2010;105(8):1181-5.
21. Stein PK. Heart rate variability and longevity. The American journal of cardiology. 2010;106(6):910.
22. Stein PK, Domitrovich PP, Hui N, Rautaharju P, Gottdiener J. Sometimes higher heart rate variability is not better heart rate variability: results of graphical and nonlinear analyses. Journal of cardiovascular electrophysiology. 2005;16(9):954-9.

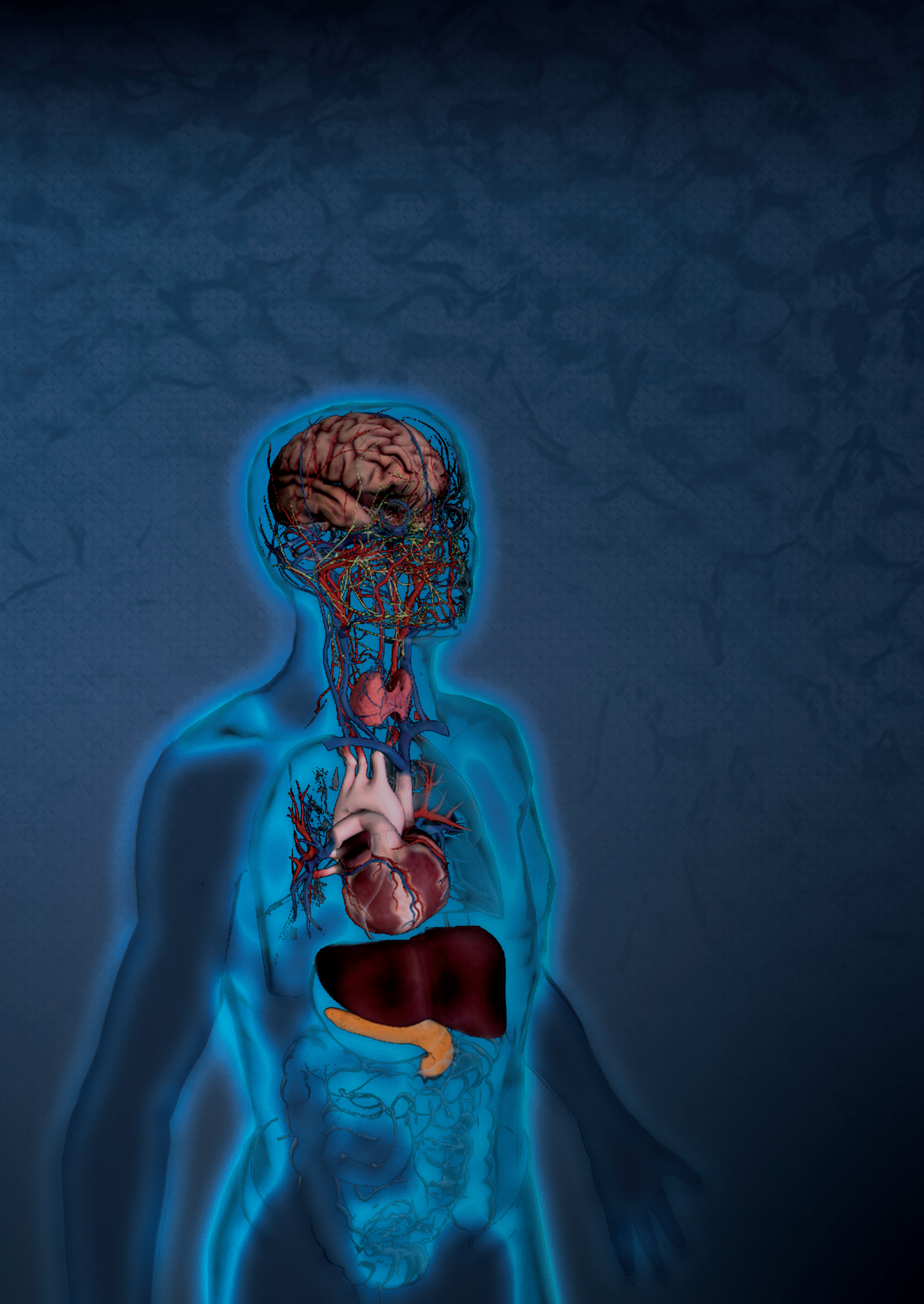

CHAPTER 12

KEY FINDINGS
GENERAL DISCUSSION
AND FUTURE PERSPECTIVES
REFLECTIONS

In this thesis, we examined three interacting systems that have been identified as contributing to a slower pace of ageing, namely the glucose/ insulin metabolism (part I), thyroid (HPT) axis (part II), and the autonomic nervous system (part III). In this chapter, the key findings of the studies will be discussed, and the results put into the context of scientific literature. Finally, directions for future practice and research will be discussed.

KEY FINDINGS

In this thesis, we found that familial longevity is associated with more pronounced relation of insulin parameters with microstructural brain parameters, and by higher TSH secretion, in the absence of differences in metabolism. In addition, familial longevity was not associated with differences in heart rate and its variability as a proxy for the autonomic nervous system. Using specialized MRI techniques (MTI), we showed that subtle changes in microstructural brain parenchymal homogeneity in relation to insulin can be detected, even in brain tissue that appears normal on conventional MR imaging sequences. From our studies, peripheral insulin action seemed to be a stronger indicator of micro- structural (perhaps early) brain integrity than glucose in normo-glycemic older adults. Furthermore, we found that intranasal application of insulin improved brain perfusion in parietal grey matter, occipital gray matter and in the thalamus. Our results strengthen the growing body of evidence that the brain plays a key role in glucose regulation.

GENERAL DISCUSSION AND FUTURE PERSPECTIVES

In literature, IGF-1/glucose/Insulin signaling (IIS), the hypothalamic/pituitary/thyroid (HPT) axis and the autonomic nervous system have been identified as part of the key modifiers of the rate of ageing. Elasticity, robustness and precision of these processes, as co- ordinated by the brain are proposed to be critical to a slower pace of ageing. Conversely, dysregulation in one or more of these systems would accelerate the pace of ageing.

Glucose/ insulin and longevity

With the global population ageing, there has been an astonishing increase in the prevalence of obesity [1], metabolic syndrome [2], type 2 diabetes [3] and neurodegenerative diseases [4]. Insulin resistance is a shared feature in these diverse pathologies [5-9]. Besides regulating peripheral glucose homeostasis, insulin is an important neuromodulator that contributes to neurobiological and other processes [10, 11].

From the magnetization transfer imaging studies, we showed that peripheral insulin action seemed to be a stronger indicator (than glucose) of micro- structural (perhaps early) brain integrity in older adults without diabetes. Higher insulin parameters were associated with measures of decreased myelin and axonal integrity, and these associations were more pronounced in offspring and "younger" older adults in whom glucose-regulatory compensatory mechanisms are probably more intact. Theoretically, the inverse association between peripheral parameters of glucose metabolism and microstructural brain parenchymal homogeneity can be due to either loss of brain integrity as a consequence of defects in glucose regulation, or explained by defects in glucose metabolism being a consequence of deficits in brain integrity.

Due to paucity of experimental studies in humans on the effects of insulin in the brain, the exact mechanism through which insulin relates to brain function remains unclear. To possibly account for our findings, we therefore propose two candidate mechanisms, which we would refer to as 'ageing brain effect' and 'ageing insulin effect'.

The first candidate mechanism is the 'ageing brain effect' (figure 1A). It is becoming clearer that the brain plays an important role in the regulation of peripheral glucose and insulin action [6]. Age related brain changes (reduced integrity of myelin and axons, and shrinkage of large neurons) are accompanied by reduction in brain volumes and function. Brain control of glucose levels may also be affected, for which the body may compensate by higher peripheral insulin secretion by the pancreas. Thus, age induced reduction in brain integrity is proposed to be the trigger for increased peripheral insulin resistance.

The second candidate mechanism is the 'ageing insulin effect' (figure 1B), in which reduced brain integrity is proposed to occur as a consequence of peripheral insulin resistance. Here, due to ageing, peripheral tissues such as muscles and adipose tissues become less sensitive to insulin, leading to increase in circulating glucose levels [12]. To compensate for this, more insulin is secreted peripherally to maintain tight glucose control [13]. Thus, the brain may become overstimulated or insulin resistant as a consequence of chronically elevated peripheral insulin levels, both of which could result in reduced brain integrity [5, 14]. Both candidate mechanisms ultimately result in peripheral hyper-insulinaemia. To protect the brain from overstimulation of neuronal insulin signalling by chronic hyper-insulinaemia, brain insulin receptors may be down regulated, resulting in central insulin resistance. The inferred inverse relation between peripheral and CSF insulin levels in humans supports this hypothesis [15, 16]. Central insulin resistance may also have adverse consequences, as insulin signalling pathways are important for regulation of neuronal growth and differentiation and insulin has neuro-protective roles against neuronal apoptosis induced by oxidative stress [17]. Thus, deficits in central insulin action may further aggravate decreased brain integrity.

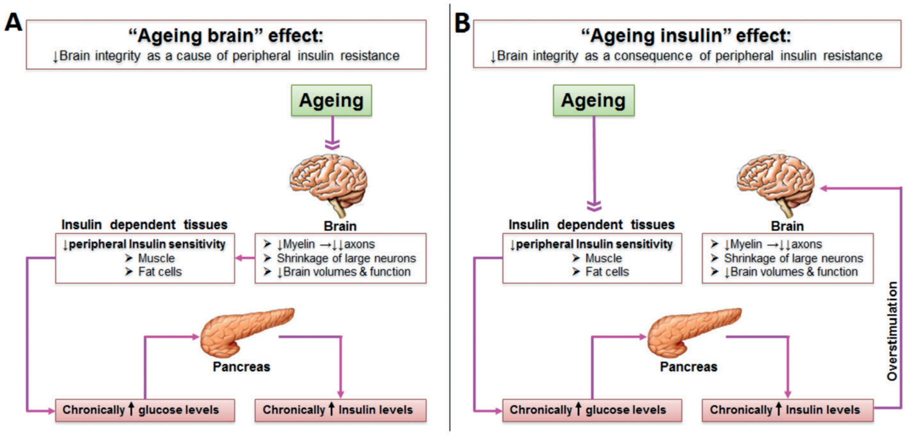

FIGURE 12.1 | Schematic diagrams showing the possible trajectories for the effect of ageing on the relationship between insulin and the brain.

Panel 1A shows the 'ageing brain' effect, in which peripheral insulin resistance occurs due to ageing- induced diminished brain function, which is then compensated for by increased insulin production. The second candidate mechanism is the 'ageing insulin' effect (panel 2B), in which ageing- induced decrease in insulin sensitivity in peripheral tissues stimulates the pancreas to secrete more insulin. The subsequent continued brain stimulation by chronically elevated insulin levels eventually lead to decreased brain integrity.

Previous studies have shown that selective administration of insulin to the brain can have beneficial effects on brain (cognition, memory) and peripheral (weight control, food intake and palatability, body fat) function [18-23]. However, the mechanisms through which insulin does this remains unclear. We showed that intranasal insulin led to increased perfusion in the parietal and occipital grey matter regions, and in the thalamus of older adults. However, the functional and clinical implications of this increased perfusion remain unclear. Future studies can be aimed at deciphering this, and establish the link (if any) between increased perfusion and the previously known and other beneficial effects of intranasal insulin. The data from our intranasal insulin study and previous studies show that insulin can be safely delivered to the brain through the intranasal route, without affecting circulating glucose and insulin levels. Further studies are also required whereby insulin is targeted at the brain of persons with metabolic disturbances, such as type 2 DM, to investigate whether intranasal insulin can rescue some of their existing metabolic disturbances.

Thyroid axis and longevity

Thyroid hormones (TH) influence a wide range of peripheral and brain-related functions including cognition and regulation of energy homeostasis. Like the glucose/ insulin axis, the hypothalamic-pituitary-thyroid (HPT) axis plays a critical role in the maintenance of energy homeostasis (intake and expenditure) by acting on metabolic tissues. TH levels tend to decline during ageing, and higher thyroid stimulating hormone (TSH) levels have been associated with longevity in humans. In our study, we looked at the mechanism underlying the link between TSH/TH and longevity. Although serum levels of TSH were higher in offspring from long-lived families at every 10- minute time point during 24 hours, TH did not differ between the groups. We also assessed energy metabolism in relation with familial longevity in humans, since metabolism has been associated with longevity in different animal models and plays a central role in different ageing theories. Familial longevity was not associated with differences in energy metabolism. Experimental studies are needed to explore how higher TSH levels are related with familial longevity.

Besides TH having marked influences over brain structure and function, their hyper- and hypo- secretion adversely affect neuronal production and survival, dendritic arborisation and other neuroplastic events, and neurotransmitter supply, all of which are reflected in disruptions of cognitive performance and mood and emotional states as well as circadian rhythms and sleep. Since subclinical hypothyroidism (SCH), considered as early thyroid failure, might also influence brain structure and function, we reviewed existing literature on the relation between SCH and cognition in older adults. No evidence was found to support the association between SCH and cognition. The review however showed that epidemiological studies on SCH have used different TSH cut- off values. There is therefore a need for standardisation of reference ranges in all ages, and for age- appropriate reference ranges when evaluating thyroid dysfunction in the elderly.

Heart rate and its variability in longevity

Heart rate and its variability patterns are believed to change with age, likely due to a change in autonomic control of the central nervous system. Using the validated Equivital (EQ02) lifemonitor, our studies confirmed that heart rate during sleep increased with calendar age. Three heart rate variability parameters (SDNN, NN50 and pNN50) also increased with calendar age, over the 24- hour period, and when analysed during daytime and sleep-time separately. However, such differences were not found when offspring enriched for longevity were compared to controls of similar age. Thus, our findings that heart rate and its variability did not differ between groups would suggest that familial longevity may not be characterized by changes in the autonomic nervous system. This may be in line with previous arguments that HRV studies in older adults could be confounded by increasing erratic rhythms, and so, differences found in previous studies may not be due to longevity [24, 25]. Future studies can be aimed at disentangling this.

REFLECTIONS ON HUMAN LONGEVITY: DOES THE BRAIN (CROSS) TALK WITH THE PERIPHERY?

In model organisms such as *Caenorhabditis elegans* and *Drosophila*, solid evidence has shown that certain brain neurons can mediate environmental influences on ageing, and longevity can be induced by neural manipulation of pathways such as insulin or IGF-1 signaling (IIS) [26-31]. Similar to insulin or IGF-1 signaling, the thyroid axis (HPT), via thyroid hormones (TH) also regulates neural development. The central nervous system is particularly dependent on TH for normal maturation and peripheral and brain function [32, 33]. TH plays a critical role in longevity. In mice, a negative correlation has been demonstrated between thyroid hormones and ageing [33], and a combination of reduced TH and IGF-I signaling results in the long-lived phenotype [32, 33]. In humans, a link has been repeatedly demonstrated between the thyroid axis and longevity [34-37]. Furthermore, experiments suggest that the brain can rapidly influence insulin sensitivity, in an age- related manner, through the autonomic nervous system (ANS) [38-42]. Thus, these metabolism-controlling signals (IIS, HPT and ANS) are linked via reciprocal controls involving the brain and periphery, and determine an organism's capacity to adapt to changing environments and to ageing.

The hypothalamus is known to have fundamental roles in growth, development, reproduction, metabolism and lifespan. The hypothalamus, via its reciprocal projections to other brain regions and the periphery, is central for the neuroendocrine interaction between the central nervous system and the periphery. Insulin, via the hypothalamus, is considered a link between the adaptive feeding (brain regulated) and changing energy requirements (periphery regulated). Insulin, a signal reflecting energy availability and reserves, provides direct negative feedback to hypothalamic nuclei that control energy and glucose homeostasis, both centrally and peripherally. Likewise, via hypothalamic control, metabolic homeostasis and ageing is integrated by thyroid hormones, possibly via effects of TH on membrane composition, inflammatory responses, stem cell renewal and synchronization of other physiological responses [33].

With the expansion of population ageing, numerous works in literature have focussed on neuro-endocrine features of ageing and longevity. Our studies contribute to existing knowledge of the crosstalk between the brain and periphery. For example, we showed that familial longevity is associated with more pronounced relation of insulin parameters with microstructural brain parameters, and by higher TSH secretion, in the absence of differences in metabolism. Building on our finding of differential TSH secretion with longevity, future studies can be aimed at deciphering the mechanisms underlying the increased TSH secretion with longevity potential. This could be via challenge experiments using recombinant TSH to decipher the thyroidal and extra- thyroidal effects of TSH, its mechanisms of action, and potential therapeutic effects.

Selective administration of insulin to the brain has been previously shown to have diverse central and peripheral effects, including beneficial effects on cognition, memory, weight control, food intake and palatability, body fat, etc. [18-23]. Our studies also show that intranasal insulin increased perfusion in the parietal and occipital brain regions in older adults. Future studies can be aimed at testing the short- and long-term effects of intranasal insulin and the consequent functional and clinical implications, especially in persons with impaired glucose metabolism. Since resetting the hypothalamic programing has been shown to accelerate or decelerate the ageing process in mice [43], further studies can thus be aimed at deciphering if resetting the hypothalamic programing can be attained in humans, using insulin that is specifically targeted to the hypothalamus. One way to measure such brain effects could be via non- invasive techniques such as measurement of blood oxygen level dependent (BOLD) brain responses, which would allow mapping of brain activities during functional MRI studies.

Indeed, as regards human longevity, the brain cross-talks with the periphery, via (but not limited to) its reciprocal connections with the metabolism-controlling signals (IIS, HPT and ANS). The links between these neuro- endocrine axes can be explored to find new therapeutic measures and strategies for slowing the pace of ageing, thereby facilitate health in old age.

REFERENCES

1. Houston DK, Nicklas BJ, Zizza CA. Weighty concerns: the growing prevalence of obesity among older adults. Journal of the American Dietetic Association. 2009;109(11):1886-95.
2. Mozumdar A, Liguori G. Persistent increase of prevalence of metabolic syndrome among U.S. adults: NHANES III to NHANES 1999-2006. Diabetes Care. 2011;34(1):216-9.
3. CfDCa. P. National Estimates and General Information on Diabetes and Prediabetes int he United States, 2011. National Diabetes Fact Sheet:. 2011.
4. Narayan KM, Boyle JP, Geiss LS, Saaddine JB, Thompson TJ. Impact of recent increase in incidence on future diabetes burden: U.S., 2005-2050. Diabetes Care. 2006;29(9):2114-6.
5. Schwartz MW, Porte D, Jr. Diabetes, obesity, and the brain. Science. 2005;307(5708):375-9.
6. Schwartz MW, Seeley RJ, Tschop MH, Woods SC, Morton GJ, Myers MG, et al. Cooperation between brain and islet in glucose homeostasis and diabetes. Nature. 2013;503(7474):59-66.
7. Sherlock M, Toogood AA. Aging and the growth hormone/insulin like growth factor-I axis. Pituitary. 2007;10(2):189-203.
8. Frolich L, Blum-Degen D, Bernstein HG, Engelsberger S, Humrich J, Laufer S, et al. Brain insulin and insulin receptors in aging and sporadic Alzheimer's disease. Journal of neural transmission (Vienna, Austria : 1996). 1998;105(4-5):423-38.
9. Zeyda M, Stulnig TM. Obesity, inflammation, and insulin resistance--a mini-review. Gerontology. 2009;55(4):379-86.
10. Gerozissis K. Brain insulin: regulation, mechanisms of action and functions. Cellular and molecular neurobiology. 2003;23(1):1-25.
11. Derakhshan F, Toth C. Insulin and the brain. Current diabetes reviews. 2013;9(2):102-16.
12. Shimokata H, Muller DC, Fleg JL, Sorkin J, Ziemba AW, Andres R. Age as independent determinant of glucose tolerance. Diabetes. 1991;40(1):44-51.
13. Lu M, Wan M, Leavens KF, Chu Q, Monks BR, Fernandez S, et al. Insulin regulates liver metabolism in vivo in the absence of hepatic Akt and Foxo1. Nature medicine. 2012;18(3):388-95.
14. Lin X, Taguchi A, Park S, Kushner JA, Li F, Li Y, et al. Dysregulation of insulin receptor substrate 2 in beta cells and brain causes obesity and diabetes. JClinInvest. 2004;114(7):908-16.
15. Hallschmid M, Benedict C, Schultes B, Born J, Kern W. Obese men respond to cognitive but not to catabolic brain insulin signaling. International journal of obesity (2005). 2008;32(2):275-82.
16. Kern W, Benedict C, Schultes B, Plohr F, Moser A, Born J, et al. Low cerebrospinal fluid insulin levels in obese humans. Diabetologia. 2006;49(11):2790-2.

17. de la Monte SM, Wands JR. Review of insulin and insulin-like growth factor expression, signaling, and malfunction in the central nervous system: relevance to Alzheimer's disease. Journal of Alzheimer's disease : JAD. 2005;7(1):45-61.
18. Hallschmid M, Benedict C, Schultes B, Fehm HL, Born J, Kern W. Intranasal insulin reduces body fat in men but not in women. Diabetes. 2004;53(11):3024-9.
19. Benedict C, Dodt C, Hallschmid M, Lepiorz M, Fehm HL, Born J, et al. Immediate but not long-term intranasal administration of insulin raises blood pressure in human beings. Metabolism: clinical and experimental. 2005;54(10):1356-61.
20. Benedict C, Hallschmid M, Schultes B, Born J, Kern W. Intranasal insulin to improve memory function in humans. Neuroendocrinology. 2007;86(2):136-42.
21. Bohringer A, Schwabe L, Richter S, Schachinger H. Intranasal insulin attenuates the hypothalamic-pituitary-adrenal axis response to psychosocial stress. Psychoneuroendocrinology. 2008;33(10):1394-400.
22. Reger MA, Watson GS, Green PS, Wilkinson CW, Baker LD, Cholerton B, et al. Intranasal insulin improves cognition and modulates beta-amyloid in early AD. Neurology. 2008;70(6):440-8.
23. Dhamoon MS, Noble JM, Craft S. Intranasal insulin improves cognition and modulates beta-amyloid in early AD. Neurology. 2009;72(3):292-3; author reply 3-4.
24. Stein PK. Heart rate variability and longevity. The American journal of cardiology. 2010;106(6):910.
25. Stein PK, Domitrovich PP, Hui N, Rautaharju P, Gottdiener J. Sometimes higher heart rate variability is not better heart rate variability: results of graphical and nonlinear analyses. Journal of cardiovascular electrophysiology. 2005;16(9):954-9.
26. Alcedo J, Kenyon C. Regulation of C. elegans longevity by specific gustatory and olfactory neurons. Neuron. 2004;41(1):45-55.
27. Fridell YW, Sanchez-Blanco A, Silvia BA, Helfand SL. Targeted expression of the human uncoupling protein 2 (hUCP2) to adult neurons extends life span in the fly. Cell Metab. 2005;1(2):145-52.
28. Lucin KM, Wyss-Coray T. Immune activation in brain aging and neurodegeneration: too much or too little? Neuron. 2009;64(1):110-22.
29. Taguchi A, Wartschow LM, White MF. Brain IRS2 signaling coordinates life span and nutrient homeostasis. Science. 2007;317(5836):369-72.
30. Wolkow CA, Kimura KD, Lee MS, Ruvkun G. Regulation of C. elegans life-span by insulinlike signaling in the nervous system. Science. 2000;290(5489):147-50.
31. Zhang G, Li J, Purkayastha S, Tang Y, Zhang H, Yin Y, et al. Hypothalamic programming of systemic ageing involving IKK-beta, NF-kappaB and GnRH. Nature. 2013;497(7448):211-6.

32. Vergara M, Smith-Wheelock M, Harper JM, Sigler R, Miller RA. Hormone-treated snell dwarf mice regain fertility but remain long lived and disease resistant. The journals of gerontology Series A, Biological sciences and medical sciences. 2004;59(12):1244-50.
33. Bowers J, Terrien J, Clerget-Froidevaux MS, Gothie JD, Rozing MP, Westendorp RG, et al. Thyroid hormone signaling and homeostasis during aging. Endocrine reviews. 2013;34(4):556-89.
34. Gussekloo J, van EE, de Craen AJ, Meinders AE, Frolich M, Westendorp RG. [Thyroid function, activities of daily living and survival in extreme old age: the 'Leiden 85-plus Study']. NedTijdschrGeneeskd. 2006;150(2):90-6.
35. Brown-Borg HM. Hormonal regulation of longevity in mammals. Ageing ResRev. 2007;6(1):28-45.
36. Ferrari E, Cravello L, Falvo F, Barili L, Solerte SB, Fioravanti M, et al. Neuroendocrine features in extreme longevity. ExpGerontol. 2008;43(2):88-94.
37. Jansen SW, Akintola AA, Roelfsema F, van der Spoel E, Cobbaert CM, Ballieux BE, et al. Human longevity is characterised by high thyroid stimulating hormone secretion without altered energy metabolism. Scientific reports. 2015;5:11525.
38. Belgardt BF, Bruning JC. CNS leptin and insulin action in the control of energy homeostasis. Annals of the New York Academy of Sciences. 2010;1212:97-113.
39. Filippi BM, Yang CS, Tang C, Lam TK. Insulin activates Erk1/2 signaling in the dorsal vagal complex to inhibit glucose production. Cell Metab. 2012;16(4):500-10.
40. Koch L, Wunderlich FT, Seibler J, Konner AC, Hampel B, Irlenbusch S, et al. Central insulin action regulates peripheral glucose and fat metabolism in mice. The Journal of clinical investigation. 2008;118(6):2132-47.
41. Macedo MP, Lima IS, Gaspar JM, Afonso RA, Patarrao RS, Kim YB, et al. Risk of postprandial insulin resistance: the liver/vagus rapport. Reviews in endocrine & metabolic disorders. 2014;15(1):67-77.
42. Obici S, Feng Z, Karkanias G, Baskin DG, Rossetti L. Decreasing hypothalamic insulin receptors causes hyperphagia and insulin resistance in rats. Nature neuroscience. 2002;5(6):566-72.
43. Obici S, Zhang BB, Karkanias G, Rossetti L. Hypothalamic insulin signaling is required for inhibition of glucose production. Nature medicine. 2002;8(12):1376-82.

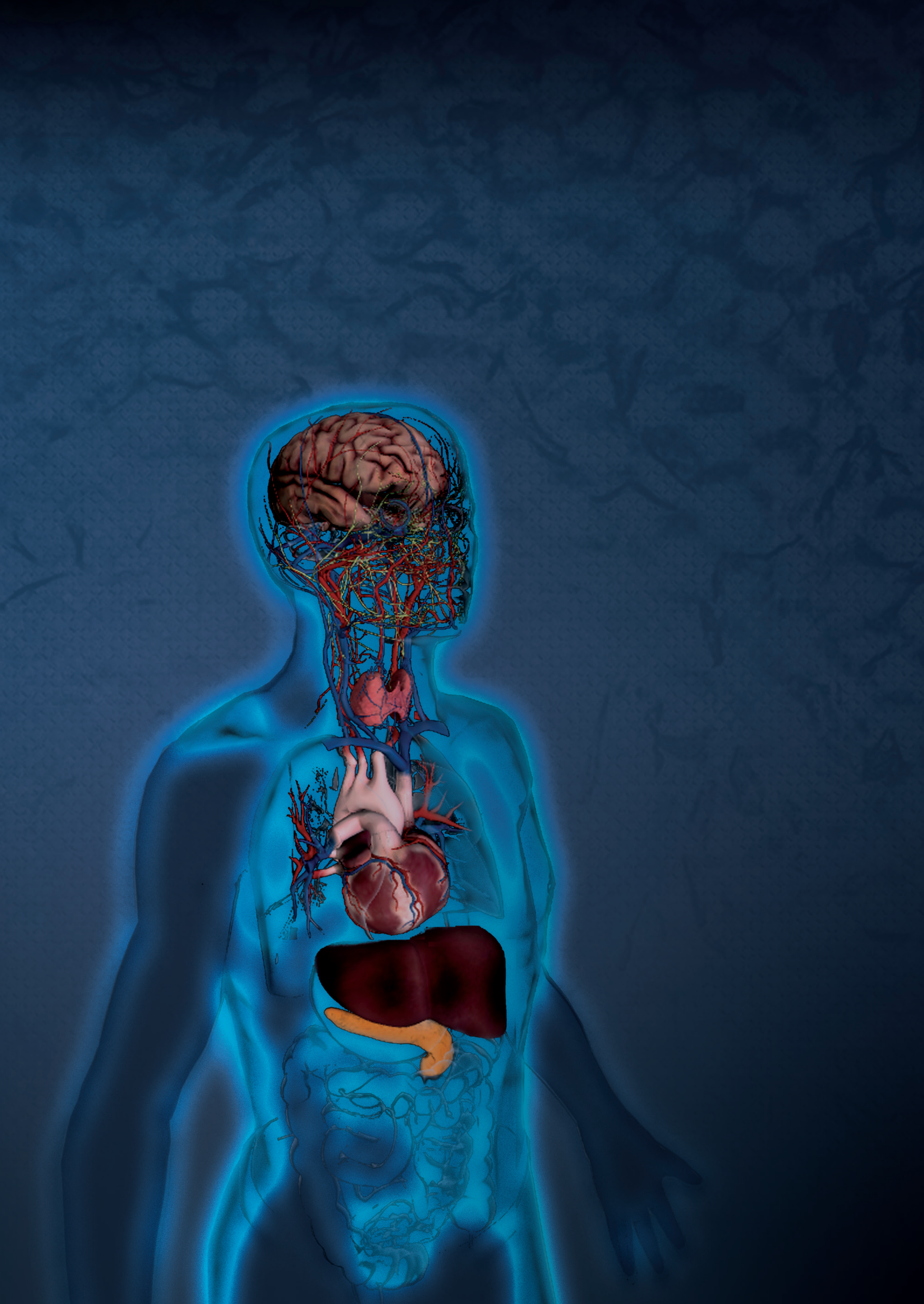

APPENDICES

NEDERLANDSE SAMENVATTING

LIST OF PUBLICATIONS

ACKNOWLEDGEMENTS

CURRICULUM VITAE

NEDERLANDSE SAMENVATTING

In dit proefschrift zijn drie interacterende systemen bestudeerd die allen invloed hebben op de snelheid van het verouderingsproces in mensen: het glucose/insuline metabolisme (deel I van dit proefschrift), de schildklier as (deel II), en het autonome zenuwstelsel (deel III).

Deel I van dit proefschrift begint met **hoofdstuk 2**. In dit hoofdstuk laten wij zien dat metingen van interstitieel glucose zoals bepaald met de "Continue Glucose Monitor" (CGM) sterk overeenkomen met veneuze glucose waarden. Echter, was er grote variatie in de 'per- persoon' Pearson correlatie coëfficiënten van de glucose bepalingen met de CGM. Bovendien waren de berekende maten van glycemie en glycemische variabiliteit lager met de CGM.

Hoofdstuk 3 en 4 beschrijven de relatie tussen maten van glucose metabolisme en maten van macro- en micro-structurele hersenintegriteit in ouderen met diabetes. We hebben gebruik gemaakt van Magnetization Transfer Imaging (MTI), een techniek die het toe laat om subtiele veranderingen in micro-structurele breinparenchym homogeniteit te detecteren, welke met conventionele MRI technieken niet zichtbaar zijn. Dit maakt MTI een gevoelige techniek om leeftijds- en ziekte gerelateerde veranderingen in het breinparenchym te detecteren. In **hoofdstuk 3** laten we zien dat alhoewel hogere bloed glucose waardes geassocieerd zijn met macro-structurele schade, verminderde insuline gevoeligheid juist sterker associeert met verminderde micro-structurele homogeniteit van het breinparenchym. In **hoofdstuk 4** tonen we aan dat hogere insuline parameters geassocieerd waren met verminderde myelinisatie en axonale integriteit, en dat deze associatie sterker was in nakomelingen van lang levende families en in "jongere" ouderen waarbij de glucose regulerende compensatie mechanismen beter intact zijn. **Hoofdstuk 3 en 4** laten beiden zien dat insuline, in vergelijking met glucose, mogelijk een sterkere indicator is voor veranderingen in micro-structurele (mogelijke vroege) brein integriteit in ouderen zonder diabetes.

Hoofdstuk 5 beschrijft een gerandomiseerde, dubbel blinde, placebo gecontroleerde cross-over trial, waarbij 40 IU insuline of placebo werd toegediend via een nasale verstuiver. Deze procedure kan veilig worden toegepast omdat er hierbij geen insuline in de perifere circulatie terecht komt, hetgeen ook bleek uit de observatie dat er geen toename was in circulerende waarden voor glucose en insuline in vergelijking met placebo. In **hoofdstuk 5** tonen we aan dat intranasaal toegediend insuline leidt tot een toename in brein perfusie bij ouderen. **Hoofdstuk 6** geeft een overzicht van de huidige kennis over glucose, insuline, veroudering en het brein.

In deel II, evalueren wij de schildklier as als één van de systemen die het verouderingsproces moduleren. Ten gevolge van het sterke circadiaanse ritme in de afscheiding en de korte halfwaardetijd van schildklier stimulerend hormoon was het noodzakelijk om herhaaldelijk bloed af te nemen om de secretie van schildklier stimulerend hormoon te kunnen berekenen.

In **hoofdstuk 7**, hebben wij bestaande venapunctie protocollen aangepast om 24 uurs bloed afname, met elke 10 minuten een afname, toe te kunnen passen in ouderen. Pragmatische aanpassingen werden gemaakt om voor, gedurende en na de bloedafnames de veiligheid en de effectiviteit van afname te garanderen. In **hoofdstuk 8** bestuderen we de TSH afscheiding en schildklier hormoon waardes gedurende 24 uur in nakomelingen uit lang levende families en hun partners zonder familiaire aanleg voor langlevendheid. Wij tonen hiermee aan dat familiare langlevendheid word gekarakteriseerd door een hogere TSH afscheiding zonder veranderingen in het energie metabolisme.

Hoewel het algemeen bekend is dat schildklier hormonen de brein functie beïnvloeden, blijft het controversieel of subklinische hypothyroïdie ook een effect heeft op cognitie. Om hier meer helderheid over te krijgen beschrijven wij in **hoofdstuk 9** een systematische meta-analyse van gepubliceerde studies over de relatie tussen subklinische hypothyroïdie en cognitieve functie in ouderen. Cross-sectionele en prospectieve analyses laten beiden geen associatie zien tussen subklinische hypothyroïdie en cognitieve functie in ouderen.

In **deel III**, bestuderen wij het autonome zenuwstelsel door meting van hartslag en hartslag variabiliteit als indicatoren van sympathische en parasympatische cardiale activiteit.

In **hoofdstuk 10**, valideren wij de werking van de "Equival EQ02 Lifemonitor" (EQ02), een gebruiksvriendelijk en veilig draadloos systeem wat de mogelijkheid biedt om continue ECG, hartslag en hartslag variabiliteit te meten, in vergelijking met de Holter monitor welke als de gouden standaard wordt gezien voor ambulante ECG metingen. Wij laten zien dat alhoewel er opvallende verschillen zijn in data kwaliteit in metingen tussen en binnen deelnemers, de hartslag en hartslag variabiliteit metingen van de EQ02 en de Holter monitor metingen zeer sterk correleren bij lage artefact percentages.

In **hoofdstuk 11** maken wij gebruik van de EQ02 om de cardiale ritmes te karakteriseren in relatie tot chronologische leeftijd en familiaire langlevendheid met behulp van continue metingen van hartslag en hartslag variabiliteit in jongeren in vergelijkingen met ouderen, en in nakomelingen van langlevende families in vergelijking met deelnemers van vergelijkbare leeftijd maar zonder familiare geschiedenis van langlevendheid. Wij tonen aan dat familiare langlevendheid niet is geassocieerd met grote verschillen in cardiale parameters. Daarentegen vonden wij verschillen in parameters van totale hartslag variabiliteit en van vagale activiteit bij jonge deelnemers in vergelijking tot ouderen.

Samenvattend laten de resultaten in dit proefschrift zien dat het brein een belangrijke rol speelt in de regulatie van het glucose en insuline metabolisme, dat insuline een sterke indicator lijkt voor micro-structurele (mogelijk vroege) verandering in brein integriteit in normoglycemische ouderen en dat intranasaal toegediend insuline een positief effect kan hebben op brein perfusie en BOLD signalen in specifieke brein gebieden. Familiare langlevendheid is geassocieerd met een meer uitgesproken relatie tussen insuline parameters en micro-structurele brein parameters en met een hogere TSH afscheiding zonder veranderingen in het energie metabolisme. Daarnaast is familiare langlevendheid niet geassocieerd met veranderingen in hartslag en hartslag variabiliteit als maat voor het autonome zenuwstelsel.

LIST OF PUBLICATIONS

Akintola AA, van de Pol V, Bimmel D, Maan AC, Van Heemst D. *Comparative analysis of the Equivital EQ02 lifemonitor with Holter ambulatory ECG device for continuous measurement of ECG, heart rate and heart rate variability: A validation study for precision and accuracy*. Front. Physiol. 7:391. doi: 10.3389/fphys.2016.00391

van der Spoel E, Jansen SW, **Akintola AA**, Ballieux BE, Cobbaert CM, Slagboom PE, Blauw GJ, Westendorp RG, Pijl H, Roelfsema F, van Heemst D. *Growth hormone secretion is diminished and tightly controlled in humans enriched for familial longevity*. Aging Cell. 2016 Sep 7. doi: 10.1111/acel.12519. [Epub ahead of print]

van der Kroef S, Noordam R, Deelen J, **Akintola AA**, Jansen SW, Postmus I, Wijsman CA, Beekman M, Mooijaart SP, Slagboom PE, van Heemst D. *Association between the rs7903146 Polymorphism in the TCF7L2 Gene and Parameters Derived with Continuous Glucose Monitoring in Individuals without Diabetes*. PLoS One. 2016 Feb 25;11(2):e0149992.

Akintola AA, Noordam R, Jansen SW, de Craen AJ, Ballieux BE, Cobbaert CM, Mooijaart SP, Pijl H, Westendorp RG, van Heemst D. *Accuracy of Continuous Glucose Monitoring Measurements in Normo-Glycemic Individuals*. PLoS One. 2015 Oct 7;10(10):e0139973

Akintola AA, Jansen SW, van Bodegom D, van der Grond J, Westendorp RG, de Craen AJ, van Heemst D. *Subclinical hypothyroidism and cognitive function in people over 60 years: a systematic review and meta-analysis*. Front Aging Neurosci. 2015 Aug 11;7:150.

Jansen SW, Roelfsema F, van der Spoel E, **Akintola AA**, Postmus I, Ballieux BE, Slagboom PE, Cobbaert CM, van der Grond J, Westendorp RG, Pijl H, van Heemst D. *Familial Longevity Is Associated With Higher TSH Secretion and Strong TSH-fT3 Relationship*. J Clin Endocrinol Metab. 2015 Oct;100(10):3806-13.

Jansen SW, Roelfsema F, **Akintola AA**, Oei NY, Cobbaert CM, Ballieux BE, van der Grond J, Westendorp RG, Pijl H, van Heemst D. *Characterization of the Hypothalamic-Pituitary-Adrenal-Axis in Familial Longevity under Resting Conditions*. PLoS One. 2015 Jul 20;10(7):e0133119.

Akintola AA, van den Berg A, Altmann-Schneider I, Jansen SW, van Buchem MA, Slagboom PE, Westendorp RG, van Heemst D, van der Grond J. *Parameters of glucose metabolism and the aging brain: a magnetization transfer imaging study of brain macro- and micro-structure in older adults without diabetes*. Age (Dordr). 2015 Aug;37(4):9802.

Akintola AA*, Jansen SW*, Wilde RB, Hultzer G, Rodenburg R, van Heemst D. *A simple and versatile method for frequent 24 h blood sample collection in healthy older adults*. MethodsX. 2014 Dec 26;2:33-8.

Jansen SW*, **Akintola AA***, Roelfsema F, van der Spoel E, Cobbaert CM, Ballieux BE, Egri P, Kvarta-Papp Z, Gereben B, Fekete C, Slagboom PE, van der Grond J, Demeneix BA, Pijl H, Westendorp RG, van Heemst D. *Human longevity is characterised by high thyroid stimulating hormone secretion without altered energy metabolism*. Sci Rep. 2015 Jun 19;5:11525.

Akintola AA, van den Berg A, van Buchem MA, Jansen SW, Slagboom EP, Westendorp RG, van der Grond J, van Heemst D. *Associations between insulin action and integrity of brain microstructure differ with familial longevity and with age*. Front Aging Neurosci. 2015 May 28;7:92.

Akintola AA, van Heemst D. *Insulin, aging, and the brain: mechanisms and implications*. Front Endocrinol (Lausanne). 2015 Feb 6;6:13

Noordam R, Jansen SW, **Akintola AA**, Oei NY, Maier AB, Pijl H, Slagboom PE, Westendorp RG, van der Grond J, de Craen AJ, van Heemst D; Leiden Longevity Study group. *Familial longevity is marked by lower diurnal salivary cortisol levels: the Leiden Longevity Study*. PLoS One. 2012;7(2):e31166.

* Equal contribution of authors

ACKNOWLEDGEMENTS

It would not have been possible to conduct and complete my doctoral research without the preparative and supportive efforts of others. I am deeply grateful to all the people whose contributions, support, help and encouragement has made it possible to complete this research project.

My profound thanks goes to the participants of the Leiden Longevity Study, especially to those who participated in Switchbox phases I and II. Without your enthusiasm, self-sacrifice and volunteering spirit, it certainly would not have been possible to successfully conduct the research whose results are contained in this thesis.

I owe the conception of my thesis to the scientific creativity of my promotor Rudi and co- promotors Diana and Jeroen. To Rudi, I deeply appreciate your thoughtful guidance, support, motivation, inspiration, and constructive criticism through the years, first as a masters student and throughout my PhD trajectory. It has helped me to grow. My warm thanks to Diana, a wonderful source of scientific inspiration and support. Words cannot express my gratitude for your belief in my abilities, for sharing your knowledge and for your continuous positive motivation and dependability. To Jeroen, I cannot thank you enough for your warmth, patience, valuable advice and enthusiastic support through my PhD trajectory.

I would like to offer my sincere thanks to the Switchbox team whose expertise, co-operation, experience and resourcefulness have made the conductance of the Switchbox studies a success. Of note is Hanno, whose guidance and continuous support have proven invaluable. Also notable are Ferdinand, Mark, Nicole, and those abroad, including Barbara and all members of the Switchbox consortium. Also to Bep Ladan and Marjan van der Elst – thanks for your resourcefulness- it was invaluable to the success of our studies. Furthermore, my heartfelt thanks goes to my dear colleagues Steffy and Annemarieke- one could not wish for better colleagues through those long research hours. Dear Steffy, we started our wonderful PhD journey together- I cherish all the thrilling and challenging moments that we have shared- thanks for being a wonderful colleague and a dear friend! Dear Annemarieke, working with you is a true delight!

I wish to express thanks to our collaborators from various departments, such as the departments of radiology, clinical chemistry and laboratory medicine, pharmacy, and the skills-lab. My sincere thanks also goes to the people that were committed to the success of

both Switchbox projects but are presently no longer at the LUMC, including Stella Henquet and Jolanda Verhagen. Thank you all for your valuable input.

I have had the pleasure of working with very cordial, warm and friendly colleagues from our department. Thank you all for the many special moments that we have shared together and for making the working at Geriatrics section of internal medicine such a pleasant experience.

To my dear mom, dad, and brothers (Femi, Anu, Sola and Joseph), thank you for everything, and for encouraging me to follow my dreams, right from an early age. Also to my brothers and sisters from the congregation- thank you for truly proving that love is the identifying mark of true Christians!

My greatest thanks goes to Ayo, and our lovely girls- Annabelle and Daniella. Annabelle and Daniella- your wonderful "hugs and kisses" and ever smiling faces, even when I have to 'flee the house' in the mornings always keeps me going. Finally to Ayo, my best friend, soulmate and husband, thank you for your love, continuous encouragement and rock-solid support. You are my inspiration and strength.

CURRICULUM VITAE

Abimbola (Abi) Akintola was born in Lagos, Nigeria on the 25th of April, 1979. After graduating with distinction from secondary school in 1994, she studied Science Laboratory Technology at the Federal Polytechnic, Ilaro, Nigeria, earning a National Diploma (with Honors) in 1997. She then studied Medicine at the Olabisi Onabanjo University in Nigeria, during which she participated in a Commonwealth exchange program with Stellenbosch University, South Africa and served as an intern at the Tygerberg Children Hospital in Stellenbosch, Cape Town. During her medical studies, she earned many awards and privileges, such as the federal government special recognition award, Ogun state recognition of excellence award, Edward Boyle Medical Elective Bursary award and Commonwealth Award for outstanding Medical students. She graduated from medical school in 2005. Immediately thereafter, she had her one-year housemanship training at the Olabisi Onabanjo University Teaching Hospital after which she practiced as a General Medical Practitioner for five years at three (international) hospitals.

In 2010, she joined the pioneer class of the Leyden Academy on Vitality and Ageing (LAVA), Leiden University, Leiden, Netherlands, for a one- year master's program for post- graduate medical doctors. While at LAVA, she served as the student assessor of the program, and graduated with the highest overall scores of the first graduating masterclass. She earned her Masters degrees in Ageing and Vitality in 2011. Immediately thereafter, she was offered a position at the department of Internal medicine, section Gerontology and Geriatrics, Leiden University Medical Center (LUMC), where she performed her doctoral research as part of the European commission funded project 'Switchbox'. For Switchbox, she co-planned and co-executed the two human- based clinical research projects (Phases I & 2) of the Netherlands arm of Switchbox. She co-wrote the Switchbox protocols that were approved by the LUMC's medical ethical committee and Dutch competent authority for medicinal research in humans. She registered the Switchbox phase II clinical trial in the European clinical trial register, screened and recruited participants, and conducted the studies from start till completion according to good clinical practice whilst collaborating with major functional areas. During this period also, she supervised many bachelor and master research students as well as lectured medical students and postgraduate doctors. She is a member of various national and international scientific and medical organizations, and has presented the results of her doctoral research at several international conferences across the globe. She plans to continue working at the LUMC.